

Department of Data Analysis and Mathematical Modelling

**Exploring the dynamics of ecological species in
intransitive competition networks**

Nathan Muyinda

Thesis submitted in fulfillment of the requirements for the degree of
Doctor (Ph.D.) of Bioscience Engineering: Mathematical Modelling

Academic year 2022-2023

Supervisors:

Prof. dr. Shodhan Rao
Center for Biotech Data Science
Ghent University Global Campus
Incheon, South Korea

Prof. dr. Bernard De Baets
Research Unit Knowledge-Based Systems (KERMIT)
Department of Data Analysis and Mathematical Modelling
Faculty of Bioscience Engineering - Ghent University

Examination committee:

Prof. dr. ir. Koen Dewettinck (Chairman)
Ghent University

Prof. dr. ir. Philippe Heynderickx
Ghent University Global Campus

Prof. dr. Joris Vankerschaver
Ghent University Global Campus

Dr. Aisling Daly
Ghent University

Prof. dr. Jae Kyoung Kim
Korea Advanced Institute of Science and Technology
South Korea

Prof. dr. Jinsu Kim
Pohang University of Science and Technology
South Korea

Dean:

Prof. dr. Els Van Damme

Rector:

Prof. dr. ir. Rik Van de Walle

Nathan Muyinda

**Exploring the dynamics of ecological species in intransitive
competition networks**

Thesis submitted in fulfilment of the requirements for the degree of
**Doctor (Ph.D) of Bioscience Engineering: Mathematical
Modelling**

Academic year 2022-2023

Dutch translation of the title:

Een exploratie van de dynamiek van ecologische soorten in niet-transitieve competitienetwerken

Please refer to this work as follows:

N. Muyinda (**2022**). Exploring the dynamics of ecological species in intransitive competition networks, PhD Thesis, Department of Data Analysis and Mathematical Modelling, Ghent University, Ghent, Belgium.

The author and the supervisors give the authorization to consult and to copy parts of this work for personal use only. Every other use is subject to the copyright laws. Permission to reproduce any material contained in this work should be obtained from the author.

Acknowledgements

I am deeply indebted to my main promoter Prof. dr. Shodhan Rao, for giving me the opportunity to travel to South Korea and to work together on this project. Thank you for the valuable guidance and feedback, and for always challenging me to grow as a scientist. In a special way, I would like to express my deepest appreciation to Prof. dr. Bernard De Baets for his, always timely, critical assessment of my work. Thank you for the support during the tough times. You have not only made me a better researcher but a resilient person. Additionally, this endeavor would not have been possible without the generous support from the Ghent University Global Campus in South Korea, who financed my research. I would also like to express my sincere gratitude to the Eastern Africa Universities Mathematics Program (EAUMP) for the financial support towards the payment of my tuition fees.

I am extremely grateful to members of the examination committee for their valuable time and effort dedicated to reading this thesis. Special thanks go to Dr. Aisling Daly for the insightful questions and comments regarding the ecological implications of this work and for pointing out some very exciting possible future directions. I am also thankful to Prof. dr. Joris Vankerschaver for the many interesting mathematical questions and observations that he pointed out in the thesis.

To all my colleagues and dear friends both at GUGC and Makerere University, thank you for all the wonderful times we spent together both in the office, and in social settings. Special thanks go to Espoir, thank you for being there for me man. Friends like you come along once in a lifetime. To Tim, Zihan, Zhenyin, Jitendra, Derrick, Kim, Mena and all the members of the Songdo Socks football team, thank you for all the good times. Life would definitely have been lonely without you guys. Lastly, I would like to thank my family, my wife Grace, and my children Abner and

Elena, for always being there for me, for always praying for me, and for being part of my journey.

Nathan Muyinda
Gent, November 2022

Contents

Preface	v
Contents	vii
Summary	xiii
Nederlandstalige samenvatting	xv
List of symbols	xviii
List of acronyms	xxii
List of Figures	xxiii
List of Tables	xxvii
1 Introduction	1
1.1 Overview	1
1.2 Research questions	7
1.3 Scope of the thesis	8

2 Ecological Background	11
2.1 Introduction to ecological communities	11
2.1.1 What is a community?	11
2.1.2 Community properties	12
2.1.3 Interspecific competition	13
2.2 Ecological communities as complex networks	14
2.2.1 Introduction	14
2.2.2 Graphs and graph theory	15
2.2.2.1 Definitions	15
2.2.2.2 Matrix representations	16
2.2.2.3 Paths, cycles and connectivity	18
2.3 Intransitive competition	19
2.3.1 What is intransitive competition?	19
2.3.2 Measuring intransitivity	21
2.3.2.1 Slater's i	22
2.3.2.2 Kendall and Babington Smith's d	22
2.3.2.3 Laird and Schamp's unbeatability (u) and always-beatability (a)	23
2.4 Kings in a tournament	23
2.5 Conclusion	24
3 Modelling Background	27
3.1 Introduction	27
3.2 Classification of mathematical models in ecology	30
3.3 Non-spatial models of competition	33
3.3.1 Mean-field ODE models	33
3.3.2 Dynamic behavior	35
3.3.2.1 Stability of equilibrium points	35
3.3.2.2 Lyapunov's stability method	37
3.3.2.3 LaSalle's invariance principle	39
3.3.3 Equilibrium stability and species coexistence	40

3.3.4	Game theory in the ecological context	42
3.3.4.1	Introduction	42
3.3.4.2	Symmetric two-person zero-sum games	43
3.3.4.3	Evolutionary game dynamics	46
3.4	Chemical reaction network theory	50
3.4.1	Introduction	50
3.4.2	Chemical reaction networks	51
3.4.3	Mass-action systems	53
3.4.4	Detailed balancing for mass-action systems	56
3.4.5	Wegscheider's conditions	57
3.5	Spatial models	58
3.5.1	Introduction	58
3.5.2	Reaction-diffusion equations	59
3.5.2.1	Reaction	60
3.5.2.2	Diffusion and random walks	60
3.5.2.3	Boundary conditions	62
3.5.2.4	The reaction-diffusion model	63
3.5.3	Metapopulation models	66
3.5.4	ODEs vs PDEs in modelling spatial dynamics	68
3.6	Numerical solution of PDEs	69
3.7	A von Neumann stability analysis	72
3.7.1	Background	72
3.7.2	Definition of stability	73
3.7.3	The von Neumann stability condition	74
3.7.4	Forward in time, centered in space	75
3.7.5	The Crank–Nicolson scheme	76
3.7.6	The fractional step theta scheme	77
3.7.7	Conclusions	79

4 The method of triads	81
4.1 Introduction	81
4.2 The method of triads	84
4.2.1 Eliminate all non-kings	84
4.2.2 Find all intransitive triads in the tournament	86
4.2.3 Establish dominance relations among the intransitive triads	88
4.2.4 Determine the final species richness	88
4.3 Example	90
4.4 Results	92
4.5 Species richness versus relative intransitivity	94
4.6 Discussion and conclusion	94
5 Dynamics of balanced metapopulation models	99
5.1 Introduction	99
5.2 Metapopulation model	102
5.3 Invariance of the unit simplex	103
5.4 Neutral stability	104
5.5 Detailed-balanced single species mass-action reaction networks	105
5.6 Balanced metapopulation model	108
5.7 Unique coexistence equilibrium	109
5.8 Some examples	112
5.9 Stability of the coexistence equilibrium	114
5.10 Discussion and conclusion	117
6 Finite-difference schemes for reaction-diffusion equations modelling cyclic competition: A stability analysis	119
6.1 Introduction	119
6.2 Linearization	122
6.3 The stability problem	123
6.4 The von Neumann stability criterion	124
6.5 Sufficient conditions for stability	127

6.6	Stability of difference schemes	128
6.6.1	The Crank–Nicolson scheme	128
6.6.2	The fractional step theta scheme	131
6.6.3	The implicit integration factor method	135
6.6.4	Implicit-explicit (IMEX) methods	140
6.7	Numerical simulations	142
6.7.1	The Brusselator model	142
6.7.2	A 3-species intransitive competition model	145
6.7.2.1	Numerical experiments	147
6.8	Matrix semi-stability	152
6.8.1	Monotone kinetics	153
6.8.2	D-semi-stability	155
6.9	Discussion and conclusion	158
7	Conclusions and future work	161
7.1	Conclusions	162
7.2	Possible future research directions	163
	Bibliography	169
	Curriculum vitae	185

Summary

Identifying the processes that preserve diversity in nature is a longstanding goal of ecology. Theoretical and empirical explanations of coexistence have focused on the role of competitive interactions in shaping ecological communities. Competition among multiple species can range from hierarchical to intransitive. Hierarchical competition occurs when species can be ranked unambiguously in order of their competitive abilities. Intransitive competition, on the other hand, occurs when the competitive superiority of species is not strictly hierarchical and is characterized by the existence of at least one competitive cycle (such as in the rock-paper-scissors game).

Over ecological time scales, competitive cycles can have stabilizing effects on species coexistence because decreasing the abundance of any competitor in the cycle propagates through the network in a way that feeds back to favour the recovery of the perturbed species. However, not all competitive cycles generate this stabilizing effect. Mathematical modelling has been used to show that cycles containing an odd number of species will stabilize coexistence, whereas cycles containing an even number of species will destabilize it. The persistence of an individual species not only depends on its pairwise competitive abilities, but also by its participation in intransitive triads (three-species cycles) which effectively rescue it periodically from extinction.

Despite decades of research, a number of questions still remain regarding how competitive intransitivity increases local species richness, whether intransitive competition alone leads to species distributions across sites in a metapopulation, and how dispersal combines with intransitive competition to predict species coexistence in a metapopulation, among others. Many questions on intransitive competition have traditionally been approached via a graph-theoretic representation

of an ecological community as a directed graph, known as a tournament. By analyzing the structure or topology of the graph, ecologists could be able to anticipate some of the dynamical properties of an ecological community and also make predictions on community structure.

In this thesis, we bring together different mathematical tools and concepts borrowed from the fields of numerical analysis, graph theory, game theory, chemical reaction network theory, and the theory of dynamical systems to explore a number of questions related to the dynamics of ecological communities under intransitive competition and the numerical stability of finite difference schemes used for solving PDEs in ecology.

More specifically, we explore how network structure (or topology) can be used to provide insights as to why some species persist while others go extinct, and provide solutions to one of community ecology's central aims, the prediction of community structure at equilibrium. Furthermore, we explore the role of dispersal or migration in the dynamics of populations living in spatially discrete habitats (patches).

Finally, we explore the mathematical problem of analyzing the stability of some of the popular finite difference schemes that have been used in the literature for the solution of reaction-diffusion equations. Such equations appear in the literature as models that govern the dynamics of populations living in spatial habitats that are viewed as a continuum, such as in aquatic systems. Since these equations have no known analytical solutions, their solutions can only be obtained via numerical methods, in particular, finite difference methods, whose stability properties are not well known, especially when applied to systems.

Nederlandstalige samenvatting

Een langetermijndoel van de ecologie is het identificeren van processen die de diversiteit in de natuur bewaren. Theoretische en empirische verklaringen voor coëxistentie focussen daarbij op de rol van competitieve interacties in de vorming van ecologische gemeenschappen. Competitie tussen meerdere soorten kan variëren van hiërarchisch tot intransitief. Enerzijds treedt hiërarchische competitie op wanneer de soorten ontegensprekelijk kunnen gerangschikt worden op basis van hun competitieve capaciteiten. Anderzijds treedt intransitieve competitie op wanneer de competitieve superioriteit van soorten niet strikt hiërarchisch is en gekarakteriseerd wordt door het bestaan van minstens één competitieve cykel (zoals in het blad-steen-schaar spel).

Over ecologische tijdschalen kunnen competitieve cycli stabiliserende effecten hebben op coëxistentie van soorten aangezien de afname van de abundantie van een soort kan propageren doorheen het netwerk op zo'n wijze dat dit leidt tot het herstel van diezelfde soort. Echter, niet alle competitieve cycli genereren dit stabiliserend effect. Wiskundige modellering heeft aangetoond dat cycli met een oneven aantal soorten coëxistentie zullen stabiliseren, terwijl cycli met een even aantal soorten deze zullen destabiliseren. Het overleven van een individuele soort hangt niet alleen af haar competitieve capaciteiten, maar ook van haar deelname aan intransitieve triades die haar effectief periodiek redden van uitsterven.

Niettegenstaande decennia van onderzoek blijven er een aantal vragen, onder andere betreffende hoe competitieve intransitiviteit lokaal het aantal soorten doet toenemen, of intransitieve competitie alleen leidt tot een metapopulatie overheen

sites en hoe verspreiding samen met intransitieve competitie toelaat coëxistentie van soorten te voorspellen. Heel wat vragen betreffende intransitieve competitie worden traditioneel aangepakt op basis van een grafentheoretische voorstelling van een ecologische gemeenschap als een gerichte graaf, in het bijzonder een tornooistructuur. Het analyseren van de structuur of de topologie van deze graaf heeft ecologen toegelaten de dynamische eigenschappen van een ecologische gemeenschap in te schatten en de structuur van een gemeenschap te voorspellen.

In deze thesis combineren we diverse wiskundige tools en concepten - uit de numerieke analyse, grafentheorie, speltheorie, theorie van chemische reactienetwerken en de theorie van dynamische systemen - voor het exploreren van een aantal relevante vragen betreffende de dynamiek van ecologische gemeenschappen onder intransitieve competitie en de numerieke stabiliteit van eindigedifferentie-schema's voor het oplossen van partiële differentiaalvergelijkingen in de ecologie. Meer specifiek exploreren we hoe netwerkstructuur (of topologie) inzicht kan verschaffen in het waarom bepaalde soorten overleven terwijl andere uitsterven, en formuleren oplossingen voor één van de centrale doelstellingen van de ecologie, nl. het voorspellen van de gemeenschapsstructuur bij evenwicht. Verder exploreren we de rol van dispersie of migratie in de dynamiek van populaties in spatiaal discrete leefgebieden. Finaal exploreren we het wiskundig probleem van het analyseren van de stabiliteit van enkele populaire eindigedifferentie-schema's die in de literatuur aangewend worden voor het oplossen van reactie-diffusie-vergelijkingen. Dergelijke vergelijkingen treden op in modellen die de dynamiek beschrijven van populaties in spatiale leefgebieden die gezien kunnen worden als een continuüm, zoals in aquatische systemen. Aangezien dergelijke vergelijkingen geen gekende analytische oplossingen hebben, kunnen deze enkel benaderd worden via numerieke methoden, in het bijzonder eindigedifferentie-methodes, waarvan de stabiliteitseigenschappen niet goed gekend zijn, in het bijzonder voor stelsels van vergelijkingen.

List of symbols

$G(V, E)$	graph with vertex set V and edge set E
$ V $	cardinality of set V
$\deg^-(v)$	in-degree of vertex v
$\deg^+(v)$	out-degree of vertex v
A	adjacency matrix
\mathbf{A}^T	the transpose of matrix A
B	incidence matrix
b_{ij}	entry in the i -th row and j -th column of B
$\ker \mathbf{B}$	the kernel of matrix B
$\mathbb{1}$	vector with all entries equal to 1
i	Slater's intransitivity index
d	number of intransitive triads
x_i	relative abundance of species i
x	vector of species relative abundances
\mathbf{x}^*	equilibrium point vector/ Nash equilibrium
T	tournament matrix/ payoff matrix
$\ \mathbf{x}\ _2$	Euclidean norm of x
$V(\mathbf{x})$	Lyapunov function
$\mathbf{x}(t; \mathbf{x}_0)$	solution with initial condition \mathbf{x}_0

$\omega(\mathbf{x}_0)$	omega limit set of $\mathbf{x}(t; \mathbf{x}_0)$
S^n	unit simplex in \mathbb{R}^n
S_+^n	interior of S^n
S	stoichiometric matrix
Z	complex stoichiometric matrix
\mathbb{R}_+^n	n -dimensional vectors of positive real numbers
Δx	space discretization step size
Δt	time discretization step size
∇^2	Laplacian
u_j^n	grid function at spatial point x_j and time t_n
\mathbf{u}^n	vector of spatial grid points at time t_n
$\hat{\mathbf{u}}^n$	discrete Fourier transform of \mathbf{u}^n
$G(\xi)$	amplification factor/matrix
$\text{Ln } \mathbf{x}$	the element-wise logarithm with $(\text{Ln } \mathbf{x})_i = \ln(x_i)$
$\frac{\mathbf{x}}{\mathbf{z}}$	the element-wise quotient vector with $(\frac{\mathbf{x}}{\mathbf{z}})_i = \frac{x_i}{z_i}$
$\text{Exp}(\mathbf{x})$	the element-wise exponential with $(\text{Exp}(\mathbf{x}))_i = e^{x_i}$
$\text{Im}(\mathbf{B})$	the image (or range) of matrix B
$\text{diag}(\mathbf{x})$	diagonal matrix with entries of \mathbf{x} on the diagonal
$\det(\mathbf{A})$	the determinant of matrix A
$\rho(G)$	the spectral radius of G
$\mathbf{M}_n(\mathbb{R})$	the set of all $n \times n$ real matrices

List of acronyms

CFL	Courant-Friedrichs-Lewy
CN	Crank-Nicolson
CRN	Chemical reaction network
CRNT	Chemical reaction network theory
DFT	Discrete Fourier transform
ESS	Evolutionarily stable strategy
ETD	Exponential time differencing
FSTS	Fractional step theta scheme
FTCS	Forward time centered space
IIF	Implicit integration factor
IMEX	Implicit-explicit
IVP	Initial value problem
NE	Nash equilibrium
ODE	Ordinary differential equation
PDE	Partial differential equation
RD	Reaction-diffusion
RI	Relative intransitivity
RPS	Rock-paper-scissors
RV	Relative variance
TIG	Triad interaction graph

List of Figures

2.1	Categorization of graphs: (a) unweighted undirected; (b) weighted undirected; (c) unweighted directed; (d) weighted directed. On the right are the corresponding adjacency matrices for the given networks. Arrow thickness in graphs (b) and (d) represents the strength of the link/interaction.	17
2.2	A complete digraph (tournament)	19
2.3	A 7-species tournament with corresponding adjacency matrix	20
2.4	(a) A transitive 7-species tournament. (b) An intransitive tournament with three of its nine intransitive triads highlighted.	21
2.5	The kings correspond to the green nodes 1, 2 and 4, while species 3 and 5 are non-kings. Among the three kings, only 1 and 4 (with thicker borders) are strong kings.	24
3.1	Schematic diagram of the modelling process	28
3.2	A Rock-Paper-Scissors game with its corresponding payoff matrix. When the players pick different objects, the winner is the one who picks the object at the head of the arrow connecting the two objects. .	43
3.3	Example of a reversible CRN with 5 chemical species ($\{X_1, \dots, X_5\}$), 6 complexes ($\{C_1 = 2X_1, C_2 = X_1 + X_2, C_3 = 2X_2, C_4 = X_1 + X_3, C_5 = X_4 + X_5, C_6 = X_2\}$) and 5 reversible reactions (edges of the network) .	57

4.1 Three five-species tournaments, each with a relative intransitivity value of $4/5$. A numerical simulation of the ODE system (3.13) for each tournament shows that the tournaments in (a) and (c) collapse to one of their intransitive triads, whereas the tournament in (b) supports coexistence of all five species. 83

4.2 An eight-species tournament with the kings shaded in green. Next to each node is shown the proportion of the population playing that node in a NE strategy. A simulation of the ODE system (3.13) is shown on the right. It is clear that all non-kings are not part of the unique NE strategy and hence they ultimately perish as shown in the simulation. 85

4.3 A nine-species tournament with the kings shaded. Next to each node is shown the proportion of the population playing that node in a NE strategy. A simulation of the ODE system (3.13) is shown on the right. 86

4.4 A seven-species tournament in which every species is king. Only species 1, 2 and 3 (with thicker borders) are strong kings. A simulation of the ODE system (3.13) for the tournament shows that species 2, although a strong king, does not persist. 86

4.5 A seven-species tournament with corresponding adjacency matrix . . . 87

4.6 Left: A nine-species tournament with the kings in green. Center: A six-species tournament obtained from elimination of the non-kings from the nine-species tournament. Right: A final five-species tournament in which every species is a king. 90

4.7 A TIG for the final five-species tournament of Fig. 4.6. The TIG contains a single cycle formed by the red arrows. 91

4.8 A simulation of the ODE system (3.13) for the nine-species tournament of Fig. 4.6. Shown on the right is the time evolution of the four species that go extinct. 91

4.9 The two non-isomorphic tournaments of size five in which every species is a king. 92

4.10 The TIG for the five-species tournament in Fig. 4.9 on the right. 93

4.11 Corresponding simulation results of the ODE system (3.13) for the two 5-species tournament of Fig. 4.9. 93

4.12 Final species richness versus relative intransitivity. The number of dots at a single point represents the number of tournaments with the same relative intransitivity value. 95

5.1 Left: A heterogeneous dispersal graph according to Nagatani et al. (2018). Right: A homogeneous dispersal graph according to our definition. 109

- 5.2 A metapopulation network composed of three patches. Each patch contains a local population composed of three species (1, 2 and 3), in cyclic competition, as shown by the black arrows. The red arrows denote migrations among the patches in the directions shown. 113
- 5.3 A metapopulation network composed of three patches. Species can migrate from patch 1 to the other two patches and vice versa. However, there exists no migrations between patches 2 and 3. 113
- 5.4 Left: Dynamics of the metapopulation model in Fig. 5.2 for patches 1 and 3 showing asymptotic stability of the coexistence equilibrium. Right: The time evolution of the proportion of species 1 in the three patches. 117
- 5.5 Left: Dynamics of the metapopulation model in Fig. 5.3 for patches 1 and 3 showing a limit cycle arising from the neutral stability of the coexistence equilibrium. Right: Time evolution of the proportion of species 1 in the three patches. Note that the dynamics in all patches are the same and thus the three graphs overlap. 117
- 6.1 Real parts of the two eigenvalues of the Jacobian at the point $x = 5.05$. The space step size is $\Delta x = 0.101$, while the time step size is $\Delta t = 0.01$ for all the schemes. 144
- 6.2 Left: Solution $v(x, t)$ of the Brusselator system at $x = 5.05$. The space step size is $\Delta x = 0.101$, while the time step size is $\Delta t = 0.0002$ for the explicit scheme and $\Delta t = 0.01$ for the rest of the schemes. Right: Spatial pattern solution. 145
- 6.3 Real parts of the two eigenvalues of the Jacobian for $D_u = 1, D_v = 8, a = 4.5, b = 21$ at the point $x = 5.05$. The space step size is $\Delta x = 0.101$, while the time step size is $\Delta t = 0.01$ for all the schemes. 146
- 6.4 Left: Solution $v(x, t)$ for $D_u = 1, D_v = 8, a = 4.5, b = 21$ at the point $x = 5.05$ with $\Delta t = 0.01$. Right: Spatial pattern. 147
- 6.5 Blow-up of solution $v(5.05, t)$ for $\Delta t = 0.255$ for the CN, $\Delta t = 0.2$ for the FSTS and $\Delta t = 0.25$ for the IIF. One of the eigenvalues of the Jacobian has a positive real part at the time of blow-up. 148

6.6 Dynamics of the ODE model system obtained from Eq. (6.72) by dropping the diffusion term. Species population densities move along periodic orbits around a coexistence equilibrium point (6.73). Left: The figure shows several such orbits for the invasion rates $\alpha_1 = 0.2$, $\alpha_2 = 0.5$ and $\alpha_3 = 0.3$. Here, u_3 ranges linearly from zero along the base of the triangle to unity at its peak; similarly u_1 and u_2 increase to unity at their respective corners. Right: The dynamics can also be visualized by plotting the population densities $u_i(t)$ as a function of time t . These simulations have been obtained by making use of MATLAB's standard ODE solver, **ode45**. 149

6.7 Real parts of the three eigenvalues of the Jacobian for for the invasion rates $\alpha_1 = 0.2$, $\alpha_2 = 0.5$ and $\alpha_3 = 0.3$ at the point $x = 5.05$. The space step size is $\Delta x = 0.1$, while the time step is $\Delta t = 0.1$ all the schemes (CN, FSTS and IIF) and $\Delta t = 0.01$ for the IMEX scheme. . . . 150

6.8 Numerical solutions of Eq. (6.72) using the CN scheme for the invasion rates $\alpha_1 = 0.2$, $\alpha_2 = 0.5$ and $\alpha_3 = 0.3$ at the point $x = 5.05$. The space step size is $\Delta x = 0.1$, while the time step is $\Delta t = 0.1, 4.0$ and 4.118 . It can be observed that the dynamics are similar for all Δt for which the scheme is stable. For $\Delta t = 4.118$, there is a blow-up of the finite difference solution and the scheme becomes unstable. 151

6.9 Numerical solutions of Eq. (6.72) using the FSTS scheme for the invasion rates $\alpha_1 = 0.2$, $\alpha_2 = 0.5$ and $\alpha_3 = 0.3$ at the point $x = 5.05$. The space step size is $\Delta x = 0.1$, while the time step size is $\Delta t = 0.1, 1.0, 3.0$ and 5.0 . It can be observed that as Δt is increased, the dynamics change from periodic orbits to quasi-periodic orbits and finally to a blow-up. 152

6.10 Numerical solutions of Eq. (6.72) using the IIF scheme for the invasion rates $\alpha_1 = 0.2$, $\alpha_2 = 0.5$ and $\alpha_3 = 0.3$ at the point $x = 5.05$. The space step size is $\Delta x = 0.1$, while the time step size is $\Delta t = 0.1, 3.5$ and 4.0 . It can be observed that the dynamics are similar for all Δt for which the scheme is stable. For $\Delta t = 4.0$, there is a blow-up of the finite difference solution and the scheme becomes unstable. 153

6.11 Numerical solutions of Eq. (6.72) using the IMEX scheme for the invasion rates $\alpha_1 = 0.2$, $\alpha_2 = 0.5$ and $\alpha_3 = 0.3$ at the point $x = 5.05$. The space step size is $\Delta x = 0.1$, while the time step size is $\Delta t = 0.02, 0.1, 1.0$ and 2.2 . It can be observed that as Δt is increased, the dynamics change from periodic orbits to quasi-periodic orbits and finally to a blow-up. 154

List of Tables

4.1 A summary of the results obtained from applying the method of triads to all non-isomorphic tournaments composed of five to nine species. Here, FSR denotes final species richness, while FSC denotes final species composition.	94
---------------------------------------------------------------------------------------------------------------------------------------------------------------------------------------------------------------------------------------------	----

1

Introduction

1.1 Overview

The coexistence of species which interact competitively has long interested ecologists and the question of what permits so many competitors to coexist in some communities remains an open question (Tilman, 1982; Chesson, 2000). The mystery of species coexistence is rooted in the *competitive-exclusion principle*, which states that two species competing for the same resource cannot coexist (Hardin, 1960; Armstrong and McGehee, 1980). The species that is better at gaining the limiting resource will eventually eliminate the inferior competitor. However, the central prediction of the competitive exclusion principle, the elimination of all but the best competitor, lies in sharp contrast with what is observed in nature. Many habitats harbor a considerable diversity of species, the most obvious among these being the *paradox of the plankton* (Hutchinson, 1961) where a number of the phytoplankton species are able to coexist in a relatively homogeneous or unstructured environment (the open ocean), all competing for the same sorts of resources. This contrast poses an enigma.

1

Coexistence has been so coupled with the concept of competition that it may be aptly defined as the absence of competitive exclusion (Aarssen, 1983). Thus, to resolve the enigma of coexistence, efforts have been geared towards establishing what factors or mechanisms prevent competitive exclusion of one species by another in a resource-limited environment. In this regard, two somewhat opposing explanatory frameworks have been proposed; the *niche* and *neutral* theories of coexistence.

The classical niche theory of coexistence, which is the oldest explanation for species coexistence, states that only those species differing sufficiently in resource use can coexist. In other words, two (or more) species cannot coexist in the same *ecological niche* (Gause, 1934). A species' ecological niche has been defined by the resources and conditions it requires to survive and reproduce (Grinnell, 1917). Hutchinson (1957) expanded on this definition of niche by disaggregating the habitat into the multiple resources it embodied. The physical space a species occupies, the temperature and moisture conditions of the space, and the seasonality in abiotic and biotic conditions that the space experiences, along with the food requirements and the interactions that a species engages in with other species are considered. In this case, a species' ecological niche can be viewed as a multidimensional space or hypervolume, in which each resource represents an independent axis. The space that each species occupies within this hypervolume is defined by its basic resource requirements (i.e., the *fundamental niche*) and is winnowed down by antagonistic interactions with other organisms (i.e., the *realized niche*) (Moore, 2013).

From the classical niche theory, each species is adapted to exploit a unique ecological niche through partitioning of resources and the very coexistence of species is only possible because their niches are different. If niche differentiation is not achieved, competitive exclusion will eventually happen. The three conditions necessary for competitive exclusion to proceed are (Aarssen, 1989);

- demands on resources sufficiently exceed supply,
- species do not make demands on sufficiently different resource units, and
- the species differ sufficiently in competitive ability.

The niche differentiation theory is, however, jeopardized by the fact that only few studies have been able to successfully quantify the importance of niche differences in maintaining the diversity observed in nature (Adler et al., 2007). It has also been argued that the coexistence of plant species may not necessarily be a result of niche differentiation, but rather the degree of *niche overlap* (i.e., similarity between species in the use of a particular set of resources) (Kim and Ohr, 2020; Shmida and Ellner, 1984; Mahdi et al., 1989). Higher plants are relatively immobile, lack any real choice in energy supply, and generally make demands on

essentially the same resources. It is thus difficult to imagine how there could not be considerable niche overlap and enormous opportunity for competition in many plant communities (Aarssen, 1983). Thus, whether niche differentiation is needed for coexistence of plants is itself open to question.

Hubbell's (2001) neutral theory directly challenged the niche paradigm by proposing that species similarities with regard to fitness, and not niche differences, explain the high diversity of many natural communities. That is, species are able to coexist or evade competitive exclusion only if these species are *ecologically equivalent* in the sense that, they are equally able to survive, reproduce, disperse and even evolve (to give rise to new species). This coexistence is not maintained by the ability of species to compete more effectively when rare, but by three processes: ecological drift (i.e., changes in species population size due to random births and deaths), dispersal and speciation. Hubbell showed that neutral models describe the abundance patterns of trees in tropical rain forests especially well. However, despite the fact that this theory has provided good fits to empirical data, it has also met resistance from many ecologists who feel that the equivalence assumption is unrealistic and violates the deeply held belief that all species are fundamentally different.

The above two theoretical frameworks, however, seem insufficient to account for all the diversity observed in many natural communities. This is because both mechanisms focus on the reduction of competitive exclusion and yet, such reduction may not be required for species coexistence (Soliveres et al., 2015).

A number of empirical and theoretical studies suggest that *intransitive competition* (or a lack of competition hierarchy) is an important mechanism that allows species to coexist within a single community even if they compete strongly (Gilpin, 1975; Laird and Schamp, 2006; Allesina and Levine, 2011; Gallien et al., 2017). This lack of competition hierarchy can emerge when, for example, species' competitive abilities differ across resources, or across species life stages (Gallien, 2017).

Alternatively, intransitivity in the competitive interactions among species can also occur if the hierarchy in species' ability to exploit resources differs from their ability to prevent resource uptake by others (Laird and Schamp, 2006). This leads to the generation of cycles in the hierarchy of competitive strength, just as in the game of rock-paper-scissors (RPS). This mechanism is stabilizing because decreasing the abundance of any competitor in the cycle propagates through the network in a way that feeds back to favour the recovery of the perturbed species.

The presence of cycles also means that, although species differ considerably in their competitive abilities, no single competing species is superior to any other at the level of the community. In other words, intransitive competition constitutes some form of "competitive equivalence" of species, which results into an equal probability of survival, reproduction and distribution within the habitat, as all participants of interactions control the abundance of each other (Permogorskiy, 2015).

1 This could allow species to coexist even without niche differences.

For any species-rich ecosystem composed of strongly competitive species, it is likely that intransitive cycles will exist (Vandermeer, 2011). Many theoretical studies have explored how such intransitive cycles benefit diversity maintenance (Laird and Schamp, 2006; Allesina and Levine, 2011), although direct empirical support for this coexistence mechanism is generally sparse. However, Kerr et al. (2002) showed that intransitive interactions occur between engineered strains of the bacterium *Escherichia coli*, whereas Sinervo and Lively (1996) demonstrated that these interactions exist between individuals with different mating strategies in a population of lizards. Although these interactions actually occur within a species (intraspecific), rather than between species (interspecific), the best species-level evidence for intransitive competition comes from patterns of colony overgrowth in marine sessile organisms (Buss and Jackson, 1979).

Mathematical models have been used to provide insights into the underlying mechanisms and ecological implications of intransitive cycles within a competition network (Laird and Schamp, 2006). One key result from modelling studies is that intransitive competition cycles formed by an odd number of species will stabilize coexistence, whereas cycles containing an even number of species are inherently unstable, with an odd number of species among the even surviving while the rest are excluded (Allesina and Levine, 2011; Vandermeer, 2011).

However, modelling studies have, so far, been unable to predict the prevalence of intransitive competition in nature, or how many species in natural communities are maintained by it (Soliveres et al., 2015; Godoy et al., 2017; Soliveres et al., 2018; Saiz et al., 2019). This could be due to the difficulty in observing and measuring intransitivity in the field, or due to the fact that broad theories on the subject are still lacking. Thus, the role of intransitive competition in maintaining diversity in real-world ecosystems remains unclear despite decades of research devoted to answering this question.

Within intransitive competition networks, one core aim of many community ecologists is the prediction of community structure at equilibrium, which is essentially the final species composition, including the number of species (species richness) and their relative abundances. However, till now, predictions on even the simplest community aspects like equilibrium species richness remains a challenge. This is because ecological communities can be highly diverse with very many species interacting in a complex network. Thus it is challenging to study how communities evolve.

On the one hand, some studies have suggested that predictions on community structure could be possible if ecologists are able to accumulate a sufficiently inclusive worldwide data set of species traits (Grime, 2006; McGill et al., 2006). But collecting enough data on the relevant traits of species sufficient enough to make prediction possible is not only difficult but also expensive in practice. Moreover,

because competitive outcomes may depend on various environmental conditions, unless one can accurately predict future environmental conditions or declare competition to be utterly unimportant in structuring communities, it seems unlikely that community structure can be predicted from a database of species traits (Koide et al., 2011).

On the other hand, other studies have suggested that predictions on community structure will require the development of metrics that explore the ranking of species involved in intransitive structures, not just aspects of their presence, absence or frequency (Laird and Schamp, 2018b).

Generating and making predictions on community composition (species richness and abundance) at equilibrium from intransitive competition networks, has led ecologists to turn to tools, concepts and results developed outside ecology, such as graph (or network) theory, game theory and chemical reaction network theory, among others, and these have proven to be extremely useful in providing insights into a number of ecological questions.

For example, game theory provides a mathematical framework in which competitive interactions among species can be treated as a game with multiple players. Using this framework, ecologists are able to elucidate evolutionary consequences of interactions, such as fitness payoffs and the proportions of strategies (phenotypes) played by each group within a population.

On the other hand, when ecological communities are represented by interaction networks, graph theory provides a robust and well-formalized framework to characterize the complexity of such networks. For example, it has provided indices that have enabled ecologists to quantify not only the degree, but also the architecture of ecological complexity.

Furthermore, in the absence of dispersal, the dynamics of ecological competition networks are often modelled by systems of ordinary differential equations (ODEs). Chemical reaction network theory (CRNT) provides a mathematical framework within which the qualitative dynamics of such ODE model systems can be linked to the structure of the interaction network.

Finally, combining intransitive competition with already established explanations for community diversity, such as the existence of a global metapopulation, in which all species coexist and from which local communities (habitat patches) are assembled by dispersal processes, could provide insights into the coexistence mechanisms of spatially structured environments.

The competition-dispersal (or competition-colonization) trade-off has long been regarded as one possible mechanism enabling coexistence, where species with inferior competitive ability can compensate by migrating more frequently, and over long distances, hence adopting the name *fugitive species*, whereas superior competitors dominate within patches, fugitive species gain an edge through the discovery and early colonization of fresh resource patches.

1

Classic metapopulation models based on the competition-dispersal tradeoff go back to Levins and Culver (1971) who demonstrated that two species can coexist in a metapopulation if one species is a superior competitor and the other species is a superior disperser. This was also confirmed by Tilman (1994) whose multi-species model predicts that an unlimited number of species competing for a single resource can coexist in a spatially subdivided habitat, given that the inferior competitors have sufficiently higher dispersal abilities than the superior competitors.

Furthermore, assuming intransitivity in the competitive interactions within the habitat patches creates some form of competitive equivalence among the species (Laird and Schamp, 2006), and could therefore provide insights into the effects of dispersal on coexistence when differences in competitive abilities among species are neutralized. Numerical simulations by Nagatani et al. (2018) have already shown that, for cyclic interactions within a patch, metapopulation dynamics are significantly different when the dispersal network is *homogeneous* compared to when the dispersal network is *heterogeneous*.

Finally, classic metapopulation models treat the environment as a discrete collection of habitat patches, and thus have model equations in the form of a system of ODEs. However, in some cases, like for many aquatic systems, the environment is viewed as a continuum and metapopulation models of such systems can only be constructed for very finely reticulated subdivisions of the continuum. For analysis of such situations, it is generally more convenient to pass to the limit and replace the discrete patch ODE system by a system of partial differential equations (PDEs).

ODEs also provide an insufficient description when continuous aspects of geometry are important or the well-mixed assumption is obviously at odds with the nature of the ecological system at hand (Daun et al., 2008). In such cases, again, PDEs (or reaction-diffusion equations) provide an appropriate framework to model such systems.

PDEs are advantageous over ODEs because they allow modellers to incorporate both temporal and spatial processes simultaneously into equations governing population dynamics. In addition, they have been used to lend insight into numerous fundamental population processes including dispersal, ecological invasions, the effect of habitat geometry and size, dispersal mediated coexistence, and the emergence of spatial patterns (Holmes et al., 1994).

Unfortunately, since the PDE model equations are often nonlinear, closed-form analytical expressions of their solutions can be found only in very special circumstances, and these are mostly of limited theoretical and practical interest. Thus scientists have naturally been led to seek numerical techniques for the approximation of solutions. However, their numerical computations are more demanding than those of ODEs, and may, in some situations, require a larger computing platform than personal computers.

The most powerful and generally applicable algorithms for the approximate solu-

tion of PDEs rely on the concept of *discretization*, whereby the PDE under consideration is replaced by equations that involve a finite number of unknowns. There are several different ways to discretize a PDE. The simplest method uses finite difference approximations for the partial derivatives in the PDE. This gives rise to a large algebraic system of equations to be solved in place of the PDE, something that is easily solved on a computer. Mathematical theory may be useful in selecting appropriate numerical simulation methods and may facilitate accuracy and efficiency of simulations.

However, a number of mathematical challenges arise when using a finite difference method to solve the underlying PDE, top among these is the problem of *numerical stability*. A given finite difference method is unstable if the small differences between the original PDE and its discretized version to be implemented on a computer lead to significant changes in the numerical solution over time with respect to the exact solution. Stability of a numerical method is a fundamental property that is necessary for the method to produce a valid solution. A standard tool for establishing the stability of a finite difference scheme is the von Neumann stability analysis.

1.2 Research questions

In this thesis, we shall bring together different mathematical tools and concepts borrowed from the fields of numerical analysis, graph theory, game theory, chemical reaction network theory, and the theory of dynamical systems to explore a number of questions related to the dynamics of ecological communities under intransitive competition and the numerical stability of finite difference schemes used for solving PDEs in ecology.

More specifically, in this thesis, we will explore how network structure (or topology) can be used to provide insights as to why some species persist while others go extinct, and provide solutions to one of community ecology's central aims, the prediction of community structure at equilibrium. Then, we shall explore the role of dispersal or migration in the dynamics of populations living in spatially discrete habitats (patches). Finally, we will explore the mathematical problem of analyzing the stability of some of the popular finite difference schemes that have been used in the literature for the solution of reaction-diffusion equations. Such equations appear in the literature as models that govern the dynamics of populations living in spatial habitats that are viewed as a continuum, such as in aquatic systems. Since these equations have no known analytical solutions, their solutions can only be obtained via numerical methods, in particular, finite difference methods, whose stability properties are not well known, especially when applied to reaction-diffusion systems.

1 For this purpose, we formulate several research questions to guide our investigations, which will be elaborated and motivated in subsequent chapters:

1. How does community structure emerge from a directed graph?
2. What properties of intransitive networks promote species richness?
3. To what extent are single-patch dynamics within a metapopulation affected by migration?
4. Do the well-known stability properties of finite difference schemes that have been derived on the linear diffusion equation extend to the full reaction-diffusion system?

These research questions will be studied through the use of both mathematical analysis and simulations.

1.3 Scope of the thesis

In Chapter 2, we introduce in detail the important ecological concepts and tools relevant to the later chapters of this thesis. We start by introducing the concept of an ecological community, and the common measures used to distinguish ecological communities. We then introduce the graphical (or network) representation of an ecological community. This allows us to introduce the notion of intransitive competition, which is the main focus of our work, and the measures of intransitivity. Finally we introduce the concept of kings/non-kings in a network, an important concept that we use in Chapter 5 to justify the competitive exclusion of some species.

In Chapter 3, we review the mathematical modelling approaches suitable for intransitive competition dynamics. We start by discussing non-spatial model formulations which take the form of ODEs and aspects of their dynamic behavior, particularly, the stability of equilibrium points. Then we introduce relevant concepts from game theory and chemical reaction network theory. We then introduce spatial models ranging from discrete metapopulation models to continuous reaction-diffusion equations. Finally, we discuss some popular numerical methods, in particular, finite difference schemes, used for the numerical solution of reaction-diffusion equations. We end the chapter with an introduction of the von Neumann stability analysis, which will provide a basis for the mathematical problem of numerical stability that is discussed in Chapter 6.

In Chapter 4, we intend to answer our first two research questions where we try to explore how community structure emerges from a complete directed graph (or tournament). To do this, we make use of the intransitive triads in the tournament

together with the concept of kings/non-kings in the tournament. By first eliminating all the non-kings and reducing the tournament to an all-kings tournament, we are then able to use the interactions among the intransitive triads to deduce the final species richness and/or composition even without the need for numerical simulations of their mean-field ODE models.

Our third research question is answered in Chapter 5, where we make use of concepts and methods from dynamical systems theory, graph theory and chemical reaction network theory, particularly the concept of detailed balancing, to explore the effects of dispersal or migration on the dynamics of a metapopulation that is composed of several subpopulations spread among distinct habitat patches. This chapter also provides a mathematical proof to some established numerical results in the literature and thus broadens the application of such results.

The final research question of this thesis is answered in Chapter 6, where we explore a well-known mathematical problem of numerical stability. Here, we perform a von Neumann stability analysis of some popular finite difference schemes that have been used for the numerical solution of reaction-diffusion equations in ecology. Stability results in the literature have been derived based on the analysis of a system of linear diffusion equations. It is not clear whether these existing stability conditions would still hold if the same schemes are applied to the full reaction-diffusion equations which are usually encountered in practice. The aim of this chapter is to shed light on this existing mathematical problem.

Finally, in Chapter 7, we present a summary of the main results of this thesis as well as their conclusions. We also outline possible future research directions.

2

2

Ecological Background

2.1 Introduction to ecological communities

2.1.1 What is a community?

An *ecological community* is an assemblage of interactions among species populations occurring together in space and time (Begon et al., 2006). Community ecology is the study of the interactions among populations of coexisting species. One important goal of community ecology is to explain the underlying mechanisms that create, maintain, and determine the fate of ecological communities.

Ecological communities can be highly diverse with many species interacting in a complex ecological network. It is challenging to study how entire communities evolve. Consequently, community ecologists work with restricted groups of organisms, focusing on readily-identified sets of species that are ecologically or taxonomically similar. For example, attention could be restricted to groups of species that are all engaged in some similar ecological function, also known as *functional*

groups, or on the feeding interactions among species, leading to what is known as a *food web*, i.e., a group of species linked by such interactions, thus describing the paths by which biomass flows through the community. A customarily used subset of a food-web is the notion of *trophic level*, which typically describes a subset of a community with similar feeding habits (Bersier, 2007), e.g., herbivores. By studying these restrictions, ecologists focus their efforts on a manageable and coherent portion of the community, manageable in terms of number of species and coherent in terms of ecological requirements.

2.1.2 Community properties

The potentially bewildering complexity of ecological communities has motivated ecologists to use various descriptors to condense and summarize information about the number, identity and relative abundance of species. It should however be noted that, although no single magic number, index or graph can provide a complete description of a community, some of these measures provide a useful way of comparing different communities.

Species richness: One way to characterize a community is to count or list the number of species that are present. The total number of species present in a community, often called species richness, is synonymous with our basic notion of biodiversity. The richness of a community is often calculated based on the number of species observed in repeated random samples of a given number of individuals, or on the volume of the habitat that has been explored (Begon et al., 2006). The most common species are likely to be represented in the first few samples, and as more samples are taken, rarer species will be added to the list. To decide whether enough sampling effort has been made, the investigator should continue to sample until the graph of the cumulative number of species versus the amount of sampling effort reaches an asymptotic value. That asymptotic value provides a reasonable estimate of the number of species present (Chao and Chiu, 2016).

Species evenness: Another basic feature of ecological communities is the distribution of relative abundances of the various species in a community. There are many aspects of this distribution that can be measured, but the simplest feature is species evenness (Smith and Wilson, 1996). Evenness (equitability) represents the degree to which individuals are split among species with low values indicating that one or a few species dominate, and high values indicating that relatively equal numbers of individuals belong to each species.

Species diversity: A combination of the number of species (richness) and their relative abundance (evenness) defines species diversity, which is a measure of what is frequently referred to as *community structure*. Several diversity

indices have been developed that mathematically combine the effects of richness and evenness. Such indices provide important information about the rarity and commonness of species in a community. The two most popular diversity indices are *Simpson's diversity index* (Simpson, 1949), and *Shannon's diversity index* (Shannon, 1948). Both indices are calculated based on the relative abundance of species.

2.1.3 Interspecific competition

Community ecologists seek to understand what drives the patterns of species co-existence, diversity and distribution that is observed in nature. A core part of how they address these questions is by examining how different species in a community interact with each other.

Species interactions represent the effects that individuals in a community have on each other. These interactions can be defined as either *intraspecific* or *interspecific*. Intraspecific interactions are those that occur between individuals of the same species while interactions that occur between two or more species are called interspecific interactions.

Interspecific interactions have long been considered to be among the key mechanisms that can influence species abundances and community composition and thus govern the structure and dynamics of ecological communities. Organisms live in a complex web of interspecific interactions, affecting one another via competition, predation, and mutualism, among various other forms of interactions.

Among the interspecific interactions, competition is probably the most frequently inferred interaction in community ecology and has received, by far, the most theoretical and empirical attention. Competition is most typically considered the interaction of individuals that vie for a common resource that is in limited supply, but more generally can be defined as the direct or indirect interaction of organisms that leads to a change in fitness (or reproductive success) when the organisms share the same resource.

Theoretically, interspecific competition for finite resources has been viewed as asymmetric (i.e., in terms of a winner and a loser) with the dominating species gaining more resources and eliminating the subordinate from the habitat or segregating them to less favorable sites. This view was first fostered by the *competitive exclusion principle* (Hardin, 1960) which states that if two or more species compete for the same limiting resource, then all but one of them will be driven to extinction.

Interspecific competition can be categorized to be of two types, interference competition and exploitative competition (Miller, 1967). Interference competition refers to any activity which either directly or indirectly limits a competitor's access

to a necessary resource such as a niche, defended space or particular habitat. For example, competition among sessile animals has been found to involve direct physical aggression: one species of barnacle outcompeted another for attachment space by undercutting or even crushing other competitors. Some animals show more formalized aggressive behaviours, with greater emphasis on display and correspondingly less on physical contact (Shigesada et al., 1984).

Exploitative competition, on the other hand, is the indirect interaction among species arising from the joint exploitation of a limited resource. Simply put, the use of the resource by one individual will decrease the amount available for other individuals. As an extreme example, one species may feed on a plant during the day, and another species may feed on the same plant during the night. Each species diminishes the resource for the other, but there is no direct contact or conflict (Jensen, 1987). Whether by interference or exploitation, over time a superior competitor can eliminate an inferior one from the area, resulting in competitive exclusion (Hardin, 1960). Therefore the distribution and structure of ecological communities can be theoretically affected by both exploitative and interference competition.

2.2 Ecological communities as complex networks

2.2.1 Introduction

Networks provide one of the best representations for ecological communities, composed of many species with dense connections between them. Network-based approaches to ecological questions have been increasingly used, particularly in recent decades, because they offer the opportunity to investigate, within a common formal mathematical framework, questions ranging from the species level to the community level (Delmas et al., 2019). This methodological framework derived from graph theory has provided ecologists with the tools needed to observe and quantify the structure of ecological communities in ways that simply were not available previously.

Network concepts, tools and techniques have a long history of use in ecology. The first attempt to represent the trophic interactions in a community as a network was made by the Italian scientist Lorenzo Camerano in 1880 (Bersier, 2007). Earlier verbal descriptions of food webs existed, but Camerano was apparently the first to provide a graphic representation of the connections of groups of species in a natural community (Cohen, 1994). Three decades later, Pierce et al. (1912) attempted to describe the predatory and parasitic interactions of the boll weevil as a network of interactions. Shortly thereafter, Summerhayes and Elton (1923) analyzed

in some detail the trophic interactions among the species inhabiting Bear Island, concluding that animal communities could be best described in terms of the food relations between species. They seized the opportunity presented by the relatively small number of species on Bear Island to present a graphic representation of the feeding relationships linking all animal species. These three pioneering works all recognized the importance of the diagrammatic approach, specifically treating the community as a network, in studying the interactions between species in order to understand the organization and dynamics of communities.

Today, the network-oriented approach permeates almost all areas in ecology and evolution and is one of the fastest growing ecological disciplines (Delmas et al., 2019). For example, scientists have used network models to investigate communities of mutualistic species (Bascompte and Jordano, 2007), general properties of ecosystems (Higashi and Burns, 1991), competitive interactions (Allesina and Levine, 2011) and the movement of genes and organisms across landscapes (Urban and Keitt, 2001; Holland and Hastings, 2008; Jacoby et al., 2012).

2.2.2 Graphs and graph theory

In recent years, graph theory (also called network theory) has established itself as one of the most useful tools that ecologists have used to study ecological networks (Proulx et al., 2005; Bunn et al., 2000). Urban and Keitt (2001) give a general description of ecological applications of graph theory. However, this section describes the graph theory concepts and terms that will be used in this thesis.

2.2.2.1 Definitions

In general, networks or graphs are used to capture relationships between entities or objects. By definition, a graph G is a mathematical object consisting of two sets: vertices (nodes/points) V and edges (links/arcs/lines) E that represent functional connections between pairs of vertices. We sometimes write $G(V, E)$ instead of G . A *subgraph* of G is a graph whose vertex and edge set are subsets of the vertex and edge set of G . We write $|V|$ to denote the number of vertices in G , and $|E|$ to denote the number of edges in G .

In ecology, individuals, populations and habitats are the main objects of interest, and thus act as the vertices to the graph, with behaviour and dispersal as the main processes that link them (Dale and Fortin, 2010). For example, a food web can be represented as a graph with species as nodes and their feeding relationships as edges. Similarly, the spatial dynamics of a metapopulation can be analyzed by connecting the patches (nodes) of suitable habitat with edges measuring dispersal between patches. We usually represent a graph pictorially (Fig. 2.1).

We say that two vertices v_i and v_j of G are *adjacent* if there is an edge $e = v_i v_j$ joining them, and the vertices v_i and v_j are then said to be *incident* with such an edge. Similarly, two distinct edges e and f are adjacent if they have a vertex in common. The graph is called *undirected* (or symmetric) when all the edges are bidirectional, meaning every edge from vertex v_i to vertex v_j is also an edge from vertex v_j to vertex v_i . It is called *directed* (or *digraph*) when every edge is assigned a direction. This is usually indicated with an arrow on the edge. In ecology, the edges in a directed graph could indicate the direction of biomass transfer (e.g., from competitive subordinate to dominant) (Otto and Day, 2007) or the direction of migration.

In addition, the edges can be *unweighted* or *weighted* leading to an unweighted or weighted graph, respectively. Weights can represent a variety of ecologically relevant quantities, depending on the system being described. For example, edge weights can quantify interaction frequency, interaction strength (e.g., per-capita effect of one species on the growth rate of another), carbon flow between trophic levels, dispersal probabilities (e.g., the rate at which individuals of a population move between patches), etc.

In a digraph G , the *in-degree* of a vertex v , denoted $\deg^-(v)$, is the number of edges coming into it. The *out-degree* of v , denoted $\deg^+(v)$, is the number of edges going out of it. The *degree* of v , denoted $\deg(v)$ is the sum of the in-degree and out-degree.

2.2.2.2 Matrix representations

Although it is convenient to represent a graph by a diagram of points joined by lines or arrows, such a representation may be unsuitable if we wish to store a large graph in a computer. One useful representation involves matrices. If G is a graph with vertices labelled $\{1, 2, \dots, n\}$, its *adjacency matrix* \mathbf{A} is the $n \times n$ matrix whose ij -entry (entry in the i -th row and j -th column) a_{ij} depends on whether the graph is weighted or unweighted. In unweighted graphs, $a_{ij} = 1$ if there exists an edge from vertex j to vertex i , otherwise $a_{ij} = 0$. (As a cautionary remark, the adjacency matrix obtained using the above definition is the transpose of what is commonly defined as the adjacency matrix). In weighted graphs, the edge weight is given instead of being set to unity. Adjacency matrices are symmetric for undirected graphs but not for digraphs. In ecology, edge weights denote the strength of the interaction between two ecological entities (individuals, populations or habitats). This strength is not necessarily between 0 and 1; if the strength of interactions depicts the raw effect of one population on another, then it can take both negative and positive values (Delmas et al., 2019) (see Fig. 2.1).

Another important matrix representation of a graph is the *incidence matrix*. The incidence matrix of G is a $|V| \times |E|$ matrix \mathbf{B} , whose ij -entry $b_{ij} = 0$ if vertex i

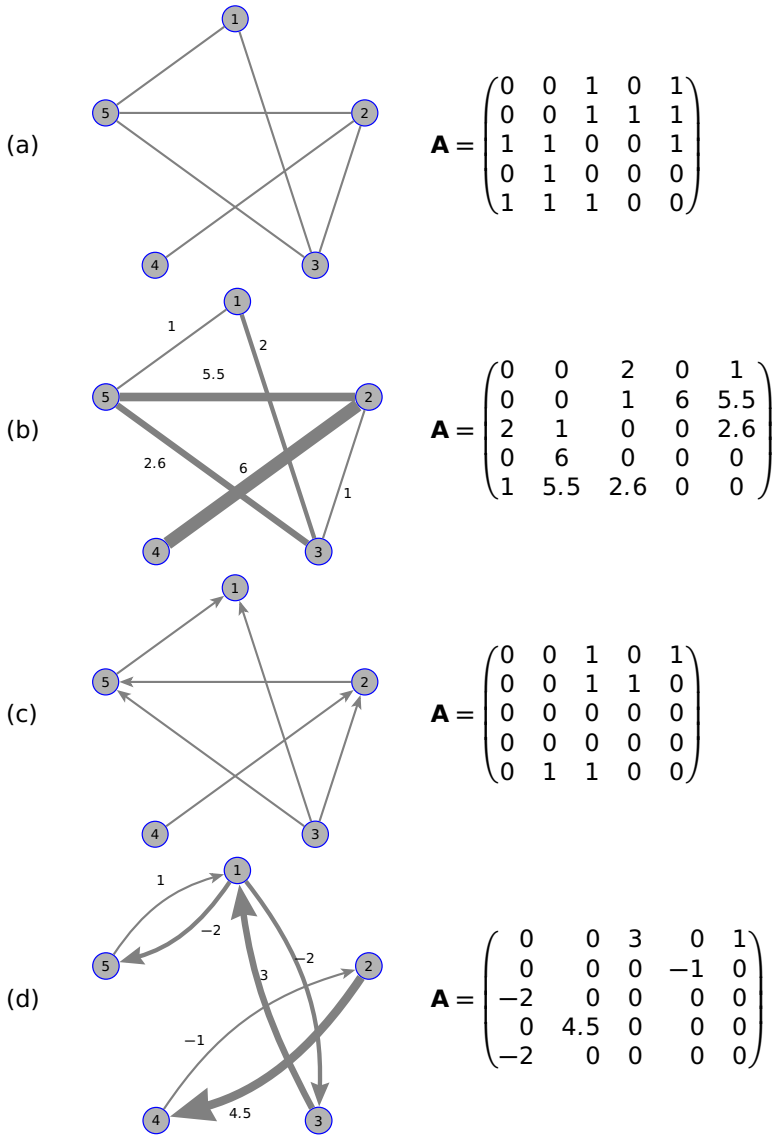


Figure 2.1: Categorization of graphs: (a) unweighted undirected; (b) weighted undirected; (c) unweighted directed; (d) weighted directed. On the right are the corresponding adjacency matrices for the given networks. Arrow thickness in graphs (b) and (d) represents the strength of the link/interaction.

and edge j are not incident, otherwise $b_{ij} = 1$ or -1 if edge j originates from, or terminates at, vertex i , respectively. Thus the sum of entries in each column of \mathbf{B} is zero. Equivalently, this can be written as $\mathbb{1}^T \mathbf{B} = 0$, where $\mathbb{1} \in \mathbb{R}^n$ denotes the n -dimensional vector with all entries equal to 1.

2.2.2.3 Paths, cycles and connectivity

Many applications of graphs involve ‘getting from one vertex to the other’. For example, you may wish to find the shortest route between two habitat patches or to identify vertices of high importance, such as keystone species in a food web, and patches acting as stepping stones in a dispersal network (Costa et al., 2019). The interaction between vertices can be thought of as a flow of information between the vertices that are linked by edges. The following definitions describe ways of going from one vertex to another.

Given a graph G , a *walk* in G is a finite sequence of edges of the form $v_0v_1, v_1v_2, \dots, v_{m-1}v_m$ also denoted by $v_0 \rightarrow v_1 \rightarrow v_2 \rightarrow \dots \rightarrow v_m$ in which any two consecutive edges are adjacent. Such a walk determines a sequence of vertices v_0, v_1, \dots, v_m . We call v_0 the *initial vertex* and v_m the *final vertex* of the walk, and speak of a *walk from v_0 to v_m* . The number of edges in a walk is called its *length*. Note that we do not require all the edges or vertices in a walk to be different.

It is sometimes useful to be able to refer to a walk under more restrictive conditions in which we require all the edges, or all the vertices, to be different. A *path* in G is a walk from v_0 to v_m such that each vertex is unique (i.e., no vertex is visited more than once, except possibly, $v_0 = v_m$). This implies that the edges of a path are also unique. A closed path (i.e., one in which $v_0 = v_m$) is called a *cycle*.

We can use the concept of a path to define a *connected graph*. A graph G is said to be (*strongly*) *connected* if, for every pair of vertices v_i, v_j in G , there exists a (directed) path from v_i to v_j , and is *disconnected or unconnected* otherwise. Every disconnected graph can be split up into a number of (strongly) connected subgraphs, called (*strongly*) *connected components* (Aldous and Wilson, 2003). For any graph G with n vertices and incidence matrix \mathbf{B} , it holds that $\text{rank } \mathbf{B} = n - \ell$, where ℓ is the number of (strongly) connected components of the graph. In particular, G is connected if and only if $\ker \mathbf{B}^T = \text{span } \mathbf{1}$.

We complete this section by describing one important type of graph known as a *complete graph*. A complete graph is a graph in which each vertex is adjacent to every other vertex in the graph. Thus, a complete graph with n vertices has $n(n-1)/2$ edges. For ecological applications, focus is often on directed graphs as many ecological processes are oriented. In this regard, we talk about complete directed graphs, also known as *tournaments* (See Fig. 2.2). Such a digraph can be used to, for example, represent interspecific competition within a community where each species is assumed to compete with every other species and these pairwise competitive interactions are asymmetric characterized with one consistently dominant species and one consistently subordinate species.

Tournaments form perhaps the most widely studied class of directed graphs, and much is known about them (e.g., see (Moon, 1968))

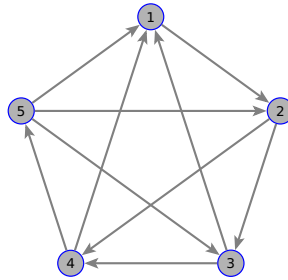


Figure 2.2: A complete digraph (tournament)

2.3 Intransitive competition

Ecologists have traditionally focused on competition as the main force structuring ecological communities. Thus our primary understanding of the preservation of species diversity both empirically and theoretically has been achieved mainly through the study of pairwise competitive interactions (Chesson, 2000). Therefore, for the remainder of the main part of this thesis, we will focus explicitly on pairwise competitive interactions between species and the networks that arise from these interactions.

2.3.1 What is intransitive competition?

In theoretical studies on the effects of interspecific competition on community structure, it is usually assumed that each species competes with every other species in the community and that the pairwise competitive interactions among species are asymmetric and characterized by a consistent outcome, with one consistently dominant species and one consistently subordinate species (Muyinda et al., 2020).

In this regard, an ecological community of n species linked by competition can be represented as a tournament graph whose vertices are the species and whose directed edges point from the competitive subordinate to the competitive dominant, indicating the transfer of energy and matter; some conventions use the reverse. Equivalently, these competitive interactions can be captured in a square $n \times n$ adjacency matrix \mathbf{A} , whose rows and columns are labelled by the species in the community ordered in a similar way. The entries of \mathbf{A} are such that $a_{ij} = 1$ if species i dominates species j , otherwise $a_{ij} = 0$ (see Fig. 2.3).

In the simplest case, where all species in a system compete for a single limiting resource, their competitive abilities should be *transitive* (Allesina and Levine, 2011). That is, one species dominates all the other species in a group, a second

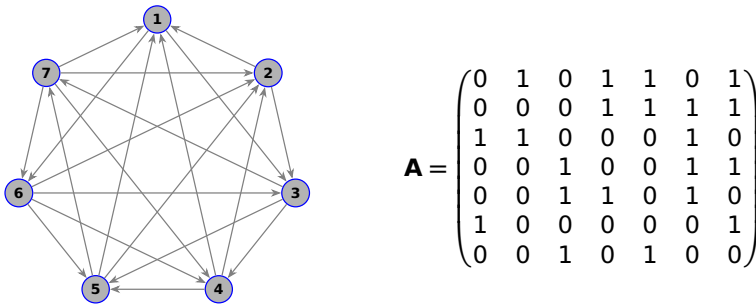


Figure 2.3: A 7-species tournament with corresponding adjacency matrix

dominates all but the first, and so on down to the last species which is dominated by all the others (Fig. 2.4 (a)). That is, for any three individuals (triad), if A dominates B and B dominates C , then A also dominates C . Transitive tournaments are consistent with a global ranking of all the competitors.

Transitivity is a common feature among many diverse taxa, including insects, fish, birds and mammals (LeBrun, 2005; French and Smith, 2005; Broom et al., 2009; Rushen, 1982; Stuble et al., 2017; Chase et al., 2002). However, transitivity associated with resources critical for a species' survival can undermine coexistence because, at equilibrium, the best competitor will drive all the others extinct (LeBrun, 2005).

By contrast, when species compete for several resources in which each competitor competes best for, yet is limited by, a different resource, then it may result in an *intransitive* tournament that is not consistent with any global ranking. Intransitivity is therefore characterized by the presence of at least one cycle within the network where the transitivity assumption fails. That is, A dominates B , B dominates C , but C dominates A . Such a three-species cycle, analogous to the classical rock-paper-scissors (RPS) game, is called an *intransitive triad* and the more intransitive triads there are in the tournament, the further the network is from transitivity (Fig. 2.4 (b)) (Chase et al., 2002).

These cyclic competitive interactions have been found to exist in a variety of real ecosystems including plant systems (Lankau et al., 2011; Taylor and Aarssen, 1990; Cameron et al., 2009), marine benthic systems (Buss and Jackson, 1979) and microbial populations (Kerr et al., 2002; Kirkup and Riley, 2004). Cyclic competition also plays a role in the mating strategy of side-blotched lizards (Sinervo and Lively, 1996), the overgrowth of marine sessile organisms (Burrows and Hawkins, 1998), competition between mutant strains of yeast (Paquin and Adams, 1983) and in explaining the oscillating frequency of lemming populations (Gilg et al., 2003). Figure 2.4 shows an example of both a transitive and intransitive competition network.

Because of the lack of irrefutable evidence that intransitivity is abundant in natu-

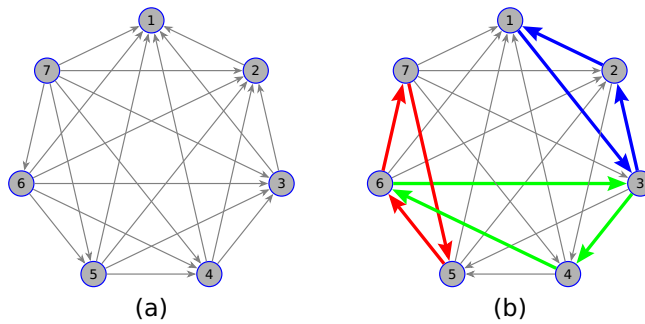


Figure 2.4: (a) A transitive 7-species tournament. (b) An intransitive tournament 7 with three of its nine intransitive triads highlighted.

ral systems, theoretical examinations of intransitivity have frequently focused on systems with few species. Theoretical models of intransitivity show clearly, for example, that hierarchies of three species quickly collapse to monocultures, while an intransitively competing triad of species can coexist indefinitely in many competition models (e.g., Gilpin (1975)). While fewer studies have considered more diverse systems, these have produced evidence that more intransitivity within a network of competing species (i.e., less hierarchical competition) results in more prolonged coexistence (e.g., Laird and Schamp (2006, 2018b)).

2.3.2 Measuring intransitivity

Intransitive competition was first explored theoretically by May and Leonard (1975) and Gilpin (1975), and since then, a few studies have tested for the occurrence of intransitive competition and its effects on coexistence, developing different indices to measure it. Such indices have shown that competition networks characterized by greater levels of intransitivity are more resistant to species extinctions, and are therefore more likely to display persistent species coexistence, than the more transitive communities (Laird and Schamp, 2006).

Several possible indices exist for measuring intransitivity and for otherwise describing the structure of competitive interactions. These indices, in general, roughly group into measures derived from matrix theory (e.g., relative variance) and measures derived from graph theory (e.g., number of cycles, out-degree statistics). The aim of each measure is to quantify in some way the degree to which a given network is not transitive. We now briefly discuss some of the known indices of intransitivity.

2.3.2.1 Slater's i

The Slater measure of intransitivity, denoted by i , is the minimum number of edge directions that need to be reversed in order to transform the tournament into a transitive network (Slater, 1961). Thus it is an intuitive way of measuring intransitivity. Low values of i correspond to more hierarchical systems, with $i=0$ corresponding to a transitive tournament. Conversely, high values of i correspond to more intransitively competing networks.

Slater's i was independently rediscovered and introduced to ecological literature by Petraitis (1979) who denoted it with s . All tournaments have a minimum value of $i=s=0$; however, the maximum value is positively related to the species richness (Laird and Schamp, 2018b). Petraitis referred to the upper bound of s as M (which is the maximum number of edge reversals across all possible n -species tournaments that are needed to transform any tournament into a transitive network) and used s and M to make a scaled index $t = 1 - s/M$, with transitive and maximally intransitive tournaments having values of $t = 1$ and $t = 0$, respectively.

A formula for computing M was given by Petraitis (1979):

$$M = \begin{cases} \frac{n^2 - 1}{8}, & \text{if } n \text{ is odd,} \\ \frac{n^2 - 2n}{8} + x, & \text{if } n \text{ is even,} \end{cases}$$

where

$$x = \begin{cases} 1, & \text{if } 6 \leq n \leq 10, \\ 2, & \text{if } 12 \leq n \leq 20, \\ 3, & \text{if } 22 \leq n \leq 30. \end{cases}$$

However, this formula has been recently established not to hold for some tournaments with $n \geq 7$ species (Laird and Schamp, 2018a). Nonetheless, there are other ways of estimating reversal-based indices, even if exact values cannot be computed (see, e.g., (Kenyon-Mathieu and Schudy, 2007)).

2.3.2.2 Kendall and Babington Smith's d

The Kendall measure (Kendall and Babington Smith, 1940) counts the number of intransitive triads among all $\binom{n}{3}$ triads in an n -species tournament. Thus, it has a very close intuitive link with intransitivity. Like in Slater's i , low values of d correspond to more hierarchical networks, with $d=0$ for a transitive tournament while higher values of d correspond to more intransitively competing networks.

The number of intransitive triads is calculated as follows (Bezembinder, 1981):

$$d = \binom{n}{3} - \frac{1}{2} \sum_{i=1}^n s_i(s_i - 1),$$

where s_i corresponds to the number of competitors that species i outcompetes (or the sum of the elements in row i of the adjacency matrix \mathbf{A}). Since the maximum value of d grows with n , a scaled index ζ is given by $\zeta = 1 - d/d_{\max}$, where $d_{\max} = (n^3 - n)/24$ for n odd and $d_{\max} = (n^3 - 4n)/24$ for n even (Kendall and Babington Smith, 1940).

Laird and Schamp (2006, 2008) independently developed two very similar indices, *relative variance* (RV) derived using variances of the *score sequence* (row sums of the adjacency matrix \mathbf{A} arranged in nondecreasing order) (Laird and Schamp, 2006) and *relative intransitivity* (RI) given by $RI = 1 - RV = d/d_{\max}$ (Laird and Schamp, 2008).

2.3.2.3 Laird and Schamp's unbeatability (u) and always-beatability (a)

Laird and Schamp (2018b) proposed two binary indices, *unbeatability* (u) and *always-beatability* (a), taking values of either 0 or 1. Unbeatability has a value $u=1$ when there is an "unbeatable" species that outcompetes every other species in the tournament, and a value of $u=0$ otherwise. Likewise, always-beatability has a value of $a=1$ when there is an "always-beatable" species that is outcompeted by every other species, and a value of $a=0$ otherwise. These two indices are inversely related to the intuitive understanding of intransitivity. A transitive tournament must have both values of u and a equal to 1, whereas intransitive networks do not necessarily have to. All tournaments with $u=1$ are expected to evolve to a monoculture of the unbeatable species, whereas for a tournament with $a=1$, the always-beatable species is expected to go extinct first.

2.4 Kings in a tournament

In his exposition on the use of tournaments to model dominance in flocks of chickens, Maurer (1980) defined a *king* in a tournament T as a species $i \in T$ such that for every other species $j \in T$, either species i dominates j , or there is a third species $k \in T$ such that i dominates k and k dominates j . This definition of kings in tournaments is due to the mathematical sociologist Landau (1953), who showed that any finite flock of chickens has a most dominant one, called a king. He associated with each tournament an ordered sequence of non-negative integers, its score sequence, formed by listing the vertex in-degrees in non-decreasing order, and

showed that every vertex of maximum score is a king. We refer to any species that is not a king as a *non-king* (see, e.g., Fig. 2.5).

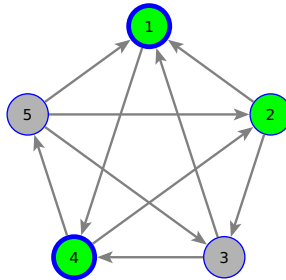


Figure 2.5: The kings correspond to the green nodes 1, 2 and 4, while species 3 and 5 are non-kings. Among the three kings, only 1 and 4 (with thicker borders) are strong kings.

In a bid to strengthen the capability of kings, Ho and Chang (2003) developed the notion of a *strong king* which represents a strong sense of dominance in tournaments. To define a strong king, denote by $b(i, j)$ the number of third species $k \in T$ through which species i dominates j indirectly. Then, a king i is said to be strong if $b(i, j) > b(j, i)$ for all species j that dominate species i . Obviously, it is not true that every king in a tournament is strong, e.g., among the three kings of the tournament shown in Fig. 2.5, only 1 and 4 are strong kings. Details on the characterization of strong kings can be found in Chen et al. (2008).

2.5 Conclusion

Despite interspecific differences in competitive ability, the high level of biodiversity present in ecological communities is a long-standing mystery in community ecology. Classical coexistence theories establish that each species inhabits a particular ecological niche, involving a given combination of abiotic and biotic factors, where it outcompetes the rest of the species in the local pool (i.e., niche theory). Under this premise, niche overlap penalizes worse competitors, which results in their competitive exclusion from a community, and supports that species coexist by being functionally different and by exploiting different niches. If true, then the species richness of a community depends on the total amount of niche space and the average size of each niche. Thus, wide niches should lead to a lower species richness than narrow ones for a given set of resources.

In contrast, neutral theory assumes that individuals and species are demographically and ecologically interchangeable and therefore equivalent in their competitive ability, i.e., none of the species shows an advantage or disadvantage over the others. According to the neutral theory, ecological drift, dispersal and speciation are the drivers of population dynamics and species coexistence. However,

each theory suffers from some shortcomings. Field evidence that classic resource-based niche differences are essential for coexistence is rare, whereas the species equivalence assumption of neutral theory is hard to reconcile with nature.

An alternative coexistence mechanism is a competitive intransitivity within the community. Theory has proposed that intransitive competition in complex ecological networks can enhance community persistence. This means that the competitive abilities of the species cannot be ordered in a strict hierarchy but instead form cycles of competitive dominance, such as in the rock-paper-scissors game. More and more empirical evidence of intransitive competition has been found in bacteria, phytoplankton, plants, vertebrate and invertebrate communities.

The use of network approaches to answer ecological questions has grown considerably in recent decades. The abstraction of ecological systems, such as communities, through networks of interactions between their components indeed provides a way to summarize this information with single objects. Concepts borrowed from graph theory, such as nodes, links, cycles, and connectivity are now commonly used in the analysis of food webs, ecological competition networks, plant-pollinator networks and predator-prey interactions. By combining the graph-theoretical framework with game theory and dynamical systems, ecologists can be able to determine the equilibrium abundance of all species from the competitive network, explore how species diversity relates to the number of limiting factors, and how spatial heterogeneity combines with intransitivity to interactively favor diversity preservation. Results from this can offer new perspectives on established ecological theories as well as tools to address new challenges. In the next chapter, we introduce the mathematical modelling frameworks commonly used in the study of ecological systems, together with game-theoretical concepts and methods.



3

Modelling Background

3.1 Introduction

The desire to formulate general rules in ecology often finds its expression in the construction of mathematical models (Begon et al., 2006). By definition, a mathematical model is a representation in mathematical terms of the behaviour or dynamics of a real object, which enables the study of the object without its experimental analysis (Dym, 2004).

Since models are attempts to represent some aspects of reality, any effort to include all aspects would overwhelm us with detail and would require a model as large as the original object (Olinick, 2014). Thus there is a large component of compromise in mathematical modelling. Almost all real ecological systems are too complicated to model in their entirety. Hence the first level of compromise is to identify the most important aspects of the system. These will be included in the model, the rest will be excluded. The second level of compromise concerns the level of mathematical manipulation that is worthwhile. Although mathematics has the potential to prove general results, these results depend critically on the

form of equations used. Small changes in the structure of equations may require enormous changes in the mathematical methods. Using computers to handle the model equations may never lead to elegant results, but it is much more robust against alterations.

Thus in constructing a mathematical model, scientists must keep in mind the type of information they wish to obtain from it. The simple schematic diagram of Fig. 3.1 illustrates the role that mathematical models play in science. Scientists begin

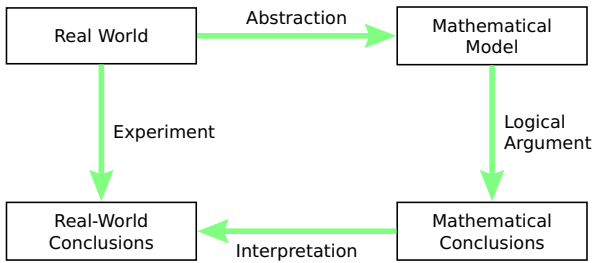


Figure 3.1: Schematic diagram of the modelling process

with some observations about the real object. They wish to make conclusions or predictions about the situation they have observed. One way to proceed is to conduct experiments and record the results. The model builder follows a different path. First, she abstracts, or translates, some of the essential features of the real world into a mathematical system. Then by logical argument, she derives some mathematical conclusions. These conclusions are then interpreted as predictions about the real object.

The real objects of ecological research are populations, communities and ecosystems. Conducting experiments on such objects is not possible, because it can lead to changes or even destruction of the ecological objects (Gertsev and Gertseva, 2004). In this situation it is clear that mathematical modelling plays a key role in ecological research.

To be useful, the mathematical model should make predictions about the real object that are expected to be actually observed when appropriate experiments are carried out. If the predictions from the model bear little resemblance to what actually occurs in the real world, then the model is not a good one. In that case, the modeler has not isolated the critical features of the situation being studied, or the axioms misrepresent the relations among these features. On the other hand, if there is good agreement between what is observed and what the model predicts, then there is some reason to believe that the mathematical model does indeed correctly capture important aspects of the real-world object.

What happens frequently is that some of the predictions of a mathematical model agree quite closely with observed events, but other predictions do not. In such

a case, we might modify the model so as to improve its accuracy. The incorrect predictions may suggest ways of rethinking the assumptions of the mathematical model. One hopes not only that the revised model will preserve the correct predictions of the original one, but also that it will make further correct predictions. The incorrect inferences of the revised model will lead, in turn, to yet another version, more sophisticated than the earlier one. Thus, by stages, we develop a sequence of models, each more accurate than the previous ones.

Mathematical modelling has played, and will continue to play, a crucial role in the development of ecology, particularly in our ability to predict outcomes. Models can be used to try to further our understanding of the fundamental mechanisms driving community patterns already observed and to make new predictions of how community dynamics should proceed under different conditions (Vellend, 2016).

Historically, mathematical modelling and its applications can be traced back to ancient civilizations as an attempt to understand and analyze the world around them. The great Belgian mathematician and ecologist Pierre-François Verhulst in 1838 developed the logistic equation to describe the self-limiting growth of populations, which included terms for intrinsic growth rate and a carrying capacity (Bacaër, 2011).

In 1910, Alfred Lotka developed a set of differential equations, heavily influenced by the logistic equation, to model the oscillating dynamics of two reacting chemical species, in which a product formed by the reaction is also one of the starting species, creating a self-sustaining feedback loop (*autocatalysis*) (Lotka, 1910). A decade later, it occurred to him to apply the same mathematics to living populations of predator-prey (or herbivore-plant) dynamics Lotka (1925). Concurrently, Vito Volterra independently developed a similar predator-prey model to explain his son-in-law's observations of fish predators in the Adriatic Sea (Volterra, 1927).

The so-called Lotka-Volterra equations (LV equations) demonstrate the inherent tendency of predator-prey populations to oscillate, e.g., a large predator population will reduce available prey to the point where predators decline from lack of food, but this will result in a population increase for the prey species and a subsequent resurgence of the predator (Levin et al., 2009). The LV system has become the classical mathematical model for explaining the predator-prey interactions in natural communities and has formed the cornerstone for much of ecology today. Many mathematical variations of the basic LV system have been developed to explain unexpected changes and temporal fluctuations in the dynamics of not only natural animal populations (e.g., snowshoe hare and the Canadian lynx) but also to show that long-term coexistence of predators and prey is possible in a laboratory using predatory and prey mites (Tahara et al., 2018).

The middle of the 20th century also witnessed a major wave of enthusiasm for the use of mathematical models in community ecology bolstered largely via contributions of Robert MacArthur and colleagues. MacArthur developed a conceptual

framework to champion the role of competition in determining the structure of ecological communities. This work led to the theory of island biogeography (MacArthur and Wilson, 1967), a classical theory postulating that species richness in isolated habitats is regulated by local extinction and colonization and should vary with habitat size and proximity to potential sources of colonizers.

Shortly after MacArthur and Wilson's seminal contributions, a cornerstone for theoretical ecology, a number of physicists entered ecology in the 1970s, and their use of mathematical tools drove a dramatic increase in dynamical systems theory in ecology. Robert May, a trained physicist, rankled ecologists in 1972 by publishing a simple mathematical model describing the relationship between diversity and stability in a theoretical ecosystem (May, 1972, 1974). The surprising result of May's model was that large or complex ecosystems were so unstable that their existence was statistically improbable. While that conclusion did not match what ecologists observe in natural systems such as rain forests, which may contain thousands of species in a single tree, the model challenged the simplistic assumption of more diversity leading to more stability. In another very influential paper in 1976, he introduced community ecology to the possibility of chaotic dynamics in even the simplest of models, ones that were taught in virtually every introductory ecology course (May, 1976).

Today, exponential gains in computing power and data storage capacity have allowed scientists to explore ever more complex models in finer detail. This is due to the fact that the formulated mathematical models can be complemented with realistic simulations in which details not amenable to analysis can be explored. The visual real-time simulations of modelled phenomena give more compelling and more accessible interpretations of what the models predict. This has made it easier to earn the recognition of ecologists.

3.2 Classification of mathematical models in ecology

All mathematical models in ecology can be divided into two groups; *isomorphic* and *homomorphic* models (Gertsev and Gertseva, 2004). An isomorphic model is one in which every aspect of the real object has a corresponding component in the model. In other words, the model is symmetric relative to the object of modelling. However, since the real objects of ecological research (i.e., populations, communities, ecosystems) are very complex, it is almost impossible to reflect all features of such objects in the model. Thus it is necessary to resort to definite assumptions and group characteristics. In this case, however, symmetry between the real object of modelling and the mathematical model is lost resulting in the so-called homomorphic relationship, and the mathematical model becomes homomorphic.

Thus it is clear that all mathematical models in ecology are homomorphic (Gertsev and Gertseva, 2004).

Since the assumptions made about the real object frequently involve a rate of change (with respect to time t) of one or more variables, the mathematical depiction of all these assumptions may be one or more equations involving derivatives. In other words, the mathematical model may be a differential equation or a system of differential equations that describe the behavior of a system that evolves with time, also known as a *dynamical system*. A solution of the model then gives the *state of the system*; in other words, the values of a set of time-dependent variables, called *state variables*, for appropriate values of t , describe the state of the system in the past, present, or future. The set of possible combinations of state variable values is called the *state space* of the system. Such a state space is often called a *phase space*. Evolution of a dynamical system corresponds to a trajectory (or an orbit) in the phase space. Different initial states result in different trajectories. The set of all trajectories forms the *phase portrait* of a dynamical system.

Mathematical models can also be classified by what role random events play in the model. A *deterministic* model has no random components; for the same initial conditions and time period projected, it always gives the same result. The most typical deterministic models encountered are difference equations or differential equations. In contrast, a *stochastic* model incorporates at least one random factor, and thus the results could be different every time the model is run.

One type of stochastic model assumes that the values of some or all parameters vary through time or across individuals and are therefore described by probability distributions (Jackson et al., 2000). Each time the model is run, the parameter values are drawn from their specified probability distributions. Other stochastic models add random errors following each calculation to simulate the effects of environmental variability. One reason to add stochasticity is to produce realistic variability in the trajectories of the state variables through time, either because the variance as well as the average value is of interest or because the effect of variability in one state variable on another state variable is of interest. Model results might be cast in terms of probabilities, for example, as the percentage of simulations in which all but one of the competing species goes extinct. A stochastic model is not necessarily more "correct" than a deterministic model, and it is more work to create. It does provide additional information, but whether this information is of value depends on the purpose of the model.

Another way in which models may differ is based on the way time is handled in the model. In *discrete-time* models, such as difference equations, time takes on values only at certain time-points (i.e., time is broken into discrete segments, usually of fixed length). A typical difference equation model of population growth takes the

general form

$$x_{t+1} = f(x_t) \quad (3.1)$$

where x_t and x_{t+1} represent the value of the state variable at the beginning of two successive time intervals, and f is the function describing the change. State variables that fall naturally into this type of analysis include populations with discrete life stages (e.g., insect larvae instars) or that have nonoverlapping generations (in which the adults die and are replaced by their offspring at fixed intervals). In contrast, *continuous-time* models, such as differential equations, describe continuous changes of an object with time and, for a scalar variable x , have the general form

$$\frac{dx}{dt} = f(x) \quad (3.2)$$

where dx/dt is the rate of change of the state variable and f is the function describing the processes that contribute to the rate of change.

Finally, mathematical models are usually composed of variables, which are abstractions of quantities of interest in the described systems, and operators that act on these variables, which can be algebraic operators, functions, differential operators, etc. If all the operators in a mathematical model exhibit linearity, the resulting mathematical model is defined as *linear*, otherwise the model is considered to be *nonlinear*. The question of linearity and nonlinearity is dependent on context, and linear models may have nonlinear expressions in them. For example, a differential equation is said to be linear if it can be written with linear differential operators, but it can still have nonlinear expressions in it.

While appropriate in some situations, linear models may obscure potentially important properties of the population, which may ultimately influence the accuracy of predictions drawn from them. For example, linear models cannot detect nonlinear density dependence and the differential influence of abiotic factors above and below certain density thresholds (Ellis and Post, 2004). Although there are exceptions, nonlinear models tend to be more difficult to study than linear ones. A common approach to nonlinear problems is linearization, but this can be problematic if one is trying to study aspects such as chaotic dynamics which are strongly tied to nonlinearity.

We focus on deterministic models of interacting species mediated by competitive interactions. Such models are termed species- or population-level models because they model changes in populations, and assume that stochasticity at the individual level can be averaged into a deterministic population-level effect (Daly, 2017). These differ from other modelling approaches such as community-level models and individual-based models. In community-level models, a multispecies community is considered as a sort of "super-organism", because it grows, adjusts under some circumstances, reproduces itself, and functionally represents higher level of integration than the individual species that make it up. From this angle, the

community can be viewed as a collection of genes and reactions, rather than a set of distinct species (Song et al., 2014). Consequently, community-level models describe the dynamics of communities in terms of interactions between genes/reactions, rather than between species. Individual-based models, on the other hand, simulate populations and communities by following individuals and their properties (DeAngelis and Grimm, 2014).

We now proceed to describe the different population-level models used in this thesis.

3.3 Non-spatial models of competition

3.3.1 Mean-field ODE models

Spatial heterogeneity is a crucial factor which shapes the dynamics of a single population and supports coexistence of large numbers of species within ecological communities and ecosystems, a fact which has been recognized both in experiments/observations and theoretical models (Morozov and Poggiale, 2012; de Souza Júnior et al., 2014; Hart et al., 2017). However, incorporating spatial effects could lead to models, such as reaction-diffusion equations, that are less tractable than their spatially homogeneous counterparts. In particular, the analytical treatment of such models becomes seriously impeded and in many cases it can be impossible. In addition, the implementation of complex spatial models normally implies the use of a large number of additional parameters and functions which are often unknown or poorly understood (Morozov and Poggiale, 2012). This makes analysis of sensitivity of the model to variation of parameters or functions substantially more complicated compared to the non-spatial cases.

However, in a large number of cases, we are interested in generic mechanisms through which an ecosystem or a community functions, and for this reason we only need a qualitative description of the system. The main questions include the possibility of persistence and coexistence of species as well as the eventual types of patterns of dynamics which include oscillatory, chaotic, stationary, etc. From this point of view, we only need to include the spatial heterogeneity in the case where the same model without space would provide qualitatively different patterns or where adding spatial dimension results in a minimal increase in model complexity.

Since the main drawback of spatially explicit models lies in their complexity, sometimes it can be possible to simplify those models and describe the population dynamics in terms of some integral characteristics averaged over a large part of the habitat or even over the entire habitat. Such reduced models are known as

mean-field models. In a mean-field ODE model, the individuals in a community are assumed to be well-mixed and the probability of interaction of a randomly chosen individual with any other individual does not depend on the individual chosen. Also the environment is considered to be homogeneous so that the proportions of species do not vary from point to point in space. Some classical examples include:

1. the classical Lotka-Volterra model for competitive interactions of S species with relative abundances x_1, \dots, x_S , which takes the general form

$$\frac{dx_i}{dt} = x_i \left(r_i - \sum_{j=1}^S \alpha_{ij} x_j \right), \quad (3.3)$$

where $r_i > 0$ is the intrinsic growth rate of species i , and α_{ij} represents the competitive effect of species j on species i . Note that the term inside the parentheses $\left(r_i - \sum_{j=1}^S \alpha_{ij} x_j \right)$ is called the per-capita growth rate of species i .

2. the well-known model for cyclic competition (May and Leonard, 1975):

$$\begin{aligned} \frac{dx_1}{dt} &= x_1(1 - x_1 - \alpha x_2 - \beta x_3), \\ \frac{dx_2}{dt} &= x_2(1 - \beta x_1 - x_2 - \alpha x_3), \\ \frac{dx_3}{dt} &= x_3(1 - \alpha x_1 - \beta x_2 - x_3), \end{aligned} \quad (3.4)$$

3. Frean and Abraham's (2001) mean-field model of rock-paper-scissors competition

$$\begin{aligned} \frac{dx_r}{dt} &= x_r(x_s P_r - x_p P_p), \\ \frac{dx_p}{dt} &= x_p(x_r P_p - x_s P_s), \\ \frac{dx_s}{dt} &= x_s(x_p P_s - x_r P_r), \end{aligned} \quad (3.5)$$

where x_r, x_s and x_p are the proportions of species r (rock), s (scissors) and p (paper) with $x_r + x_s + x_p = 1$. An individual of species r can invade a species s with probability P_r , a species s invades a species p with probability P_s , a species p invades a species r with probability P_p , and all other invasion probabilities are zero, and

4. Laird and Schamp's (2009) multispecies extension of the model in Eq. (3.5)

$$\frac{dx_i}{dt} = \sum_{j=1}^S \mathbf{T}(i, j) x_i x_j \quad (3.6)$$

where $\mathbf{x} = (x_1, \dots, x_S)^\top$ is the vector of species abundances and \mathbf{T} is the tournament matrix (i.e., $\mathbf{T}(i, j) = 1$ if species i outcompetes species j , $\mathbf{T}(i, j) = -1$ if species j outcompetes species i , and $\mathbf{T}(i, j) = 0$ if $i = j$).

It can be noted from the above four models that the considered mean-field ODE system takes the general form

$$\frac{dx_i}{dt} = f_i(x_1, x_2, \dots, x_S) = x_i g_i(x_1, x_2, \dots, x_S), \quad (3.7)$$

for some given linear function g_i . This is because for models of biological systems, $x_i = 0$ implies $f_i(x_1, x_2, \dots, x_S) = 0$ such that a non-existent species cannot increase (Williams and Chow, 1978).

3.3.2 Dynamic behavior

We now give a brief discussion of the behavior of dynamical systems, focused on systems modelled by nonlinear ODEs. This allows us to discuss equilibrium points, stability of equilibrium points in the sense of Lyapunov, limit cycles and other key concepts of dynamical systems. We also introduce some methods for analyzing global behavior of solutions.

3.3.2.1 Stability of equilibrium points

The goal here is to discuss some results on the stability of solutions to the nonlinear ODE system of the form

$$\dot{\mathbf{x}} = f(\mathbf{x}), \quad (3.8)$$

where the dot represents the derivative with respect to time t , $\mathbf{x} = (x_1, \dots, x_n)^\top$ and $f(\mathbf{x}) = (f_1(\mathbf{x}), \dots, f_n(\mathbf{x}))^\top$. Equation (3.8) is called *time-invariant* because f does not explicitly depend on t .

The components of the n -dimensional vector $f(\mathbf{x})$ are assumed to be *locally Lipschitz functions* of \mathbf{x} defined for all $\mathbf{x} \in D \subset \mathbb{R}^n$. A function $f(\mathbf{x})$ is locally Lipschitz at a point \mathbf{x}_0 if it satisfies the *Lipschitz condition*

$$\|f(\mathbf{x}) - f(\mathbf{y})\|_2 \leq L \|\mathbf{x} - \mathbf{y}\|_2 \quad (3.9)$$

for all \mathbf{x}, \mathbf{y} in some neighborhood of \mathbf{x}_0 , where L is a positive constant, and $\|\cdot\|_2$ denotes the Euclidean norm of an n -dimensional vector; that is,

$$\|\mathbf{x}\|_2 = \sqrt{x_1^2 + x_2^2 + \dots + x_n^2}. \quad (3.10)$$

The Lipschitz condition guarantees that Eq. (3.8) has a unique solution that satisfies the initial condition $\mathbf{x}(0) = \mathbf{x}_0$ (Levine, 1996).

An *equilibrium point* for the dynamical system (3.8) represents a stationary condition for the dynamics. We say that $\mathbf{x}^* = (x_1^*, x_2^*, \dots, x_n^*)^T \in D$ is an equilibrium point of Eq. (3.8) if $f(\mathbf{x}^*) = 0$. Whenever the state of the system starts at \mathbf{x}^* , it will remain at \mathbf{x}^* for all future time. Equilibrium points are one of the most important features of a dynamical system since they define the states corresponding to constant operating conditions. As discussed in many textbooks, the equilibrium solutions often dictate the long term behavior of the general solutions.

It is often important to know whether an equilibrium point is *stable* or not. Stability of equilibrium points is usually characterized in the sense of Lyapunov, a Russian mathematician and engineer who laid the foundation of the theory which now carries his name. Generally speaking, we say that an equilibrium point is *locally stable* if all solutions which start near \mathbf{x}^* (meaning that the initial conditions are in a neighborhood of \mathbf{x}^*) remain near \mathbf{x}^* for all time; otherwise it is *unstable*. It is said to be *locally asymptotically stable* if it is locally stable, and furthermore, all solutions starting near \mathbf{x}^* asymptotically approach \mathbf{x}^* as time approaches infinity. We now make these definitions precise.

Definition 3.1. We say that an equilibrium point \mathbf{x}^* is *locally stable* if for all $\epsilon > 0$, there exists a $\delta > 0$ such that

$$\|\mathbf{x}(0) - \mathbf{x}^*\|_2 < \delta \Rightarrow \|\mathbf{x}(t) - \mathbf{x}^*\|_2 < \epsilon \text{ for all } t > 0.$$

Note that this definition does not imply that $\mathbf{x}(t)$ gets closer to \mathbf{x}^* as time increases, but rather just that it stays nearby. Furthermore, the value of δ may depend on ϵ , so that if we wish to stay very close to the equilibrium point, we may have to start very, very close ($\delta \ll \epsilon$). This type of stability is sometimes called stability "in the sense of Lyapunov".

Definition 3.2. An equilibrium point \mathbf{x}^* is *locally asymptotically stable* if it is stable and also there exists a $\delta > 0$ such that $\|\mathbf{x}(0) - \mathbf{x}^*\|_2 < \delta$ implies that $\mathbf{x}(t) \rightarrow \mathbf{x}^*$ as $t \rightarrow \infty$.

Furthermore, an equilibrium point may be stable but not asymptotically stable. Such an equilibrium is said to be *neutrally stable*.

Finally, we say that an equilibrium point is *unstable* if it is not stable. More specifically, we say that \mathbf{x}^* is unstable if given $\epsilon > 0$, there always exists an initial condition $\mathbf{x}(0)$ with $\|\mathbf{x}(0) - \mathbf{x}^*\|_2 < \epsilon$ such that $\mathbf{x}(t)$ grows unbounded as time increases.

Definitions 3.1 and 3.2 are local definitions; they describe the behavior of a system near an equilibrium point. The *region of attraction* (also called region of local

asymptotic stability, domain of attraction or basin) is defined as the set of all points $\mathbf{x}_0 \in D$ such that the solution of Eq. (3.8) that starts from \mathbf{x}_0 at time $t = 0$ approaches \mathbf{x}^* as $t \rightarrow \infty$. When the region of attraction is the whole space \mathbb{R}^n , we say that \mathbf{x}^* is *globally asymptotically stable*.

The goal now is to characterize the stability of the equilibrium point \mathbf{x}^* of Eq. (3.8). For convenience, we take $\mathbf{x}^* = 0$. There is no loss of generality in doing this because any equilibrium point \mathbf{x}^* can be shifted to the origin via the change of variables $\tilde{\mathbf{x}} = \mathbf{x} - \mathbf{x}^*$. Therefore we assume, $f(0) = 0$, and study the stability of the origin $\mathbf{x}^* = 0$.

For a linear system, $\dot{\mathbf{x}} = A\mathbf{x}$ where A is a constant-coefficient matrix, the equilibrium point $\mathbf{x}^* = 0$ is globally asymptotically stable if all eigenvalues of A have negative real parts. However for a nonlinear system $\dot{\mathbf{x}} = f(\mathbf{x})$, establishing any kind of stability is usually very difficult.

3.3.2.2 Lyapunov's stability method

In 1892, Lyapunov introduced a method to determine the stability properties of an equilibrium point without explicitly integrating the differential equation (3.8). The method is a generalization of the idea that if there is some "measure of energy" in a system, then we can study the rate of change of the energy of the system to ascertain stability. The "Lyapunov function" plays the role of this energy. The equilibrium state of a physical system is stable if the energy decreases (or at least does not increase) continuously in the neighborhood of this equilibrium state.

Before stating the method, we start by looking at a number of functional properties that we shall use in describing Lyapunov functions.

Definition 3.3. Let $V : D \rightarrow \mathbb{R}$ be a continuously differentiable function defined on a domain $D \subset \mathbb{R}^n$ that contains the origin. V is said to be positive definite if

- (a) $V(0) = 0$, and
- (b) $V(\mathbf{x}) > 0$ for $\mathbf{x} \in D$, and $\mathbf{x} \neq 0$.

It is said to be positive semidefinite if condition (b) is replaced by the weaker condition $V(\mathbf{x}) \geq 0$ for $\mathbf{x} \neq 0$. A function $V(\mathbf{x})$ is said to be negative definite or negative semidefinite if $-V(\mathbf{x})$ is positive definite or positive semidefinite, respectively. If $V(\mathbf{x})$ does not have a definite sign as per one of these four cases, it is said to be indefinite.

Using these definitions, the following theorem allows us to determine stability for a system by constructing an appropriate energy function. Roughly, this theorem states that when $V(\mathbf{x})$ is a positive definite function and $\dot{V}(\mathbf{x}) \leq 0$ along the trajectories of a system, then we can conclude stability of the equilibrium point $\mathbf{x}^* = 0$.

The time derivative of V taken along the trajectories of the system (3.8) is as follows:

$$\begin{aligned}\dot{V}(\mathbf{x}) &= \sum_{i=1}^n \frac{\partial V}{\partial x_i} \dot{x}_i = \sum_{i=1}^n \frac{\partial V}{\partial x_i} f_i(\mathbf{x}) \\ &= \begin{bmatrix} \frac{\partial V}{\partial x_1} & \frac{\partial V}{\partial x_2} & \cdots & \frac{\partial V}{\partial x_n} \end{bmatrix} \begin{bmatrix} f_1(\mathbf{x}) \\ f_2(\mathbf{x}) \\ \vdots \\ f_n(\mathbf{x}) \end{bmatrix} = \left(\frac{\partial V}{\partial \mathbf{x}} \right)^T f(\mathbf{x}).\end{aligned}\quad (3.11)$$

Lyapunov's stability theorem is stated as follows.

3

Theorem 3.1. (Khalil, 1996)[Lyapunov's theorem] Let $\mathbf{x} = 0$ be an equilibrium point of (3.8) and $D \subset \mathbb{R}^n$ be a domain containing $\mathbf{x} = 0$. Let $V : D \rightarrow \mathbb{R}$ be a continuously differentiable function with $\dot{V}(\mathbf{x})$ given by Eq. (3.11) denoting the derivative of V along the trajectories of (3.8). The origin is stable if $V(\mathbf{x})$ is positive semidefinite and $\dot{V}(\mathbf{x})$ is negative semidefinite, and it is asymptotically stable if $\dot{V}(\mathbf{x})$ is negative definite. That is, if

1. $V(0) = 0$ and $V(\mathbf{x}) \geq 0$ in $D \setminus \{0\}$, and
2. $\dot{V}(0) = 0$ and $\dot{V}(\mathbf{x}) \leq 0$ in $D \setminus \{0\}$,

then $\mathbf{x} = 0$ is locally stable. It is locally asymptotically stable if condition (2) is replaced by

$$\dot{V}(0) = 0 \text{ and } \dot{V}(\mathbf{x}) < 0, \forall \mathbf{x} \in D \setminus \{0\}.$$

Furthermore, if $D = \mathbb{R}^n$ and V is radially unbounded (that is, $\|\mathbf{x}\| \rightarrow \infty \Rightarrow V(\mathbf{x}) \rightarrow \infty$), then the origin is globally asymptotically stable. A continuously differentiable function $V(\mathbf{x})$ satisfying the stability conditions above is called a Lyapunov function for the system.

Note that if the origin $\mathbf{x} = 0$ is a globally asymptotically stable equilibrium point of a system, then it must be the unique equilibrium point. For if there was another equilibrium point \mathbf{x}^* , the trajectory starting at \mathbf{x}^* would remain at \mathbf{x}^* for all $t \geq 0$; hence, it would not approach the origin which contradicts the claim that the origin is globally asymptotically stable. Therefore global asymptotic stability is not studied for multiple equilibria systems.

Lyapunov's theorem is a powerful tool for studying the stability of equilibrium points without solving the differential equation (3.8). However, there are two drawbacks. First, there is no systematic method for finding a Lyapunov function for a given ODE system. In some cases, there are natural Lyapunov function candidates like energy functions in electrical or mechanical systems. In other cases, it is basically a matter of trial and error (Khalil, 1996). Second, the theorem's conditions

for stability are only sufficient; they are not necessary. Failure of a Lyapunov function candidate to satisfy the conditions for stability or asymptotic stability does not mean that the equilibrium is not stable or asymptotically stable. It only means that such a stability property cannot be established by using this Lyapunov function candidate. But the search for an appropriate Lyapunov function is rooted in the fact that the converse of Theorem 3.1 exists. That is, if an equilibrium point is stable, then there exists a continuously differentiable function $V(\mathbf{x})$ satisfying the conditions of the theorem (Murray et al., 1994).

3.3.2.3 LaSalle's invariance principle

For local and global asymptotic stability, Lyapunov's theorem requires that the Lyapunov function is strictly decreasing outside the equilibrium point, i.e., $\dot{V}(\mathbf{x}) < 0$ for any $\mathbf{x} \neq 0$. In many situations, however, we are unable to find such a Lyapunov function. If the Lyapunov function is not strictly decreasing, then the solution can remain on a level surface of the Lyapunov function ($V(\mathbf{x}) = c$ for some $c > 0$) and not be attracted towards the equilibrium point. LaSalle introduced a theorem which enables one to conclude asymptotic stability of the equilibrium point even when $\dot{V}(\mathbf{x}) = 0$ for some $\mathbf{x} \neq 0$. To state LaSalle's invariance principle, we need to introduce a few definitions.

Definition 3.4. Let $\mathbf{x}(t; \mathbf{x}_0)$ denote the solution to (3.8) with initial condition \mathbf{x}_0 . A point \mathbf{p} is called an *omega limit point* of solution $\mathbf{x}(t; \mathbf{x}_0)$ if there exists a sequence $\{t_n\}$ of time points, with $t_n \rightarrow \infty$ as $n \rightarrow \infty$, such that

$$\mathbf{x}(t_n; \mathbf{x}_0) \rightarrow \mathbf{p} \text{ as } n \rightarrow \infty.$$

The set of all such points of $\mathbf{x}(t; \mathbf{x}_0)$ is called the *ω -limit* (or *forward*) set of $\mathbf{x}(t; \mathbf{x}_0)$ and denoted by $\omega(\mathbf{x}_0)$.

Similarly, for $t_n \rightarrow -\infty$ an *alpha limit point* and *α -limit* (or *backward*) set $\alpha(\mathbf{x}_0)$ are defined.

A simple example of an ω -limit set is an asymptotically stable equilibrium point. Another example is a closed (periodic) orbit that attracts a trajectory. Such an orbit is called a *stable limit cycle*. Thus, a limit cycle is a periodic orbit γ that is the omega- or alpha-limit set of a point $\mathbf{x} \notin \gamma$.

Definition 3.5. A set $M \subset \mathbb{R}^n$ is said to be (positively) *invariant* w.r.t. (3.8) if

$$\mathbf{x}_0 \in M, \Rightarrow \mathbf{x}(t; \mathbf{x}_0) \in M, \forall t \geq 0.$$

We also say that $\mathbf{x}(t; \mathbf{x}_0) \rightarrow M$ as $t \rightarrow \infty$ if there exists a point $\mathbf{p} \in M$ such that

$$\|\mathbf{x}(t; \mathbf{x}_0) - \mathbf{p}\|_2 \rightarrow 0 \text{ as } t \rightarrow \infty.$$

The equilibrium point and the limit cycle are invariant sets, since any solution starting in either set remains in the set for all future time. Moreover, if $\mathbf{x}(t; \mathbf{x}_0)$ is bounded for all $t \geq 0$, then the ω -limit set $\omega(\mathbf{x}_0)$ is nonempty, compact (i.e., bounded and closed) and invariant (Murray et al., 1994; Khalil, 1996). In addition,

$$\mathbf{x}(t; \mathbf{x}_0) \rightarrow \omega(\mathbf{x}_0) \text{ as } t \rightarrow \infty.$$

For a set E that is not invariant, we can talk about its *maximal (largest) invariant set* $M \subset E$.

We are now ready to state LaSalle's invariance principle.

Theorem 3.2 (Khalil, 1996, LaSalle's invariance principle). *Let $\Omega \subset D$ be a compact set that is positively invariant w.r.t. (3.8). Let $V : D \rightarrow \mathbb{R}$ be a continuously differentiable function such that $\dot{V}(\mathbf{x}) \leq 0$ in Ω . Let E be the set of all points in Ω where $\dot{V}(\mathbf{x}) = 0$. Let M be the largest invariant set in E . Then every solution starting in Ω approaches M as $t \rightarrow \infty$.*

Since our interest is in the asymptotic stability of the origin, that is $\mathbf{x}(t; \mathbf{x}_0) \rightarrow \mathbf{0}$ as $t \rightarrow \infty$, we need to have $M = \{\mathbf{0}\}$. That is, set E contains no invariant sets other than the origin. In this case, LaSalle's invariance principle is commonly stated through the following two corollaries of Theorem 3.2. The first one establishes conditions for (local) asymptotic stability, and the second one establishes conditions for global asymptotic stability.

Corollary 3.1 ((The local) LaSalle's invariance principle). *Let $\mathbf{x} = \mathbf{0}$ be an equilibrium point for (3.8). Let $V : D \rightarrow \mathbb{R}$ be a continuously differentiable, positive definite function on a domain D containing the origin $\mathbf{x} = \mathbf{0}$, such that $\dot{V}(\mathbf{x}) \leq 0$ in D . Let $S = \{\mathbf{x} \in D : \dot{V}(\mathbf{x}) = 0\}$ and suppose that no solution can stay indefinitely in S , other than the trivial solution $\mathbf{x}(t) \equiv \mathbf{0}$. Then, the origin is asymptotically stable.*

Corollary 3.2 ((The global) LaSalle's invariance principle). *Let $\mathbf{x} = \mathbf{0}$ be an equilibrium point for (3.8). Let $V : \mathbb{R}^n \rightarrow \mathbb{R}$ be a continuously differentiable, radially bounded, positive definite function such that $\dot{V}(\mathbf{x}) \leq 0$ for all $\mathbf{x} \in \mathbb{R}^n$. Let $S = \{\mathbf{x} \in \mathbb{R}^n : \dot{V}(\mathbf{x}) = 0\}$ and suppose that no solution can stay indefinitely in S , other than the trivial solution $\mathbf{x}(t) \equiv \mathbf{0}$. Then, the origin is globally asymptotically stable.*

Not only does LaSalle's invariance principle relax the negative definiteness requirement of Lyapunov's stability theorem, but it can also be used in cases where the system has an equilibrium set rather than an isolated equilibrium point.

3.3.3 Equilibrium stability and species coexistence

We have already seen that for ODE models governing the dynamics of n intrinsically competing species, the components of the n -dimensional vector f in (3.8)

take the general form

$$f_i(\mathbf{x}) = x_i g_i(\mathbf{x}),$$

where $\mathbf{x} = (x_1, \dots, x_n)^T$ is the vector of species abundances and $g_i : D \subset \mathbb{R}^n \rightarrow \mathbb{R}$ are given functions. Generally, it is assumed that the functions g_i , together with their first derivatives, are defined and continuous for all nonnegative values of \mathbf{x} . The particular ecological situation will dictate additional specific conditions on the n functions g_1, \dots, g_n .

An equilibrium point \mathbf{x}^* is called a *coexistence equilibrium* (even when it does not describe actual coexistence) if all species have positive abundances ($x_i^* > 0$ for all i) at this point (Barabás et al., 2016). If such a coexistence equilibrium point exists, it has to be the solution of the following set of n linear equations (with one equation for each species i):

$$g_i(x_1, x_2, \dots, x_5) = 0. \quad (3.12)$$

The equilibrium point is said to be *locally stable* if species' abundances tend to return to this point when perturbed from it, and it is *globally stable* if species' abundances approach this point for any combination of starting abundances.

Analyses of the Lotka–Volterra population dynamics model have analytically demonstrated that a necessary condition for species coexistence is the existence of a coexistence equilibrium point (Hofbauer and Sigmund, 1998). However, although necessary, the existence of a coexistence equilibrium point is not sufficient to guarantee species coexistence in n -species systems. For example, it has been shown that competition between two species can lead to the extinction of one of them even if a coexistence equilibrium point exists (Hofbauer and Sigmund, 1998).

On the other hand, although the stability of a coexistence equilibrium point is not required for coexistence in higher dimensional systems, it has been shown that the global stability of a coexistence equilibrium point is a sufficient condition for species coexistence (Saavedra et al., 2017). Therefore species coexistence can be studied by looking into the conditions necessary for species to coexist (that is, existence of a coexistence equilibrium point) and the necessary and sufficient conditions (i.e., existence and global stability) for species persistence. Unfortunately, many times, global stability is difficult to prove and one may only rely on the necessary conditions for species coexistence.

3.3.4 Game theory in the ecological context

3.3.4.1 Introduction

The structure of the competitive network is an important driver of biodiversity and coexistence in natural communities. In addition to determining which species survive, the nature and intensity of competitive interactions within the network also affect the growth, productivity, and abundances of those individuals that persist. However, competitive interactions are costly. Energy is invested by each organism in both exploitative and interference competition as a means to acquire the resource. The energy spent is a cost to the organism, and the resources are benefits. Comparing the relative cost to the benefits obtained following an interaction determines the net gain or loss incurred by the organism, and this value is referred to as the *payoff* (Cowden, 2012). An individual's payoff depends on both her competitive strategy, such as exploitation or interference, and the competitive strategies of the organisms with which it interacts. Organisms with the most dominant strategy maximize their payoff and, in turn, increase their fitness. In this regard, the network of competitive interactions can be viewed as an evolutionary game, and here, we review the game-theoretical methods that have been applied to questions in ecology.

A game, in the mathematical sense, is a situation in which players make rational decisions according to defined rules in an attempt to receive some sort of payoff. Game theory is the branch of mathematics which focuses on the analysis of such games. Game theory is useful for creating a precise mathematical model linking strategy combinations to payoff. The origins of game theory can be traced back to the Renaissance, when the first analyses of strategy games appeared, although no formal theory existed until 1928 when John von Neumann first published the paper *On the Theory of Games of Strategy*, and with his subsequent 1944 book with Oskar Morgenstern titled, *Theory of Games and Economic Behavior* (von Neumann and Morgenstern, 1944). Inspired by the equilibrium concept of von Neumann for two-person, zero-sum games, John Nash (1950) defined and characterized equilibrium for general-sum n -person games. This notion, now called the *Nash equilibrium* (NE), proved to be so successful in various applications, especially in economics. Originally, game theory was studied by economists and mathematicians, but in 1973, Maynard Smith and Price published an article where they adapted the methods of traditional game theory to the context of biological natural selection (Maynard Smith and Price, 1973). They introduced the concept of *evolutionarily stable strategy* (ESS), which is closely related to the Nash equilibrium, as a way of explaining the existence of ritualized animal conflict. Evolutionary game theory was greatly advanced through the introduction of the *Replicator Equation* (RE), which has strong connection with the classical Lotka–Volterra model and the intransitive competition model (3.6). In fact, in this thesis, the ODE model

system that is employed in all non-spatial cases is the replicator equation

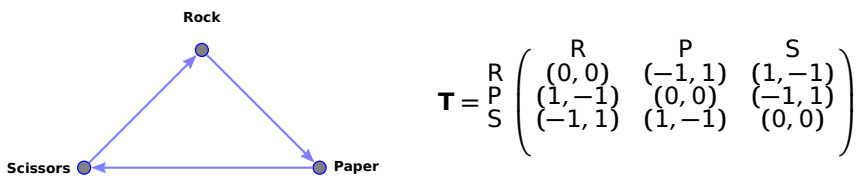
$$\frac{dx_i}{dt} = x_i(\mathbf{T}\mathbf{x})_i \quad (3.13)$$

for a two-player, symmetric, zero-sum game defined by the payoff matrix \mathbf{T} . For a detailed introduction to evolutionary game theory, see Hofbauer and Sigmund (1998).

3.3.4.2 Symmetric two-person zero-sum games

We start by analyzing games in which two players face each other, each choosing one strategy out of a set. Importantly, we consider static games in which each player makes his/her decision without having knowledge of the decision of the other player. Player 1 (row player) has to choose between n options, or *strategies* which we denote by $\mathbf{e}_1, \dots, \mathbf{e}_n$ and Player 2 (column player) between m strategies $\mathbf{f}_1, \dots, \mathbf{f}_m$. If Player 1 chooses \mathbf{e}_i and Player 2 chooses \mathbf{f}_j , then Player 1 obtains a *payoff* a_{ij} and Player 2 obtains a payoff b_{ij} . You can think of the payoff as, for example, a monetary payoff paid to the player after they choose their strategy and played the game but many interesting other interpretations arise. The game, then, is described by two $n \times m$ payoff matrices $A = (a_{ij})$ and $B = (b_{ij})$. Alternatively, we can describe it by one matrix \mathbf{T} whose element in the i -th row and j -th column, is the pair (a_{ij}, b_{ij}) of payoff values.

For example, suppose the two players engaged in a Rock-Paper-Scissors game. In this game, each player has to opt between the three strategies, numbered in that order. The loser pays one dollar to the winner and no money is exchanged in case of a tie. The rules of the game, together with the payoff matrix are shown in Fig. 3.2. This game is an example of a *zero-sum* game. In a zero-sum game,



$$\mathbf{T} = \begin{matrix} & \begin{matrix} \text{R} & \text{P} & \text{S} \end{matrix} \\ \begin{matrix} \text{R} \\ \text{P} \\ \text{S} \end{matrix} & \begin{pmatrix} (0, 0) & (-1, 1) & (1, -1) \\ (1, -1) & (0, 0) & (-1, 1) \\ (-1, 1) & (1, -1) & (0, 0) \end{pmatrix} \end{matrix}$$

Figure 3.2: A Rock-Paper-Scissors game with its corresponding payoff matrix. When the players pick different objects, the winner is the one who picks the object at the head of the arrow connecting the two objects.

the payoffs to the players are opposite in the sense that whatever the first player wins, the second player loses and vice versa. That is, $b_{ij} = -a_{ij}$. Thus the sum of their payoffs is 0, hence the name zero-sum game. A zero-sum game is called *symmetric* if the corresponding payoff matrix is square and skew-symmetric. Thus

a symmetric two-person zero-sum game is defined by a single, square payoff matrix $\mathbf{T} = (T_{ij})$. A positive entry T_{ij} represents a gain for Player 1 of that amount (and a corresponding loss to Player 2 of the same amount) and vice versa. A zero-sum game that is played on a tournament is called a *tournament game*. For example, the payoff matrix for the zero-sum RPS game above is

$$\mathbf{T} = \begin{matrix} & \begin{matrix} \text{R} & \text{P} & \text{S} \end{matrix} \\ \begin{matrix} \text{R} \\ \text{P} \\ \text{S} \end{matrix} & \begin{pmatrix} 0 & -1 & 1 \\ 1 & 0 & -1 \\ -1 & 1 & 0 \end{pmatrix} \end{matrix}$$

Let us enumerate the strategies by $1, 2, \dots, n$. Suppose that Player 1 opts to play strategy i with probability x_i . This *mixed strategy* is thus given by the probability vector $\mathbf{x} = (x_1, x_2, \dots, x_n)^T \in \mathbb{R}^n$ (with $x_i \geq 0$ and $\sum_{i=1}^n x_i = 1$). We denote the set of all such mixed strategies by S^n , which is a unit simplex in \mathbb{R}^n , spanned by the standard unit vectors \mathbf{e}_i , which are said to be the *pure strategies*, and correspond to the original set of alternatives. That is,

$$S^n = \left\{ \mathbf{x} \in \mathbb{R}^n : \sum_{i=1}^n x_i = 1, 0 \leq x_i \leq 1 \right\}.$$

A strategy $\mathbf{x} \in S^n$ is called *completely mixed* if it belongs to the interior of S^n (which we will denote by S^n_+). That is, $\mathbf{x} \in S^n_+$ if $x_i > 0$ for all i .

If Player 1 plays the pure strategy i and Player 2 uses a mixed strategy \mathbf{y} , then the payoff for Player 1 (or more precisely, its expected value) is

$$(\mathbf{T}\mathbf{y})_i = \sum_{j=1}^n T_{ij}y_j. \quad (3.14)$$

On the other hand, if Player 1 uses the mixed strategy \mathbf{x} and Player 2 uses \mathbf{y} , then the expected payoff for Player 1 (which is the same as the negative payoff for Player 2) is

$$\mathbf{x} \cdot \mathbf{T}\mathbf{y} = \sum_i x_i (\mathbf{T}\mathbf{y})_i = \sum_{i,j} T_{ij}x_i y_j. \quad (3.15)$$

In playing the game, Player 2 wants to select a strategy to minimize Player 1's payoff (as it is a zero-sum game this will increase her payoff). On the other hand, Player 1 wants to maximize his own payoff as well. Thus if Player 1 knows the strategy \mathbf{y} of the co-player, then Player 1 should use a strategy \mathbf{x}^* which is a best reply to \mathbf{y} . The set of best replies is the set

$$\{ \mathbf{x}^* \in S^n : \mathbf{x} \cdot \mathbf{T}\mathbf{y} \leq \mathbf{x}^* \cdot \mathbf{T}\mathbf{y} \quad \forall \mathbf{x} \in S^n \}. \quad (3.16)$$

If Player 1 has found a best reply to the strategy \mathbf{y} of Player 2, then Player 1 has no incentive to deviate from \mathbf{x}^* , as long as Player 2 sticks to \mathbf{y} . But will Player 2 stick to \mathbf{y} ? Only if Player 2 has no incentive either to use another strategy, i.e., he has also hit upon a best reply. Two strategies \mathbf{x}^* and \mathbf{y}^* are said to form a *Nash equilibrium* (NE) pair for a two-player zero-sum game if no player can improve his payoff by changing his strategy from his equilibrium strategy to another strategy provided his opponent keeps his equilibrium strategy. That is,

$$\mathbf{x} \cdot \mathbf{T}\mathbf{y}^* \leq \mathbf{x}^* \cdot \mathbf{T}\mathbf{y}^* \leq \mathbf{x}^* \cdot \mathbf{T}\mathbf{y} \quad (3.17)$$

for all $\mathbf{x}, \mathbf{y} \in S^n$. In other words, $(\mathbf{x}^*, \mathbf{y}^*)$ is a NE pair if and only if \mathbf{x}^* is a best reply to \mathbf{y}^* and \mathbf{y}^* is a best reply to \mathbf{x}^* . The strategies \mathbf{x}^* and \mathbf{y}^* are also called *optimal strategies*. The *fundamental theorem of game theory* due to Von Neumann states that there always exist at least one NE pair for any two-person zero-sum finite game. The quantity $v = \mathbf{x}^* \cdot \mathbf{T}\mathbf{y}^*$ is called the *value* of the game. For a symmetric game, $v = 0$ and any strategy optimal for Player 1 is also optimal for Player 2 (i.e., $\mathbf{y}^* = \mathbf{x}^*$) (Fisher and Ryan, 1992). A *symmetric NE* for a zero-sum game is, thus, specified by a strategy \mathbf{x}^* having the property that it is the best reply to itself, that is

$$\mathbf{x} \cdot \mathbf{T}\mathbf{x}^* \leq 0 \quad (3.18)$$

for all $\mathbf{x} \in S^n$. The NE is said to be *strict* if equality holds only for $\mathbf{x} = \mathbf{x}^*$. Nash (1951) has showed that every finite symmetric game admits a symmetric NE.

A useful tool to find Nash equilibria is to eliminate strategies from the game, a priori, because they will never be a part of a NE strategy. In a symmetric, two-person zero-sum game with payoff matrix \mathbf{T} , a strategy i is *dominated* by strategy k if, $T_{ij} \leq T_{kj}$ for all j and $T_{ij} < T_{kj}$ for at least one j . The *dominance principle* states that a rational player should never play a dominated strategy since his payoffs would be less than his payoffs if he uses the dominant strategy. The importance behind dominant strategies is that they are useful in ruling out other strategies to play within a game. It would not be logical to play a strategy that is inferior to another. Indeed we have

Proposition 3.1 (Sultan, 1993, p.294). *Suppose i is a dominated strategy in a symmetric, two-person zero-sum game with payoff matrix \mathbf{T} . Then for any symmetric NE \mathbf{x}^* , $x_i^* = 0$. Moreover, any NE for the game obtained by removing the rows (and columns) from \mathbf{T} corresponding to dominated strategies will also be a NE for the original game.*

This allows to eliminate dominated strategies in an iterative manner until we obtain a payoff matrix \mathbf{T}' for a game which does not contain dominated strategies.

3.3.4.3 Evolutionary game dynamics

In Section 3.3.4.2, we have considered two-player games in the framework of classical game theory, where the outcome depends on the choices made by rational and consciously reasoning individuals. The solution for this type of game (the NE) was based on the idea that each player uses a strategy that is a best response to the strategy chosen by the other, so neither would change what they were doing. The 1970s witnessed the birth of evolutionary game theory marked by the publication of a series of papers by mathematical biologist John Maynard Smith (1973; 1974; 1979). Maynard Smith adapted the methods of classical game theory, which were created to model the behaviour of rational economic agents, to the context of evolutionary biology, particularly for understanding the behaviour of animals in game-theoretic situations. It required a radical shift in perspective and the introduction of thinking in terms of populations.

In evolutionary game theory, players are interpreted as populations (of animals or individuals) which are genetically programmed to play a particular strategy (or phenotype) that is inherited by its offspring (Webb, 2007). The game is the *game of life*. From time to time, two individuals meet randomly and play the game, using their strategies. The outcome of each encounter yields a payoff which represents a gain in biological fitness (expected number of offspring). Thus individuals with more successful strategies have higher fitness and leave more offspring also programmed to play in the same way. So in the next generation, the composition of the population will change.

In order to analyze this set-up, it is convenient to assume that the population is well-mixed so that the individuals (players) differ only by their strategy. This applies well to games where both players are on an equal footing (e.g., symmetric games). Thus much of evolutionary game theory is concerned with symmetric two player games.

Evolutionarily stable strategies

A strategy \mathbf{x}^* for a symmetric zero-sum game with payoff matrix \mathbf{T} is an *evolutionarily stable strategy* (or ESS) if two conditions are met (Hofbauer and Sigmund, 1998, p.63):

(a) equilibrium condition:

$$\mathbf{x} \cdot \mathbf{T}\mathbf{x}^* \leq 0 \quad \forall \mathbf{x} \in S^n; \quad (3.19)$$

(b) stability condition:

$$\text{if } \mathbf{x} \neq \mathbf{x}^* \text{ and } \mathbf{x} \cdot \mathbf{T}\mathbf{x}^* = 0, \text{ then } \mathbf{x}^* \cdot \mathbf{T}\mathbf{x} > \mathbf{x} \cdot \mathbf{T}\mathbf{x} = 0. \quad (3.20)$$

Note that Eq. (3.19) is just the definition of a NE; strategy \mathbf{x}^* is a best reply against itself. This, however, does not guarantee uninvadability since it allows the existence of another strategy \mathbf{x} which is an alternative best reply. The stability condition states that in such a case, \mathbf{x}^* does better against \mathbf{x} than \mathbf{x} against itself. Thus it is clear that a strict NE implies ESS and ESS implies NE.

We now connect NE and ESS with dynamical systems.

Replicator dynamics

Assume that the population evolves in the sense that the proportions (or relative abundancies) x_i change with time. Thus we let $\mathbf{x}(t)$ depend on time, and denote by $\dot{x}_i(t)$ the rate of change of x_i . The assumption of differentiability implies an infinitely large population (Sigmund, 2011). The per capita growth rate \dot{x}_i/x_i of the relative abundance of strategy i is a measure of its evolutionary success. The differential equation for \dot{x}_i/x_i is derived using the basic tenet of Darwinism which is that the reproductive success of a given individual using strategy i should be proportional to the difference between the fitness $f_i(\mathbf{x})$ of individuals using i and the average fitness $\bar{f}(\mathbf{x}) = \sum_i x_i f_i(\mathbf{x})$ of the population (Hofbauer and Sigmund, 1998). Thus we have

$$\frac{\dot{x}_i}{x_i} = \text{fitness of type } i - \text{average fitness}, \quad (3.21)$$

which yields the *replicator equation*

$$\dot{x}_i = x_i(f_i(\mathbf{x}) - \bar{f}(\mathbf{x})), \quad i = 1, \dots, n. \quad (3.22)$$

Under the usual smoothness assumption on $f_i(\mathbf{x})$ (e.g., if $f_i(\mathbf{x})$ is locally Lipschitz continuous), the ODE (3.22) with initial condition \mathbf{x}_0 has a unique solution (for sufficiently small t) which we denote by $\mathbf{x}(t; \mathbf{x}_0)$. Equation (3.22) has the following elementary properties.

- Lemma 3.1.** 1. The simplex S^n is invariant under the replicator dynamics (3.22): if $\mathbf{x}_0 \in S^n$ then $\mathbf{x}(t; \mathbf{x}_0) \in S^n$ for all $t \in \mathbb{R}$.
2. Every face of the simplex S^n is invariant under the dynamics (3.22).

Proof. 1. Let $K = x_1 + \dots + x_n$, then we have

$$\frac{dK}{dt} = (1 - K)\bar{f}(\mathbf{x}),$$

which has $K(t) = 1$ as a solution. Thus if $\mathbf{x}_0 = (x_1(0), \dots, x_n(0)) \in S^n$ (or $K(0) = \sum_{i=1}^n x_i(0) = 1$), then $K(t) = \sum_{i=1}^n x_i(t) = 1$ for all t .

2. Note that if $x_i(0) = 0$, then $\dot{x}_i = 0$ and thus $x_i(t) = 0$ for all t , so that the faces of the simplex, and therefore S^n itself, are invariant. \square

Thus we will restrict Eq. (3.22) to the simplex S^n . In addition, item 2 of Lemma 3.1 means that if a certain strategy is not present in the population, the dynamics will not introduce it. So the replicator dynamics do not include mutation (generation of new strategies) but only selection mechanisms (where only the fittest strategies propagate in the population). If certain strategies are absent from the population then the population stays on the corresponding face of the simplex.

In the context of a symmetric game, $f_i(\mathbf{x})$ is linear and corresponds to the expected fitness (or payoff) for a player using the strategy i against a population state \mathbf{x} and the average fitness $\bar{f}(\mathbf{x})$ corresponds to the average fitness in the population. Thus the replicator equation (3.22) becomes

$$\frac{dx_i}{dt} = x_i((\mathbf{T}\mathbf{x})_i - \mathbf{x} \cdot \mathbf{T}\mathbf{x}) \quad (3.23)$$

for $i = 1, \dots, n$. Accordingly, the proportion of individuals using strategy i increases (decreases) if its payoff is bigger (smaller) than the average payoff in the population. For a symmetric zero-sum game, $\mathbf{x} \cdot \mathbf{T}\mathbf{x} = 0$ and Eq. (3.23) becomes

$$\frac{dx_i}{dt} = x_i(\mathbf{T}\mathbf{x})_i, \quad (3.24)$$

which is the same as the mean-field ODE in Eq. (3.6) describing the dynamics of n interacting species.

If a certain strategy is absent at initial times, for example, let us assume that $x_1(0) = 0$, then by Lemma 3.1 the trajectories of the dynamics do not leave the face of the simplex $\{\mathbf{x} \in S^n, x_1 = 0\}$. Let us set $\tilde{\mathbf{x}} = (x_2, \dots, x_n)^\top$ and let $\tilde{\mathbf{T}}$ the $(n-1) \times (n-1)$ matrix obtained from \mathbf{T} by deleting its first row and first column. Then we have

$$\frac{dx_i}{dt} = x_i(\tilde{\mathbf{T}}\tilde{\mathbf{x}})_i, \quad i = 2, \dots, n, \quad (3.25)$$

and so the dynamics on the face of the simplex is simply the dynamics for the reduced game with strategies $\{2, \dots, n\}$ and payoff matrix $\tilde{\mathbf{T}}$.

An equilibrium point of the replicator equation is a population state $\mathbf{x}^* \in S^n$ for which $\dot{x}_i^*(t) = 0$ for all i . In particular, all vertices of S^n (i.e., population states in which only one strategy is present) are equilibrium points. The replicator equation (3.24) admits a coexistence equilibrium $\mathbf{x}^* \in S_+^n$ if there exists a solution (in S_+^n) of the linear equations

$$(\mathbf{T}\mathbf{x})_i = 0, \quad i = 1, \dots, n. \quad (3.26)$$

Similarly all equilibrium points on each face can be obtained by solving a corresponding system of linear equations. Generically, each sub-simplex (and S^n itself) contains one or no coexistence equilibria (Hofbauer and Sigmund, 1998). Thus, if a coexistence equilibrium for Eq. (3.24) exists, then it is unique.

It can also be shown that if no coexistence equilibrium exists, then all orbits in S^n_+ converge to the boundary, for $t \rightarrow \pm\infty$. In particular, if strategy i is dominated, then $x_i(t) \rightarrow 0$ for $t \rightarrow +\infty$ (Sigmund, 2011). Conversely, if there exists an orbit $\mathbf{x}(t)$ bounded away from the boundary of S^n (i.e., such that for some $a > 0$ the inequality $x_i(t) > a$ for all $t > 0$ and all $i = 1, \dots, n$), then there exists a coexistence equilibrium in S^n_+ (Hofbauer and Sigmund, 1988).

The equilibrium points of the replicator equation (3.24) are closely related to the NE of the symmetric zero-sum game with payoff matrix \mathbf{T} . Recall that a point $\mathbf{x}^* \in S^n$ is a (symmetric) NE if

$$\mathbf{x} \cdot \mathbf{T}\mathbf{x}^* \leq \mathbf{x}^* \cdot \mathbf{T}\mathbf{x}^* = 0 \quad (3.27)$$

for all $\mathbf{x} \in S^n$, and an *evolutionarily stable state* if

$$\mathbf{x}^* \cdot \mathbf{T}\mathbf{x} > \mathbf{x} \cdot \mathbf{T}\mathbf{x} \quad (3.28)$$

for all $\mathbf{x} \neq \mathbf{x}^*$ in a neighborhood of \mathbf{x}^* .

The following two theorems relate the NE of the game to the equilibrium points of Eq. (3.24).

Theorem 3.3 (Hofbauer and Sigmund, 1998, Theorem 7.2.1).

- (a) If $\mathbf{x}^* \in S^n$ is a NE of the game described by the payoff matrix \mathbf{T} , then \mathbf{x}^* is an equilibrium point of (3.24).
- (b) If \mathbf{x}^* is the ω -limit of an orbit $\mathbf{x}(t)$ in the interior of S^n , then \mathbf{x}^* is a NE.
- (c) If \mathbf{x}^* is a Lyapunov stable equilibrium point, then it is a NE.

Theorem 3.4 (Hofbauer and Sigmund, 1998, Theorem 7.2.4). If $\mathbf{x}^* \in S^n$ is an evolutionarily stable state for the game with payoff matrix \mathbf{T} , then it is an asymptotically stable equilibrium point of (3.24). In fact, if $\mathbf{x}^* \in S^n_+$ is evolutionarily stable, then it is a globally stable equilibrium point for (3.24)

The above two theorems imply that ecologists can predict the number of coexisting species by examining NE behaviour of the underlying zero-sum game. Importantly, the problem of computing the NE for a two-person zero-sum game can be reduced to solving an appropriately defined linear programming problem (Fisher and Ryan, 1992). In fact, it has been shown that the converse is also true, i.e., every linear

programming problem can be solved by finding a symmetric NE to a corresponding zero-sum game (Adler, 2013).

In situations where coexistence of all species is required, the ODE system (3.24) should admit a coexistence equilibrium point which is stable. In such a case, it is convenient to consider competition tournaments for which the corresponding zero-sum game is *completely mixed*. In a completely mixed game, the symmetric NE is unique and lies in S_+^n . It has already been shown that all symmetric, two-person zero-sum games with an even number of pure strategies are never completely mixed, which implies that the coexistence of an even number of species is not possible Allesina and Levine (2011). Kaplansky (1945) provided the necessary and sufficient conditions for the game to be completely mixed, i.e., a symmetric, two-person zero-sum game is completely mixed if its payoff matrix \mathbf{T} has rank $n - 1$ and all its cofactors are different from zero and have the same sign. Furthermore, for games whose payoff matrices are of order 3 or 5, he went ahead to provide specific conditions for the game to be completely mixed. For instance, for $n = 3$, the game with pay-off matrix

$$\mathbf{T} = \begin{bmatrix} 0 & c & -b \\ -c & 0 & a \\ b & -a & 0 \end{bmatrix}$$

is completely mixed if and only if a, b, c are different from zero and have the same sign. The unique symmetric NE is then given by $(a/(a+b+c), b/(a+b+c), c/(a+b+c))$. For $n = 5$, the symmetric game is completely mixed if and only if the five expressions

$$\begin{aligned} & T_{25}T_{34} - T_{35}T_{24} + T_{45}T_{23} \\ & -T_{15}T_{34} + T_{35}T_{14} - T_{45}T_{13} \\ & T_{15}T_{24} - T_{25}T_{14} + T_{45}T_{12} \\ & -T_{15}T_{23} + T_{25}T_{13} - T_{35}T_{12} \\ & T_{14}T_{23} - T_{24}T_{13} + T_{34}T_{12} \end{aligned}$$

have the same sign and the unique NE is then proportional to them. These conditions were later extended to odd-ordered skew-symmetric payoff matrices Kaplansky (1995).

3.4 Chemical reaction network theory

3.4.1 Introduction

Chemical reaction network theory (CRNT) has been developed over the last 50 years to study the dynamical evolution of the concentrations of the chemical

species involved in a known set of reactions (Feinberg, 1987). A primary aim of the theory is to make assertions about connections between the qualitative dynamics of a kinetic system and properties of its underlying reaction network. If the graph underlying the kinetic system in a given reaction network has some special properties, then the associated dynamical system is known (or conjectured) to have certain dynamical properties. Questions regarding the existence of positive equilibria, their stability, and the nonextinction, or persistence, of species which are the constituents of the system can be answered even without knowledge of the exact values of key system parameters, called *rate constants*, which are usually difficult to find experimentally, and, hence, are often times unknown.

For example, if the underlying reaction network is *reversible* (i.e., for every edge, there is an edge in the reverse direction), then the kinetic (mass-action) system admits a positive equilibrium point in each positive *stoichiometric compatibility class* (invariant set) for any choice of positive rate constants (Boros, 2019). In addition, if the rate constants satisfy some algebraic constraints such as the *Wegscheider conditions* (Wegscheider, 1902), the mass-action system is in a state of *thermodynamic equilibrium*, where the rate of any forward reaction is balanced by the rate of the reverse reaction. Such a system, said to be *detailed-balanced*, enjoys remarkable dynamical properties, like the existence of a globally defined Lyapunov function, and uniqueness of a positive equilibrium point in each positive stoichiometric compatibility class (Schaff et al., 2013).

In this section, we introduce the necessary mathematical concepts, results and notation from the CRNT that will be useful in the analysis of some of the ecological models discussed in this thesis.

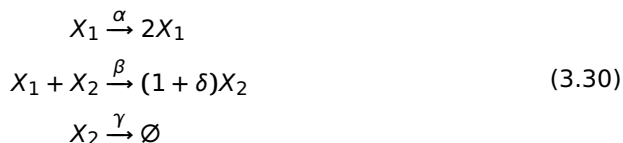
3.4.2 Chemical reaction networks

Chemical reaction networks provide an efficient way to model mechanisms of local interactions in disciplines ranging from chemistry, biochemistry, epidemiology to population dynamics. In these systems, entities interact to form other entities as prescribed by a directed graph, the reaction network.

In ecology, a number of models enjoy compact representations in the form of chemical reactions. Examples of these include, the classic Lotka–Volterra predator–prey model

$$\begin{aligned}\frac{dx_1}{dt} &= \alpha x_1 - \beta x_1 x_2 \\ \frac{dx_2}{dt} &= -\gamma x_2 + \kappa x_1 x_2\end{aligned}\tag{3.29}$$

from a hypothetical chemical reaction network



with $\kappa = \beta\delta$. We can easily interpret these reactions as, respectively: the birth of new prey from a prey, a predator consuming a prey and giving birth to δ new predators, and a predator dying.

Here, we introduce the mathematical concepts and notation relevant for the study of chemical reaction networks.

Roughly, a chemical reaction network (CRN) is a finite set of chemical reactions of the form

$$\mathcal{R}_j : \sum_{i=1}^n \alpha_{ij} X_i \xrightleftharpoons[k_j^-]{k_j^+} \sum_{i=1}^n \beta_{ij} X_i, \quad j = 1, \dots, r \quad (3.31)$$

where $S = \{X_1, \dots, X_n\}$ is called the set of chemical species, $\mathcal{R} = \{\mathcal{R}_1, \dots, \mathcal{R}_r\}$ is called the reaction set. The nonnegative integers α_{ij} and β_{ij} are called the *stoichiometric coefficients*. They control the number of individual molecules which are either consumed by, or produced as a result of, each individual reaction. Finally, the constants $k_j^+ > 0$ and $k_j^- \geq 0$ are the reaction rate constants. Note that if $k_j^- = 0$, then reaction \mathcal{R}_j only happens in the forward direction and is thus not reversible.

The species on the left-hand and right-hand side are usually referred to as the *reactants/substrates* and, the *products* of reaction \mathcal{R}_j , respectively. If a reaction happens spontaneously (no reactants) or when there are physical inflows in the system, then \emptyset may appear at the left-hand side of (3.31). Similarly, if some reactants are degraded into something whose concentration is unimportant, or if there are physical outflows to the system, then \emptyset may appear at the right-hand side of (3.31).

The stoichiometric coefficients of a CRN are often represented in a more compact form called the stoichiometric matrix, denoted by \mathbf{S} . Matrix \mathbf{S} is organized such that every column corresponds to a reaction and every row corresponds to a chemical species. Thus it is an $n \times r$ matrix given by

$$\mathbf{S} = (\gamma_{ij}) \quad \text{where} \quad \gamma_{ij} = \beta_{ij} - \alpha_{ij} \quad (3.32)$$

for $i = 1, \dots, n$ and $j = 1, \dots, r$

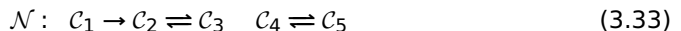
It is more common within chemical reaction network literature to index the reactions by the net terms on the left-hand or right-hand side of a reaction, which are called *complexes*. This eliminates redundancies so that, if a stoichiometrically

equivalent complex appears multiply in the network (3.31), it is only indexed once. Consequently we associate to network (3.31) a set of complexes: $\mathcal{C} = \{C_1, \dots, C_m\}$, the union of all distinct left-hand or right-hand sides of the reactions in the network. Thus each C_i represents a distinct non-negative integer linear combination of species corresponding to products or reactants of the reactions in (3.31), specifically $\sum_{j=1}^n \alpha_{ij} X_j$ or $\sum_{j=1}^n \beta_{ij} X_j$. It is typically assumed that: (a) every species in \mathcal{S} appears in at least one complex in \mathcal{C} ; (b) every complex in \mathcal{C} appears in at least one reaction in \mathcal{R} ; and (c) there are no self reactions (i.e., $C_i \rightleftharpoons C_i$). Thus a CRN is a triplet $\mathcal{N} = (\mathcal{S}, \mathcal{C}, \mathcal{R})$ of the three nonempty finite sets.

Viewing CRNs as interactions between distinct complexes naturally gives rise to their interpretation as directed graphs $G(V, E)$ where the vertices are the complexes (i.e., $V = \mathcal{C}$) and the edges are the reactions (i.e., $E = \mathcal{R}$). In the literature this graph has been termed the *complex graph* of the network (Rao et al., 2012). Connectivity concepts from graph theory also apply to the complex graph of a CRN. If there is a path between two vertices C_i and C_j , then they are said to be connected. If there is a directed path from vertex C_i to vertex C_j and vice versa, then they are said to be *strongly connected*. If any two vertices of a subgraph are (strongly) connected, then the subgraph is said to be a (*strongly*) *connected component*. The connected components are precisely the *linkage classes*, whereas the strongly connected components are the *strong linkage classes* of a CRN.

A CRN is called *reversible* if every reaction in the network is reversible. It is said to be *weakly reversible* if the existence of a path from C_i to C_j implies the existence of a path from C_j to C_i .

For example, consider the chemical reaction network



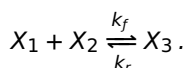
There are two linkage classes: $\mathcal{L}_1 = \{C_1, C_2, C_3\}$ and $\mathcal{L}_2 = \{C_4, C_5\}$. It is not hard to see that the linkage classes completely partition the complex set \mathcal{C} of a CRN. For example, we have $\mathcal{L}_1 \cap \mathcal{L}_2 = \emptyset$ and $\mathcal{L}_1 \cup \mathcal{L}_2 = \mathcal{C}$ in (3.33).

3.4.3 Mass-action systems

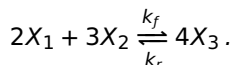
In the mean-field ODE models of Section 3.3.1 the default rule for describing the dynamics of two interacting species is the *law of mass-action*. The law of mass-action is a powerful concept that describes the average behavior of a system that consists of many interacting parts, such as molecules, that react with each other, or interacting populations. The law originates in the theory and practice of chemical reaction kinetics and states that the rate at which molecules of type A and B collide (i.e., the number of collisions per unit volume per unit of time) in a well-stirred reaction vessel, is proportional to the product of the concentrations of A

and B . Translated into individuals of species 1 and species 2 making pairwise contacts in a homogeneously mixing population, the assumption reads that the number of contacts per unit area per unit of time is proportional to the product of the density of species 1 and the density of species 2. Its use in ecology began with the pioneering work of Alfred Lotka (Lotka, 1925) who used it to justify the encounter term in his predator-prey ODE model. Since then, the law has become ubiquitous in mathematical ecology for modelling the interactions between individuals of different groups. The use of the law is appealing since it permits the use of powerful results from CRNT. Moreover, the simplicity of the interaction term widens the possibilities to analytically study the behaviour of the resulting systems of differential equations.

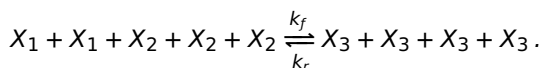
3 In order to model how the concentrations of the chemical species evolve over time, we assume that the reaction vessel is spatially homogeneous (well-stirred solution) and that the reacting species are in sufficient quantity to be modelled as chemical concentrations. We furthermore assume that the system obeys mass-action kinetics, so that the rate of each reaction is proportional to the product of concentrations of the reactant species each raised to a power equal to the corresponding stoichiometric coefficient. For example, consider the chemical reaction



By the law of mass-action, the rate of reaction in the forward direction is given by $v_f = k_f x_1 x_2$, while the rate of reaction in the reverse direction is $v_r = k_r x_3$. The net reaction rate v is thus given by $v = v_f - v_r = k_f x_1 x_2 - k_r x_3$. Now consider the chemical reaction



This can alternatively be written as



Again applying the law of mass-action, the rate of reaction in the forward direction is given by

$$v_f = k_f x_1 \cdot x_1 \cdot x_2 \cdot x_2 \cdot x_2 = k_f x_1^2 x_2^3,$$

while the rate of reaction in the reverse direction is

$$v_r = k_r x_3 \cdot x_3 \cdot x_3 \cdot x_3 = k_r x_3^4,$$

and the net reaction rate is given by $v = k_f x_1^2 x_2^3 - k_r x_3^4$.

Thus, for reaction \mathcal{R}_j in (3.31), by the law of mass-action,

$$\begin{aligned} \text{rate of forward reaction, } v_j^{\text{forward}} &= k_j^+ \prod_{i=1}^n x_i^{\alpha_{ij}} \quad \text{and} \\ \text{rate of backward reaction, } v_j^{\text{backward}} &= k_j^- \prod_{j=1}^n x_j^{\beta_{ij}} \end{aligned} \quad (3.34)$$

Therefore the net reaction rate v_i in the presence of both forward and backward reactions is

$$v_i(\mathbf{x}) = v_i^{\text{forward}} - v_i^{\text{backward}} = k_i^+ \prod_{j=1}^n x_j^{\alpha_{ij}} - k_i^- \prod_{j=1}^n x_j^{\beta_{ij}}, \quad (3.35)$$

where $\mathbf{x} \in \mathbb{R}^n$ is the vector of concentrations of chemical species and $i = 1, 2, \dots, r$. Then the mass-action rate for the complete reaction set is given by the vector

$$\mathbf{v}(\mathbf{x}) = [v_1(\mathbf{x}) \quad \dots \quad v_r(\mathbf{x})]^T. \quad (3.36)$$

We can now write the ODE system governing the dynamics of a CRN under mass-action kinetics as

$$\frac{d\mathbf{x}}{dt} = \mathbf{S}\mathbf{v}(\mathbf{x}) \quad (3.37)$$

where \mathbf{S} is the $n \times r$ stoichiometric matrix.

In order to most clearly emphasize the connection between the reaction graph of a chemical reaction network and the behaviour of solutions under mass-action kinetics, it is common to reformulate the dynamical representation (3.37) by splitting the stoichiometric matrix \mathbf{S} into forms which emphasize the connections between stoichiometrically distinct complexes.

Note from graph theory that the complex graph can also be characterized by its $m \times r$ incidence matrix $\mathbf{B} = (b_{ij})$ defined as follows:

$$b_{ij} = \begin{cases} -1 & \text{if } C_i \text{ is the reactant complex of reaction } \mathcal{R}_j \\ 1 & \text{if } C_i \text{ is the product complex of reaction } \mathcal{R}_j \\ 0 & \text{otherwise} \end{cases}.$$

Since each of the m complexes is a combination of the n chemical species, we can define an $n \times m$ matrix $\mathbf{Z} = (z_{ij})$ where z_{ij} is the stoichiometric coefficient of species X_i in the complex C_j . Thus the k^{th} column of \mathbf{Z} represents the stoichiometric coefficients of the chemical species in the complex C_k . The matrix \mathbf{Z} is called the *complex stoichiometric matrix* (Rao et al., 2012). Notice that every column of \mathbf{S} is the difference of two columns of \mathbf{Z} . It can be easily verified that

$$\mathbf{S} = \mathbf{Z}\mathbf{B}. \quad (3.38)$$

Hence the dynamical system (3.37) for the evolution of the species concentrations can also be written as

$$\frac{d\mathbf{x}}{dt} = \mathbf{Z}\mathbf{B}\mathbf{v}(\mathbf{x}) \quad (3.39)$$

For some purposes, description (3.37) is useful, but for others (3.39) is.

3.4.4 Detailed balancing for mass-action systems

The nonlinearity in the mass-action system (3.37) or (3.39) makes it very difficult, if not impossible, to create general mathematical criteria about qualitative properties of such systems, like existence of positive equilibria, stability properties of equilibria, or persistence (non-extinction) of variables. However, CRNT provides a framework that answers this type of questions for mass-action systems. The theory introduces new concepts such as the *deficiency* of a reaction network, and gives conditions on such networks for the existence, uniqueness and stability of equilibrium points. These conclusions sometimes hold independent of the precise values of the system parameters (rate constants) which are usually difficult to find experimentally, and, hence, are often times unknown in practical applications.

Mass-action systems give rise to very diverse dynamics. For example, weakly reversible deficiency zero mass-action systems have a unique, positive and locally asymptotically stable equilibrium (within the same stoichiometric compatibility class or invariant set) (Feinberg, 1987). Yet there are other mass-action systems that have periodic orbits or limit cycles, and others that admit multiple positive equilibria within the same stoichiometric compatibility class. Here, we focus on one important characterization of equilibrium points of mass-action systems which have proven useful in the literature: *detailed-balanced* equilibrium concentrations.

We begin with some definitions.

Definition 3.6. A vector of concentrations $\mathbf{x}^* \in \mathbb{R}_+^n$ is called an equilibrium of the dynamical system (3.37) if

$$\mathbf{S}\mathbf{v}(\mathbf{x}^*) = 0. \quad (3.40)$$

Definition 3.7. For a reversible CRN, an equilibrium $\mathbf{x}^* \in \mathbb{R}_+^n$ of (3.37) is called detailed balanced if

$$v_i(\mathbf{x}^*) = 0, \text{ for } i = 1, 2, \dots, r. \quad (3.41)$$

That is, for every reversible reaction, the forward and backward rates are equal. An equilibrium that is detailed balanced is also called a thermodynamic equilibrium.

It has been shown that for mass-action systems, if one positive equilibrium point of the deterministic model is detailed balanced, then every positive equilibrium point is detailed balanced (Feinberg, 1989). Thus, we have the following definition.

Definition 3.8. A mass-action system is said to be detailed balanced if the network is reversible and there exists a positive equilibrium point which is detailed balanced.

Detailed balanced equilibria have particularly nice properties in the context of mass-action systems. For example, It has been shown that if a mass-action system is detailed balanced then there exists a unique positive equilibrium in each stoichiometric compatibility class, and this equilibrium is detailed-balanced. Moreover, such an equilibrium is locally asymptotically stable in its stoichiometric compatibility class due to the existence of a strict Lyapunov function (Schaft et al., 2013).

3.4.5 Wegscheider's conditions

In a reversible CRN, the principle of detailed-balance requires that, at equilibrium, the net reaction rate for each reaction is zero. This implies that, for a given equilibrium, detailed-balance results in a system of linear algebraic conditions on the reaction rate constants. On the contrary, if we assume the existence of an a priori unknown equilibrium point with the detailed-balance property, then a system of nonlinear conditions on rate constants appear (Gorban and Yablonsky, 2011). These conditions are known now as the *Wegscheider conditions* named after Rudolf Wegscheider (1901) who introduced the principle of detailed-balance in the field of chemical kinetics.

For example, consider the reversible CRN in Fig. 3.3. An equilibrium is said to

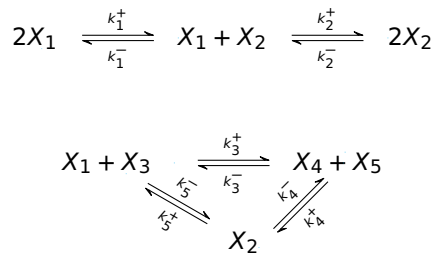


Figure 3.3: Example of a reversible CRN with 5 chemical species ($\{X_1, \dots, X_5\}$), 6 complexes ($\{C_1 = 2X_1, C_2 = X_1 + X_2, C_3 = 2X_2, C_4 = X_1 + X_3, C_5 = X_4 + X_5, C_6 = X_2\}$) and 5 reversible reactions (edges of the network)

be detailed-balanced if at the equilibrium concentration, the net reaction rate for each reversible reaction is zero. Thus, if x_i^* denotes the equilibrium concentration of species X_i , $i = 1, \dots, 5$, then the full set of conditions, arising from the five reactions, required for the mass-action equilibrium to be detailed balanced is given

as:

$$\begin{aligned}
 k_1^+ x_1^{*2} &= k_1^- x_1^* x_2^* \\
 k_2^+ x_1^* x_2^* &= k_2^- x_2^{*2} \\
 k_3^+ x_1^* x_3^* &= k_3^- x_4^* x_5^* \\
 k_4^+ x_4^* x_5^* &= k_4^- x_2^* \\
 k_5^+ x_2^* &= k_5^- x_1^* x_3^* .
 \end{aligned} \tag{3.42}$$

Assuming that a detailed-balance equilibrium exists for this network, the set of conditions (3.42) can be simultaneously satisfied only if the reaction rate constants are appropriately constrained. Some algebraic manipulation of (3.42) allows us to identify the required constraints as follows

$$\frac{k_1^+}{k_1^-} = \frac{k_2^+}{k_2^-} \tag{3.43}$$

$$k_3^+ k_4^+ k_5^+ = k_3^- k_4^- k_5^- . \tag{3.44}$$

Note that the second constraint (3.44) does not require precise knowledge of the constituent species in the complexes \mathcal{C}_4 , \mathcal{C}_5 and \mathcal{C}_6 , but only the fact that the three complexes form a cycle. On the other hand, the first constraint cannot be obtained without knowledge of the constituent species in the complexes \mathcal{C}_1 , \mathcal{C}_2 and \mathcal{C}_3 . The set of constraints on the rate constants, such as the ones in (3.43 and 3.44) is not only necessary but also sufficient in the sense that if the constraints are satisfied for a reversible CRN with mass-action kinetics, then every equilibrium of the CRN is detailed-balanced (Feinberg, 1989). Thus we say that a CRN is detailed-balanced when its equilibria are detailed-balanced, or equivalently, when the rate constants satisfy the appropriate constraints, known as the Wegscheider's conditions.

3.5 Spatial models

3.5.1 Introduction

Spatial heterogeneity, i.e., differences between populations and individuals at different geographical locations, is one of the most obvious features of the natural world. Spatial structure and dynamics determine the way the interactions among species living within a given habitat are interconnected (Gibert and Yeakel, 2019) to form the complex networks that characterize ecological communities. In addition, heterogeneities in the spatial landscape have been shown to have profound effects on the dynamics of populations and the structure of communities (Kareiva et al., 1990; Cantrell and Cosner, 2003). For example, early theoretical studies on the cyclic competition among three species were based on the Lotka–Volterra

ODE system, which ignores spatial effects and predicts a solution of unstable periodic dynamics that leads to the extinction of two of the species after a short transient (May and Leonard, 1975; Berr et al., 2009). However, numerous theoretical models have shown that the three competing species can coexist indefinitely if ecological processes such as dispersal, migration and the cyclic competitive interactions occur over small spatial scales (Kerr et al., 2002; Durrett and Levin, 1998). Space therefore plays a central role in mediating ecological dynamics and the use of spatial models in ecology has grown enormously over the last two decades.

There are many ways in which space and the organisms inhabiting it can be represented in models. However, the most fundamental distinction between the different models is the way in which the spatial dimension is represented. Some models treat space explicitly, giving some sort of description at each spatial location at any given time, or implicitly, incorporating parameters that vary with spatial scale or following only the percent cover of different species across the landscape (Cantrell and Cosner, 2003; Sommer and Worm, 2002; White et al., 2018). Among the models that treat space explicitly, some treat space as a continuum, while others treat space as a discrete collection of patches (metapopulation). The continuum models take the form of partial differential equations (PDEs), or specifically *reaction-diffusion (RD) equations* while metapopulation models usually consist of a system of ODEs that describe movement of individuals between discrete spatial patches.

3.5.2 Reaction-diffusion equations

RD equations arise as models for the densities of organisms that disperse through space by random walks and that interact with each other and their surroundings in ways that affect their local densities. These models are in themselves deterministic, but they can be derived as limits of stochastic processes under suitable scaling. Specifically, they provide a modelling approach that allows us to translate assumptions about stochastic local movement into deterministic descriptions of global densities.

RD models are spatially explicit, describe population densities and treat space and time as continuous. These features distinguish them from other principal approaches that have been used in studies of spatially structured populations such as metapopulation patch models and individual-based cellular automata models. These equations have been used to describe a number of relevant ecological phenomena that include travelling wavefronts corresponding to biological invasions; critical patch size problems which study the minimum habitat size necessary for a population to persist and the formation of spatial patterns in ecology (Cosner, 2008). In a RD equation, 'reaction' refers to the mathematical description of local population growth, and 'diffusion' refers to the mathematical description of dispersal or migration. We now describe how reaction-diffusion models are derived.

3.5.2.1 Reaction

In the context of ecological models, the reaction terms in RD equations are typically the same as those that are used in nonspatial models for interacting populations that are based on ODEs, i.e.,

$$\frac{dx_i}{dt} = f_i(x_1, \dots, x_n), \quad (3.45)$$

where, as before, $f_i(x_1, \dots, x_n)$ has the form $f_i(x_1, \dots, x_n) = x_i g(x_1, \dots, x_n)$. In the case of a single species with population density $u(t)$, common choices for $f(u)$ are $f(u) = ru$ (*exponential growth*) or $f(u) = ru(1 - u/K)$ (*logistic growth*). For multispecies systems, typical reaction terms include those from the classic Lotka–Volterra equations and from the classical replicator dynamics of evolutionary game theory.

3.5.2.2 Diffusion and random walks

Diffusion is a phenomenon by which matter, particle groups, population, etc., spread out within a given space according to individual random walks (Okubo and Levin, 2001). The diffusive description of random motion emerges as a continuum limit of such random walks when the length Δx of each space step and the time Δt required for each time step go to zero in such a way that the ratio $(\Delta x)^2/\Delta t$ remains constant. To understand how this works it is useful to consider a simple example in a one-dimensional spatial domain.

Suppose that an individual moves along a line by moving a distance Δx to the left with probability $1/2$ or a distance Δx to the right with probability $1/2$ at each time step Δt . Let $P(x, t)$ denote the probability that the individual is at location x at time t , or equivalently, the fraction of a population of individuals that are at x at time t . The probability $P(x, t + \Delta t)$ that the individual is at location x at time $t + \Delta t$ can be computed by observing that to arrive at that point at that time the individual must have been either one step to the left at time t and then moved to the right, or one step to the right and have moved to the left. Thus, we have

$$P(x, t + \Delta t) = \frac{1}{2}P(x + \Delta x, t) + \frac{1}{2}P(x - \Delta x, t). \quad (3.46)$$

If we subtract $P(x, t)$ from both sides and divide by Δt we obtain

$$\frac{P(x, t + \Delta t) - P(x, t)}{\Delta t} = \frac{1}{2\Delta t} [P(x + \Delta x, t) - 2P(x, t) + P(x - \Delta x, t)]. \quad (3.47)$$

Suppose that we now impose the diffusive scaling

$$2D = \frac{(\Delta x)^2}{\Delta t}. \quad (3.48)$$

Then Eq. (3.47) becomes

$$\frac{P(x, t + \Delta t) - P(x, t)}{\Delta t} = D \frac{P(x + \Delta x, t) - 2P(x, t) + P(x - \Delta x, t)}{(\Delta x)^2}. \quad (3.49)$$

The expression on the left is a difference quotient in t ; the expression on the right is a second order difference in x . Thus taking the limit of Eq. (3.49) as $\Delta t, \Delta x \rightarrow 0$ while (3.48) remains valid yields

$$\frac{\partial P}{\partial t} = D \frac{\partial^2 P}{\partial x^2}. \quad (3.50)$$

This is the diffusion equation for the density $P(x, t)$, which is the diffusion part of typical reaction-diffusion models. Mathematically this equation is identical to the heat equation. The relation given in Eq. (3.48) suggests that D can be viewed as being half of the square of the distance that is moved by an individual in unit time by symmetric random movements to the left or right. This interpretation of the diffusion coefficient D is valid in any number of spatial dimensions.

A completely different approach to deriving Eq. (3.50) is based on *Fick's law* and the notion of flux. This states that the flux, J , of material, which can be cells, amount of chemical, number of animals and so on, is proportional to the gradient of the concentration of the material. That is, in a one-dimensional spatial domain,

$$J \propto -\frac{\partial P}{\partial x} \Rightarrow J = -D \frac{\partial P}{\partial x}, \quad (3.51)$$

where $P(x, t)$ is the concentration of species and D is the diffusion coefficient. The minus sign simply indicates that diffusion transports matter from a high to a low concentration.

We now write a general conservation equation which says that the rate of change of the amount of material in a region is equal to the rate of flow across the boundary plus any that is created within the boundary. If the region is $x_1 < x < x_2$ and no material is created,

$$\frac{\partial}{\partial t} \int_{x_1}^{x_2} P(x, t) dx = J(x_1, t) - J(x_2, t). \quad (3.52)$$

Assuming that P and J have continuous first order partial derivatives, we have

$$\int_{x_1}^{x_2} \frac{\partial P(x, t)}{\partial t} dx = - \int_{x_1}^{x_2} \frac{\partial J(x, t)}{\partial x} dx. \quad (3.53)$$

Thus

$$\int_{x_1}^{x_2} \left(\frac{\partial P(x, t)}{\partial t} + \frac{\partial J(x, t)}{\partial x} \right) dx = 0. \quad (3.54)$$

Since this is true for any choice of x_1 and x_2 , it follows that

$$\frac{\partial P(x, t)}{\partial t} = - \frac{\partial J(x, t)}{\partial x}. \quad (3.55)$$

Using Eq. (3.51), we get the classical diffusion equation in a one-dimensional spatial domain, namely

$$\frac{\partial P}{\partial t} = \frac{\partial}{\partial x} \left(D \frac{\partial P}{\partial x} \right), \quad (3.56)$$

which, if D is constant reduces to Eq. (3.50).

In higher spatial dimensions, Eq. (3.50) becomes

$$\frac{\partial P}{\partial t} = D \nabla^2 P = D \left(\frac{\partial^2 P}{\partial x^2} + \frac{\partial^2 P}{\partial y^2} + \frac{\partial^2 P}{\partial z^2} \right), \quad (3.57)$$

where ∇^2 is the Laplacian. The coefficient D in Eq. (3.57) still represents half of the mean square distance travelled by an individual in unit time in all space dimensions. The single species diffusion equation given in (3.50) can be extended to multispecies system. In this case P denotes the vector of species densities, $P = (P_1, \dots, P_n)^T$ and $D = \text{diag}(D_1, \dots, D_n)$ is a diagonal matrix with constant diffusion coefficients $D_i \geq 0$ for all i .

3.5.2.3 Boundary conditions

For models involving diffusion in a region $\Omega \subset \mathbb{R}^n$, $n = 1, 2, 3$, with boundary $\partial\Omega$, it is necessary to specify what happens at the boundary. In the context of ecological models, habitat boundaries can be created by physical features such as rivers, roads or (for aquatic systems) shorelines, but they can also arise from interfaces between different types of ecological communities such as forests and grasslands. These boundaries can influence population dynamics in various ways. For example, they can act as a barrier to movement of some species or act as a source of mortality for others. Typical boundary conditions involve specifying the flux of individuals across the boundary, the density at the boundary or a relation between

those. If the density is specified, we have a *Dirichlet* boundary condition

$$P(x, t)|_{\partial\Omega} = h(x), \quad (3.58)$$

where h is a known function defined on the boundary $\partial\Omega$. If the flux is specified, we have a *Neumann* boundary condition

$$\left. \frac{\partial P}{\partial \mathbf{n}} \right|_{\partial\Omega} = h(x), \quad (3.59)$$

where \mathbf{n} is the outward pointing unit normal vector on $\partial\Omega$ and $\partial P/\partial \mathbf{n}$ is the directional derivative of P in the direction of \mathbf{n} . If both the flux across the boundary and the density at the boundary are specified, we have a *Robin* boundary condition

$$\left(aP + b \frac{\partial P}{\partial \mathbf{n}} \right) \Big|_{\partial\Omega} = h(x) \quad (3.60)$$

for some nonzero constants a and b .

In many ecological models, homogeneous boundary conditions, in which $h(x) = 0$, are often used. Here, the Dirichlet condition $P(x, t) = 0$ corresponds to what is termed as a lethal (or hostile) boundary because it can be interpreted to mean that all individuals who encounter $\partial\Omega$ die. The no-flux boundary condition $\partial P/\partial \mathbf{n} = 0$ corresponds to a situation where individuals encountering $\partial\Omega$ are always “reflected” back into Ω so that no individual crosses the boundary of the habitat. The Robin condition $aP + b \frac{\partial P}{\partial \mathbf{n}} = 0$, with $0 \leq a \leq 1$ and $a + b = 1$, can be interpreted to mean that when individuals reach the boundary $\partial\Omega$, a fraction a of those individuals die while the rest are reflected back into Ω .

3.5.2.4 The reaction-diffusion model

Once we have specified a habitat Ω , the dispersal properties and local population dynamics of species inhabiting Ω and the behaviour (or fate) of individuals encountering the boundary $\partial\Omega$ of Ω , we can assemble a complete RD model. Since most of the ODE models considered involve Lotka–Volterra interaction terms, or other smooth interaction terms, the traditional way to obtain a reaction-diffusion model would be to simply add diffusion to the mean-field ODE model system. This leads to the RD system that takes the form

$$\frac{\partial u_i}{\partial t} = D_i \nabla^2 u_i + f_i(\mathbf{u}), \quad (x, t) \in \Omega \times \mathbb{R}^+, \quad (3.61a)$$

where $\mathbf{u} = (u_1, \dots, u_n)^T$ and $u_i = u_i(x, t)$ is the proportion (relative abundance) of species i at location x at time t . However, if the ODE is governed by the replicator dynamics (3.24), just adding the diffusion term involving the Laplacian to the

ODE does not work because of the fact that there is an additional condition that $\sum_{i=1}^n u_i = 1$. This only works in the case when all the diffusion coefficients D_i are identical. To complete the model formulation we need to specify initial conditions,

$$u_i(x, 0) = v_i(x), \quad (3.61b)$$

and boundary conditions

$$\alpha_i \frac{\partial u_i}{\partial \mathbf{n}} + (1 - \alpha_i) u_i = 0, \quad (x, t) \in \partial\Omega \times \mathbb{R}^+, \quad (3.61c)$$

where $0 \leq \alpha_i \leq 1$. Thus $\alpha_i = 1$ corresponds to the zero-flux Neumann boundary conditions while $\alpha_i = 0$ corresponds to the homogeneous Dirichlet boundary conditions.

Examples of RD models in ecology include:

- the equation for the logistic growth of a single population distributed along a single environmental axis x , and subject to random dispersal,

$$\dot{u} = D\nabla^2 u + ru(1 - u/K), \quad (3.62)$$

where the dot represents the partial derivative with respect to time t ;

- the predator-prey model (Garvie, 2007),

$$\begin{aligned} \dot{u} &= \nabla^2 u + u(1 - u) - vh(au), \\ \dot{v} &= \delta \nabla^2 v + bv h(au) - cv, \end{aligned} \quad (3.63)$$

where $u(x, t)$ and $v(x, t)$ are the population densities of prey and predators at time t and position x , and the parameters a, b, c and δ are strictly positive. The functional response $h(\cdot)$ is assumed to be a \mathcal{C}^2 function (i.e., h is continuous and has continuous first and second derivatives) that represents the prey consumption rate per predator;

- the three-species intransitive (cyclic) competition model obtained from the RPS mean-field ODE model (3.5) of Frean and Abraham (2001) by assuming that the competing populations are spatially distributed on a line:

$$\begin{aligned} \dot{u}_1 &= \nabla^2 u_1 + u_1(\alpha_1 u_2 - \alpha_3 u_3), \\ \dot{u}_2 &= \nabla^2 u_2 + u_2(\alpha_2 u_3 - \alpha_1 u_1), \\ \dot{u}_3 &= \nabla^2 u_3 + u_3(\alpha_3 u_1 - \alpha_2 u_2), \end{aligned} \quad (3.64)$$

where u_1, u_2 and u_3 are the (non-negative) proportions of the three competing populations, and the parameters α_i denote the invasion rates. That is, an

individual of species 1 can invade another from species 2 with probability α_1 , an individual from species 2 invades another from species 3 with probability α_2 , whereas an individual from species 3 invades one from species 1 with probability α_3 . All other invasion probabilities are set to zero.

In most of the cases, it is assumed that the above RD equations are defined on a bounded domain (habitat), Ω , and are augmented with appropriate initial conditions and the no-flux boundary conditions which reflect the assumption that the individual species cannot leave the domain.

Because the reaction terms in typical RD models are usually nonlinear, the RD system is called nonlinear (or semilinear). In general, the nonlinearity makes it hard, if not impossible, to solve the RD system analytically, which is also the case with many nonlinear systems of ODEs. Thus numerical methods have an important part to play in investigating the behavior of solutions of the RD system. On the other hand, standard results from the general theory of nonlinear PDEs (see Logan (2008); Cantrell and Cosner (2003)) can be used to show that a given RD model is *well-posed*, i.e., a solution exists, the solution is unique and the solution's behavior changes continuously with the initial conditions. For example, in the single-species case, if the function f and the boundary $\partial\Omega$ of Ω are smooth and the initial condition $v(x)$ is continuous on both the interior and boundary of Ω , then Eq. (3.61) will be well-posed in the sense that it will have a unique solution $u_1(x, t)$ on $\Omega \times [0, T]$ for some $T > 0$ with $u_1(x, t)$ depending continuously on $v(x)$. Such standard results are, however, not trivial to prove.

Due to the unavailability of analytical solutions of Eq. (3.61), attempts have been made to look for numerical solutions to reveal more dynamical behaviors of the RD system. Typically, finite-difference methods are used to approximate the equation in space, equipped with some time integration method. These numerical methods can also be used to get the density values of species at each point of space in every instant of time. A major issue that arises in the use of these methods is *numerical stability*. Numerical stability concerns how errors introduced during the execution of an algorithm propagate through the method. It is a property of the numerical method rather than of the problem being solved. In a stable method, any numerical errors (e.g., round-off, truncation, discretization), introduced at some stage of the computation do not get amplified as the computation proceeds. Obviously this is very important, since errors are impossible to avoid in any numerical calculation. If errors are amplified, pretty soon they will dominate any computation (making it useless). Ensuring numerical stability usually boils down to certain constraints on the time step. For example, for classical explicit methods, the time step is restricted by the famous *Courant-Friedrichs-Lewy* (CFL) condition to ensure stability. For example, for the one-dimensional heat equation $u_t = cu_{xx}$, where $c > 0$, the CFL condition for the stability of the explicit forward Euler scheme is $\Delta t \leq \Delta x^2/2c$. Implicit schemes, on the other hand, allow for a

larger time step, but require more computations. In an unconditionally stable method, there is no restriction on the time step for obtaining a numerical solution. In the single species case (scalar form of Eq. (3.61)), existing unconditionally stable methods are all implicit methods. However, as we shall show later, these methods have conditional numerical stability conditions in the multispecies (higher dimensional) case.

3.5.3 Metapopulation models

Metapopulation theory constitutes a useful framework for explicitly incorporating spatial effects in models for population dynamics in ecology. Whereas classical population models treat local populations as closed systems (no immigration or emigration), this assumption is probably not valid for many species. Movement of individuals among populations is common and can have profound effects on the dynamics of local populations.

Metapopulation models describe an open system in which extinction and persistence of local populations depend on the movement of individuals among a set of habitat patches. Many species often inhabit discrete areas of the landscape (ponds, woodlands in agricultural landscapes, and so on) where demographic processes occur within patches, and dispersal occurs between them. The movement of organisms between patches leads to local differences in colonization and extinction rates, which can influence the spatial distribution of a species over time (Gibert and Yeakel, 2019; Hanski and Gilpin, 1997).

Levins (1969), modelling the dynamics of insect pests across a region within which local populations fluctuate asynchronously, coined the term metapopulation to describe a population comprising many subpopulations, living in spatially discrete habitats (patches) connected to each other through dispersal or migration (Hanski, 1998).

Levins' original theoretical model incorporated a series of identical habitat patches that are classified as either occupied by subpopulations of individuals or empty at any point in time. The model is a differential equation that specifies how patches become occupied or vacant through time and predicts the percentage of habitat patches that would hold populations at equilibrium. There are two key parameters: the local extinction rate and the migration rate of individuals to other patches. If p denotes the proportion of occupied patches at any time t , the equation for the model is,

$$\frac{dp}{dt} = mp(1-p) - ep, \quad (3.65)$$

where m is the migration rate (the probability that migrants from any given subpopulation reach another site), and e is the rate at which local populations (in a

single patch) go extinct. The model is analyzed to give the number (proportion) of occupied patches at equilibrium.

If the colonization rate is larger than the extinction rate, $m > e$, then Eq. (3.65) admits a unique equilibrium fraction p^* of occupied patches given by $p^* = 1 - e/m$ which is globally stable (Amarasekare, 1998). Global stability means that the fraction of occupied patches eventually approaches its equilibrium value p^* for all possible initial conditions (except $p = 0$), and returns to this equilibrium after any size perturbation away from equilibrium (except one that gives $p = 0$). The important and intriguing conclusion from the Levins model is that the persistence of the entire metapopulation is guaranteed as long as individuals can successfully disperse from one patch to another and this migration rate exceeds the local extinction rate.

Note that the simple Levins model describes the state of the population by a scalar variable, namely the fraction of occupied habitat patches. But in doing so the model ignores two important forms of population structure. One structure that is ignored is the distribution of local population sizes, as only the presence or absence of the species in the habitat patches are modelled. This is why the original Levins model and its derivatives have also been called *patch-occupancy* models or *extinction-colonization* models or *presence-absence* models (Fahrig, 2007).

The second structure missing from the Levins model is the spatial configuration of the landscape, as the model assumes an infinitely large network of discrete habitat patches of equal size and equal connectivity.

Not surprisingly, the simplicity of the Levins model has attracted criticism because of its lack of biological realism (Harrison and Taylor, 1997). However, interest in his conclusion about persistence has led to a number of models of metapopulation dynamics with increasing sophistication. For example, Hanski and Ovaskainen (2000) extended Levins' formulation to realistic landscapes in which the habitat patches may differ from each other, e.g., in terms of their size, quality and connectivity to the remaining network. Metz and Diekmann (1986) formulated and solved a model incorporating explicit local population sizes. Other models have incorporated several realistic biological processes, such as the rescue effect (Hanski, 1983) (where occupied patches on the brink of extinction are rescued by immigration of individuals into the patch (Brown and Kodric-Brown, 1977)), patch preference effect (Etienne, 2000) (where dispersers have a preference for either occupied or empty patches), Allee effect (Amarasekare, 1998) (where the per capita growth rate of populations at low densities increases with an increase in density), and multispecies competition (Levin, 1974; Tilman, 1994).

3.5.4 ODEs vs PDEs in modelling spatial dynamics

We have seen in the previous section that ODEs can still be used to study spatial effects on the dynamics of an ecological community especially if the community is considered as a collection of discrete well-mixed habitat patches that interact only via dispersal of individuals. As long as the factors driving inter-patch migrations can be reasonably modelled mathematically, ODEs remain a viable and relatively simple option for characterizing spatially structured systems.

3 However, in some settings, the particular geometry of a habitat patch, its size and the permeability of its edges (or boundaries) are potentially important in dictating system behavior. For example, in marine communities, it has been suggested that changes in the ratio of perimeter length to area, and patch shape, might affect the number of species able to inhabit a patch (Koivisto et al., 2011). ODEs provide an insufficient description when continuous aspects of geometry are important or the well-mixed assumption is obviously at odds with the nature of the ecological system at hand (Daun et al., 2008). In such a case, PDEs (or RD equations) provide an appropriate framework to model such systems.

PDEs have also been used to lend insight into numerous fundamental population processes including dispersal, ecological invasions, the effect of habitat geometry and size, dispersal-mediated coexistence, and the emergence of spatial patterns (Holmes et al., 1994). As with ODEs, formal mathematical theory has been developed for many types of PDEs, unfortunately this theory is more complicated, and often farther removed from insights about the dynamic structure of the underlying system than is the theory for ODEs (Daun et al., 2008). Many of the PDEs relevant to detailed ecological modelling are too complex for analytical treatment and therefore the output that can be feasibly obtained from such models is limited to numerical simulations. However, their computations are more demanding, with simulations often requiring a larger computing platform than personal computers. Mathematical theory may be useful in selecting appropriate numerical simulation methods and may facilitate accuracy and efficiency of simulations, even when this theory cannot give any direct information about possible model behavior.

PDEs and ODEs are often complimentary modelling tools and may coexist in analysis of the same system, especially when one is attempting to include several scales of description. Due to the difficulty in solving a PDE, there are instances when the large time behavior of solutions of the PDE decay to spatially homogeneous functions of time which are solutions of the associated ODE. In this case, the qualitative properties of solutions of the PDE are determined, at least for large t , by the phase portrait of the associated ODE. The question to ask is, when and under what conditions can PDE (3.66) be replaced by ODE (3.67)? According to Conway et al. (1978), the answer to this question depends upon whether an invariant region for the PDE exists. An invariant region is a subset of the phase space such that if the

values of the solution of the PDE are contained in the region for one value of t the same is true for all later times. It has already been shown that for a set Σ to be invariant for the PDE, it must be a rectangle that is invariant for the associated ODE (Conway et al., 1978). Recall that the reaction term $f(\mathbf{x})$ that is used in this work is the replicator dynamics.

In this work, the PDE system that is used is

$$\frac{\partial x_i}{\partial t} = D_i \nabla^2 x_i + f_i(\mathbf{x}) \quad (3.66)$$

where $\mathbf{x} = (x_1, \dots, x_n)^\top$, $f_i(\mathbf{x}) = x_i(\mathbf{T}\mathbf{x})_i$ is the replicator dynamics and the diffusion coefficients D_i are such that $D_i = D$ (so that $\sum_{i=1}^n x_i = 1$). The associated ODE is given by

$$\frac{dx_i}{dt} = x_i(\mathbf{T}\mathbf{x})_i. \quad (3.67)$$

We have already shown in Lemma 3.1 that the unit simplex S^n is invariant under the flow of (3.67). Hence the RD system (3.66) admits an invariant set $\Sigma = S^n$.

Let $\sigma = D\lambda - M$, where $-\lambda$ is the first nonzero (smallest positive) eigenvalue of the Laplacian subject to homogeneous Neumann boundary conditions on the spatial domain considered and M is the maximum norm for $\nabla f(\mathbf{x})$ (the gradient or Jacobian of f) for $\mathbf{x} \in S^n$. It has been shown that for $\sigma > 0$, the qualitative behaviour of solutions of (3.66) is really determined by the behaviour of the associated ODE (3.67) (Conway et al., 1978). However, to check whether $\sigma > 0$ for models of many multidimensional systems is a nontrivial task and we are often resigned to solving the PDE (3.66) itself instead of its associated ODE (3.67).

3.6 Numerical solution of PDEs

Choosing the right method for the numerical solution of Eq. (3.66) subject to boundary conditions is very important. The overall goal is to obtain a solution with sufficiently small error in a sufficiently small time (or with limited available computational resources).

The most powerful and generally applicable algorithms for the approximate solution of PDEs rely on the concept of *discretization*, whereby the PDE under consideration is replaced by equations that involve a finite number of unknowns. There are several different ways to discretize a PDE. The simplest method uses finite difference approximations for the partial derivatives in the PDE. This gives rise to a large algebraic system of equations to be solved in place of the PDE, something that is easily solved on a computer.

Let us consider the scalar PDE

$$\frac{\partial u}{\partial t} = d\nabla^2 u + f(u) \quad (3.68)$$

coupled with the appropriate boundary conditions. Here u denotes the concentration (or density) of a chemical/biological species of interest at any time t , and d is the diffusion coefficient.

To solve (3.68) numerically using a finite difference method, the first step is to apply the *method of lines* approach (Hyman, 1976), where the PDE is discretized first in space and then in time. That is, we first approximate the spatial derivative by finite difference formulas from a Taylor series expansion. This reduces the PDE to a semi-discrete form, consisting of a system of nonlinear ODEs in time,

$$\mathbf{u}_t = C\mathbf{u} + F(\mathbf{u}). \quad (3.69)$$

Here, \mathbf{u} is a vector of the concentration u at the grid points, C is a constant matrix arising out of the discretization of the Laplacian plus boundary conditions and $F(\mathbf{u})$ is a vector of the nonlinear reaction term evaluated at the grid points.

Next we discretize in time by, again, approximating the time derivative in the ODE system with finite difference formulas. The way we discretize the time derivative (i.e., whether we approximate the derivative using forward, backward or central differences etc.) gives rise to different finite difference schemes like, the FTCS (Forward Time Centered Space), CN (Crank-Nicolson), FSTS (fractional step θ -scheme), etc. The resulting finite difference formulation is then solved, instead of the PDE, to give rise to the numerical solution.

The error between the numerical solution and the exact solution is determined by the error between the true (analytical) derivative and its finite difference approximation. This error is called the *discretization error* or *truncation error*. The term truncation error reflects the fact that a finite part of a Taylor series is used in the approximation.

There are three important features that a derived finite difference scheme must possess: *consistency*, *stability* and *convergence*. A finite difference approximation is considered consistent if by reducing the mesh (space) and time step size, the truncation error could be made to approach zero. The scheme is said to be stable if any numerical errors introduced at any stage of the computation decay as the computation proceeds from one time step to the next. Stability of a finite difference approximation is assessed using von Neumann stability analysis. Finally, convergence means that the numerical solution from the finite difference equations approaches the true solution of the PDE when the mesh is refined. The famous *Lax equivalence theorem* states that a consistent finite difference approximation for a well-posed PDE is convergent if and only if it is stable.

Stability is thus one of the most important properties of a numerical scheme and it plays a major role in determining which method to use. Several researchers propose the use of implicit schemes given the fact that such schemes have already been proven to be unconditionally stable for the linear diffusion equation. The belief is that this unconditional stability extends to the full RD equation with the (in general) nonlinear reaction term, although, as we shall see, this is only true subject to certain conditions on the reaction term.

Implicit schemes also could permit the use of larger time steps compared to explicit schemes whose time step is very limited by the so-called CFL (Courant–Friedrichs–Lewy) condition. The main drawback of implicit schemes, especially for nonlinear RD systems, is the computational complexity in their implementation.

Another important concept that arises in the derivation of finite difference schemes for the solution of (3.68) is the notion of *stiffness*. From the method of lines approach, it has been stated in the literature that the choice of whether to use an explicit or implicit scheme for the time integration of the ODE system (3.69) depends on whether the ODE system is stiff or not.

Several attempts at a rigorous definition for the stiffness of an ODE system exist in the literature. Among all these definitions, it is generally agreed that the essence of stiffness consists of the fact that the exact solution being sought includes components with vastly differing time scales that are hard to follow by the numerical solution (Brugnano et al., 2011).

In other words, the spectrum of the linearized system (or Jacobian matrix) is such that some eigenvalues have a very large negative real part, whereas other eigenvalues are much smaller in magnitude. Hence some components of the solution decay much more rapidly than others. Interestingly, the component of the exact solution corresponding to such large negative eigenvalues is almost irrelevant, as it becomes almost instantaneously tiny. However, the presence of such an eigenvalue continues to render the numerical solution to the system very difficult even to the point of exhausting any available computing resources.

Lambert (1992) points out that stiffness occurs when stability requirements, rather than those of accuracy, severely constrain the time step length. A familiar consequence of this is expressed by Hairer and Wanner (1996) who state that an ODE system is stiff whenever standard explicit methods do not work or are unacceptably time consuming, because the time step is forced down to be very small, even in regions where the solution is smooth.

We proceed to briefly describe the Von-Neumann stability analysis of some popular finite difference schemes applied to scalar linear RD equations.

3.7 A von Neumann stability analysis

3.7.1 Background

Studying the stability of finite difference schemes has a long history. Courant et al. (1928) showed in their pioneering work that the stability of a finite difference scheme used for the solution of a PDE is obtained only if the ratio of the mesh widths in different directions satisfies certain inequalities. Since then, these inequalities are known as the CFL (Courant-Friedrichs-Lewy) conditions.

3

Later, Charney et al. (1950), while attempting to answer the question of how to prevent the amplification of a disturbance that may be introduced to a system, used the method of Courant et al. (1928) to derive a criterion that ensures that no such amplification occurs for discretized linear PDEs with constant coefficients. This attempt resulted in a rigorous method for investigating the stability behavior of numerical schemes which, in the literature, is often referred to as the von Neumann stability analysis (Ehlers et al., 2013).

This approach is based on the Fourier series (transform) expansion of the numerical solution, or error, in a spatial frequency domain and studies the behavior of the Fourier coefficients as time increases. Unstable schemes cause a growth in the coefficients. A numerical scheme is called stable if the generated numerical solution always remains in a bounded neighborhood of the initial condition.

The use of the Fourier transform is supported by Parseval's identity (Thomas, 1995), which states that the norm of the solution and its transform are equal in their respective spaces. Thus, the boundedness of the Fourier transform of the solution is equivalent to the boundedness of the solution itself.

To determine the conditions under which this prerequisite is satisfied, one has to first assemble the so-called amplification factor (or matrix for systems), which is a number (or matrix, for systems) relating the Fourier transform of the solution vectors of the system in two consecutive time steps.

Subsequently, it can be shown that the numerical solution may be stable only if the magnitude (spectral radius) corresponding to the amplification factor (matrix) remains smaller than unity. Hence, to keep the magnitude (spectral radius) of the amplification factor (matrix) smaller than unity becomes the necessary stability condition for the scheme. More details on this can be found in Thomas (1995).

Because Fourier transforms are used, von Neumann stability analysis is restricted to linear equations with constant coefficients, uniform grids and periodic boundary conditions (Wesseling, 2001). This restriction thus leaves us in an uncomfortable situation of hoping that the results obtained from this analysis extend to the com-

plicated, nonlinear mathematical models of interest and this fact should not be forgotten.

For linear PDEs that are posed with non-periodic boundary conditions, a rigorous stability analysis is more difficult, but the von Neumann method still provides a useful way of weeding out obviously unsuitable schemes. Moreover, for problems with variable coefficients, the method is applicable locally by replacing the variable coefficients by constants, because instability is usually a local phenomenon.

Finally, when dealing with nonlinear problems, the method can be used for the locally linearized problem to provide initial guidance on the stability limits; then numerical tests should be performed to confirm the stability restrictions for the nonlinear problem. This decision has been made considering that although the linear stability is not a sufficient condition for guaranteeing the nonlinear stability, it is still a necessary condition for achieving the nonlinear stability (Hirsch, 1988).

3.7.2 Definition of stability

Since the von Neumann method is restricted to linear PDEs with constant coefficients, our stability analysis in this section will be for finite difference schemes applied to the scalar linear RD equation

$$\frac{\partial u}{\partial t} = d\nabla^2 u + au \quad (3.70)$$

where a is a real constant. For simplicity, let us consider Eq. (3.70) in a one-dimensional spatial domain although the results will analogously hold in three spatial dimensions. Thus, the version of Eq. (3.70) that we use takes the form

$$\frac{\partial u}{\partial t} = d \frac{\partial^2 u}{\partial x^2} + au. \quad (3.71)$$

We start by giving a formal definition of stability. To do this, consider a two-level finite difference scheme for solving (3.71) on a subset of \mathbb{R} that takes the form

$$\mathbf{u}^{n+1} = Q\mathbf{u}^n, \quad n \geq 0, \quad (3.72)$$

where $n+1$ and n denote the time levels t_{n+1} and t_n , respectively. Stability of the difference scheme (3.72) is defined as follows Thomas (1995);

Definition 3.9. *The difference scheme (3.72) is said to be stable with respect to the l_2 norm if there exist positive constants Δx_0 and Δt_0 and non-negative constants K and β so that*

$$\|\mathbf{u}^{n+1}\|_{l_2} \leq Ke^{\beta t} \|\mathbf{u}^0\|_{l_2} \quad (3.73)$$

for $0 \leq t = (n+1)\Delta t \leq T$ for any T , $0 < \Delta x \leq \Delta x_0$ and $0 < \Delta t \leq \Delta t_0$, and where

$$\|\mathbf{u}^n\|_{\ell_2} = \left(\Delta x \sum_j |u_j^n|^2 \right)^{1/2}. \quad (3.74)$$

The above definition of stability implies that for a difference scheme to be stable, the solutions to the difference equation must be exponentially bounded.

3.7.3 The von Neumann stability condition

A von Neumann stability analysis makes use of the discrete Fourier transform (DFT) defined as follows (Thomas, 1995);

Definition 3.10. For a function $\mathbf{u}^n = (u_j^n)_{j \in \mathbb{Z}}$ defined at the grid points j , its discrete Fourier transform $\hat{\mathbf{u}}^n$ is defined as

$$\hat{\mathbf{u}}^n(\xi) = \frac{1}{\sqrt{2\pi}} \sum_{j \in \mathbb{Z}} e^{-ij\xi} u_j^n, \quad i = \sqrt{-1}, \quad (3.75)$$

for $\xi \in [-\pi, \pi]$.

The importance of using the DFT in the analysis of the stability of difference schemes can be seen when applied to the shift operator \mathcal{S} defined by

$$\mathcal{S}_+ \mathbf{u}^n := (u_{j+1}^n)_{j \in \mathbb{Z}} \quad \text{and} \quad \mathcal{S}_- \mathbf{u}^n := (u_{j-1}^n)_{j \in \mathbb{Z}}$$

That is,

$$\begin{aligned} \widehat{\mathcal{S}_+ \mathbf{u}^n}(\xi) &= \frac{1}{\sqrt{2\pi}} \sum_{j \in \mathbb{Z}} e^{-ij\xi} u_{j+1}^n = \frac{1}{\sqrt{2\pi}} \sum_{j \in \mathbb{Z}} e^{-i(j-1)\xi} u_j^n \quad (j \rightarrow j-1) \\ &= \frac{1}{\sqrt{2\pi}} \sum_{j \in \mathbb{Z}} e^{-ij\xi} e^{i\xi} u_j^n = e^{i\xi} \frac{1}{\sqrt{2\pi}} \sum_{j \in \mathbb{Z}} e^{-ij\xi} u_j^n \\ &= e^{i\xi} \hat{\mathbf{u}}^n(\xi). \end{aligned}$$

Similarly

$$\widehat{\mathcal{S}_- \mathbf{u}^n}(\xi) = e^{-i\xi} \hat{\mathbf{u}}^n(\xi).$$

Thus, taking the DFT of the left- and right-hand side of Eq. (3.72), the difference scheme can be transformed to the form

$$\hat{\mathbf{u}}^{n+1} = G(\xi) \hat{\mathbf{u}}^n \quad (3.76)$$

where the quantity $G(\xi)$ is known as the amplification factor of the difference scheme. A necessary and sufficient condition for the stability of the difference scheme (3.72) is given in the following proposition.

Proposition 3.2. (Thomas, 1995, Proposition 3.1.7) Consider the difference scheme (3.72) with amplification factor $G(\xi)$. The scheme is stable according to Definition 3.9 if and only if there exist positive constants Δt_0 , Δx_0 and C so that

$$|G(\xi)| \leq 1 + C\Delta t \quad (3.77)$$

for $0 < \Delta t \leq \Delta t_0$, $0 < \Delta x \leq \Delta x_0$ and all $\xi \in [-\pi, \pi]$.

Inequality (3.77) is called the von Neumann stability condition and a scheme whose amplification factor satisfies this condition is said to be *von Neumann-stable*.

Equipped with the DFT and Proposition 3.2, we are now in position to analyze the stability of the FTCS scheme, the CN scheme and the fractional step θ -scheme for Eq. (3.71).

3.7.4 Forward in time, centered in space

The FTCS scheme, also known as the explicit Euler scheme, is an explicit finite difference scheme that is first order accurate in time. A discretization of Eq. (3.71) using the FTCS scheme is given by

$$\frac{u_j^{n+1} - u_j^n}{\Delta t} = d \left(\frac{u_{j+1}^n - 2u_j^n + u_{j-1}^n}{\Delta x^2} \right) + \alpha u_j^n, \quad (3.78)$$

where the exponents on u indicate the time level and the subscripts indicate the spatial grid point. Equation (3.78) can be rewritten as

$$u_j^{n+1} = r(S_+ u_j^n + S_- u_j^n) + (1 - 2r + \alpha \Delta t) u_j^n \quad (3.79)$$

where $r = \frac{d\Delta t}{\Delta x^2}$. Taking the DFT of both sides of Eq. (3.79) leads to

$$\begin{aligned} \hat{u}^{n+1}(\xi) &= \left(r(e^{i\xi} + e^{-i\xi}) + (1 - 2r + \alpha \Delta t) \right) \hat{u}^n(\xi) \\ &= (2r(\cos \xi - 1) + 1 + \alpha \Delta t) \hat{u}^n(\xi) \\ &= \left(1 - 4r \sin^2 \frac{\xi}{2} + \alpha \Delta t \right) \hat{u}^n(\xi). \end{aligned} \quad (3.80)$$

From (3.80), the amplification factor of the FTCS scheme is given by

$$G(\xi) = 1 - 4r \sin^2(\xi/2) + a\Delta t. \quad (3.81)$$

Thus

$$|G(\xi)| = |1 - 4r \sin^2(\xi/2) + a\Delta t| \leq |1 - 4r \sin^2(\xi/2)| + |a|\Delta t.$$

If we restrict r so that

$$|1 - 4r \sin^2(\xi/2)| \leq 1, \quad (3.82)$$

then,

$$|G(\xi)| \leq 1 + |a|\Delta t,$$

which is the von Neumann stability condition inequality with $C = |a|$. Thus the FTCS scheme is stable whenever (3.82) is satisfied. That is

$$|1 - 4r \sin^2(\xi/2)| \leq 1 \Leftrightarrow r \leq 1/2.$$

Hence the FTCS is a conditionally stable scheme and the condition for stability is

$$0 < r = \frac{d\Delta t}{\Delta x^2} \leq 1/2.$$

This is the well-known CFL (Courant-Friedrichs-Lewy) condition for the stability of the FTCS scheme.

3.7.5 The Crank–Nicolson scheme

The Crank–Nicolson (CN) scheme is a second order accurate in time implicit scheme commonly employed for the time integration of initial value problems (IVPs). A CN discretization of Eq. (3.71) is given by

$$\begin{aligned} \frac{u_j^{n+1} - u_j^n}{\Delta t} &= \frac{d}{2} \left(\frac{u_{j+1}^{n+1} - 2u_j^{n+1} + u_{j-1}^{n+1}}{\Delta x^2} \right) + \\ &\frac{d}{2} \left(\frac{u_{j+1}^n - 2u_j^n + u_{j-1}^n}{\Delta x^2} \right) + \frac{a}{2} (u_j^{n+1} + u_j^n). \end{aligned} \quad (3.83)$$

Equation (3.83) can be rewritten as

$$\begin{aligned} \left(1 + r - \frac{a\Delta t}{2} \right) u_j^{n+1} - \frac{r}{2} (S_+ u_j^{n+1} + S_- u_j^{n+1}) &= \left(1 - r + \frac{a\Delta t}{2} \right) u_j^n \\ &+ \frac{r}{2} (S_+ u_j^n + S_- u_j^n), \end{aligned} \quad (3.84)$$

where $r = d\Delta t/\Delta x^2$. Taking the DFT of Eq. (3.84) leads to the simplified form

$$\left(1 + 2r \sin^2 \frac{\xi}{2} - \frac{\alpha \Delta t}{2}\right) \hat{\mathbf{u}}^{n+1} = \left(1 - 2r \sin^2 \frac{\xi}{2} + \frac{\alpha \Delta t}{2}\right) \hat{\mathbf{u}}^n. \quad (3.85)$$

From Eq. (3.85), the amplification factor of the CN scheme is given by

$$G(\xi) = \frac{1 - \left(2r \sin^2 \frac{\xi}{2} - \frac{\alpha \Delta t}{2}\right)}{1 + \left(2r \sin^2 \frac{\xi}{2} - \frac{\alpha \Delta t}{2}\right)}. \quad (3.86)$$

Note from Eq. (3.86) that if $\alpha \leq 0$, the amplification factor G can be written as

$$G(\xi) = \frac{1-p}{1+p}, \quad \text{where } p = 2r \sin^2 \frac{\xi}{2} - \frac{\alpha \Delta t}{2} \geq 0. \quad (3.87)$$

Thus $|G(\xi)| < 1$ for all $\xi \in [-\pi, \pi]$. Hence, from Proposition 3.2, the CN-scheme is unconditionally stable.

However, if $\alpha > 0$, then as Δt approaches $(1 + 2r \sin^2(\xi/2))/\alpha$, $|G| \rightarrow \infty$ and the CN-scheme will be unstable. Thus the unconditional stability of the CN-scheme is only guaranteed when $\alpha \leq 0$.

3.7.6 The fractional step theta scheme

The FSTS is an operator splitting technique introduced by Glowinski (2003) for the time integration of initial value problems. The method has also been used by Madzvamuse and Chung (2014) to solve a system of RD equations. To introduce the scheme, consider an IVP

$$u_t = \mathcal{A}(u), \quad u(0) = u_0, \quad (3.88)$$

where \mathcal{A} is a (possibly nonlinear) operator that has a nontrivial decomposition

$$\mathcal{A} = \mathcal{A}_1 + \mathcal{A}_2. \quad (3.89)$$

To derive the FSTS, the time step is divided into three portions and over each portion, the operators \mathcal{A}_1 and \mathcal{A}_2 are alternately treated implicitly and explicitly.

Let $\theta \in]0, 1/2[$ and divide the time interval $[n, n+1]$ into three subintervals $[n, n+\theta]$, $[n+\theta, n+1-\theta]$ and $[n+1-\theta, n+1]$. A FSTS for Eq. (3.88) proceeds as follows:

Assuming u^n is known, compute $u^{n+\theta}$, $u^{n+1-\theta}$ and u^{n+1} as follows:

Step 1: Solve for $\mathbf{u}^{n+\theta}$ using:

$$\frac{\mathbf{u}^{n+\theta} - \mathbf{u}^n}{\theta\Delta t} = \mathcal{A}_1(\mathbf{u}^{n+\theta}) + \mathcal{A}_2(\mathbf{u}^n)$$

Step 2: Solve for $\mathbf{u}^{n+1-\theta}$ using:

$$\frac{\mathbf{u}^{n+1-\theta} - \mathbf{u}^{n+\theta}}{(1-2\theta)\Delta t} = \mathcal{A}_1(\mathbf{u}^{n+\theta}) + \mathcal{A}_2(\mathbf{u}^{n+1-\theta})$$

Step 3: Solve for \mathbf{u}^{n+1} using:

$$\frac{\mathbf{u}^{n+1} - \mathbf{u}^{n+1-\theta}}{\theta\Delta t} = \mathcal{A}_1(\mathbf{u}^{n+1}) + \mathcal{A}_2(\mathbf{u}^{n+1-\theta})$$

In the case of RD equations, it is natural to take the operators \mathcal{A}_1 and \mathcal{A}_2 to be the diffusion and reaction terms, respectively. Thus, a FSTS for Eq. (3.71) is given by

$$\left\{ \begin{array}{l} \frac{u_j^{n+\theta} - u_j^n}{\theta\Delta t} = d \frac{[u_{j+1}^{n+\theta} - 2u_j^{n+\theta} + u_{j-1}^{n+\theta}]}{\Delta x^2} + au_j^n, \\ \frac{u_j^{n+1-\theta} - u_j^{n+\theta}}{(1-2\theta)\Delta t} = d \frac{[u_{j+1}^{n+\theta} - 2u_j^{n+\theta} + u_{j-1}^{n+\theta}]}{\Delta x^2} + au_j^{n+1-\theta}, \\ \frac{u_j^{n+1} - u_j^{n+1-\theta}}{\theta\Delta t} = d \frac{[u_{j+1}^{n+1} - 2u_j^{n+1} + u_{j-1}^{n+1}]}{\Delta x^2} + au_j^{n+1-\theta}. \end{array} \right. \quad (3.90)$$

Define $r = \Delta t/\Delta x^2$. The three equations in (3.90) can be rewritten as

$$\left\{ \begin{array}{l} (1 + 2rd\theta)u_j^{n+\theta} - rd\theta(u_{j+1}^{n+\theta} + u_{j-1}^{n+\theta}) = (1 + a\theta\Delta t)u_j^n, \\ (1 - (1 - 2\theta)a\Delta t)u_j^{n+1-\theta} = (1 - 2(1 - 2\theta)rd)u_j^{n+\theta} + (1 - 2\theta)rd(u_{j+1}^{n+\theta} + u_{j-1}^{n+\theta}), \\ (1 + 2rd\theta)u_j^{n+1} - rd\theta(u_{j+1}^{n+1} + u_{j-1}^{n+1}) = (1 + a\theta\Delta t)u_j^{n+1-\theta}. \end{array} \right. \quad (3.91)$$

Taking the DFT of Eq. (3.91) and combining the three resulting equations gives

$$\hat{\mathbf{u}}^{n+1} = \frac{(1 + a\theta\Delta t)^2 (1 - 4rd(1 - 2\theta) \sin^2(\frac{\xi}{2}))}{(1 - a(1 - 2\theta)\Delta t) (1 + 4rd\theta \sin^2(\frac{\xi}{2}))^2} \hat{\mathbf{u}}^n. \quad (3.92)$$

The amplification factor for the FSTS will therefore be given by

$$G = \frac{(1 + a\theta\Delta t)^2 (1 - 4rd(1 - 2\theta)\sin^2(\frac{\xi}{2}))}{(1 - a(1 - 2\theta)\Delta t)(1 + 4rd\theta\sin^2(\frac{\xi}{2}))^2}. \quad (3.93)$$

For stability, we need to compute $|G|$. Now,

$$|G| = \left| \frac{1 + a\theta\Delta t}{1 - a(1 - 2\theta)\Delta t} \right| \cdot \left| \frac{1 - 4rd(1 - 2\theta)\sin^2(\frac{\xi}{2})}{1 + 4rd(2\theta + 4rd\theta^2\sin^2(\frac{\xi}{2}))\sin^2(\frac{\xi}{2})} \right| \cdot |1 + a\theta\Delta t|.$$

Assume that $a \leq 0$ and $\frac{1}{4} \leq \theta \leq \frac{1}{3}$. Then

$$\left| \frac{1 + a\theta\Delta t}{1 - a(1 - 2\theta)\Delta t} \right| \leq 1$$

follows from $a \leq 0$ and $\theta \leq \frac{1}{3}$, and

$$\left| \frac{1 - 4rd(1 - 2\theta)\sin^2\frac{\xi}{2}}{1 + 4rd(2\theta + 4rd\theta^2\sin^2\frac{\xi}{2})\sin^2\frac{\xi}{2}} \right| \leq 1$$

follows from $a \leq 0$ and $\theta \geq \frac{1}{4}$. Hence

$$|G| \leq 1 + \theta|a|\Delta t \leq 1 + \frac{1}{3}|a|\Delta t, \quad (3.94)$$

which is the von Neumann stability condition.

Thus, if $a \leq 0$ and $\theta \in [1/4, 1/3]$, then from Proposition 3.2, the FSTS is linearly unconditionally stable. In addition, the FSTS is second order accurate in time only if $\theta = 1 - 1/\sqrt{2}$. Note that $1/4 < 1 - 1/\sqrt{2} < 1/3$. However, if $a > 0$, then as Δt approaches $1/a(1 - 2\theta)$, $|G| \rightarrow \infty$ and the FSTS will be unstable. Thus the unconditional stability of the FSTS is only guaranteed when $a \leq 0$ and $1/4 \leq \theta \leq 1/3$.

3.7.7 Conclusions

From the stability analysis of the FTCS, CN and FSTS finite difference schemes applied to the linear RD equation, it is clear that the explicit FTCS scheme is conditionally stable with the time step restricted by the CFL condition. Both the implicit CN and FSTS schemes could be unconditionally stable, with no restriction on the time step size, provided the reaction term of the equation satisfies certain conditions, in particular, the coefficient of the linear reaction term should be non-

positive and $1/4 \leq \theta \leq 1/3$ for the FSTS. This results from this analysis, although carried out when Eq. (3.71) is restricted to a one-dimensional spatial domain, analogously hold in higher spatial dimensions. However, many mathematical models of ecological communities are not scalar equations and are generally nonlinear. It is not clear whether the stability conditions derived from an analysis of the scalar linear RD equation would still hold when the same schemes are applied to the multidimensional nonlinear RD models commonly encountered in ecology.

Thus, in cases where the dynamics of an ecological community can only be modelled by a system of nonlinear RD equations, questions regarding the stability of finite difference schemes that can be used to obtain the numerical solution of the model still remain. This is because analyzing the stability of a numerical scheme applied to a nonlinear RD system can be a complicated task. In addition, the available stability conditions obtained from a linear analysis may not necessarily apply to the nonlinear problem. This is due to the fact that linear stability is a necessary condition for nonlinear problems but is certainly not sufficient (Hirsch, 1988). Thus, later in this thesis, we shall explore the question of stability of finite difference schemes when applied to systems of nonlinear RD equations to try and establish some necessary and possibly sufficient conditions under which some of the well-known implicit schemes are stable.

4

The method of triads

The material of this chapter is based on the following publications:

- Muyinda, N., Baetens, J.M., De Baets, B., and Rao, S. (2020). Using intransitive triads to determine final species richness of competition networks. *Physica A - Statistical Mechanics and its Applications*, 540. <https://doi.org/10.1016/j.physa.2019.123249>
- Muyinda, N., De Baets, B., and Rao, S. (2020). Non-king elimination, intransitive triad interactions, and species coexistence in ecological competition networks. *Theoretical Ecology*, 13, 385–397. <https://doi.org/10.1007/s12080-020-00459-6>

4.1 Introduction

One of the central concerns in community ecology is how species coexist as they do in the face of competition. In the quest for mechanisms of species coexistence, competitive intransitivity has been identified as an important mechanism

that can theoretically lead to the coexistence of multi-species communities despite intense competition among species (Gilpin, 1975; May and Leonard, 1975; Laird and Schamp, 2006; Vandermeer, 2011). In addition, the discovery of compelling empirical examples of competitive intransitivity in a range of taxa including bacteria (Kerr et al., 2002), lizards (Sinervo and Lively, 1996), coral reef invertebrates (Buss and Jackson, 1979) and plants (Lankau et al., 2011) have further aroused interest in the issue.

Studies have shown that intransitive competition not only promotes species richness within a community, but also fosters coexistence among highly dissimilar species with different competitive strategies by creating some form of competitive equivalence among the species (Laird and Schamp, 2006; Soliveres et al., 2015). However, despite the fact that indices of intransitivity have been key in demonstrating the effect of intransitive competition on species coexistence, ecologists have been unable to use these indices to predict the final species richness or final species composition of competition networks that are modelled by complete directed graphs (or tournaments). Indeed, there are tournaments that have the same level of intransitivity, as measured by a particular index, but that evolve to a completely different final species richness. An example of such a case is shown in Fig. 4.1, where all three 5-species tournaments have a relative intransitivity value of $4/5$, but two tournaments evolve to one of their intransitive triads, whereas the third tournament supports coexistence of all the five species. This implies that the final species richness cannot be derived from the degree of intransitivity provided by the current indices. It further suggests that species coexistence may be influenced by certain topological variations that are not accounted for (or captured) in the current indices.

Laird and Schamp (2018b) have stated that predicting the final species richness in competition networks will require the development of metrics that explore the ranking of species involved in intransitive structures, not just aspects of their presence, absence or frequency. In that regard, they proposed the two binary indices, unbeatability (u) and always-beatability (a). All tournaments with $u = 1$ are expected to have a final species richness of 1, whereas for an n -species tournament with $a = 1$, the final species richness is at most $n - 1$. However, predicting the final species richness in tournaments with no unbeatable species remains an open problem.

In a two-dimensional spatial domain in which three species compete intransitively for survival, coexistence is characterized by the formation of spiral wave patterns and the interactions among the different species are characterized by the entanglement of the corresponding spirals (Reichenbach et al., 2007; Cheng et al., 2014). From numerical simulations of a 5-species cyclic system, Cheng et al. (2014) observed that the competition among the species at the microscopic level leads to the emergence of mesoscopic groups, each involving three species, and it is the interaction among these groups that fundamentally determine the final

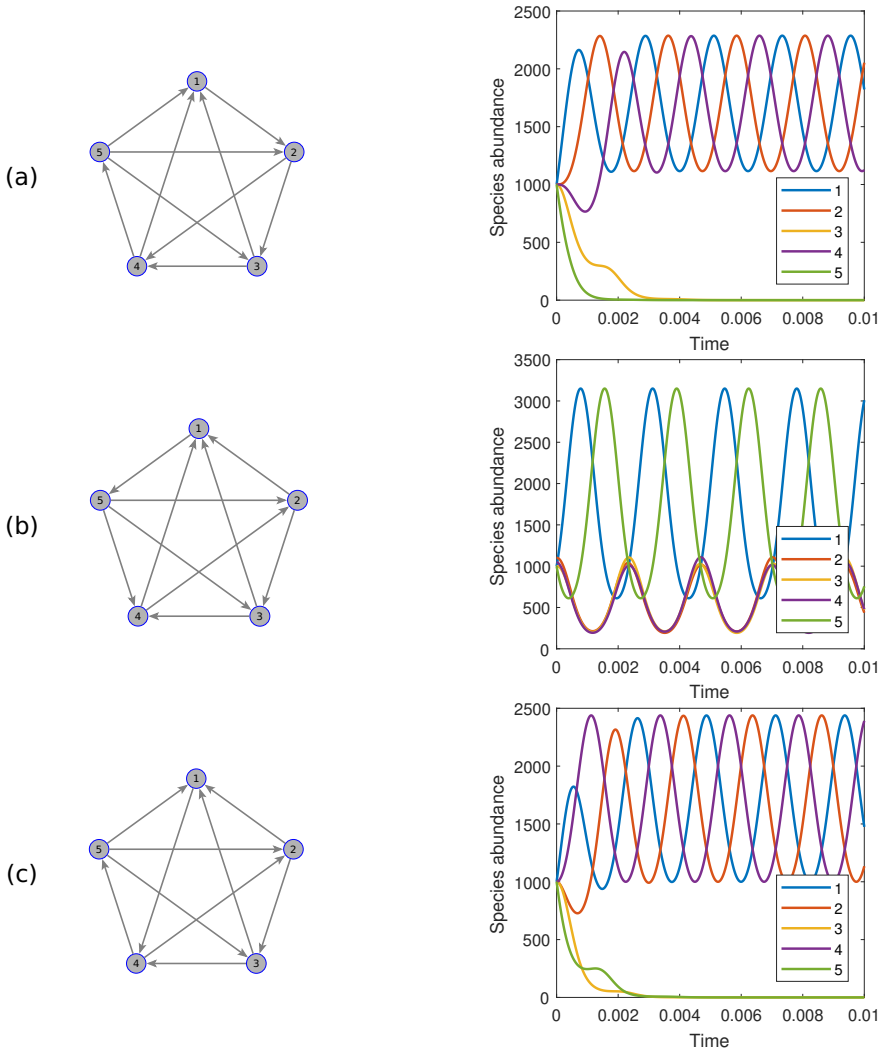


Figure 4.1: Three five-species tournaments, each with a relative intransitivity value of 4/5. A numerical simulation of the ODE system (3.13) for each tournament shows that the tournaments in (a) and (c) collapse to one of their intransitive triads, whereas the tournament in (b) supports coexistence of all five species.

species richness. These mesoscopic groups are the intransitive triads of the competition network.

In this chapter, we propose an approach that makes use of the interactions among the intransitive triads in a tournament to deduce the final species richness and composition in a number of competition networks, and also give explanations as to why some species survive while others are excluded. The proposed approach, which we call the “the method of triads” (Muyinda et al., 2019, 2020) involves two steps. In the first step, it is assumed that community structure is governed by

the pairwise interactions among the species and it is these interactions that fundamentally determine the survival or competitive exclusion of each species. This step involves the recursive competitive exclusion of all non-kings in the tournament resulting into smaller and smaller tournaments until the point at which the resulting tournament is such that every species is a king. At this point, the pairwise interactions among species are not sufficient to guarantee survival of individual species as simulations have shown that even the so-called strong kings can get excluded. It is the interactions among the intransitive triads of the tournament that fundamentally determine the survival or competitive exclusion of species in an all-kings tournament.

In the second step, focus is on tournaments in which every species is a king. In such tournaments, interactions occur at the group level and it is the interactions among the intransitive triads of the tournament that fundamentally determine the final richness and composition. We establish dominance relations among the intransitive triads in the tournament, which allows us to generate a competition network of the intransitive triads. This competition network is then represented by an oriented graph known as the triad-interaction graph (TIG), in which the nodes are the intransitive triads and the arrows point from the subordinate triad to the dominant one. The structure of the TIG is then used to deduce the possible final species richness and/or composition.

4.2 The method of triads

Consider an n -species tournament with adjacency matrix $\mathbf{A} = (a_{ij})$. The method of triads proceeds as follows.

4.2.1 Eliminate all non-kings

The first step in the application of the method of triads is the elimination of all non-kings in the tournament. In Section 2.4, we defined a king in a tournament as any species that dominates every other species either directly or through a third species. We thus defined a non-king as any species that is not a king.

In a tournament containing both kings and non-kings, it is believed that the survivorship of individual species is governed by their pairwise competitive abilities. At this stage, all non-kings in the tournament will eventually get excluded resulting in a smaller tournament. To show this, we view the competition network as a game-theoretical problem, in particular, as a symmetric two-player zero-sum game in which the species correspond to the pure strategies available to the players. We then show that any strategy corresponding to a non-king is a dominated

strategy and hence will not be part of the unique NE strategy of the game. This result is presented in Lemma 4.1.

Lemma 4.1. Consider an n -species tournament whose corresponding symmetric zero-sum game has payoff matrix \mathbf{T} . If species i is a non-king in the tournament, then strategy i in the corresponding game is a dominated strategy.

Proof. Suppose species i is a non-king. Then there exists at least one other species, say species k , such that species k not only dominates species i , but also dominates every other species that is dominated by species i .

This implies that in the corresponding zero-sum game, the payoff matrix \mathbf{T} is such that $T_{ki} = 1$ (which implies $T_{ik} = -1$) and $T_{kj} = 1$ for all j for which $T_{ij} = 1$. Thus $T_{ij} \leq T_{kj}$ for all j , and hence strategy i is dominated by strategy k . \square

A consequence of Lemma 4.1 is the following result.

Lemma 4.2. In a competition network represented by a complete directed graph (tournament), all non-kings will ultimately perish.

Proof. The proof follows from Lemma 4.1, Proposition 3.1 and Theorem 3.3. \square

To illustrate the result in Lemma 4.2, we use two examples shown in Figs. 4.2 and 4.3.

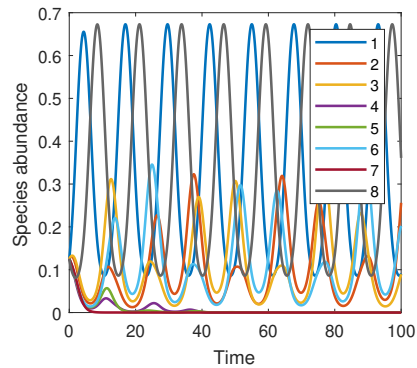
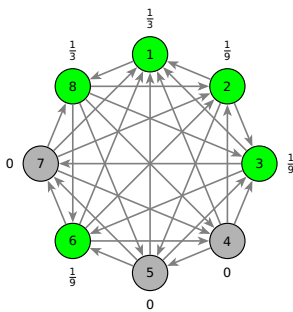


Figure 4.2: An eight-species tournament with the kings shaded in green. Next to each node is shown the proportion of the population playing that node in a NE strategy. A simulation of the ODE system (3.13) is shown on the right. It is clear that all non-kings are not part of the unique NE strategy and hence they ultimately perish as shown in the simulation.

Lemma 4.2 allows us to eliminate all the non-kings in the tournament resulting in a smaller tournament. If the resulting tournament also contains non-kings, these also get eliminated. This process is continued until the point at which the resulting tournament is such that every species is a king. At this point, pairwise interactions

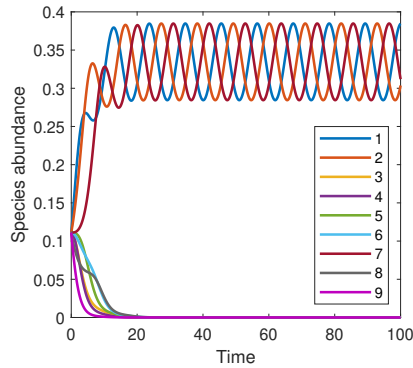
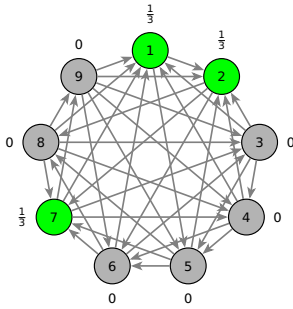


Figure 4.3: A nine-species tournament with the kings shaded. Next to each node is shown the proportion of the population playing that node in a NE strategy. A simulation of the ODE system (3.13) is shown on the right.

among species are insufficient to drive coexistence as simulations have shown that even the so-called strong kings can face competitive exclusion (see, e.g., Fig. 4.4).

4

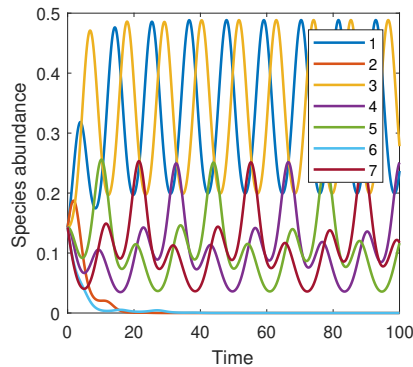
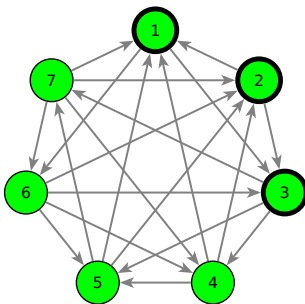


Figure 4.4: A seven-species tournament in which every species is king. Only species 1, 2 and 3 (with thicker borders) are strong kings. A simulation of the ODE system (3.13) for the tournament shows that species 2, although a strong king, does not persist.

We postulate that, at the point where every species is a king, it is the group interactions, in particular, the interactions among the intransitive triads, that fundamentally determine the final species richness and composition.

4.2.2 Find all intransitive triads in the tournament

After recursively eliminating all the non-kings and thus reducing the tournament to one in which every species is a king, the next step is to identify all the intransitive triads in the tournament. Recall from Section 2.3.2.2 that the number of

intransitive triads (which we denoted with d) in an n -species tournament is given by

$$d = \frac{n(n-1)(n-2)}{6} - \frac{1}{2} \sum_{i=1}^n s_i(s_i-1), \tag{4.1}$$

where s_i corresponds to the number of competitors that species i outcompetes (or the sum of the elements in row i of the adjacency matrix \mathbf{A}). For illustration, consider the all-kings seven-species tournament of Fig. 4.5, where the s_i are shown in the right-hand column outside the adjacency matrix.

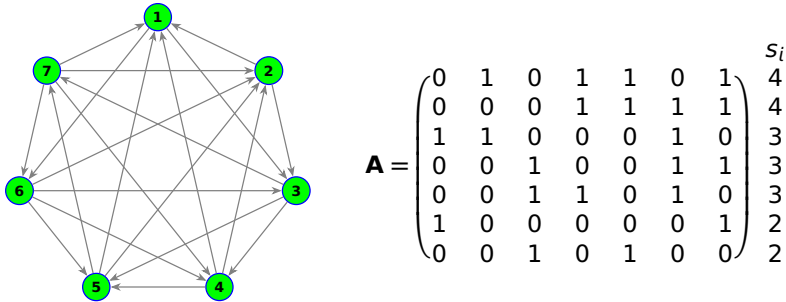


Figure 4.5: A seven-species tournament with corresponding adjacency matrix

Note that the sum of the s_i equals $n(n-1)/2$, the number of edges in the graph. Then

$$d = \frac{(7)(6)(5)}{6} - \frac{1}{2}(12 + 12 + 6 + 6 + 6 + 2 + 2) = 35 - 23 = 12.$$

Hence the seven-species tournament of Fig. 4.5 has 12 intransitive triads.

To retrieve these intransitive triads, we compute the determinants of all 3×3 principal submatrices of the adjacency matrix \mathbf{A} . By definition, an $m \times m$ matrix P is a principal submatrix of \mathbf{A} if P is obtained from \mathbf{A} by deleting any $n-m$ rows and the same $n-m$ columns. The species involved in an intransitive triad correspond to the row indices of any 3×3 principal submatrix of \mathbf{A} whose determinant is equal to 1. In fact, all 3×3 principal submatrices of \mathbf{A} , except those corresponding to the intransitive triads, have determinant zero.

For example, the 12 intransitive triads in the 7-species tournament of Fig. 4.5 are 126, 143, 153, 173, 146, 156, 243, 253, 273, 367, 475 and 567.

After listing the intransitive triads in the tournament, we proceed to establish a dominance relationship among them.

4.2.3 Establish dominance relations among the intransitive triads

In the case where the tournament T contains only one intransitive triad ($d = 1$) and considering the fact that the tournament contains no unbeatable species (since every species is a king), we expect the tournament to evolve to the single intransitive triad. In this case, the final species richness will be 3 whereas the final species composition will be the three species involved in the lone intransitive triad.

Suppose that the tournament with adjacency matrix \mathbf{A} contains $d (\geq 2)$ intransitive triads. Denote the set of intransitive triads with

$$T = \{T_1, T_2, \dots, T_d\} \quad \text{where } T_j = j_1 j_2 j_3,$$

with species $j_i \in \{1, 2, \dots, n\}$, $i = 1, 2, 3$.

From the set T , form all the $\binom{d}{2}$ possible pairs $\{T_i, T_j\}_{i < j}$ of intransitive triads. For each pair $\{T_i, T_j\}$, proceed as follows:

1. If T_i and T_j have two species in common, say, $i_1 = j_1$ and $i_2 = j_2$, then, if $a_{i_3 j_3} = 1$, then T_i dominates T_j and vice versa.
2. If T_i and T_j have only one species in common, say, $i_1 = j_1$, and if $a_{i_2 j_2} = 1$ & $a_{i_3 j_3} = 1$, or, $a_{i_3 j_2} = 1$ & $a_{i_3 j_3} = 1$, then T_i dominates T_j .
3. Finally, if T_i and T_j have no common species, but one of the triads has at least one species that dominates all the three species in the second triad, then the first triad will dominate. Otherwise no conclusion can be made about the dominance relation between the two triads and the TIG contains no edge between the two triads.

The above three rules allow us to construct a TIG that may or may not be a complete directed graph. The TIG can also be coded in a $d \times d$ adjacency matrix $\mathbf{A}^* = (a_{ij}^*)$ in which $a_{ij}^* = 1$ if T_i dominates T_j , otherwise $a_{ij}^* = 0$. If no dominance relation can be established between T_i and T_j , then $a_{ij}^* + a_{ji}^* = 0$; otherwise $a_{ij}^* + a_{ji}^* = 1$. The structure of the TIG could then be used to deduce the final species richness and/or composition of the original n -species tournament.

4.2.4 Determine the final species richness

From the structure of the TIG, the final species richness and composition of the tournament can be deduced by making use of the following hypotheses.

1. If there exists a $k \in \{1, 2, \dots, d\}$ such that $\sum_{j=1}^d a_{kj}^* = d - 1$, that is, T_k is an ‘unbeatable’ triad in the TIG, then the network will evolve to T_k .
2. Suppose, on the other hand, that there exists no unbeatable triad and yet the k -th column of matrix \mathbf{A}^* is a zero column. This implies that triad T_k dominates every other triad T_j for which there exists an edge between T_k and T_j . In addition, if, for any other triad T_i for which there exists no edge between T_i and T_k , T_k dominates T_i through a third triad, then the competition network will evolve to T_k .
3. Finally, if there exists no unbeatable triad and \mathbf{A}^* contains no zero column, then, like in the case of a competition network with no unbeatable species, the tournament cannot evolve to a three-species system and thus the final species richness is greater than 3. Thus we expect the final species richness and composition to be determined from the cycles formed by the intransitive triads.

Thus, in the case where the TIG contains no unbeatable triad and \mathbf{A}^* contains no zero column, the final species richness and composition is derived as follows.

- (a) Determine all cycles formed by the intransitive triads by evaluating the determinants of all principal submatrices of \mathbf{A}^* of size $\{3, 4, \dots, d\}$. The cycles will correspond to the indices of all those principal submatrices with determinant equal to 1 or -1 .
- (b) Ignore all cycles in which the total number of species that form the triads in the cycle is even. This is because coexistence of an even number of species is not possible (Allesina and Levine, 2011).
- (c) From (a) and (b), the final species richness and composition can be deduced by making use of the following hypotheses.
 - H1. If the TIG contains a single cycle of triads, the competition network will evolve to a community whose composition are the species that form the intransitive triads involved in the cycle of triads. Thus the final species richness is equal to the number of unique species that make up the triads that form the lone cycle.
 - H2. If the TIG contains a cycle in which every triad in the cycle dominates every other triad outside the cycle, in other words, a dominant cycle of triads, then the network will evolve to a community composed of the species that make up the intransitive triads involved in the dominant cycle.
 - H3. If the TIG contains multiple cycles of triads, and the total number of individual species involved in each of the cycles is equal, then the final species richness will be equal to the number of individual

species that form any one of the cycles of triads. However, although we can deduce the exact final species richness, we are unable to exactly state the final species composition as the network could evolve to any of the cycles of triads.

On the other hand, if the TIG contains multiple cycles of triads, with different numbers of individual species, the current method is unable to exactly deduce both the final species richness and composition as the network could evolve to any of the cycles of triads. However, the method is able to narrow down both the final species richness and composition to a few possibilities.

4.3 Example

To illustrate the method of triads, consider a nine-species tournament for which the iterative elimination of non-kings reduces the tournament to a five-species tournament in which every species is a king as shown in Fig. 4.6.

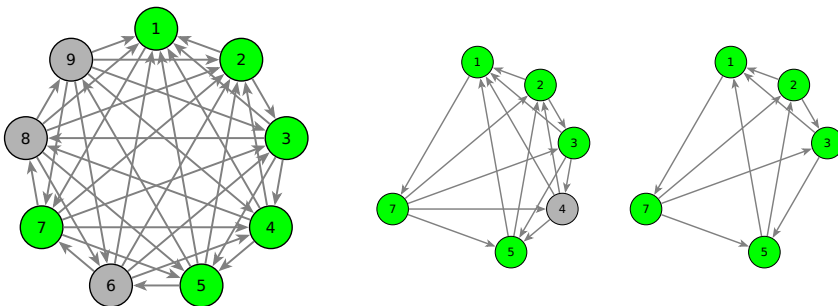


Figure 4.6: Left: A nine-species tournament with the kings in green. Center: A six-species tournament obtained from elimination of the non-kings from the nine-species tournament. Right: A final five-species tournament in which every species is a king.

The resulting five-species tournament contains four intransitive triads 127, 137, 157 and 253. Dominance relations among these intransitive triads lead to the TIG shown in Fig. 4.7. The TIG contains a single cycle in which all the triads in the cycle, that is, 127, 137 and 157, dominate every other triad outside the cycle, which in this case is triad 253. Since the total number of individual species in this cycle is odd, it is concluded, from hypotheses H1 or H2, that the final five-species tournament supports coexistence of all the five species $\{1, 2, 3, 5, 7\}$ that form the cycle of triads. Thus the original nine-species competition network will evolve to a community of five species composed of 1, 2, 3, 5 and 7.

Computing the unique NE strategy of the corresponding symmetric zero-sum game for the nine-species tournament yields $\mathbf{x}^* = \left(\frac{1}{3}, \frac{1}{9}, \frac{1}{9}, 0, \frac{1}{9}, 0, \frac{1}{3}, 0, 0\right)$, which also

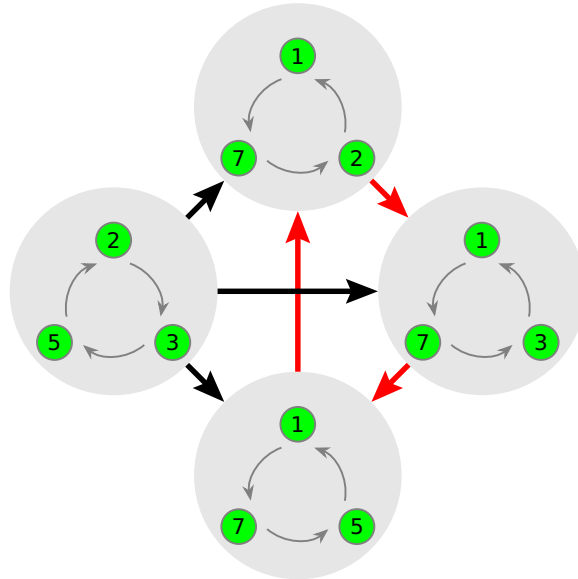


Figure 4.7: A TIG for the final five-species tournament of Fig. 4.6. The TIG contains a single cycle formed by the red arrows.

confirms the competitive exclusion of species 4, 6, 8, and 9. A simulation of the ODE system (3.13) for this nine-species tournament is shown in Fig. 4.8.

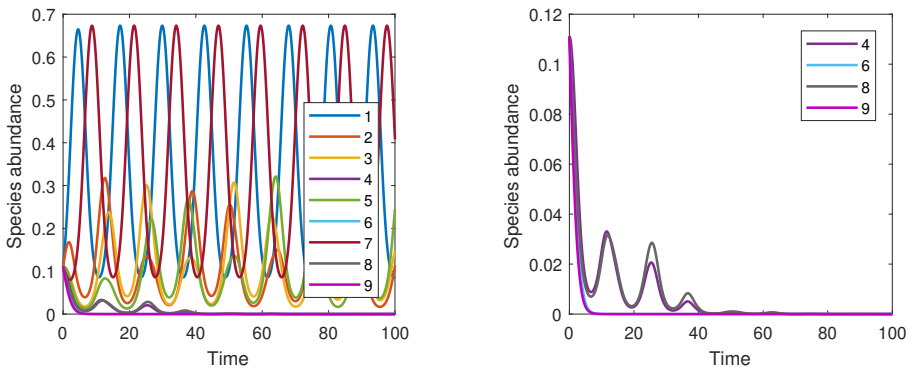


Figure 4.8: A simulation of the ODE system (3.13) for the nine-species tournament of Fig. 4.6. Shown on the right is the time evolution of the four species that go extinct.

Thus, both the simulation of the ODE system (3.13) and the unique NE strategy of the corresponding zero-sum game confirm that species $\{1, 2, 3, 5, 7\}$ form the final species composition as predicted by the method of triads. Hence the final species richness of the nine-species tournament is 5.

4.4 Results

The method of triads has been tested on all non-isomorphic tournaments composed of five to nine species and on a number of non-isomorphic tournaments composed of 10 species. To validate the predictions from the method of triads, we have used the computation from the game-theoretical framework where the tournament has been treated as a two-person, zero-sum game and computed the Nash equilibrium optimal strategy for each tournament. In addition, we have also carried out ODE simulations for a number of selected cases. Two useful results have been derived regarding the final species richness and composition for all networks whose non-king elimination reduces the tournament to an all-kings tournament of size three and five. These two results are presented in the following propositions.

Proposition 4.1. *For a three-species network in which every species is a king, all the three species coexist.*

4

Proof. A three-species community in which every species is a king is an intransitive triad. Thus the three species coexist. \square

Proposition 4.2. *For a five-species community in which every species is a king, all the five species coexist.*

Proof. It can be verified that there exist exactly two non-isomorphic tournaments of size five in which every species is a king. These two tournaments are shown in Fig. 4.9. Note that the tournament on the left is isomorphic to the final five-species



Figure 4.9: The two non-isomorphic tournaments of size five in which every species is a king.

tournament of Fig. 4.6 which has been shown to support coexistence of all the five species.

Applying the method of triads, it can be verified that the tournament on the right contains five intransitive triads that form the TIG shown in Fig. 4.10. From the TIG, it is clear that the triads form a single cycle that involves all the five individual species. Thus from hypothesis H1, we conclude that this tournament supports coexistence of all the five species. Computing the unique NE strategy

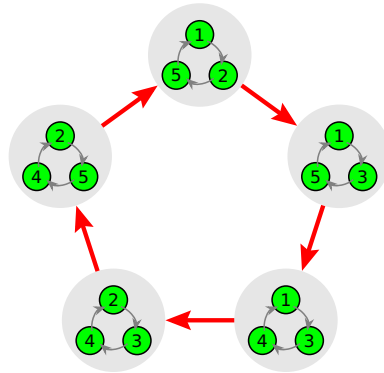


Figure 4.10: The TIG for the five-species tournament in Fig. 4.9 on the right.

of the corresponding symmetric zero-sum for this five-species tournament yields $\mathbf{x}^* = \left(\frac{1}{5}, \frac{1}{5}, \frac{1}{5}, \frac{1}{5}, \frac{1}{5}\right)$, which confirms coexistence of all the five species.

Figure 4.11 shows results from the simulation of the ODE system (3.13) for the two tournaments of Fig. 4.9.

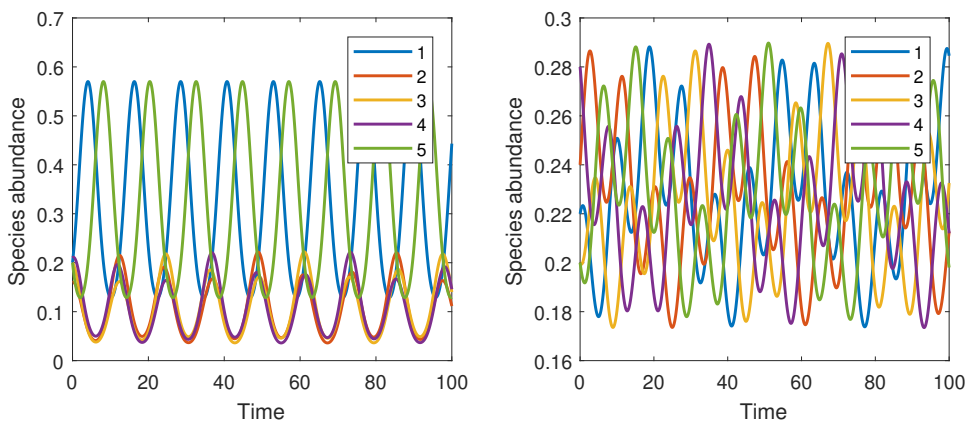


Figure 4.11: Corresponding simulation results of the ODE system (3.13) for the two 5-species tournament of Fig. 4.9.

□

Propositions 4.1 and 4.2 lead to the exact determination of the final species composition and richness in 8 out of the 12 non-isomorphic tournaments composed of five species, 41 out of the 56 tournaments composed of six species, 322 out of the 456 tournaments composed of seven species, 4142 out of the 6880 tournaments composed of eight species and 87638 out of the 191536 tournaments composed of nine species.

In Table 4.1, we present a summary of the number of ecological networks composed of five to nine species for which the method of triads is able to accurately predict the final species richness and/or composition.

Table 4.1: A summary of the results obtained from applying the method of triads to all non-isomorphic tournaments composed of five to nine species. Here, FSR denotes final species richness, while FSC denotes final species composition.

#Species	# non-isomorphic Tourn.	%Tourn. for which the exact FSR can be deduced	%Tourn. in which the exact FSC can be deduced
5	12	100	100
6	56	100	96.4
7	456	94.5	65.1
8	6880	83.1	70.3
9	191536	66.6	53.8

4.5 Species richness versus relative intransitivity

We try to further explore how the level of intransitivity of a tournament relates to the final species richness in tournaments that contain neither unbeatable nor always-beatable species. In Fig. 4.12, we plot graphs of the final species richness versus the relative intransitivity of such tournaments containing five, six, seven and eight species.

Although it may be early to infer a relationship between the level of intransitivity and the final species richness, an observation from Fig. 4.12 is that there is a critical value of the relative intransitivity below which maximum possible coexistence is not possible. For example, in the case of five species, all tournaments with a relative intransitivity below 0.8 cannot support coexistence of all the five species. Similarly, in the case of six species, all tournaments with a relative intransitivity below 0.625 cannot support coexistence of five species, which is the maximum coexistence possible in this case, while in the case of seven and eight species, it is 0.6429 and 0.5, respectively. However, having a relative intransitivity value greater than the above-mentioned critical values does not necessarily imply that maximum coexistence of the species will occur.

4.6 Discussion and conclusion

Interaction networks are basic descriptions of ecological communities and are at the core of community dynamics models (Alcántara and Rey, 2012). An analysis of

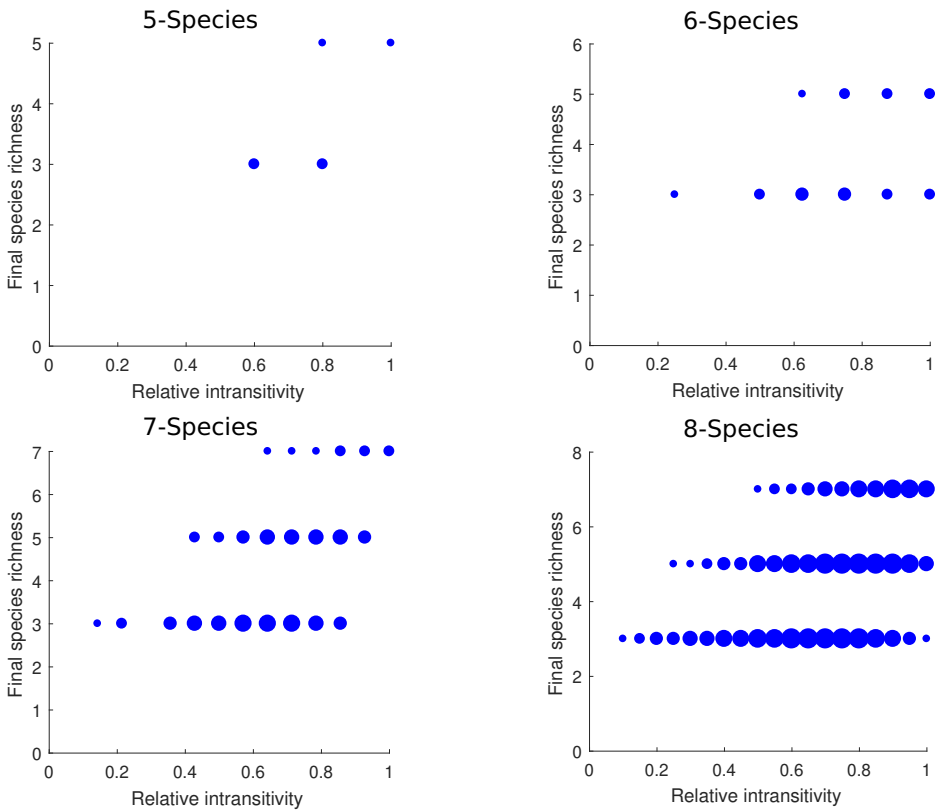


Figure 4.12: Final species richness versus relative intransitivity. The number of dots at a single point represents the number of tournaments with the same relative intransitivity value. The size of the points is therefore proportional to the log of the number of overlapping points. The graph also confirms that the FSR is always odd.

these networks should enable us to anticipate some of the dynamical properties of ecological communities. This is based on the intuition that many of the dynamical properties of networks depend on the particular arrangement of their nodes (i.e., the topology of the network). For example, it has been observed that an intransitive cycle within a network can act as a stabilizing force, in that other species may be influenced by it in a way that prevents what would otherwise be a competitive exclusion (Vandermeer, 2011). The survivorship of an individual species is determined not only by its pairwise competitive ability, but also by its participation in intransitive triads, which effectively rescue it periodically from extinction (Vandermeer, 2013).

In this chapter, we have highlighted an approach that can be used to predict the dynamical properties of ecological communities governed by intransitive competition by considering the competition networks, represented by complete directed graphs, directly rather than via numerical simulations of their mean-field differential equation models. The simulation of differential equations is essential when making precise predictions about how an ecological community will evolve over time in particular situations. However, to gain a more intuitive understanding of how community structure emerges from a directed graph, an analysis of the topology of the network is needed (Vandermeer and Perfecto, 2018).

The approach introduced, coined the method of triads, makes use of the pairwise competitive abilities of individual species to partition the nodes of the network into two disjoint groups, the kings and non-kings based on Maurer's definition of kings in a tournament (Maurer, 1980). By using a game-theoretical framework, we have mathematically proven that every non-king species will ultimately face competitive exclusion resulting in an all-king community in which every species is involved in at least one intransitive triad with every other species.

In the resulting all-king community, it is postulated that the pairwise competitive abilities of species are not sufficient to guarantee the survival of individual species and it is the competitive interactions among the intransitive triads of the network that fundamentally determine the community structure. This has also been observed in simulations of spatial competition models where the intransitive triads are shown to form spiral wave patterns and the interactions among the different species are characterized by the entanglement of the corresponding spirals which ultimately determine the community structure at equilibrium (Vandermeer and Yitbarek, 2012; Cheng et al., 2014). A triad interaction graph (TIG) is therefore constructed and the final community composition and/or richness can then be deduced based on the structure of the TIG.

The hypotheses H1-H3 stated in the method of triads have been derived out of intuition and confirmed through model simulations. Numerical simulations show that the proposed hypotheses hold for all non-isomorphic tournaments composed of five to nine species and for all examples of 10-species tournaments that we have tested them on. Results show that an all-king community of size five is

persistent in that all the five species will coexist in perpetuity. In addition, the proposed approach leads to the exact deduction of the final species composition and richness in a number of ecological networks composed of five to nine species as the results in Table 4.1 show.

By comparing the second column of Table 4.1 with the last two columns, it can be observed that the method of triads is unable to deduce the exact final species richness and composition for a number of non-isomorphic tournaments. This is because for such tournaments, the TIG contains multiple cycles of triads of different size. Here size is used to refer to the total number of unique individual species that make up the triads involved in the cycle. In such case, the method can, however, narrow down the final species richness and composition to a few possibilities, which are, respectively, the sizes of the cycles of triads and sets of individual species that make up the cycles. However, for a network whose TIG contains multiple cycles of triads but whose size is the same, the exact final species richness can be deduced, which is the size of the cycle of triads. Here, the network will still evolve to one of the sets of individual species that make up the cycles of triads. Deducing the exact final species richness and composition for a network whose TIG contains multiple cycles of triads is still a subject of future research.

5

Dynamics of balanced metapopulation models

The material of this chapter is based on the following publication:

- Rao, S., Muyinda, N., and De Baets, B. (2021). Stability analysis of the coexistence equilibrium of a balanced metapopulation model. *Scientific Reports*, 11(1). <https://doi.org/10.1038/s41598-021-93438-8>

5.1 Introduction

In Chapter 4, we highlighted an approach that can be used to predict the final species richness and composition of ecological communities governed by intransitive competition by considering the competition networks, represented by tournaments, directly rather than via numerical simulations of their mean-field ODE models. To validate our prediction for each tournament, we carried out numerical simulations of its mean-field ODE model system that was derived under the

assumption that all individuals of all species live in a well-mixed, homogeneous, non-spatial landscape. However, spatial heterogeneity is one of the most obvious features of the natural world. Species are rarely distributed continuously in space but rather are organized into local populations (habitat patches), interconnected to varying degrees through dispersal. The issue of how species coexist in patchy environments is central to both basic and applied ecology. Even if local populations go extinct, species can persist at a regional scale through immigration from other habitats. The idea that colonization and extinction dynamics of patches could promote coexistence of competitors was first conceptualized in Hutchinson's notion of a *fugitive species*. Hutchinson (1951) proposed the term *fugitive* to describe a species that is able to coexist with a competitively dominant species due to its better dispersal capabilities. The fugitive species is quicker to occupy any vacant patches in the environment and establish populations before competitively superior species arrive and eventually displace them. The colonization of new patches allows the fugitive species to continually flee from competition as long as the landscape contains some unoccupied patches. Because competition for resources is asymmetric, a trade-off between dispersal and local competitive abilities among species can lead to coexistence in a patchy environment (Tilman, 1994; Gordon, 2000).

5 Mathematical representations of this idea began with Levins' (1969) one-species patch-occupancy model (discussed in Section 3.5.3) and generated the metapopulation concept, defined as an assemblage of local populations connected by dispersal. His simple model predicts that a metapopulation will persist only when the rate of local extinction is exceeded by the rate of recolonizations by dispersers from occupied patches. If, instead, the local extinction rate happens to exceed the rate of recolonization, then Levins' model predicts extinction on a global scale. In the 50 years since Levins first introduced his model, hundreds of papers have analyzed and expanded on its basic structure. Current metapopulation models with a more complex structure than Levins' patch-occupancy model and its variants allow for a broader range of population phenomena to be examined, such as changes in local population size, variations in patch size, quality and connectivity, and multispecies competition.

In typical metapopulation modelling, the landscape is assumed to be composed of multiple habitat patches, where population dynamics takes place and homogeneous mixing of individuals is assumed, connected to each other through dispersal. This effectively defines the landscape as a network (directed graph) in which the nodes are the patches and the weighted edges express the migration or colonization rate constants. Nagatani et al. (2018) assume that the migrations between patches are random with the migration rate constant being equal to the reciprocal of the number of dispersal links from a given patch to other patches. They therefore define a dispersal graph to be homogeneous if all nodes (patches) have the same number of links, otherwise the graph is considered heterogeneous.

For many ecologists, the central question is how the structure or connectivity pattern of the underlying graph influences the dynamics of the metapopulation. Intriguingly, initial research indicated that spatial structure has in fact very little effect, with criteria for metapopulation stability appearing to be identical to the stability conditions for a single patch (Rohani et al., 1996). However, many model-based and empirical studies have shown that variability or heterogeneity in patch connectivity may play a role in enhancing the persistence of metapopulations (Artzy-Randrup and Stone, 2010; Perry and Lee, 2019). For example, numerical simulations by Nagatani et al. (2018) have shown that in a metapopulation model for the rock-paper-scissors game, the dynamics are significantly different when the dispersal network is homogeneous compared to when the network is heterogeneous. Specifically, their simulations show that the coexistence equilibrium within each habitat patch is asymptotically stable in the case of a heterogeneous network, while the same equilibrium remains neutrally stable in the case of a homogeneous graph (as in the single patch case). That is, heterogeneity leads to the indefinite coexistence of all three species with abundances equal to the coexistence equilibrium values, whereas homogeneity leads to the perpetual coexistence of all three species with periodically oscillating abundances (i.e., there exists a limit cycle around the coexistence equilibrium to which the trajectories converge). However, these numerical results have been provided without mathematical proof.

In this chapter, we show, mathematically, that the numerical observations of Nagatani et al. (2018) are not only valid for RPS competition systems, but also extend to a broader class of competition networks. We first broaden the class of competition networks under consideration by giving a more general definition of homogeneity/heterogeneity that is based on the adjacency matrix of the dispersal graph without imposing any restrictions on the values of the migration rate constants. Then by combining concepts and results from game theory, chemical reaction network theory (CRNT) and dynamical systems theory, we provide a mathematical proof for the numerical observations of Nagatani et al. (2018), generalizing the scope of application to cover this broader class of competition networks within the patches. Specifically, we perform a stability analysis of the coexistence equilibrium point of a metapopulation model that is based on Levin's (1974) metapopulation model. In performing the analysis we borrow from CRNT the concept of *detailed-balancedness* (van der Schaft et al., 2013, 2015), a key feature for this kind of metapopulation model, that has not been previously explored. We define a metapopulation model to be detailed-balanced if there exist positive equilibrium species proportions (or relative abundances) for which the overall migration rate of each species between any two patches is zero. Then, by assuming that our metapopulation model is detailed-balanced, we provide a mathematical proof for the numerical observations of Nagatani et al. (2018), which shows that these numerical observations are not only valid for a three-species cyclic competition system, but also apply to any n -species tournament for which a coexistence equi-

librium exists.

5.2 Metapopulation model

Consider an interconnected network of m discrete patches each being inhabited by the same n species. Let $x_{i,j}$ denote the density of species i ($i = 1, \dots, n$) in patch j ($j = 1, \dots, m$). Within each patch, each species can compete against every other species and this competition is asymmetric such that for any pair of species, one is dominant over the other. In addition, we assume that the densities of species within each patch are affected by other patches only via migration. Let $\phi_{i,j}$ denote the rate of change of the proportion of species i in patch j in the absence of migration. Since the dominance relationships among the species (described by a tournament matrix \mathbf{T}) are assumed to be the same for all patches, and since the habitat patches are assumed to be spatially homogeneous, the intra-patch dynamics are governed by the replicator equation (3.13). Thus we have

$$\phi_{i,j} = x_{i,j} (\mathbf{T}\mathbf{p}_j)_i, \quad (5.1)$$

where $\mathbf{p}_j := (x_{1,j}, x_{2,j}, \dots, x_{n,j})^\top$, $i = 1, \dots, n$ and $j = 1, \dots, m$.

5 Allowing migrations between the patches, assume that species can migrate from one patch to some or all of the other patches. The rate of migration of each species between two patches is directly proportional to the proportion of the particular species in the originating patch, with a (nonnegative) constant of proportionality being the same across species. This constant of proportionality will be referred to as the rate constant associated with the migration. It is assumed that if there is migration between two given patches, then it is bidirectional, *i.e.*, the rate constant of migration from patch j to patch k is strictly positive if and only the same holds for the migration from k to j . In addition, such an inter-patch migration may be described by a weighted finite directed graph $G_1 = (V_1, E_1)$ where $V_1 = \{1, \dots, m\}$ is the set of patches (vertices) and an edge $(j, k) \in E_1$ means that every species can migrate from patch j to patch k . Thus a directed edge from patch j to patch k exists if and only if the rate constant of migration from patch j to patch k is strictly positive. Each edge of the graph has an associated weight which is equal to the (positive) rate constant associated with the corresponding migration.

The flow of species between the patches can be summarized in a weighted $m \times m$ adjacency matrix \mathbf{A} with entry A_{jk} being equal to the rate constant of migration of species from the patch j to patch k . The diagonal elements of \mathbf{A} are hence equal to 0. Due to the bidirectional nature of migration, it holds that $A_{jk} > 0 \Leftrightarrow A_{kj} > 0$ and $A_{jk} = 0 \Leftrightarrow A_{kj} = 0$, for any $j \neq k$. Let $\Delta = \text{diag}(\delta_1, \dots, \delta_m)$ denote the m -dimensional

diagonal matrix whose j -th entry is given by

$$\delta_j = \sum_{k=1}^m A_{jk}. \quad (5.2)$$

Define $\mathbf{L} := \Delta - \mathbf{A}^\top$ and denote by $\psi_{i,j}$ the net migration of species i from other patches to patch j . In the simplest case, the net exchange of species i from patch k to patch j is

$$A_{kj}x_{i,k} - A_{jk}x_{i,j}$$

where A_{kj} (resp. A_{jk}) is the rate constant of migration of any species from patch k to patch j (resp. reverse). Thus $\psi_{i,j}$ takes the form

$$\psi_{i,j} = \sum_{k=1}^m (A_{kj}x_{i,k} - A_{jk}x_{i,j}) = \sum_{k=1}^m A_{kj}x_{i,k} - \delta_j x_{i,j} = - \sum_{k=1}^m L_{jk}x_{i,k}. \quad (5.3)$$

Let us denote $\Psi_i := (\psi_{i,1}, \psi_{i,2}, \dots, \psi_{i,m})^\top$ and $\mathbf{r}_i := (x_{i,1}, x_{i,2}, \dots, x_{i,m})^\top$, then

$$\Psi_i = -\mathbf{L}\mathbf{r}_i. \quad (5.4)$$

With migration among the patches, the proportion of a species within a patch is influenced by two factors: the first is the interaction with other species within the patch and the second is the migration of that particular species to or from other patches. Thus, the metapopulation model describing the dynamics of the n species in the m -patch network is described by the system of mn differential equations;

$$\dot{x}_{i,j} = \phi_{i,j} + \psi_{i,j} = x_{i,j}(\mathbf{T}\mathbf{p}_j)_i - (\mathbf{L}\mathbf{r}_i)_j, \quad i = 1, \dots, n, \quad j = 1, \dots, m. \quad (5.5)$$

This system evolves on the unit simplex S^{mn} .

5.3 Invariance of the unit simplex

We now proceed to show that the unit simplex S^{mn} is positively invariant for the dynamical system (5.5).

Proposition 5.1. *The unit simplex S^{mn} is positively invariant for System (5.5).*

Proof. To show the invariance of the unit simplex S^{mn} under the flow of System (5.5), it suffices to show that each of the faces of the simplex cannot be crossed, i.e., the vector field points inward from the faces of S^{mn} .

On the one hand, if $x_{i,j} = 0$ for some i, j , then

$$\frac{dx_{i,j}}{dt} = \sum_{k=1}^m A_{kj} x_{i,k} \geq 0,$$

which implies that $x_{i,j} = 0$ cannot be crossed from positive to negative. In an ecological context, this condition simply states the obvious fact that an extinct species is in no danger of declining. On the other hand, if $x_{i,j} = 1$ for some i, j , then obviously $x_{l,k} = 0$ for any $l \neq i$ or $k \neq j$ and

$$\frac{dx_{i,j}}{dt} = -\delta_j < 0.$$

Hence, the vector field associated with System (5.5) points inward from the faces of S^{mn} . So, S^{mn} is positively invariant under the flow of System (5.5). \square

Note that Proposition 5.1 does not exclude the solution trajectories of System (5.5) from approaching the boundary equilibria of the system as $t \rightarrow \infty$. The metapopulation is said to be persistent if for every $\mathbf{x}_0 \in S_+^{mn}$, the ω -limit set $\omega(\mathbf{x}_0)$ does not intersect the boundary of S^{mn} . In other words, a metapopulation is persistent if the initial existence of all the species implies that none of the species goes extinct with the passage of time.

5.4 Neutral stability

In the absence of migration, the local population dynamics are independent and are governed by the replicator equation

$$\frac{dx_i}{dt} = x_i(\mathbf{T}\mathbf{x})_i, \quad (5.6)$$

where x_i is the proportion of species i within the patch and $\mathbf{x} = (x_1, \dots, x_n)^\top$. Following Grilli et al. (2017), we show that if System (5.6) admits a feasible equilibrium \mathbf{x}^* , then it is neutrally stable. In other words, we show that if all the species coexist, then their proportions cycle neutrally around the feasible equilibrium. To do so, we consider the Lyapunov function

$$V(\mathbf{x}) = -\sum_{i=1}^n x_i^* \ln \frac{x_i}{x_i^*}. \quad (5.7)$$

By Gibbs inequality (Brémaud, 1988), $V(\mathbf{x})$ is positive in S_+^n and $V(\mathbf{x}) = 0$ only if $\mathbf{x} = \mathbf{x}^*$. Taking the time derivative of V , we have (using $T_{ij} = -T_{ji}$):

$$\begin{aligned}\dot{V}(\mathbf{x}) &= -\sum_{i=1}^n x_i^* \frac{\dot{x}_i}{x_i} = -\sum_{i=1}^n x_i^* (\mathbf{T}\mathbf{x})_i = -\sum_{i=1}^n x_i^* \left(\sum_{j=1}^n T_{ij} x_j \right) \\ &= \sum_{j=1}^n x_j \left(\sum_{i=1}^n T_{ji} x_i^* \right) = \sum_{j=1}^n x_j (\mathbf{T}\mathbf{x}^*)_j = 0.\end{aligned}$$

Hence, V is a constant of motion: all orbits $t \rightarrow \mathbf{x}(t)$ of the mean-field model remain on constant level sets of V . This implies that all orbits in S_+^n are closed orbits surrounding \mathbf{x}^* .

In the following sections, we explore one fundamental ecological question: To what extent are the single-patch dynamics affected by migration?

5.5 Detailed-balanced single species mass-action reaction networks

The CRNT concept of detailed-balancing (introduced in Section 3.4.4) will be instrumental when deriving the main results of this chapter. With this formulation, the modelling of dispersion among patches is carried out analogously as in the case of detailed-balanced mass-action chemical reaction networks (van der Schaft et al., 2013, 2015). We briefly explain the relevant aspects.

Consider a network of r reversible chemical reactions occurring among the chemical species C_1, C_2, \dots, C_m . Each of these r reversible reactions has a species C_j as substrate and another species C_k as product (with $j \neq k$). Let A_{jk} (resp. A_{kj}) denote the mass action rate constant of the forward (resp. reverse) reaction in (5.8):



Since all reactions are reversible, it holds that $A_{jk} > 0 \Leftrightarrow A_{kj} > 0$ and $A_{jk} = 0 \Leftrightarrow A_{kj} = 0$, for any $j \neq k$.

We associate a finite asymmetric directed graph $G_2 = (V_2, E_2)$ with the reaction network, where $V_2 = \{1, \dots, m\}$ is the set of chemical species and an edge (j, k) in E_2 is associated with each reversible reaction (5.8). Let x_j denote the concentration of species C_j , for $j = 1, \dots, m$. Let v_p denote the overall rate of the p^{th} reaction in the direction of the p^{th} edge in G_2 . Then the dynamics of the chemical reaction network can be described by the equation

$$\dot{\mathbf{x}} = \mathbf{B}\mathbf{v}, \quad (5.9)$$

where $\mathbf{x} = (x_1, x_2, \dots, x_m)^\top$, \mathbf{B} is the $m \times r$ incidence matrix of G_2 and $\mathbf{v} = (v_1, v_2, \dots, v_r)^\top$. Since each reaction of the network is governed by mass action kinetics, if the p^{th} reaction of the network is described by (5.8), then

$$v_p = A_{jk}x_j - A_{kj}x_k. \quad (5.10)$$

Define $k_p^{\text{forw}} := A_{jk}$ and $k_p^{\text{rev}} := A_{kj}$. Recall that, a reversible chemical reaction network is said to be *detailed balanced* if it admits a detailed balanced (or thermodynamic) equilibrium. In other words, a detailed balanced single species (or unimolecular) reversible reaction network is one for which there exists an equilibrium \mathbf{x}^* at which the overall reaction rate of every reversible reaction of the network is zero. Thus, if x_j^* and x_k^* denote the concentrations of C_j and C_k at a detailed balanced equilibrium \mathbf{x}^* , then it holds that

$$A_{jk}x_j^* = A_{kj}x_k^*.$$

It is clear from Eq. (5.10) that if \mathbf{u} is a detailed balanced equilibrium, then also $q\mathbf{u}$ is, for any $q \in \mathbb{R}_+$. Hence, we can choose a detailed balanced equilibrium $\mathbf{z}^* \in S_+^m$.

Now define

$$K_p^{\text{eq}} := \frac{z_k^*}{z_j^*} = \frac{A_{jk}}{A_{kj}} = \frac{k_p^{\text{forw}}}{k_p^{\text{rev}}}.$$

Define $\mathbf{K}^{\text{eq}} := (K_1^{\text{eq}}, K_2^{\text{eq}}, \dots, K_r^{\text{eq}})^\top$ and note that

$$\mathbf{K}^{\text{eq}} = \text{Exp}(\mathbf{B}^\top \text{Ln}(\mathbf{z}^*)), \quad (5.11)$$

where $\text{Ln}(\mathbf{z}^*)$ is the element-wise natural logarithm of \mathbf{z}^* . That is, $(\text{Ln} \mathbf{z}^*)_i = \text{Ln}(z_i^*)$.

From this, the condition for detailed balancing of a reversible single species chemical reaction network can be derived.

Proposition 5.2. *A reversible single species mass action chemical reaction network is detailed balanced if and only if*

$$\text{Ln}(\mathbf{K}^{\text{eq}}) \in \text{Im}(\mathbf{B}^\top). \quad (5.12)$$

As mentioned in (van der Schaft et al., 2013, Remark 3.1), from condition (5.12), it follows that any $\mathbf{w} \in \mathbb{R}^r$ satisfying $\mathbf{B}\mathbf{w} = \mathbf{0}^m$ will also satisfy

$$\sum_{p=1}^r w_p \text{Ln}(K_p^{\text{eq}}) = 0.$$

This leads to the well-known Wegscheider conditions (Wegscheider, 1902) for de-

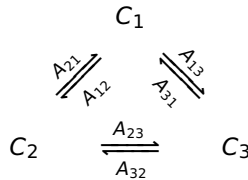
tailed balancing given by

$$\prod_{p=1}^r (k_p^{\text{forw}})^{w_p} = \prod_{p=1}^r (k_p^{\text{rev}})^{w_p}.$$

Hence, the reversible reaction network



with strictly positive rate constants is always detailed balanced, whereas the cyclic reversible reaction network



with strictly positive rate constants is detailed balanced if and only if

$$A_{12}A_{23}A_{31} = A_{21}A_{32}A_{13}.$$

We now describe the compact mathematical formulation for a detailed balanced network derived in (van der Schaft et al., 2013). This formulation will be crucially used for deriving the main results of this chapter.

Let (5.8) denote the p^{th} reaction of a detailed balanced single species network with a thermodynamic equilibrium $\mathbf{z}^* \in \mathbb{R}_+^m$. Define

$$\kappa_p := A_{jk}z_j^* = A_{kj}z_k^*.$$

For any other vector of concentrations $\mathbf{x} \in \mathbb{R}_+^m$, it follows from Eq. (5.10) that the overall rate of the p^{th} reaction in the forward direction is given by

$$v_p = \kappa_p \left(\frac{x_j}{z_j^*} - \frac{x_k}{z_k^*} \right).$$

Define $\mathcal{K} := \text{diag}(\kappa_1, \kappa_2, \dots, \kappa_r)$. Then it can be verified that the vector \mathbf{v} of reaction rates is given by

$$\mathbf{v} = -\mathcal{K}\mathbf{B}^T \left(\frac{\mathbf{x}}{\mathbf{z}^*} \right).$$

Define $\mathbf{Z}^* := \text{diag}(\mathbf{z}^*)$. From Eq. (5.9), it now follows that the dynamics of the detailed-balanced single species reaction network is described by the equation

$$\dot{\mathbf{x}} = -\mathbf{B}\mathcal{K}\mathbf{B}^T \left(\frac{\mathbf{x}}{\mathbf{z}^*} \right) = -(\mathbf{B}\mathcal{K}\mathbf{B}^T(\mathbf{Z}^*)^{-1})\mathbf{x}. \tag{5.14}$$



Equation (5.14) can then be used to provide an analogous formulation for the metapopulation model (5.5).

5.6 Balanced metapopulation model

We say that the inter-patch migration of a metapopulation network is detailed balanced if the overall migration rate of any species between any two patches is zero for a certain positive set of proportions of that species in the different patches. From the theory of detailed balanced reaction networks described in Section 5.5, it follows that a detailed-balanced inter-patch migration network corresponds to a detailed-balanced single species mass-action reaction network. Let \mathbf{B} denote the incidence matrix corresponding to the directed graph G_1 describing the inter-patch migrations and let r denote the number of edges in G_1 . Comparing Eqs. (5.4) and (5.14), it follows that if the inter-patch migration is detailed balanced, then there exist diagonal matrices $\mathcal{K} \in \mathbb{R}^{r \times r}$ and $\mathbf{Z}^* \in \mathbb{R}^{m \times m}$ with positive diagonal entries such that $(\mathbf{1}^m)^\top \mathbf{Z}^* \mathbf{1}^m = 1$ and

$$\mathbf{L} = \mathbf{B} \mathcal{K} \mathbf{B}^\top (\mathbf{Z}^*)^{-1}.$$

Let $\mathbf{Z}^* = \text{diag}(\mathbf{z}^*)$. Equation (5.4) can now be rewritten as

$$\psi_i = -\mathbf{B} \mathcal{K} \mathbf{B}^\top \left(\frac{\mathbf{r}_i}{\mathbf{z}^*} \right). \quad (5.15)$$

On the other hand, if the interactions within each patch, in the absence of migrations, correspond to a tournament whose corresponding zero-sum game is completely mixed, then the replicator equation governing the population dynamics within the patch admits a unique coexistence equilibrium $\mathbf{y}^* \in S_+^n$ with $\mathbf{T} \mathbf{y}^* = \mathbf{0}^n$. Thus, Eq. (5.1) can also be written as

$$\phi_{i,j} = x_{i,j} \left(\mathbf{T} \mathbf{Y}^* \left(\frac{\mathbf{p}_j}{\mathbf{y}^*} \right) \right)_i, \quad (5.16)$$

where $\mathbf{Y}^* := \text{diag}(\mathbf{y}^*)$.

Consequently, from Eqs. (5.5), (5.15) and (5.16), it follows that the dynamics of a metapopulation can be described by the mn differential equations

$$\frac{dx_{i,j}}{dt} = x_{i,j} \left(\mathbf{T} \mathbf{Y}^* \left(\frac{\mathbf{p}_j}{\mathbf{y}^*} \right) \right)_i - \left(\mathbf{B} \mathcal{K} \mathbf{B}^\top \left(\frac{\mathbf{r}_i}{\mathbf{z}^*} \right) \right)_j, \quad (5.17)$$

for $i = 1, \dots, n$ and $j = 1, \dots, m$.

Henceforth in this thesis, we restrict our analysis to metapopulation models of

type (5.17) for which the interactions within each patch correspond to a tournament game with a completely mixed NE strategy and whose inter-patch migration is detailed-balanced. Such metapopulation models will be referred to as *balanced metapopulation models*.

If all the elements of \mathbf{z}^* in Eq. (5.17) are equal, *i.e.*, if $z_j^* = \frac{1}{m}$ for $j = 1, \dots, m$, then we say that the balanced metapopulation model is *homogeneous*, otherwise we call it *heterogeneous*. Whether a balanced metapopulation model is homogeneous or not can be checked from the adjacency matrix \mathbf{A} corresponding to its inter-patch migration graph G_2 . If \mathbf{A} is symmetric, then the model is homogeneous, otherwise it is heterogeneous.

Remark 5.1. Nagatani et al. (2018) assume that migrations from one patch to other patches are random with a probability of migration (or migration constant) equal to the reciprocal of the number of dispersal links from a patch to other patches. They thus define a dispersal graph to be homogeneous if all nodes have the same degree (number of links), otherwise the graph is heterogeneous. With this definition, homogeneity, in general, is equivalent to the existence of cycles in the dispersal graph, whereas heterogeneity is equivalent to their absence. However, with our new definition, it is clear that this is not necessary. An example of such a case is shown in Fig. 5.1.

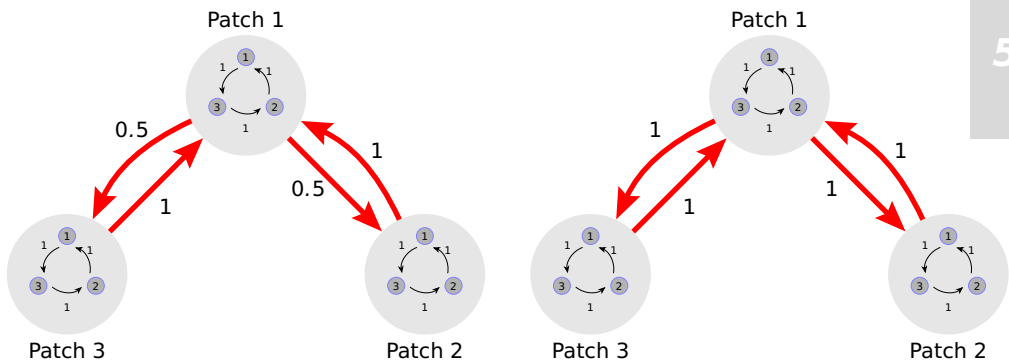


Figure 5.1: Left: A heterogeneous dispersal graph according to Nagatani et al. (2018). Right: A homogeneous dispersal graph according to our definition.

5.7 Unique coexistence equilibrium

In this section, we present a theorem that gives an expression for the coexistence equilibrium of the balanced metapopulation model (5.17). Before we state our main theorem in this section, we need the following lemma.



Lemma 5.1. Let $\mathbf{B} \in \mathbb{R}^{m \times r}$ denote the incidence matrix of a finite connected directed graph G_2 and let $\mathcal{K} \in \mathbb{R}^{r \times r}$ denote a diagonal matrix with positive diagonal entries. For any $\mathbf{w} \in \mathbb{R}_+^m$, it holds that $-\mathbf{w}^\top \mathbf{B} \mathcal{K} \mathbf{B}^\top \left(\frac{\mathbf{1}^m}{\mathbf{w}} \right) \geq 0$. Moreover $-\mathbf{w}^\top \mathbf{B} \mathcal{K} \mathbf{B}^\top \left(\frac{\mathbf{1}^m}{\mathbf{w}} \right) = 0$ if and only if $\mathbf{w} = q \mathbf{1}^m$, where $q \in \mathbb{R}_+$.

Proof. Assume that the p^{th} edge of the graph G_2 is directed from vertex i_p to vertex j_p . Hence, $B_{i_p p} = -1$, $B_{j_p p} = 1$ and $B_{k p} = 0$ for $i_p \neq k \neq j_p$. Thus,

$$-\mathbf{w}^\top \mathbf{B} \mathcal{K} \mathbf{B}^\top \left(\frac{\mathbf{1}^m}{\mathbf{w}} \right) = \sum_{p=1}^m (w_{j_p} - w_{i_p}) \kappa_p \left(\frac{1}{w_{i_p}} - \frac{1}{w_{j_p}} \right) = \sum_{p=1}^m \frac{\kappa_p}{w_{i_p} w_{j_p}} (w_{j_p} - w_{i_p})^2 \geq 0.$$

Moreover, $-\mathbf{w}^\top \mathbf{B} \mathcal{K} \mathbf{B}^\top \left(\frac{\mathbf{1}^m}{\mathbf{w}} \right) = 0$ if and only if $w_{j_p} = w_{i_p}$ for $p = 1, \dots, m$, which is equivalent with $\mathbf{B}^\top \mathbf{w} = \mathbf{0}^r$.

Since the graph G_2 is connected, we recall from Bollobás (1998) that $\text{rank}(\mathbf{B}) = m - 1$ and furthermore $\ker(\mathbf{B}^\top) = \mathbf{1}^m$. Therefore $\mathbf{B}^\top \mathbf{w} = \mathbf{0}^r$ if and only if $\mathbf{w} = q \mathbf{1}^m$, where $q \in \mathbb{R}_+$. This completes the proof. \square

We now state the main theorem of this section.

Theorem 5.1. The balanced metapopulation model (5.17) admits a unique coexistence equilibrium $\mathbf{x}^* \in S_+^{mn}$. The proportion $x_{i,j}^*$ of species i in patch j at the unique coexistence equilibrium is given by

$$x_{i,j}^* = y_i^* z_j^*. \quad (5.18)$$

for $i = 1, \dots, n$ and $j = 1, \dots, m$.

Proof. We divide the proof into two parts. In the first part we prove that System (5.18) indeed yields an equilibrium for the model. In the second part, we prove that this coexistence equilibrium is unique.

Let us define

$$\mathbf{p}_j^* := \left(x_{1,j}^*, x_{2,j}^*, \dots, x_{n,j}^* \right)^\top = z_j^* \mathbf{y}^* \quad \text{and} \quad \mathbf{r}_i^* := \left(x_{i,1}^*, x_{i,2}^*, \dots, x_{i,m}^* \right)^\top = y_i^* \mathbf{z}^*.$$

For \mathbf{x}^* to be an equilibrium of System (5.17), it should render the right-hand side equal to zero. Note that

$$\mathbf{T} \mathbf{Y}^* \begin{pmatrix} \mathbf{p}_j^* \\ \mathbf{y}^* \end{pmatrix} = z_j^* \mathbf{T} \mathbf{Y}^* \mathbf{1}^n = z_j^* \mathbf{T} \mathbf{y}^* = \mathbf{0}^n$$

and

$$\mathbf{B} \mathcal{K} \mathbf{B}^\top \begin{pmatrix} \mathbf{r}_i^* \\ \mathbf{z}^* \end{pmatrix} = y_i^* \mathbf{B} \mathcal{K} \mathbf{B}^\top \mathbf{1}^m = \mathbf{0}^m.$$

In addition,

$$(\mathbf{1}^{mn})^\top \mathbf{x}^* = \sum_{i=1}^n \sum_{j=1}^m x_{i,j}^* = \sum_{i=1}^n y_i^* \sum_{j=1}^m z_j^* = 1.$$

Thus, \mathbf{x}^* is a coexistence equilibrium of System (5.17).

Assume that there exists another coexistence equilibrium $\mathbf{x}^{**} \in S_+^{mn}$. Let $x_{i,j}^{**}$ denote the corresponding proportion of species i in patch j and define

$$\mathbf{p}_j^{**} := (x_{1,j}^{**}, x_{2,j}^{**}, \dots, x_{n,j}^{**})^\top, \quad \text{and} \quad \mathbf{r}_i^{**} := (x_{i,1}^{**}, x_{i,2}^{**}, \dots, x_{i,m}^{**})^\top.$$

It follows that for any i, j it holds that

$$x_{i,j}^{**} \left(\mathbf{T}\mathbf{Y}^* \left(\frac{\mathbf{p}_j^{**}}{\mathbf{y}^*} \right) \right)_i - \left(\mathbf{B}\mathcal{K}\mathbf{B}^\top \left(\frac{\mathbf{r}_i^{**}}{\mathbf{z}^*} \right) \right)_j = 0. \quad (5.19)$$

Multiplying both sides of Eq. (5.19) with $\frac{x_{i,j}^*}{x_{i,j}^{**}}$, we get

$$x_{i,j}^* \left(\mathbf{T}\mathbf{Y}^* \left(\frac{\mathbf{p}_j^{**}}{\mathbf{y}^*} \right) \right)_i - \frac{x_{i,j}^*}{x_{i,j}^{**}} \left(\mathbf{B}\mathcal{K}\mathbf{B}^\top \left(\frac{\mathbf{r}_i^{**}}{\mathbf{z}^*} \right) \right)_j = 0.$$

Summing the left-hand side of the above expression over the different species and patches, we get

$$\sum_{j=1}^m \sum_{i=1}^n x_{i,j}^* \left(\mathbf{T}\mathbf{Y}^* \left(\frac{\mathbf{p}_j^{**}}{\mathbf{y}^*} \right) \right)_i - \sum_{i=1}^n \sum_{j=1}^m \frac{x_{i,j}^*}{x_{i,j}^{**}} \left(\mathbf{B}\mathcal{K}\mathbf{B}^\top \left(\frac{\mathbf{r}_i^{**}}{\mathbf{z}^*} \right) \right)_j = 0. \quad (5.20)$$

Now consider the two terms in the left-hand side Eq. (5.20) separately. For the first term, note that, for any j , it holds that

$$\begin{aligned} \sum_{i=1}^n x_{i,j}^* \left(\mathbf{T}\mathbf{Y}^* \left(\frac{\mathbf{p}_j^{**}}{\mathbf{y}^*} \right) \right)_i &= \sum_{i=1}^n x_{i,j}^* (\mathbf{T}\mathbf{p}_j^{**})_i = \sum_{i=1}^n x_{i,j}^* \left(\sum_{l=1}^n T_{il} x_{l,j}^{**} \right) = - \sum_{l=1}^n x_{l,j}^{**} \left(\sum_{i=1}^n T_{li} x_{i,j}^* \right) \\ &= - \sum_{l=1}^n x_{l,j}^{**} \left(\sum_{i=1}^n T_{li} y_i^* z_j^* \right) = -z_j^* \sum_{l=1}^n x_{l,j}^{**} (\mathbf{T}\mathbf{y}^*)_l = 0. \end{aligned}$$

Hence,

$$\sum_{j=1}^m \sum_{i=1}^n x_{i,j}^* \left(\mathbf{T}\mathbf{Y}^* \left(\frac{\mathbf{p}_j^{**}}{\mathbf{y}^*} \right) \right)_i = 0.$$

For the second term, we find

$$\begin{aligned} -\sum_{i=1}^n \sum_{j=1}^m \frac{x_{ij}^*}{x_{ij}^{**}} \left(\mathbf{BK}\mathbf{B}^\top \left(\frac{\mathbf{r}_i^{**}}{\mathbf{z}^*} \right) \right)_j &= -\sum_{i=1}^n y_i^* \sum_{j=1}^m \frac{z_j^*}{x_{ij}^{**}} \left(\mathbf{BK}\mathbf{B}^\top \left(\frac{\mathbf{r}_i^{**}}{\mathbf{z}^*} \right) \right)_j \\ &= -\sum_{i=1}^n y_i^* \left(\frac{\mathbf{z}^*}{\mathbf{r}_i^{**}} \right)^\top \mathbf{BK}\mathbf{B}^\top \left(\frac{\mathbf{r}_i^{**}}{\mathbf{z}^*} \right). \end{aligned}$$

Thus, Eq. (5.20) can be simplified as

$$-\sum_{i=1}^n y_i^* \left(\frac{\mathbf{z}^*}{\mathbf{r}_i^{**}} \right)^\top \mathbf{BK}\mathbf{B}^\top \left(\frac{\mathbf{r}_i^{**}}{\mathbf{z}^*} \right) = 0.$$

Since $y_i^* > 0$ for $i = 1, \dots, n$, it holds for any $i = 1, \dots, n$ that

$$-\left(\frac{\mathbf{z}^*}{\mathbf{r}_i^{**}} \right)^\top \mathbf{BK}\mathbf{B}^\top \left(\frac{\mathbf{r}_i^{**}}{\mathbf{z}^*} \right) = 0. \quad (5.21)$$

From Eq. (5.21) and Lemma 5.1, it follows that $\mathbf{r}_i^{**} = q_i \mathbf{z}^*$ with $q_i \in \mathbb{R}_+$ for $i = 1, \dots, n$. Thus, $x_{ij}^{**} = q_i z_j^*$ and $\mathbf{p}_j^{**} = z_j^* \mathbf{q}$ for $i = 1, \dots, n$ and $j = 1, \dots, m$. Substituting the latter in the left-hand side of Eq. (5.19), we get

$$\begin{aligned} x_{ij}^{**} \left(\mathbf{T}\mathbf{Y}^* \left(\frac{\mathbf{p}_j^{**}}{\mathbf{y}^*} \right) \right)_i - \left(\mathbf{BK}\mathbf{B}^\top \left(\frac{\mathbf{r}_i^{**}}{\mathbf{z}^*} \right) \right)_j &= q_i z_j^{*2} \left(\mathbf{T}\mathbf{Y}^* \left(\frac{\mathbf{q}}{\mathbf{y}^*} \right) \right)_i - q_i (\mathbf{BK}\mathbf{B}^\top \mathbf{1}^m)_j \\ &= q_i z_j^{*2} (\mathbf{T}\mathbf{q})_i. \end{aligned}$$

Since $q_i > 0$ for $i = 1, \dots, n$, for Eq. (5.19) to hold, we should have $\mathbf{T}\mathbf{q} = \mathbf{0}^n$. Also note that

$$(\mathbf{1}^{mn})^\top \mathbf{x}^{**} = \sum_{i=1}^n \sum_{j=1}^m x_{ij}^{**} = \sum_{i=1}^n q_i \sum_{j=1}^m z_j^* = \sum_{i=1}^n q_i = 1.$$

Since the metapopulation model is balanced, it follows that $\mathbf{q} = \mathbf{y}^*$. Thus,

$$x_{i,j}^{**} = y_i^* z_j^* = x_{i,j}^*$$

for $i = 1, \dots, n$ and $j = 1, \dots, m$. This proves the uniqueness of the coexistence equilibrium \mathbf{x}^* . \square

5.8 Some examples

We now give examples of two balanced metapopulation models.

Example 1: Consider the following metapopulation network.

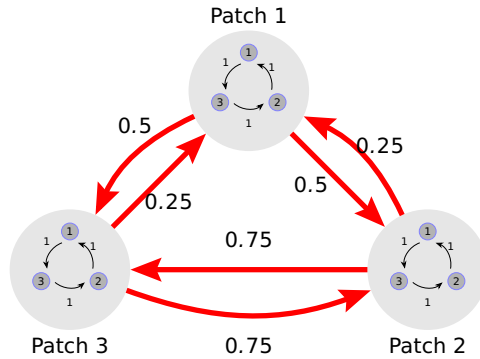


Figure 5.2: A metapopulation network composed of three patches. Each patch contains a local population composed of three species (1, 2 and 3), in cyclic competition, as shown by the black arrows. The red arrows denote migrations among the patches in the directions shown.

It is easy to verify that the network shown in Figure 5.2 corresponds to a balanced metapopulation model governed by System (5.17) with

$$\mathbf{T} = \begin{bmatrix} 0 & 1 & -1 \\ -1 & 0 & 1 \\ 1 & -1 & 0 \end{bmatrix}; \quad \mathbf{B} = \begin{bmatrix} -1 & 0 & 1 \\ 1 & -1 & 0 \\ 0 & 1 & -1 \end{bmatrix};$$

$$\mathbf{y}^* = \left(\frac{1}{3}, \frac{1}{3}, \frac{1}{3}\right)^T, \quad \mathbf{z}^* = \left(\frac{1}{5}, \frac{2}{5}, \frac{2}{5}\right)^T \text{ and } \mathcal{K} = \text{diag}\left(\frac{1}{10}, \frac{3}{10}, \frac{1}{10}\right).$$

Note that this metapopulation model is heterogeneous. From Theorem 5.1, it follows that the species proportions at the unique coexistence equilibrium for this model are given by $x_{i,1}^* = \frac{1}{15}$ and $x_{i,2}^* = x_{i,3}^* = \frac{2}{15}$.

Example 2: Consider the following metapopulation network.

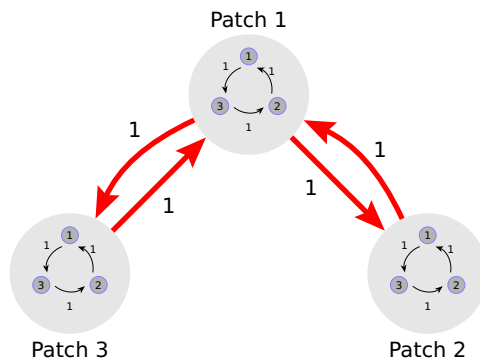


Figure 5.3: A metapopulation network composed of three patches. Species can migrate from patch 1 to the other two patches and vice versa. However, there exists no migrations between patches 2 and 3.

It is easy to verify that the network shown in Figure 5.3 corresponds to a balanced metapopulation model governed by System (5.17) with

$$\mathbf{T} = \begin{bmatrix} 0 & 1 & -1 \\ -1 & 0 & 1 \\ 1 & -1 & 0 \end{bmatrix}; \quad \mathbf{B} = \begin{bmatrix} 1 & -1 \\ 0 & 1 \\ -1 & 0 \end{bmatrix};$$

$\mathbf{y}^* = \mathbf{z}^* = \left(\frac{1}{3}, \frac{1}{3}, \frac{1}{3}\right)^\top$ and $\mathcal{K} = \frac{1}{3} \text{diag}(\mathbb{1}_2)$. Note that this metapopulation model is homogeneous. From Theorem 5.1, it follows that the species proportions at the unique coexistence equilibrium in this case are all given by $x_{i,j}^* = \frac{1}{9}$ for $i, j = 1, 2, 3$.

5.9 Stability of the coexistence equilibrium

We now prove the local stability of the unique coexistence equilibrium corresponding to the balanced metapopulation model (5.17). For the proof, we make use of the same Lyapunov function (5.7) as in Section 5.4, coupled with LaSalle's invariance principle stated in Theorem 3.2.

Theorem 5.2. *Consider the balanced metapopulation model (5.17) with coexistence equilibrium $\mathbf{x}^* \in S_+^{mn}$.*

1. *If the model is heterogeneous, then \mathbf{x}^* is locally asymptotically stable w.r.t. all initial conditions in S_+^{mn} in the neighbourhood of \mathbf{x}^* . Furthermore, if the model is persistent, then \mathbf{x}^* is globally asymptotically stable w.r.t. all initial conditions in S_+^{mn} .*
2. *If the model is homogeneous and persistent, then as $t \rightarrow \infty$, the solution trajectories converge to a limit cycle satisfying the equation*

$$\dot{x}_{i,j} = x_{i,j}(\mathbf{T}\mathbf{p}_j)_i$$

with $x_{i,j} = x_{i,k}$, for $i = 1, \dots, n$ and $j, k = 1, \dots, m$.

Proof. Let $x_{i,j}$ denote the proportion of species i in patch j . Assuming that $\mathbf{x} \in S_+^{mn}$, consider the Lyapunov function

$$V(\mathbf{x}) = -(\mathbf{x}^*)^\top \text{Ln} \left(\frac{\mathbf{x}}{\mathbf{x}^*} \right). \quad (5.22)$$

By Gibbs inequality, $V(\mathbf{x})$ is positive on S_+^{mn} and is equal to zero only if $\mathbf{x} = \mathbf{x}^*$.

Taking the time derivative of V , we have

$$\dot{V}(\mathbf{x}) = - \sum_{j=1}^m \sum_{i=1}^n \left(\frac{x_{i,j}^*}{x_{i,j}} \right) \dot{x}_{i,j}.$$

From Eq. (5.17), it follows that

$$\dot{V}(\mathbf{x}) = -\sum_{j=1}^m \sum_{i=1}^n x_{i,j}^* \left(\mathbf{T}\mathbf{Y}^* \left(\frac{\mathbf{p}_j}{\mathbf{y}^*} \right) \right)_i + \sum_{i=1}^n \sum_{j=1}^m \frac{x_{i,j}^*}{x_{i,j}} \left(\mathbf{B}\mathcal{K}\mathbf{B}^\top \left(\frac{\mathbf{r}_i}{\mathbf{z}^*} \right) \right)_j.$$

As in the proof of Theorem 5.1, it can be verified that

$$\sum_{j=1}^m \sum_{i=1}^n x_{i,j}^* \left(\mathbf{T}\mathbf{Y}^* \left(\frac{\mathbf{p}_j}{\mathbf{y}^*} \right) \right)_i = 0$$

and

$$\sum_{i=1}^n \sum_{j=1}^m \frac{x_{i,j}^*}{x_{i,j}} \left(\mathbf{B}\mathcal{K}\mathbf{B}^\top \left(\frac{\mathbf{r}_i}{\mathbf{z}^*} \right) \right)_j = \sum_{i=1}^n y_i^* \left(\frac{\mathbf{z}^*}{\mathbf{r}_i} \right)^\top \mathbf{B}\mathcal{K}\mathbf{B}^\top \left(\frac{\mathbf{r}_i}{\mathbf{z}^*} \right).$$

Thus,

$$\dot{V}(\mathbf{x}) = \sum_{i=1}^n y_i^* \left(\frac{\mathbf{z}^*}{\mathbf{r}_i} \right)^\top \mathbf{B}\mathcal{K}\mathbf{B}^\top \left(\frac{\mathbf{r}_i}{\mathbf{z}^*} \right).$$

Since $y_i^* > 0$ for $i = 1, \dots, n$, it follows from Lemma 5.1 that $\dot{V}(\mathbf{x}) \leq 0$ and $\dot{V}(\mathbf{x}) = 0$ if and only if $\mathbf{r}_i = q_i \mathbf{z}^*$ with $q_i \in \mathbb{R}_+$, for $i = 1, \dots, n$.

Thus,

$$x_{i,j} = q_i z_j^*, \quad (5.23)$$

for $i = 1, \dots, n$ and $j = 1, \dots, m$. Since $(\mathbb{1}^{mn})^\top \mathbf{x} = 1$, we obtain

$$\sum_{i=1}^n \sum_{j=1}^m x_{i,j} = \sum_{i=1}^n q_i \sum_{j=1}^m z_j^* = \sum_{i=1}^n q_i = 1.$$

Let $\mathcal{E} \subset S_+^{mn}$ be the set of all vectors \mathbf{x} for which condition (5.23) is satisfied with $(\mathbb{1}^n)^\top \mathbf{q} = 1$. We now determine the largest subset of \mathcal{E} that is positively invariant w.r.t. System (5.17). Assume that \mathbf{x} continuously takes values from \mathcal{E} and satisfies System (5.17). Since \mathbf{x} takes values from \mathcal{E} , we have $\dot{x}_{i,j} = z_j^* \dot{q}_i$. Since \mathbf{x} also satisfies System (5.17), we have

$$\dot{x}_{i,j} = x_{i,j} (\mathbf{T}\mathbf{p}_j)_i - \left(\mathbf{B}\mathcal{K}\mathbf{B}^\top \left(\frac{\mathbf{r}_i}{\mathbf{z}^*} \right) \right)_j = q_i z_j^{*2} (\mathbf{T}\mathbf{q})_i - q_i (\mathbf{B}\mathcal{K}\mathbf{B}^\top \mathbb{1}^m)_j = q_i z_j^{*2} (\mathbf{T}\mathbf{q})_i.$$

Thus, $z_j^* \dot{q}_i = q_i z_j^{*2} (\mathbf{T}\mathbf{q})_i$ which implies that

$$\dot{q}_i = z_j^* q_i (\mathbf{T}\mathbf{q})_i, \quad (5.24)$$

for $i = 1, \dots, n$ and $j = 1, \dots, m$. We now consider two cases.

Case 1: The model is heterogeneous

The model is heterogeneous if the vector \mathbf{z}^* is not parallel to $\mathbf{1}^m$. In this case, Eq. (5.24) will be satisfied only if

$$q_i(\mathbf{Tq})_i = 0$$

for $i = 1, \dots, n$. Since $q_i \in \mathbb{R}_+$ for $i = 1, \dots, n$, it follows that

$$\mathbf{Tq} = \mathbf{0}^n.$$

Since $(\mathbf{1}^n)^\top \mathbf{q} = 1$, we have $\mathbf{q} = \mathbf{y}^*$. This implies that

$$x_{i,j} = y_i^* z_j^* = x_{i,j}^*$$

for $i = 1, \dots, n$ and $j = 1, \dots, m$.

Thus, the largest subset of \mathcal{E} that is positively invariant w.r.t. System (5.17) consists of just the unique equilibrium $\mathbf{x}^* \in S_+^{mn}$.

By LaSalle's invariance principle, it follows that the equilibrium \mathbf{x}^* is locally asymptotically stable w.r.t. all initial conditions in S_+^{mn} in the neighbourhood of \mathbf{x}^* , and globally asymptotically stable w.r.t. all initial conditions in S_+^{mn} provided that System (5.17) is persistent.

5

Case 2: The model is homogeneous, i.e., $\mathbf{z}^* = \frac{1}{m} \mathbf{1}^m$

In this case, Eq. (5.24) takes the form $\dot{q}_i = \frac{q_i}{m} (\mathbf{Tq})_i$. We have

$$x_{i,j} = q_i z_j^* = \frac{q_i}{m}$$

and

$$\dot{x}_{i,j} = \frac{\dot{q}_i}{m} = \frac{q_i}{m^2} (\mathbf{Tq})_i = x_{i,j} (\mathbf{Tp}_j)_i.$$

Consequently, the largest subset of \mathcal{E} that is positively invariant w.r.t. System (5.17) consists of all vectors $\mathbf{x}(t) \in S_+^{mn}$ satisfying

$$\dot{x}_{i,j} = x_{i,j} (\mathbf{Tp}_j)_i$$

with $x_{i,j} = x_{i,k}$ for $i = 1, \dots, n$ and $j, k = 1, \dots, m$.

The proof for Case 2 again follows from LaSalle's invariance principle. \square

The above results can be illustrated by simulating System (5.17) for the metapopulation models shown in Figs. 5.2 and 5.3 of Section 5.8. The results of the simulations are shown in Figs. 5.4 and 5.5, respectively.

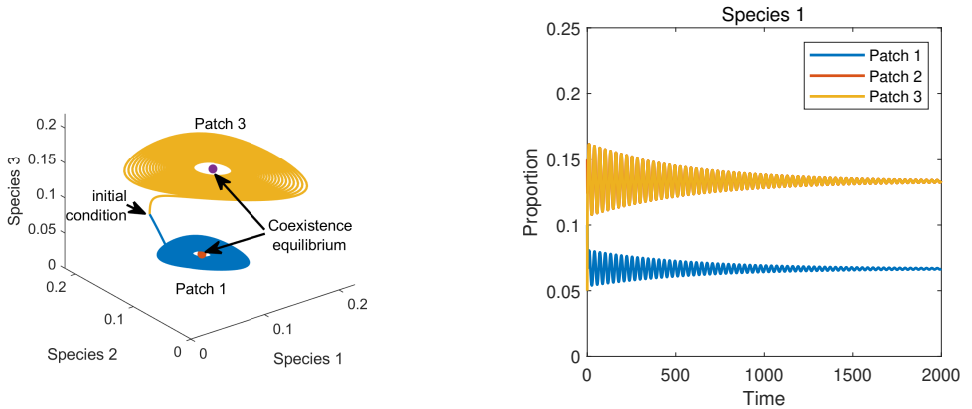


Figure 5.4: Left: Dynamics of the metapopulation model in Fig. 5.2 for patches 1 and 3 showing asymptotic stability of the coexistence equilibrium. Right: The time evolution of the proportion of species 1 in the three patches.

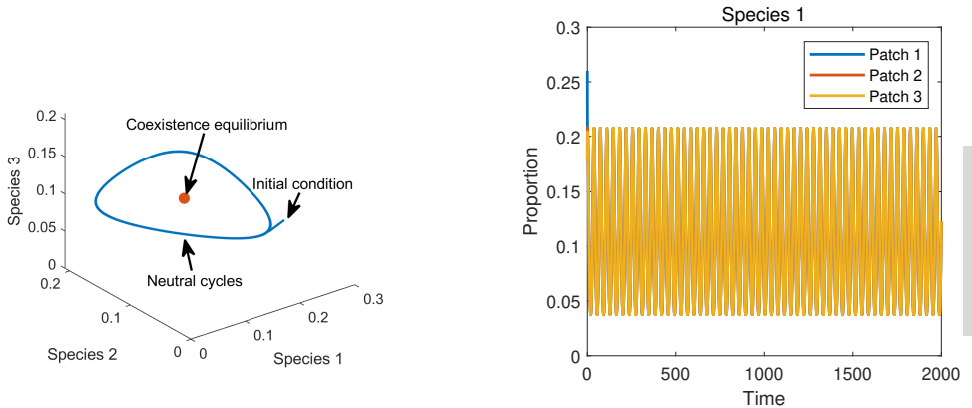


Figure 5.5: Left: Dynamics of the metapopulation model in Fig. 5.3 for patches 1 and 3 showing a limit cycle arising from the neutral stability of the coexistence equilibrium. Right: Time evolution of the proportion of species 1 in the three patches. Note that the dynamics in all patches are the same and thus the three graphs overlap.

5.10 Discussion and conclusion

In this chapter, we have expanded the class of competition networks for which the numerical observations of Nagatani et al. (2018) are valid. This has been done, firstly, by giving a more general definition of homogeneity/heterogeneity of a metapopulation network that is based on the nature of the adjacency matrix of its inter-patch migrations rather than on the number of dispersal links as was previously done in Nagatani et al. (2018).

Secondly, we have performed a stability analysis of the coexistence equilibrium of a metapopulation model whose inter-patch migration is assumed to be detailed

balanced and whose intra-patch dynamics is governed by a mean-field ODE system with a feasible (coexistence) equilibrium.

Detailed balancing, a well-known concept in CRNT, is a key feature of many metapopulation models and previous studies had not explicitly explored this concept. The motivation behind using concepts from CRNT is based on the fact that much of the interesting dynamical behavior observed in biological systems can be understood by analyzing the underlying chemical components and CRNT provides a unified mathematical approach to the study of chemical processes.

The assumption of detailed balancing thus allows us to view the inter-patch migrations as a detailed balanced single species mass action reaction network and make use of the already available results on the latter.

Results show that the considered metapopulation model admits a unique coexistence equilibrium. By making use of the Lyapunov function constructed by Grilli et al. (2017), coupled with LaSalle's invariance principle, it is shown that:

1. if the model is heterogeneous, then the coexistence equilibrium is locally asymptotically stable; it is globally stable if the considered metapopulation is persistent;
2. if the model is homogeneous and persistent, then the dynamics of the model is analogous to that of a single well-mixed patch; in this case, the coexistence equilibrium is neutrally stable.

5 These results provide a mathematical support for the numerical results of Nagatani et al. (2018) and demonstrate that the numerical observations extend beyond the three-species cyclic systems to a larger class of networks.

It should, however, be noted that, as in (Nagatani et al., 2018) and most metapopulation models, the above results have been achieved by examining the simplified case in which the patches are assumed to be spatially homogeneous and contain a local population in which individuals are well mixed. In addition, it is assumed that all the patches contain the same species.

Although this assumption is far from real metapopulations, it makes the mathematical analysis tractable and provides a starting point for future analysis of more realistic metapopulation models.

However, the results reaffirm the prevailing ecological theory that spatial heterogeneities in the landscape can have profound effects on the dynamics of populations within an environment. In the metapopulation framework, these heterogeneities come in many forms ranging from differences in dispersal rates among the patches to patch size distributions, among others. Also the fact that fragmented habitats are more likely to present some level of spatial heterogeneity underlies the importance of the metapopulation framework in studies for nature conservation.

6

Finite-difference schemes for reaction-diffusion equations modelling cyclic competition: A stability analysis

The material of this chapter is based on the following publication:

- Muyinda, N., De Baets, B., and Rao, S. (2018). On the linear stability of some finite difference schemes for nonlinear reaction-diffusion models of chemical reaction networks. *Communications in Applied and Industrial Mathematics*, 9(1),121–140. <https://doi.org/10.2478/caim-2018-0016>

6.1 Introduction

In Chapter 5, we explored the dynamics of metapopulation models which provide a useful theoretical framework for modelling the dynamics of populations living

in highly fragmented landscapes composed of discrete habitat patches. If the environment is a continuum (such as in aquatic systems), models of this type can be constructed for very finely reticulated subdivisions of the continuum, and these can provide very good approximations. However, for analysis of such situations, it is generally more convenient to pass to the limit and replace discrete patch models by continuum models. This replaces the metapopulation ODEs by a system of PDEs (in particular, reaction-diffusion (RD) equations), and greatly reduces the number of equations (Levin, 1976).

The simplest RD models considered take the general form

$$\frac{\partial u_i}{\partial t} = D_i \nabla^2 u_i + f_i(u_1, \dots, u_n), \quad (6.1)$$

or, equivalently, in matrix form,

$$\frac{\partial \mathbf{u}}{\partial t} = D \nabla^2 \mathbf{u} + \mathbf{f}(\mathbf{u}), \quad (6.2)$$

where, as before, $\mathbf{u} = \mathbf{u}(\mathbf{x}, t)$ is vector of species population densities at location \mathbf{x} at time t , D is a constant positive diagonal matrix of diffusion coefficients, ∇^2 is the Laplacian, and $\mathbf{f}(\mathbf{u})$ is a vector of functions representing the (in general, nonlinear) reaction (interaction) terms. The choice of the reaction forms may vary ranging from interactions governed by the simple law of mass-action to the somewhat more complicated functional forms such as the Holling types II and III (Volpert and Petrovskii, 2009).

A common procedure in analyzing the RD model system (6.2) is to assume constant values of the parameters, and to study accordingly the asymptotic (long-term) behaviour of the system. That is, to search for stable equilibrium points and stable periodic solutions. In this regard, it is convenient to first consider the corresponding ODE system by deleting the diffusion term from the model.

Studies have shown that, in the absence of diffusion and with no more than two interacting species, every bounded solution tends either to a stable equilibrium or to a stable periodic pattern (e.g., a limit cycle) (Hastings and Harrison, 1994; Levin, 1976). However, if the local equilibrium in the absence of diffusion is unstable, adding diffusion to the model does not make it more stable (Hastings and Harrison, 1994). On the contrary, an equilibrium that is stable in the absence of diffusion can become unstable after diffusion is included. This phenomenon is now well-known as *diffusion-driven instability* (Turing, 1952).

Diffusion-driven instability, however, seems to contradict the predictions of the metapopulation model, in which dispersal (in particular, heterogeneous migration) has a stabilizing effect on species coexistence since it moves the coexistence equilibrium from the knife-edge neutral stability to local asymptotic stability. This apparent contradiction comes from the focus on equilibrium behavior of the RD

models. Studies have shown that within the RD framework, a predator-prey system that would not persist in the absence of dispersal will persist with diffusion added to the system (Nisbet et al., 1993). However, persistence is not via a stable equilibrium but through cyclic or more complex dynamics (Hastings and Harrison, 1994).

Even in the absence of diffusion, it remains very hard, if not impossible, to solve a nonlinear ODE system analytically. With the introduction of diffusion, the analysis of the whole system remains difficult and is hence rare in the literature. Therefore, numerical methods have an important part to play in investigating the behaviour of solutions to such models.

Typically, finite-difference methods are used where the RD equation is first discretized in space, and then in time. These numerical methods can also be used to get approximate population density values of species at each point of space at every instant of time. A crucial question that arises in the use of these methods is whether the method will behave stably or not.

The importance of stability in numerical analysis is stressed by the *Lax-Richtmyer equivalence theorem* which states that, under certain natural assumptions, a finite difference scheme is convergent (*i.e.*, approaches the unknown exact analytic solution) if and only if it is stable. Here we use the term stability to designate that any numerical errors, introduced at some stage of the computation, do not magnify (blow up) over time. Obviously this is very important, since errors are an inevitable property of any numerical solution. If the algorithm is not stable, then numerical errors will be amplified with each time step and pretty soon they will dominate the computation (making it useless).

In this chapter, we explore a mathematical problem concerned with stability of finite difference schemes for systems of coupled nonlinear RD equations. The aim is to establish sufficient conditions for the stability of some popular finite difference schemes for the numerical solution of the general nonlinear RD model system (6.2) in a one-dimensional spatial domain. The motivation for this stems from the fact that majority of the sufficient conditions for the stability of finite difference schemes in the literature have been established based on an analysis of systems of linear diffusion equations (see, e.g., Thomas (1995)) and yet these conditions are only necessary and not sufficient in the case of systems of RD equations. Since most ecological competition networks involve at least two species, the RD models of such networks are nonlinear systems due to mass-action type of interactions. Thus this chapter is aimed at carrying out a rigorous study of stability of finite difference schemes, applied to coupled nonlinear RD systems, something that has been lacking in the literature.

To illustrate the results from the stability analysis, we shall study the numerical solutions of two RD model systems, first from CRNT (the Brusselator model) and second from population dynamics (the cyclic competition model).

This chapter is organized as follows. We start with a linearization of the model system (6.2) in Section 6.2. We then give a formal definition of stability of a finite difference scheme in Section 6.3. In Section 6.4, we extend the scalar definitions of the DFT and the von Neumann stability conditions given in Section 3.7.3 to the multivariable (systems) case. Note that in the scalar case, the von Neumann stability condition was both necessary and sufficient for stability. However, this condition is only necessary but not sufficient in the systems case. In Section 6.5, we give sufficient conditions for stability. Then, in Section 6.6, a local linear stability analysis of some popular finite difference schemes is carried out. We then perform some numerical experiments in Section 6.7, on the Brusselator RD model and a cyclic competition model. Finally, we show, in Section 6.8, that for RD systems whose reactions are governed by a variety of enzyme kinetic rate laws, some of the established sufficient conditions are naturally satisfied implying that these implicit schemes are expected to work for the solution of such RD systems. We end the chapter with a discussion and conclusions in Section 6.9.

6.2 Linearization

As it has been stated, the von Neumann stability method makes use of Fourier transforms and this restricts its application to linear equations with constant coefficients, uniform grids and periodic boundary conditions (Wesseling, 2001). Moreover, because nonlinear problems have no known analytic solutions, analyzing the stability of a finite difference scheme applied to a nonlinear problem like (6.2) can be a complicated task. Thus, in most cases, the stability analysis of a finite difference scheme applied to a nonlinear problem is often reduced to an analysis of stability of the difference scheme applied to the corresponding locally linearized problem. However, although the linearization substantially simplifies the stability analysis, conditions derived from the linear stability analysis may not necessarily apply to the nonlinear problem. This is due to the fact that linear stability is a necessary condition for nonlinear problems but is certainly not sufficient (Hirsch, 1988).

We have, so far, defined stability in terms of the boundedness of the errors introduced during the application of the numerical method. Numerical stability can also be defined in terms of the deviation between two numerical solutions. That is, for a numerically stable scheme, the deviation between two numerical solutions arising, for example, due to round-off error, does not grow with time. But the goal of any numerical method is to generate numerical solutions that can closely match the unknown analytical solutions. In this regard, stability of a difference scheme can as well be discussed in terms of the deviation between two analytic solutions. Using this framework, we proceed to perform a linearization of Eq. (6.2).

Suppose \mathbf{u} and \mathbf{v} are two analytical solutions to Eq. (6.2) that are close to each

other. Then their difference satisfies

$$\frac{\partial}{\partial t}(\mathbf{u} - \mathbf{v}) = D\nabla^2(\mathbf{u} - \mathbf{v}) + \mathbf{f}(\mathbf{u}) - \mathbf{f}(\mathbf{v}).$$

Define $\mathbf{z} := \mathbf{u} - \mathbf{v}$. A Taylor expansion of $\mathbf{f}(\mathbf{u})$ about \mathbf{v} leads to

$$\frac{\partial \mathbf{z}}{\partial t} = D\nabla^2 \mathbf{z} + A\mathbf{z} + \mathcal{O}(\mathbf{z}^2),$$

where A is the Jacobian matrix of \mathbf{f} evaluated at \mathbf{v} , and so at any instant in space and time, it is a matrix of constants. When \mathbf{z} is small, which corresponds to the two solutions \mathbf{u} and \mathbf{v} being near each other, such that the $\mathcal{O}(\mathbf{z}^2)$ terms are small compared to the linear term $A\mathbf{z}$, the difference between the two solutions satisfies:

$$\frac{\partial \mathbf{z}}{\partial t} \approx D\nabla^2 \mathbf{z} + A\mathbf{z}. \quad (6.3)$$

Equation (6.3) is the local linear approximation (or linearization) of Eq. (6.2) about the solution \mathbf{v} . In all the analyses of this chapter, we assume that the Jacobian A is real with finite entries in the space and time domains under consideration.

6.3 The stability problem

We consider the initial-value problem for a system of linear RD equations given by

$$\frac{\partial \mathbf{z}}{\partial t} = D\nabla^2 \mathbf{z} + A\mathbf{z}, \quad \mathbf{z}(\mathbf{x}, 0) = \mathbf{z}_0(\mathbf{x}) \quad (6.4)$$

where $\mathbf{z} = (z_1, \dots, z_m)^\top$ and $z_i = z_i(\mathbf{x}, t)$, D is a positive diagonal matrix of diffusion coefficients and A is a real constant matrix. For simplicity, we restrict Eq. (6.4) to a one-dimensional spatial domain $\Omega \subset \mathbb{R}$ for time $t \in]0, T[$, although the results will analogously hold in three spatial dimensions.

The von Neumann stability analysis requires a uniform grid, so let Δt denote the time step and Δx the space step. The discrete set of points in space-time is given by

$$x_j = j\Delta x, \quad t_n = n\Delta t,$$

and the continuous function \mathbf{z} is approximated by the grid function \mathbf{z}_j^n ,

$$\mathbf{z}_j^n \approx \mathbf{z}(x_j, t_n).$$

The ℓ_2 norm of the grid function \mathbf{z}^n is defined by

$$\|\mathbf{z}^n\|_{\ell_2} = \sqrt{\Delta x \sum_j \|\mathbf{z}_j^n\|_2^2}.$$

where the norm in the summation is the Euclidean norm defined as

$$\|\mathbf{z}\|_2 = \sqrt{\sum_{j=1}^m |z_j|^2}.$$

A general two-step difference scheme of width N for the PDE in Eq. (6.4) at the point (x_j, t_n) takes the form

$$\sum_{|k| \leq N} A_k^1 \mathbf{z}_{j+k}^{n+1} = \sum_{|k| \leq N} A_k^0 \mathbf{z}_{j+k}^n, \tag{6.5}$$

where A_k^1 and A_k^0 are $m \times m$ constant matrices whose entries depend on the parameters of the PDE and the numerical scheme. A numerical solution of Eq. (6.4) is obtained by solving the discrete equations (6.5). Thus the numerical solution gives only approximate values of the exact solution of the PDE at the grid points.

This approximation introduces a number of errors such as truncation and round-off errors. A good numerical solution is one for which the error is small in some sense (Liska and Steinberg, 1993). When the numerical error in the solution increases with increasing time, the solution may begin to oscillate with larger and larger amplitudes and consequently become unstable.

Intuitively, a numerical scheme is stable when the errors are not amplified with increasing time. More precisely, stability requires that for $0 \leq t = n\Delta t \leq T$, there exists a positive constant K such that

$$\|\mathbf{z}_j^{n+1}\|_{\ell_2} \leq K \|\mathbf{z}_j^n\|_{\ell_2}. \tag{6.6}$$

Here K is independent of the step sizes and n but may depend on any other parameters in the PDE or the discretization scheme. Because of the time-translation invariance, condition (6.6) only needs to hold for $n = 0$ (Liska and Steinberg, 1993). It should also be noted that stability is purely a property of the difference scheme (6.5) and has nothing to do with the original initial-value problem (6.2).

6.4 The von Neumann stability criterion

We now proceed to establish the condition under which relation (6.6) holds, i.e., the stability condition. We have already stated that the standard tool for achieving

this is the von Neumann stability analysis, which makes use of the discrete Fourier transform (DFT).

In Section 3.7.3, we have defined the DFT, the amplification matrix and also stated the von Neumann stability condition in the scalar case. We proceed to extend these definitions to the multivariable (or systems) case.

Suppose that $\mathbf{z} = (\dots, \mathbf{z}_{-1}, \mathbf{z}_0, \mathbf{z}_1, \dots)^\top$ with $\mathbf{z}_j = (z_{1j}, \dots, z_{mj})^\top$ is a vector in ℓ_2 . We define the discrete Fourier transform $\hat{\mathbf{z}}$ of \mathbf{z} as follows (Thomas, 1995);

$$\hat{\mathbf{z}}(\xi) = \frac{1}{\sqrt{2\pi}} \sum_{j \in \mathbb{Z}} e^{-ij\xi} \mathbf{z}_j \quad (6.7)$$

for $\xi \in [-\pi, \pi]$. The inverse discrete Fourier transform is given by

$$\mathbf{z}_j = \frac{1}{\sqrt{2\pi}} \int_{-\pi}^{\pi} e^{ij\xi} \hat{\mathbf{z}}(\xi) d\xi \quad (6.8)$$

for $-\infty < j < \infty$.

Like in Section 3.7.3, the DFTs of the shift operators are given by

$$\widehat{S_{\pm} \mathbf{z}}(\xi) = e^{\pm i\xi} \hat{\mathbf{z}}(\xi). \quad (6.9)$$

The approach that we use to analyze the stability is to take the DFT of Eq. (6.5) to get

$$\sum_{|k| \leq N} A_k^1 e^{ik\xi} \hat{\mathbf{z}}^{n+1} = \sum_{|k| \leq N} A_k^0 e^{ik\xi} \hat{\mathbf{z}}^n. \quad (6.10)$$

Assuming that the matrix $\sum_{|k| \leq N} A_k^1 e^{ik\xi}$ is invertible, which is not a significant restriction, and from (6.10) we have

$$\hat{\mathbf{z}}^{n+1}(\xi) = G(\xi) \hat{\mathbf{z}}^n, \quad (6.11)$$

where

$$G(\xi) = \left(\sum_{|k| \leq N} A_k^1 e^{ik\xi} \right)^{-1} \left(\sum_{|k| \leq N} A_k^0 e^{ik\xi} \right). \quad (6.12)$$

The matrix $G(\xi)$ is called the amplification matrix of the difference scheme (6.5), and reduces to the previously defined amplification factor when there is only one equation to be discretized. Notice that

$$\begin{aligned} \hat{\mathbf{z}}^{n+1}(\xi) &= G(\xi) \hat{\mathbf{z}}^n \\ &= G^{n+1}(\xi) \hat{\mathbf{z}}^0. \end{aligned} \quad (6.13)$$

So, the growth of $\hat{\mathbf{z}}^n$ (and \mathbf{z}^n) and, hence, the stability of the difference scheme, depends on the growth of the amplification matrix raised to the n -th power, G^n .

In using the DFT, we have transformed our problem from the solution space (ℓ_2 -space) containing numerical spatial derivatives to a problem with no spatial variation in a vector L_2 -space (the transform space). Then, by Parseval's identity ($\|\mathbf{z}\|_2 = \|\hat{\mathbf{z}}\|_2$ where the first two-norm is the vector ℓ_2 norm and the second two-norm is the vector L_2 norm on $[-\pi, \pi]$), an equivalent form of the stability inequality (6.6) reads

$$\|\hat{\mathbf{z}}^{n+1}\|_2 \leq K \|\hat{\mathbf{z}}^n\|_2. \tag{6.14}$$

In order for all $\hat{\mathbf{z}}^n$ (and hence \mathbf{z}^n) to remain bounded, and hence the difference scheme (6.5) to be stable, requires that the matrix $[G(\xi)]^n$ remains uniformly bounded for all values of ξ . Establishing bounds makes use of the matrix norm

$$\|G\|_2 = \max_{\mathbf{z} \neq 0} \frac{\|G \cdot \mathbf{z}\|_2}{\|\mathbf{z}\|_2}.$$

Since G is an $m \times m$ matrix with m eigenvalues $\lambda_1, \dots, \lambda_j, \dots, \lambda_m$ obtained as roots of a polynomial

$$\det|G - \lambda I| = 0, \tag{6.15}$$

its spectral radius is defined by the modulus of the largest eigenvalue:

$$\rho(G) = \max_j |\lambda_j|. \tag{6.16}$$

From linear algebra, it is known that

$$\|G\|_2 \geq \max_j \frac{\|G\mathbf{v}_j\|_2}{\|\mathbf{v}_j\|_2} = \max_j |\lambda_j| = \rho(G), \tag{6.17}$$

where \mathbf{v}_j are the eigenvectors of G , and

$$\|G\|_2^n \geq \|G^n\|_2 \geq \rho^n(G). \tag{6.18}$$

In addition, for any matrix A , $\|A\|_2 = \sqrt{\rho(A^*A)}$, where A^* is the conjugate transpose of A . If A is a real symmetric matrix, then $A^* = A$ such that $\rho(A^*A)\rho(A^2) = \rho^2(A)$, and thus $\|A\|_2 = \rho(A)$.

The von Neumann stability criterion requires that for a stable scheme, the spectral radius of the amplification matrix satisfies (Richtmyer and Morton, 1967)

$$\rho(G) \leq 1 + C\Delta t, \tag{6.19}$$

for finite Δt , $C \geq 0$ and for all $\xi \in [-\pi, \pi]$.

Using the von Neumann criterion (6.19) with a nonzero C allows for exponential growth in the solution. Although any growth in the solution is viewed as the scheme tending towards instability, this is special since this growth is less than or equal to an exponential (Thomas, 1995). Generally, this stability condition is only necessary. It is also sufficient, for example, in the scalar case ($m = 1$).

Verifying the sufficient condition is usually an even more complicated problem. In any case, the necessary condition for stability gives substantial insight into the stability properties of the difference scheme.

6.5 Sufficient conditions for stability

An attempt at establishing sufficient conditions for stability can be achieved by making use of the next two propositions and lemma.

Proposition 6.1 (Richtmyer and Morton, 1967, p. 84). *Suppose that the amplification matrix G associated with the difference scheme (6.5) satisfies the von Neumann condition (6.19). Then, if G is "uniformly diagonalizable", that is, for each G , there exists a matrix S such that $S^{-1}GS = \Lambda$ is diagonal and S and S^{-1} are bounded independent of ξ and Δt , then the scheme is stable.*

Proposition 6.2 (Horn and Johnson, 2013, p. 368). *There is a matrix norm $\|\cdot\|_s$ such that $\|A\|_s = \rho(A)$ if and only if every eigenvalue of A of maximum modulus is semisimple. That is, for all $\lambda \in \sigma(A)$ such that $|\lambda| = \rho(A)$, the algebraic multiplicity of λ is equal to its geometric multiplicity. We call $\|\cdot\|_s$ the spectral radius norm.*

Lemma 6.1. *Let B be an n -square matrix. Suppose that B is uniformly diagonalizable such that $S^{-1}BS$ is a diagonal matrix, for some nonsingular matrix S . Furthermore, suppose there exists a constant δ such that $\Delta \geq \delta > 0$, where $\Delta^2 := \det(S^*S)$, S^* is the conjugate transpose of S , then the matrix S together with its inverse are uniformly bounded.*

Proof. Since B is diagonalizable, the columns of the matrix S are the linearly independent eigenvectors of B . Assume that the eigenvectors are normalized. The norm of any n -square matrix does not exceed n times the absolute value of its largest element (Richtmyer and Morton, 1967). Thus $\|S\|_2 \leq n$. In addition, $|(S^{-1})_{ij}| \leq 1/\Delta$ (Richtmyer and Morton, 1967), and since Δ is bounded away from zero, then $\|S^{-1}\|_2 \leq n/\Delta$. Thus the matrices S and S^{-1} are uniformly bounded. \square

In addition, we shall also make use of the concept of semi-stability, and D-semi-stability, of matrices in our attempt to establish sufficient conditions for stability.

By definition, an n -square matrix A is said to be *stable* (*semi-stable*) if every eigenvalue of A has a negative (non-positive) real part. It is said to be *semi-stable* if

every eigenvalue of A has a non-positive real part. It is said to be D -stable (D -semi-stable) if for all positive diagonal matrices D , the matrix DA is stable (semi-stable) (Horn and Johnson, 2013). Note that if a matrix A is D -semi-stable, then $IA = A$ is semi-stable, where I is the identity matrix. Thus D -semi-stability implies semi-stability.

6.6 Stability of difference schemes

We are now in a position to establish sufficient conditions for the stability of some popular difference schemes used for the solution of Eq. (6.2). We shall assume that the matrix A in the linearized Eq. (6.4) is real with finite entries. Thus any matrix norm of A is bounded by the size of A times the absolute value of its largest element (Richtmyer and Morton, 1967), which implies that the matrix A is bounded. We shall make use this fact.

We shall perform a stability analysis of the Crank–Nicolson (CN) scheme, the fractional step theta scheme (FSTS), the implicit integration factor (IIF) scheme and an implicit-explicit (IMEX) scheme.

6.6.1 The Crank–Nicolson scheme

The Crank–Nicolson (CN) scheme is a second order accurate in time implicit scheme commonly employed for the time integration of initial-value problems. A CN scheme for the linearized Eq. (6.4) in a one-dimensional spatial domain is

$$\frac{1}{\Delta t}(\mathbf{z}_j^{n+1} - \mathbf{z}_j^n) = \frac{1}{2\Delta x^2}D \left[(\mathbf{z}_{j+1}^{n+1} - 2\mathbf{z}_j^{n+1} + \mathbf{z}_{j-1}^{n+1}) + (\mathbf{z}_{j+1}^n - 2\mathbf{z}_j^n + \mathbf{z}_{j-1}^n) \right] + \frac{1}{2}A(\mathbf{z}_j^{n+1} + \mathbf{z}_j^n). \tag{6.20}$$

Equation (6.20) can be rewritten as

$$\left(I + rD - \frac{\Delta t}{2}A \right) \mathbf{z}_j^{n+1} - \frac{r}{2}D(S_+ \mathbf{z}_j^{n+1} + S_- \mathbf{z}_j^{n+1}) = \left(I - rD + \frac{\Delta t}{2}A \right) \mathbf{z}_j^n + \frac{r}{2}D(S_+ \mathbf{z}_j^n + S_- \mathbf{z}_j^n), \tag{6.21}$$

where $r := \frac{\Delta t}{\Delta x^2}$.

Taking the discrete Fourier transform of Eq. (6.21) gives

$$\left(I + 2r\sin^2\left(\frac{\xi}{2}\right)D - \frac{\Delta t}{2}A \right) \hat{\mathbf{z}}^{n+1} = \left(I - 2r\sin^2\left(\frac{\xi}{2}\right)D + \frac{\Delta t}{2}A \right) \hat{\mathbf{z}}^n. \tag{6.22}$$

Thus, from Eq. (6.22), the amplification matrix for the CN scheme is given by

$$G = \left(I + \rho D - \frac{\Delta t}{2} A \right)^{-1} \left(I - \rho D + \frac{\Delta t}{2} A \right), \quad (6.23)$$

where $p := 2r \sin^2\left(\frac{\xi}{2}\right) \geq 0$ for $\xi \in [-\pi, \pi]$.

Let us rewrite G in the form

$$G = \left(I - \frac{\Delta t}{2} (I + \rho D)^{-1} A \right)^{-1} (I + \rho D)^{-1} \left(I - \rho D + \frac{\Delta t}{2} A \right). \quad (6.24)$$

Since D is a positive diagonal matrix, $(I + \rho D)$ and its inverse are both positive diagonal and invertible. It is known, from linear algebra, that every n -square matrix is similar to a matrix in Jordan canonical form. That is, if $\lambda_1, \lambda_2, \dots, \lambda_k$ are the distinct eigenvalues of $(I + \rho D)^{-1} A$, there exists a nonsingular matrix S such that

$$(I + \rho D)^{-1} A = S J S^{-1}, \quad (6.25)$$

where J is the Jordan canonical form of $(I + \rho D)^{-1} A$, and takes the form

$$J = \text{diag}(J_{n_1}, J_{n_2}, \dots, J_{n_l}),$$

with $l \geq k$ and each J_{n_i} is a square Jordan block of size n_i having eigenvalue λ_i on the diagonal, 1's on the superdiagonal and zeros elsewhere, and $n_1 + n_2 + \dots + n_l = m$, the size of G .

Substituting (6.25) in (6.24), the amplification matrix G can be written as

$$G = X Y + \frac{\Delta t}{2} X H, \quad (6.26)$$

where

$$\begin{aligned} X &:= S \left(I - \frac{\Delta t}{2} J \right)^{-1} S^{-1}, \\ Y &:= (I + \rho D)^{-1} (I - \rho D), \text{ and} \\ H &:= (I + \rho D)^{-1} A. \end{aligned} \quad (6.27)$$

Since $D = \text{diag}(d_1, d_2, \dots, d_m)$, Y is a diagonal matrix, with diagonal entries

$$y_j = \frac{1 - \rho d_j}{1 + \rho d_j}, \quad j = 1, 2, \dots, m. \quad (6.28)$$

The next theorem establishes sufficient conditions for the stability of the CN scheme (6.20).

Theorem 6.1. *Suppose that the matrix A is D -semi-stable, matrix G is diagonal-*

izable and matrix X is such that every eigenvalue of maximum modulus is semi-simple. Then

- (i) matrix G satisfies the von Neumann condition, and
- (ii) the CN scheme (6.20) is unconditionally stable.

Proof. (i) Taking the spectral radius norm of G in Eq. (6.26), we have

$$\|G\|_s \leq \|X\|_s \|Y\|_s + \frac{\Delta t}{2} \|X\|_s \|H\|_s. \tag{6.29}$$

Since Y is a diagonal matrix, Proposition 6.2 implies that $\|Y\|_s = \rho(Y)$.

Since $pd_j \geq 0$, the eigenvalues of Y are its diagonal entries given by

$$y_j = \frac{1 - pd_j}{1 + pd_j}$$

and satisfy $|y_j| \leq 1$ for all $j = 1, 2, \dots, m$. Thus $\rho(Y) \leq 1$.

From Eq. (6.27), the eigenvalues of X are the same as the eigenvalues of

$$\left(I - \frac{\Delta t}{2} J \right)^{-1}.$$

If A is D -semi-stable, all the eigenvalues of J , which are, of course, the eigenvalues of $(I + \rho D)^{-1} A$, have non-positive real parts. Thus, for any Δt , if μ is an eigenvalue of $\left(I - \frac{\Delta t}{2} J \right)$, then $\text{Re}(\mu) \geq 1$. This implies that $|\mu| \geq 1$. Hence any eigenvalue of $\left(I - \frac{\Delta t}{2} J \right)^{-1}$, given by $1/\mu$ will satisfy $|\mu^{-1}| \leq 1$. Thus $\rho(X) \leq 1$.

Since G is diagonalizable and X is such that every eigenvalue of maximum modulus is semi-simple, from Proposition 6.2, we have $\|G\|_s = \rho(G)$ and $\|X\|_s = \rho(X)$. Thus Eq. (6.29) reduces to

$$\begin{aligned} \rho(G) &\leq \rho(X)\rho(Y) + \frac{\Delta t}{2} \rho(X)\|H\|_s \\ &\leq 1 + \frac{\Delta t}{2} \|H\|_s. \end{aligned} \tag{6.30}$$

Since $(I + \rho D)^{-1}$ is a positive diagonal matrix for any $p \in [0, 2r]$ and matrix A is bounded, matrix $H = (I + \rho D)^{-1} A$ is bounded. Let us denote this bound by $2C$ for some positive constant C . Then Eq. (6.30) reduces to

$$\rho(G) \leq 1 + C\Delta t.$$

(ii) Since G is diagonalizable and satisfies the von Neumann condition in (i), the proof follows from Lemma 6.1 and Proposition 6.1. \square

Thus, although the CN scheme has been proven to be linearly unconditionally stable for the linear diffusion equation, this cannot be established for the full RD equation unless some reasonable assumptions are made. In our case, we have proved this by making the assumption that the Jacobian matrix A of the reaction part is D-semi-stable, the amplification matrix is diagonalizable and the matrix $X := \left(I - \frac{\Delta t}{2}(I + \rho D)^{-1}A\right)^{-1}$ is such that every eigenvalue of maximum modulus is semi-simple.

The assumption of diagonalizability is reasonable since the set of real matrices that are diagonalizable within $\mathbf{M}_n(\mathbb{C})$ is dense in $\mathbf{M}_n(\mathbb{R})$ (Serre, 2010, p. 87). The assumption of the maximum absolute eigenvalue being semi-simple is even less restrictive than the diagonalizability assumption. D-semi-stability will be proven for RD systems whose reaction terms are governed by a variety of enzyme kinetic rate laws

6.6.2 The fractional step theta scheme

The fractional step theta scheme (FSTS) is an operator splitting technique for the time integration of initial-value problems of the form

$$\mathbf{u}_t = \mathcal{A}(\mathbf{u}), \quad \mathbf{u}(0) = \mathbf{u}_0, \quad (6.31)$$

where \mathcal{A} is a nonlinear operator that has a nontrivial decomposition

$$\mathcal{A} = \mathcal{A}_1 + \mathcal{A}_2. \quad (6.32)$$

For RD equations, operators \mathcal{A}_1 and \mathcal{A}_2 are the diffusion and reaction terms, respectively.

Let $\theta \in]0, 1/2[$, divide the time interval $[n, n+1]$ into three sub-intervals $[n, n+\theta]$, $[n+\theta, n+1-\theta]$ and $[n+1-\theta, n+1]$. An FSTS for the linearized Eq. (6.4) in a one-dimensional spatial domain is given by

$$\begin{aligned} \frac{\mathbf{z}_j^{n+\theta} - \mathbf{z}_j^n}{\theta \Delta t} &= \frac{1}{\Delta x^2} D \left(\mathbf{z}_{j+1}^{n+\theta} - 2\mathbf{z}_j^{n+\theta} + \mathbf{z}_{j-1}^{n+\theta} \right) + A \mathbf{z}_j^n, \\ \frac{\mathbf{z}_j^{n+1-\theta} - \mathbf{z}_j^{n+\theta}}{(1-2\theta)\Delta t} &= \frac{1}{\Delta x^2} D \left(\mathbf{z}_{j+1}^{n+\theta} - 2\mathbf{z}_j^{n+\theta} + \mathbf{z}_{j-1}^{n+\theta} \right) + A \mathbf{z}_j^{n+1-\theta}, \\ \frac{\mathbf{z}_j^{n+1} - \mathbf{z}_j^{n+1-\theta}}{\theta \Delta t} &= \frac{1}{\Delta x^2} D \left(\mathbf{z}_{j+1}^{n+1} - 2\mathbf{z}_j^{n+1} + \mathbf{z}_{j-1}^{n+1} \right) + A \mathbf{z}_j^{n+1-\theta}. \end{aligned} \quad (6.33)$$

Using an eigenvalue analysis and assuming the operator \mathcal{A} in Eq. (6.31) to be a constant $N \times N$ matrix, symmetric and positive definite, and where $\mathcal{A}_1, \mathcal{A}_2$ in

Equation (6.32) are given by $\mathcal{A}_1 = \alpha\mathcal{A}$, $\mathcal{A}_2 = \beta\mathcal{A}$, with $\alpha + \beta = 1$, $0 < \alpha, \beta < 1$, Glowinski (2003) showed that the FSTS is second order accurate in time if $\theta = 1 - 1/\sqrt{2}$, otherwise the scheme is first order accurate in time.

This can also be confirmed for the FSTS given in Eq. (6.33) by multiplying the first and last equations in (6.33) by $\theta\Delta t$ and the second equation by $(1 - 2\theta)\Delta t$, summing up the three equations and carrying out a Taylor series expansion about the point $(n + 1/2, j)$.

To perform a stability analysis of the FSTS (6.33), let us first rewrite the three equations in the form

$$\begin{aligned} (I + 2r\theta D)\mathbf{z}_j^{n+\theta} - r\theta D(\mathbf{z}_{j+1}^{n+\theta} + \mathbf{z}_{j-1}^{n+\theta}) &= (I + \theta\Delta tA)\mathbf{z}_j^n, \\ (I - (1 - 2\theta)\Delta tA)\mathbf{z}_j^{n+1-\theta} &= (I - 2(1 - 2\theta)rD)\mathbf{z}_j^{n+\theta} + (1 - 2\theta)rD(\mathbf{z}_{j+1}^{n+\theta} + \mathbf{z}_{j-1}^{n+\theta}), \\ (I + 2r\theta D)\mathbf{z}_j^{n+1} - r\theta D(\mathbf{z}_{j+1}^{n+1} + \mathbf{z}_{j-1}^{n+1}) &= (I + \theta\Delta tA)\mathbf{z}_j^{n+1-\theta}, \end{aligned}$$

where, as before, $r = \Delta t/\Delta x^2$.

Now taking the discrete Fourier transform of the above three equations and combining the resulting equations gives

$$\begin{aligned} \hat{\mathbf{z}}^{n+1} &= \left(I + 4r\theta \sin^2\left(\frac{\xi}{2}\right)D \right)^{-1} (I + \theta\Delta tA)(I - (1 - 2\theta)\Delta tA)^{-1} \\ &\quad \left(I - 4r(1 - 2\theta) \sin^2\left(\frac{\xi}{2}\right)D \right) \left(I + 4r\theta \sin^2\left(\frac{\xi}{2}\right)D \right)^{-1} (I + \theta\Delta tA)\hat{\mathbf{z}}^n. \end{aligned} \tag{6.34}$$

From Eq. (6.34), it is clear that the amplification matrix for the FSTS is given by

$$\begin{aligned} G &= \left(I + 4r\theta \sin^2\left(\frac{\xi}{2}\right)D \right)^{-1} (I + \theta\Delta tA)(I - (1 - 2\theta)\Delta tA)^{-1} \\ &\quad \left(I - 4r(1 - 2\theta) \sin^2\left(\frac{\xi}{2}\right)D \right) \left(I + 4r\theta \sin^2\left(\frac{\xi}{2}\right)D \right)^{-1} (I + \theta\Delta tA). \end{aligned} \tag{6.35}$$

We already saw in Section 3.7.6 that, in the scalar case ($m = 1$), the FSTS scheme is linearly unconditionally stable provided that the derivative, a , of the reaction part evaluated at any positive solution is nonpositive ($a \leq 0$) and $\theta \in [1/4, 1/3]$. In the multivariable case where $m > 1$ and G given by Eq. (6.35), we can only establish linear unconditional stability for the case when $\theta = \frac{1}{3}$.

In this case, matrix G reduces to

$$G = PQR \left(I + \frac{1}{3}\Delta tA \right), \tag{6.36}$$

where

$$\begin{aligned} P &:= \left(I + \frac{4}{3} r \sin^2 \left(\frac{\xi}{2} \right) D \right)^{-1}, \\ Q &:= \left(I + \frac{1}{3} \Delta t A \right) \left(I - \frac{1}{3} \Delta t A \right)^{-1}, \text{ and} \\ R &:= \left(I - \frac{4}{3} r \sin^2 \left(\frac{\xi}{2} \right) D \right) \left(I + \frac{4}{3} r \sin^2 \left(\frac{\xi}{2} \right) D \right)^{-1}. \end{aligned} \quad (6.37)$$

Sufficient conditions for the stability of the FSTS when $\theta = 1/3$ are established in the next theorem.

Theorem 6.2. *Consider the amplification matrix G in Eq. (6.36). Assume that G is diagonalizable, matrix A is semi-stable and matrix Q in (6.37) is such that every eigenvalue of maximum modulus is semi-simple. Then*

- (i) G satisfies the von Neumann condition, and
- (ii) the FSTS with $\theta = \frac{1}{3}$ is unconditionally stable.

Proof. (i) Taking the spectral radius norm of G , we have

$$\|G\|_s \leq \|P\|_s \|Q\|_s \|R\|_s \left(1 + \frac{1}{3} \Delta t \|A\|_s \right). \quad (6.38)$$

Since G is diagonalizable, P and R are diagonal and Q is such that every eigenvalue of maximum modulus is semi-simple, by using Proposition 6.2, Eq. (6.38) reduces to

$$\rho(G) \leq \rho(P) \rho(Q) \rho(R) \left(1 + \frac{1}{3} \|A\|_s \Delta t \right). \quad (6.39)$$

Since matrix A is bounded, let us denote its bound by $3C$, where C is some non-negative constant. Equation (6.39) reduces to

$$\rho(G) \leq \rho(P) \rho(Q) \rho(R) (1 + C \Delta t). \quad (6.40)$$

Matrices P and R are both diagonal with entries, and hence eigenvalues,

$$\mu_i = \frac{1}{1 + \frac{4}{3} r d_i \sin^2 \left(\frac{\xi}{2} \right)}$$

and

$$\nu_i = \frac{1 - \frac{4}{3} r d_i \sin^2 \left(\frac{\xi}{2} \right)}{1 + \frac{4}{3} r d_i \sin^2 \left(\frac{\xi}{2} \right)},$$

respectively, for $i = 1, \dots, m$.

Since $d_i > 0$, it is clear that both $|\mu_i| \leq 1$ and $|\nu_i| \leq 1$. Hence

$$\rho(P) \leq 1 \quad \text{and} \quad \rho(R) \leq 1. \tag{6.41}$$

To find $\rho(Q)$, let J be the Jordan canonical form of A . There exists a nonsingular matrix S such that $A = SJ S^{-1}$. Matrix Q can then be written as

$$Q = S \left(I + \frac{1}{3} \Delta t J \right) \left(I - \frac{1}{3} \Delta t J \right)^{-1} S^{-1}.$$

The eigenvalues of Q are the same as the eigenvalues of

$$\left(I + \frac{1}{3} \Delta t J \right) \left(I - \frac{1}{3} \Delta t J \right)^{-1}.$$

Let $\lambda_1, \dots, \lambda_k$ be the distinct eigenvalues of A . The matrices

$$\left(I + \frac{1}{3} \Delta t J \right)$$

and

$$\left(I - \frac{1}{3} \Delta t J \right)^{-1}$$

are both upper triangular with diagonal entries $1 + \frac{1}{3} \Delta t \lambda_j$ and $1 - \frac{1}{3} \Delta t \lambda_j$, respectively. Thus the matrix $\left(I + \frac{1}{3} \Delta t J \right) \left(I - \frac{1}{3} \Delta t J \right)^{-1}$ is also upper triangular with distinct eigenvalues

$$\delta_j = \frac{1 + \frac{1}{3} \Delta t \lambda_j}{1 - \frac{1}{3} \Delta t \lambda_j}, \quad j = 1, \dots, k.$$

Since matrix A is semi-stable, that is, $\text{Re}(\lambda_j) \leq 0$ for all j , then $|\delta_j| \leq 1$ for all j . Hence

$$\rho(Q) \leq 1. \tag{6.42}$$

Combining Eqs. (6.40) to (6.42) leads to

$$\rho(G) \leq 1 + C \Delta t. \tag{6.43}$$

(ii) Proceeds as in the proof for Theorem 6.1 part (ii). □

6.6.3 The implicit integration factor method

The implicit integration factor (IIF) method is a semi-implicit exponential integrator method due to Nie et al. (2006). In the IIF method, like in all exponential integrator methods, stiffness arising due to the discretization of the spatial diffusion term is overcome by evaluating the diffusion term exactly whereas the stiffness due to the reactions is handled by carrying out an implicit treatment of the nonlinear reaction terms. In the single variable case, this method has been proven to be linearly unconditionally stable (Nie et al., 2006).

To derive an IIF scheme, we make use of the ODE model system arising out of the method of lines application to the RD system (6.2). That is, the spatial discretization of (6.2) which reduces the PDE to a semi discrete form, consisting of a system of nonlinear ODEs in time,

$$\mathbf{u}_t = \mathcal{C}\mathbf{u} + \mathcal{F}(\mathbf{u}). \quad (6.44)$$

Here \mathcal{C} is a constant matrix arising out of the discretization of the Laplacian plus boundary conditions and $\mathcal{F}(\mathbf{u})$ is a vector of the nonlinear reaction terms evaluated at the grid points.

To derive an IIF method, start by multiplying Eq. (6.44) by an integrating factor $e^{-t\mathcal{C}}$ and then integrating over a single time step from $t = t_n$ to $t = t_{n+1} = t_n + \Delta t$ to obtain

$$\mathbf{u}(t_{n+1}) = e^{\Delta t\mathcal{C}}\mathbf{u}(t_n) + e^{\Delta t\mathcal{C}} \int_0^{\Delta t} e^{-\tau\mathcal{C}} \mathcal{F}(\mathbf{u}(t_n + \tau)) d\tau. \quad (6.45)$$

This formula is exact and various exponential integrator methods arise from the choice of approximation of the integral in Eq. (6.45). For example, in the exponential time differencing (ETD) scheme of Cox and Mathews (2002), the integrand is approximated first through interpolation polynomials of the function $\mathcal{F}(\mathbf{u}(t_n + \tau))$ with $e^{-\tau\mathcal{C}}$ unchanged. Then a direct integration of the interpolation polynomial with coefficient $e^{-\tau\mathcal{C}}$ yields the ETD method.

In the case of IIF, the whole integrand $e^{-\tau\mathcal{C}}\mathcal{F}(\mathbf{u}(t_n + \tau))$ is approximated by an interpolation polynomial and a direct integration of the polynomial is done. The scheme will be explicit if the interpolation points used for the integrand are $t_n, t_{n-1}, t_{n-2}, \dots$ and implicit when the interpolation points contain t_{n+1} .

Define the vector $G(\tau) = e^{-\tau\mathcal{C}}\mathcal{F}(\mathbf{u}(t_n + \tau))$, to be the integrand in Eq. (6.45). To construct an r -th order accurate IIF scheme, we approximate $G(\tau)$ with an $(r-1)$ -th degree Lagrange interpolation polynomial, $P(\tau)$, valid on the interval $0 \leq \tau \leq \Delta t$, using interpolation points at $t_{n+1}, t_n, \dots, t_{n+2-r}$, where $t_{n+i} = t_n + i\Delta t$. Using the substitution $\tau = t - t_n$, we have $G(t) = e^{-(t-t_n)\mathcal{C}}\mathcal{F}(\mathbf{u}(t))$ and using the notation

$\mathbf{u}(t_n) = \mathbf{u}_n$, we have the Lagrange interpolation polynomial

$$P(t) = \sum_{i=-1}^{r-2} G(t_{n-i}) \prod_{\substack{j=-1 \\ j \neq i}}^{r-2} \frac{t - t_{n-j}}{t_{n-i} - t_{n-j}} = \sum_{i=-1}^{r-2} e^{i\Delta t C} \mathcal{F}(\mathbf{u}_{n-i}) \prod_{\substack{j=-1 \\ j \neq i}}^{r-2} \frac{t - t_n + j\Delta t}{(j-i)\Delta t}. \quad (6.46)$$

Thus we have

$$P(\tau) = \sum_{i=-1}^{r-2} e^{i\Delta t C} \mathcal{F}(\mathbf{u}_{n-i}) \prod_{\substack{j=-1 \\ j \neq i}}^{r-2} \frac{\tau + j\Delta t}{(j-i)\Delta t}. \quad (6.47)$$

Equation (6.45) can then be written as

$$\mathbf{u}_{n+1} = e^{\Delta t C} \mathbf{u}_n + e^{\Delta t C} \int_0^{\Delta t} P(\tau) d\tau. \quad (6.48)$$

For the second order IIF scheme ($r = 2$), we have,

$$P(\tau) = \frac{1}{\Delta t} (\tau e^{-\Delta t C} \mathcal{F}(\mathbf{u}_{n+1}) + (\Delta t - \tau) \mathcal{F}(\mathbf{u}_n)).$$

Substituting in (6.48) and integrating results into the second order IIF scheme (IIF2)

$$\mathbf{u}_{n+1} = e^{\Delta t C} \left(\mathbf{u}_n + \frac{\Delta t}{2} \mathcal{F}(\mathbf{u}_n) \right) + \frac{\Delta t}{2} \mathcal{F}(\mathbf{u}_{n+1}). \quad (6.49)$$

By computing boundaries for the stability region, Nie et al. (2006), proved that, in the case of a scalar equation (where $m = 1$), the second order IIF scheme is linearly unconditionally stable. We use a direct approach to establish sufficient conditions for the linear stability of this scheme in the multivariable case ($m > 1$).

For the stability analysis, we consider the linearized PDE (6.4) in one spatial dimension. Its discretization in space using a central difference scheme on a grid with N internal grid points and assuming $\mathbf{z} = 0$ at the boundary, we have

$$\frac{\partial \mathbf{z}_k}{\partial t} = \frac{1}{\Delta x^2} D(\mathbf{z}_{k-1} - 2\mathbf{z}_k + \mathbf{z}_{k+1}) + A\mathbf{z}_k, \quad k = 1, 2, \dots, N, \quad (6.50)$$

where $\mathbf{z}_k = [z_{1k}, z_{2k}, \dots, z_{mk}]^T$. Here the first subscript represents the index of the chemical species whereas the second subscript represents the grid point. The boundary condition implies that $\mathbf{z}_0 = \mathbf{z}_{N+1} = 0$. The linear system (6.50) is a system of Nm equations in Nm unknowns.

Rearrange the equations in (6.50) so that the first N equations are time derivatives of z_1 at the N grid points, the next N equations are for z_2 , and so on. Then system

(6.50) can be written in matrix form as

$$\mathbf{Z}_t = \mathcal{C}\mathbf{Z} + \mathcal{A}\mathbf{Z}, \quad (6.51)$$

where $\mathbf{Z} = [z_{11}, \dots, z_{1N}, \dots, z_{m1}, \dots, z_{mN}]^T \in \mathbb{R}^{Nm}$, \mathcal{C} is an Nm -square block diagonal matrix arising due to diffusion and is given by

$$\mathcal{C} = \text{diag}(B_1, B_2, \dots, B_m) \text{ with } B_i = \frac{d_i}{\Delta x^2} \begin{pmatrix} -2 & 1 & & 0 \\ 1 & \ddots & \ddots & \\ & \ddots & \ddots & 1 \\ 0 & & 1 & -2 \end{pmatrix}_{N \times N}, \quad (6.52)$$

and \mathcal{A} is a block matrix with blocks of size N , arising due to reaction, and is given by

$$\mathcal{A} = \begin{pmatrix} a_{11}I_N & a_{12}I_N & \cdots & a_{1m}I_N \\ a_{21}I_N & a_{22}I_N & \cdots & a_{2m}I_N \\ \cdots & \cdots & \cdots & \cdots \\ a_{m1}I_N & a_{m2}I_N & \cdots & a_{mm}I_N \end{pmatrix} \quad (6.53)$$

where I_N is the identity matrix of size N , a_{ij} is the ij -entry of the Jacobian matrix A .

We can express matrix \mathcal{A} as a *Kronecker product* which we define below (Laub, 2005).

Definition 6.1. Let $A \in \mathbb{R}^{m \times n}$, $B \in \mathbb{R}^{p \times q}$. The *Kronecker product* of A and B is defined as the matrix

$$A \otimes B = \begin{pmatrix} a_{11}B & \cdots & a_{1n}B \\ \vdots & \ddots & \vdots \\ a_{m1}B & \cdots & a_{mn}B \end{pmatrix} \in \mathbb{R}^{mp \times nq}$$

Thus the matrix \mathcal{A} in (6.53) can be written as

$$\mathcal{A} = A \otimes I_N. \quad (6.54)$$

To determine the eigenvalues of \mathcal{A} , we shall make use of the following theorem.

Theorem 6.3 (Laub, 2005, p. 141). Let $A \in \mathbb{R}^{n \times n}$ have eigenvalues $\lambda_1, \lambda_2, \dots, \lambda_n$ and let $B \in \mathbb{R}^{m \times m}$ have eigenvalues $\mu_1, \mu_2, \dots, \mu_m$. Then the mn eigenvalues of $A \otimes B$ are $\lambda_1\mu_1, \dots, \lambda_1\mu_m, \lambda_2\mu_1, \dots, \lambda_2\mu_m, \dots, \lambda_n\mu_m$.

We are now in position to analyze the stability of the second order IIF scheme (6.49)

when applied to the linear system (6.51). This scheme takes the form

$$\left(I - \frac{\Delta t}{2} \mathcal{A}\right) \mathbf{z}_{n+1} = e^{\Delta t \mathcal{C}} \left(I + \frac{\Delta t}{2} \mathcal{A}\right) \mathbf{z}_n, \quad (6.55)$$

where \mathcal{C} is given by (6.52) and $\mathcal{A} = A \otimes I_N$.

Assume that the matrix A is semi-stable. Then the matrix $I - \frac{\Delta t}{2} \mathcal{A}$ is nonsingular, and Eq. (6.55) can be written in the form

$$\mathbf{z}_{n+1} = \left(I - \frac{\Delta t}{2} \mathcal{A}\right)^{-1} e^{\Delta t \mathcal{C}} \left(I + \frac{\Delta t}{2} \mathcal{A}\right) \mathbf{z}_n = Q \mathbf{z}_n, \quad (6.56)$$

where $Q := \left(I - \frac{\Delta t}{2} \mathcal{A}\right)^{-1} e^{\Delta t \mathcal{C}} \left(I + \frac{\Delta t}{2} \mathcal{A}\right)$.

Notice that since we have not employed Fourier transforms, Eq. (6.56) does not contain an amplification matrix. Thus, Proposition 6.1 that was used for the CN and FSTS cannot be applied to establish sufficient conditions for the stability of the second order IIF scheme. We shall instead make use of the following proposition.

Proposition 6.3 (Thomas, 1995, Proposition 3.1.14). *Suppose Q is similar to a symmetric matrix P , i.e., there exists a nonsingular matrix S such that $Q = SPS^{-1}$. If $\|S\|$ and $\|S^{-1}\|$ are uniformly bounded for any matrix norm $\|\cdot\|$, a necessary and sufficient condition for the stability of the scheme (6.56) is that $\rho(Q) \leq 1 + \beta \Delta t$ for some non-negative β , where $\rho(Q)$ is the spectral radius of Q .*

Define $X := \left(I - \frac{\Delta t}{2} \mathcal{A}\right)^{-1}$ and $Y := e^{\Delta t \mathcal{C}}$. Matrix Q can be written as

$$Q = XY \left(I + \frac{\Delta t}{2} \mathcal{A}\right), \quad \text{where } \mathcal{A} = A \otimes I_N. \quad (6.57)$$

Sufficient conditions for the stability of the IIF scheme are established below.

Theorem 6.4. *Suppose that matrix Q in Equation (6.57) is diagonalizable, the Jacobian matrix A is semi-stable and matrix X is such that every eigenvalue of maximum modulus is semi-simple. Then*

- (i) *there exists a nonzero constant β such that $\rho(Q) \leq 1 + \beta \Delta t$, and*
- (ii) *the second order IIF scheme $\mathbf{z}_{n+1} = Q \mathbf{z}_n$ is unconditionally stable.*

Proof. (i) Applying the spectral radius norm on Eq. (6.57), we have

$$\|Q\|_s \leq \|X\|_s \|Y\|_s \left(1 + \frac{\Delta t}{2} \|A\|_s\right). \quad (6.58)$$

Since Q is diagonalizable and X is such that every eigenvalue of maximum modulus is semi-simple, Proposition 6.2 implies that $\|Q\|_s = \rho(Q)$ and $\|X\|_s = \rho(X)$.

To find $\rho(X)$, let $\lambda_1, \lambda_2, \dots, \lambda_k$ be the distinct eigenvalues of the Jacobian matrix A . From Theorem 6.3, $\lambda_1, \lambda_2, \dots, \lambda_k$ will also be the distinct eigenvalues of $\mathcal{A} = A \otimes I_N$. Let J be the Jordan canonical form of \mathcal{A} . There exists a nonsingular matrix S such that $\mathcal{A} = SJS^{-1}$. Matrix X can then be written as

$$X = S\left(I - \frac{\Delta t}{2}J\right)^{-1}S^{-1}.$$

The eigenvalues of X are the same as the eigenvalues of $\left(I - \frac{\Delta t}{2}J\right)^{-1}$.

Since matrix A is semi-stable, the distinct eigenvalues of $\left(I - \frac{\Delta t}{2}J\right)$, given by

$$1 - \frac{\Delta t}{2}\lambda_1, 1 - \frac{\Delta t}{2}\lambda_2, \dots, 1 - \frac{\Delta t}{2}\lambda_k,$$

have positive real parts greater than or equal to 1. Hence $|1 - \frac{\Delta t}{2}\lambda_i| \geq 1$ for all i and for any Δt . Therefore all the distinct eigenvalues of $\left(I - \frac{\Delta t}{2}J\right)^{-1}$, which are in fact the eigenvalues of X , and given by

$$\left(1 - \frac{\Delta t}{2}\lambda_1\right)^{-1}, \left(1 - \frac{\Delta t}{2}\lambda_2\right)^{-1}, \dots, \left(1 - \frac{\Delta t}{2}\lambda_k\right)^{-1},$$

have modulus less than or equal to 1. Thus

$$\rho(X) \leq 1. \quad (6.59)$$

For matrix $Y := e^{\Delta t C}$, matrix $\Delta t C$ is real and block diagonal given by Eq. (6.52) with each B_i multiplied by Δt . Thus Y is a real block diagonal matrix given by

$$Y = \text{diag}\left(e^{\Delta t B_1}, e^{\Delta t B_2}, \dots, e^{\Delta t B_m}\right).$$

Since each of the matrices B_j is real symmetric, each of the matrices $e^{\Delta t B_j}$ is also real symmetric and therefore Y is a real symmetric block diagonal matrix.

We know from linear algebra that every real symmetric matrix is diagonalizable. This implies that every eigenvalue of Y is semi-simple and thus from Proposition 6.2,

$$\|Y\|_s = \rho(Y).$$

The spectrum of a block diagonal matrix is the union of the spectra of the diagonal blocks (Dasgupta, 2006). Thus the set of eigenvalues of Y is the union of the sets of eigenvalues of

$$e^{\Delta t B_j}, \quad j = 1, \dots, m.$$

Note that the matrices $\Delta t B_j$ are symmetric tridiagonal and thus can be diagonalized. That is, there exists a nonsingular E_j such that $\Delta t B_j = E_j \Lambda_j E_j^{-1}$, where Λ_j is

diagonal with diagonal entries being the eigenvalues of $\Delta t B_j$. Thus

$$e^{\Delta t B_j} = E_j e^{\Lambda_j} E_j^{-1} \text{ and } e^{\Lambda_j} = \text{diag}(e^{\mu_1}, e^{\mu_2}, \dots, e^{\mu_N}),$$

where μ_k is an eigenvalue of $\Delta t B_j$, $k = 1, \dots, N$. The eigenvalues of $\Delta t B_j$ are given by

$$\mu_k = -2rd_j + 2rd_j \cos(\theta_k) = -4rd_j \sin^2\left(\frac{\theta_k}{2}\right),$$

where $\theta_k = \frac{k\pi}{N+1}$ and $r = \frac{\Delta t}{\Delta x^2}$. Thus

$$0 < e^{\mu_k} = e^{-4rd_j \sin^2\left(\frac{\theta_k}{2}\right)} \leq 1 \quad k = 1, \dots, N.$$

Hence

$$\rho(e^{\Delta t B_j}) \leq 1 \text{ for } j = 1, \dots, m, \text{ which implies } \rho(Y) \leq 1. \quad (6.60)$$

Combining Eqs. (6.58) to (6.60), we have

$$\rho(Q) \leq 1 + \frac{\Delta t}{2} \|A\|_s.$$

Since matrix A is a constant matrix of size Nm , $\|A\|_s$ is bounded by Nm times the absolute value of its largest element (Richtmyer and Morton, 1967). Let us denote this bound by 2β . Thus we have

$$\rho(Q) \leq 1 + \beta \Delta t.$$

(ii) Since Q is diagonalizable and satisfies part (i) above, the proof follows from Lemma 6.1 and Eq. (3.73). □

6

6.6.4 Implicit-explicit (IMEX) methods

We have already stated that the spatial discretization of a PDE system under the method of lines approach may result in a stiff system of ODEs which requires more restrictive stability conditions on the spatial term than other terms. Stiff problems abound in nature, and could also arise when modelling a coupled set of physical systems, wherein each physical process operates at a slightly different time scale. For such problems, instead of employing a single explicit or implicit method, on the full problem (6.44), a more reasonable approach is to apply an explicit method on the non-stiff portion (the nonlinear reaction terms) and an implicit method to the stiff portion (the linear diffusion).

Such methods abound in the scientific literature, where scientists often somewhat arbitrarily combine their favorite explicit and implicit methods together to form

an implicit-explicit (IMEX) method. IMEX methods, in the case of nonlinear RD systems, have the advantage that the resulting algebraic system is linear and can thus be solved without the need for nonlinear iterative solvers which makes the computation cheaper compared to a fully implicit scheme. For details on IMEX methods, we refer to (Wang et al., 2015; Ascher et al., 1995).

An IMEX scheme for the linearized Eq. (6.4) in a one-dimensional spatial domain is

$$\frac{1}{\Delta t}(\mathbf{z}_j^{n+1} - \mathbf{z}_j^n) = \frac{1}{\Delta x^2} D \left(\mathbf{z}_{j+1}^{n+1} - 2\mathbf{z}_j^{n+1} + \mathbf{z}_{j-1}^{n+1} \right) + A\mathbf{z}_j^n. \quad (6.61)$$

Equation (6.61) can be written as

$$(I + 2rD)\mathbf{z}_j^{n+1} - rD(\mathbf{z}_{j+1}^{n+1} + \mathbf{z}_{j-1}^{n+1}) = (I + \Delta tA)\mathbf{z}_j^n, \quad (6.62)$$

where as before $r := \Delta t/\Delta x^2$. Taking the discrete Fourier transform of Eq. (6.62) gives

$$\left(I + 4rD \sin^2 \frac{\xi}{2} \right) \hat{\mathbf{z}}^{n+1} = (I + \Delta tA)\hat{\mathbf{z}}^n, \quad (6.63)$$

from which the amplification matrix for the IMEX scheme is given by

$$G = (I + pD)^{-1} (I + \Delta tA), \quad (6.64)$$

where $p := 4r \sin^2 \frac{\xi}{2}$, $\xi \in [-\pi, \pi]$.

Sufficient conditions for the stability of the IMEX scheme are now established in Theorem 6.5.

Theorem 6.5. *Suppose that matrix G in (6.64) is diagonalizable. Then*

- (i) G satisfies the von Neumann condition, and
- (ii) the IMEX scheme in Eq. (6.61) is unconditionally stable.

Proof. (i) Applying the spectral radius norm to Eq. (6.64), we have

$$\|G\|_s \leq \|(I + pD)^{-1}\|_s \|I + \Delta tA\|_s. \quad (6.65)$$

Since matrix G is diagonalizable,

$$\|G\|_s = \rho(G).$$

Matrix $(I + pD)^{-1}$ is diagonal with diagonal entries $1/(1 + pd_i)$ and

$$\|(I + pD)^{-1}\|_s = \rho((I + pD)^{-1}).$$

Thus

$$\rho(G) \leq \rho((I + pD)^{-1}) \cdot \|I + \Delta t A\|_s. \quad (6.66)$$

The eigenvalues of $(I + pD)^{-1}$ are its diagonal entries $1/(1 + pd_i)$ and each of them is less than 1 since $p, d_i \geq 0$. Thus $\rho((I + pD)^{-1}) \leq 1$. Equation (6.66) reduces to

$$\rho(G) \leq \|I + \Delta t A\|_s \leq \|I\|_s + \Delta t \|A\|_s = 1 + \Delta t \|A\|_s.$$

Since matrix A is bounded, G satisfies the von Neumann condition.

(ii) Proceeds as in the proof of Theorem 6.1 part (ii). □

6.7 Numerical simulations

Most of the conditions derived in the previous section are difficult to verify. However, we can verify the necessary condition of semi-stability of the Jacobian matrix by carrying out a numerical simulation of two RD model systems, one from CRNT and the other from population dynamics, using the finite difference schemes discussed above.

6.7.1 The Brusselator model

The Brusselator model (Perelson, 1978; Prigogine and Lefever, 1968; Marek and Schreiber, 1991) is a well-known theoretical model widely used in the modelling and simulation of oscillating chemical systems. In its classical form, the Brusselator model is associated with the CRN



The CRN is considered to be 'far from equilibrium', so that the rates of the reverse reactions are set to zero. In addition, the assumption is made that the concentrations of the chemical species A and B (the initial reactants) and D and E (the final products) remain constant over the time scale of interest. This leaves only two varying concentrations, those of the intermediates U and V , the minimum number required for an isothermal oscillatory system (Gray et al., 1988).

Assuming that all rate constants of the reactions are unity, the conventional di-

dimensionless Brusselator model in a one-dimensional spatial domain is given by

$$\begin{aligned}\frac{\partial u}{\partial t} &= D_u \frac{\partial^2 u}{\partial x^2} + u^2 v + a - (b + 1)u \\ \frac{\partial v}{\partial t} &= D_v \frac{\partial^2 v}{\partial x^2} - u^2 v + bu,\end{aligned}\tag{6.68}$$

for $(x, t) \in [0, L] \times [0, \infty[$ and where u and v denote the concentrations of U and V , respectively, with D_u and D_v their diffusion coefficients. We complete the model system by imposing homogeneous Neumann boundary conditions

$$u_x(0, t) = u_x(L, t) = 0 \quad \text{and} \quad v_x(0, t) = v_x(L, t) = 0,$$

and nonnegative initial conditions

$$u(x, 0) = u_0(x) \geq 0, \quad v(x, 0) = v_0(x) \geq 0.$$

There are no known analytical solutions to the Brusselator RD system (6.68) and thus it has to be solved numerically.

The system admits a unique homogeneous equilibrium solution at

$$u = a, \quad v = b/a.\tag{6.69}$$

In the absence of diffusion, this equilibrium solution is stable when the parameters (a, b) satisfy

$$b < a^2 + 1.\tag{6.70}$$

In order for the system to exhibit spatial patterns, Turing's diffusion-driven instability requires the homogeneous equilibrium to be unstable in the presence of diffusion. This is achieved when

$$b > \left(1 + a \sqrt{\frac{D_u}{D_v}}\right)^2.\tag{6.71}$$

Simulation results

The schemes described in this chapter are used to simulate the Brusselator system using MATLAB for $x \in [0, 10]$ and taking the initial condition to be a small perturbation of the homogeneous equilibrium solution (6.69). The simulations are carried out for two cases; one case where the Jacobian of the reaction part is semi-stable at every time step of the simulation and another case in which it is not semi-stable. The results from the simulations are compared to those generated by an explicit scheme (forward in time, centered in space).

Case I: Jacobian is semi-stable

The parameter values chosen are $D_u = 1, D_v = 8, a = 4.5, b = 9$ and $\theta = 1/3$ for the FSTS. The results are shown in Figs. 6.1 and 6.2.

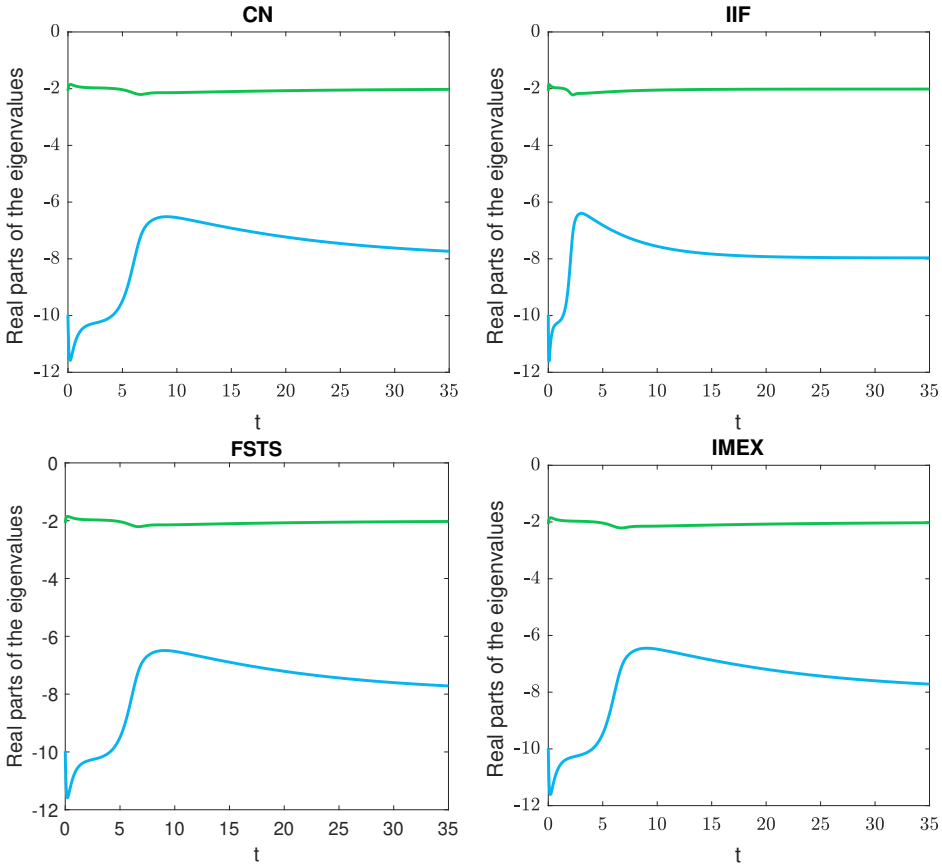


Figure 6.1: Real parts of the two eigenvalues of the Jacobian at the point $x = 5.05$. The space step size is $\Delta x = 0.101$, while the time step size is $\Delta t = 0.01$ for all the schemes.

Case II: Jacobian is not semi-stable

Here all the parameter values stay the same as above except b which we set to 21. In this case, the Jacobian is not semi-stable for certain Δt (as shown in Fig. 6.3). This implies that there exists at least one Δt for which the described schemes are unstable. For example, setting $\Delta t = 0.01$, the solutions generated by the CN, FSTS, IIF and IMEX all converge to the solution generated by the explicit scheme as shown in Fig. 6.4, whereas, setting $\Delta t = 0.255$ for the CN scheme, $\Delta t = 0.2$ for

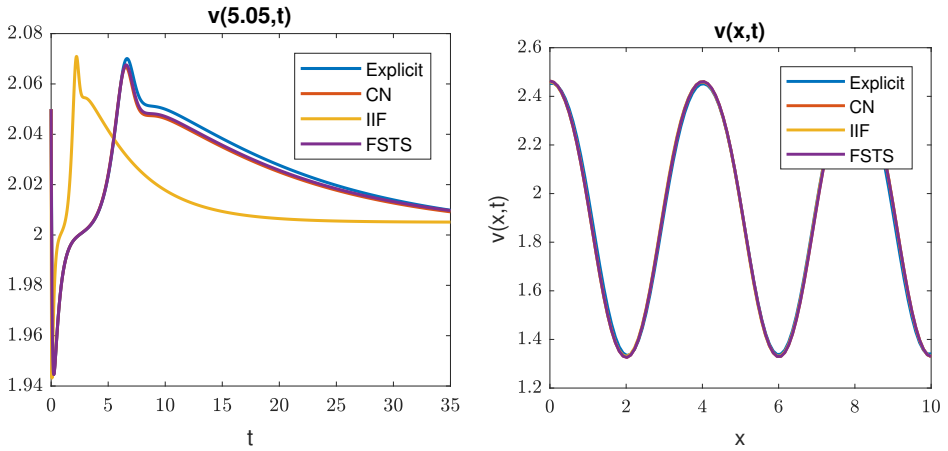


Figure 6.2: Left: Solution $v(x, t)$ of the Brusselator system at $x = 5.05$. The space step size is $\Delta x = 0.101$, while the time step size is $\Delta t = 0.0002$ for the explicit scheme and $\Delta t = 0.01$ for the rest of the schemes. Right: Spatial pattern solution.

the FSTS and $\Delta t = 0.25$ for the IIF leads to a blow-up of the solutions as shown in Fig. 6.5. Thus, when the Jacobian is not semi-stable for certain Δt , the described schemes are unstable.

6.7.2 A 3-species intransitive competition model

We now verify the necessary condition of semi stability of the Jacobian by studying the numerical solutions of an RD model system governing the dynamics of three intransitively competing populations that are spatially distributed on a line. This RD model takes the form

$$\begin{aligned}
 \dot{u}_1 &= \nabla^2 u_1 + u_1(\alpha_1 u_2 - \alpha_3 u_3), \\
 \dot{u}_2 &= \nabla^2 u_2 + u_2(\alpha_2 u_3 - \alpha_1 u_1), \\
 \dot{u}_3 &= \nabla^2 u_3 + u_3(\alpha_3 u_1 - \alpha_2 u_2),
 \end{aligned}
 \tag{6.72}$$

where $u_1(x, t)$, $u_2(x, t)$ and $u_3(x, t)$ are the (non-negative) proportions of the three competing populations, and the parameters α_i denote the invasion rates. We study the numerical simulations of this model subject to homogeneous Neumann boundary conditions

$$\frac{\partial u_i}{\partial x}(0, t) = \frac{\partial u_i}{\partial x}(L, t) = 0, \text{ for } i = 1, 2, 3,$$

and nonnegative initial conditions

$$u_1(x, 0) = g_1(x) \geq 0, \quad u_2(x, 0) = g_2(x) \geq 0, \quad \text{and } u_3(x, 0) = g_3(x) \geq 0.$$

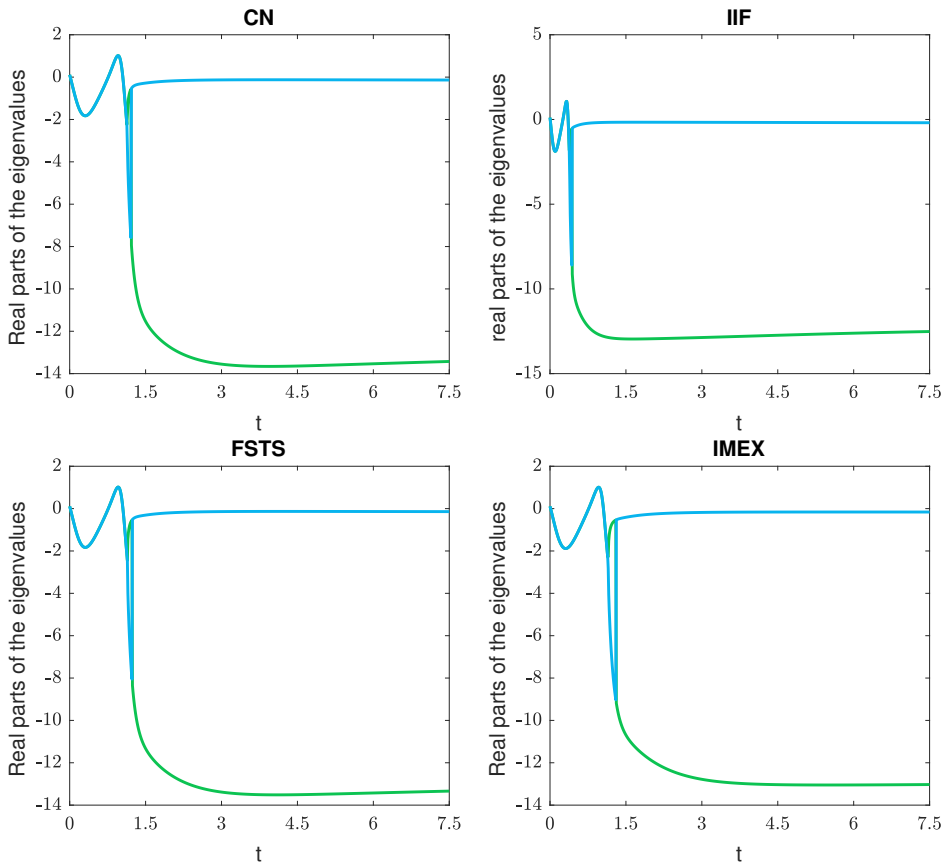


Figure 6.3: Real parts of the two eigenvalues of the Jacobian for $D_u = 1, D_v = 8, a = 4.5, b = 21$ at the point $x = 5.05$. The space step size is $\Delta x = 0.101$, while the time step size is $\Delta t = 0.01$ for all the schemes.

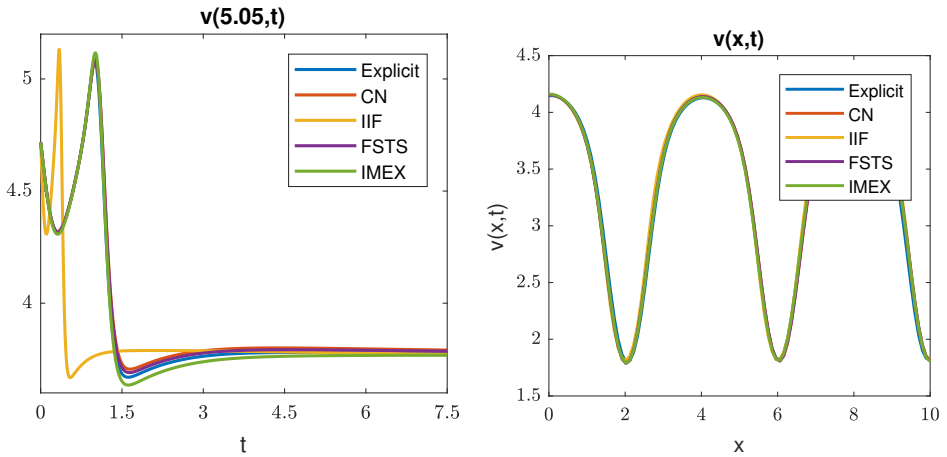


Figure 6.4: Left: Solution $v(x, t)$ for $D_u = 1, D_v = 8, a = 4.5, b = 21$ at the point $x = 5.05$ with $\Delta t = 0.01$. Right: Spatial pattern.

In the spatially homogeneous case (i.e., in the absence of diffusion), model system (6.72) reduces to an ODE system. In this case, the population densities form closed orbits around the coexistence equilibrium point (u_1^*, u_2^*, u_3^*) (see Fig. 6.6) given by

$$\begin{aligned} u_1^* &= \frac{\alpha_2}{\alpha_1 + \alpha_2 + \alpha_3}, \\ u_2^* &= \frac{\alpha_3}{\alpha_1 + \alpha_2 + \alpha_3}, \\ u_3^* &= \frac{\alpha_1}{\alpha_1 + \alpha_2 + \alpha_3}, \end{aligned} \quad (6.73)$$

which is neutrally stable. It is the intransitivity in the pairwise competition which underlies the cyclic behavior; the phenomenon clearly requires at least three competitors, which is why it cannot occur in models with two competitors.

A natural question to ask is: what happens to the periodic orbits in the ODEs (Fig. 6.6) once the spatial component (diffusion) is added back to the system. An attempt to answer this question lies in obtaining the numerical solutions of the PDE system (6.72). Here, we shall employ the numerical schemes whose stability has been discussed above to not only test the results from the stability analysis but also to investigate the behaviour of the solutions of Eq. (6.72).

6.7.2.1 Numerical experiments

The results we present are all generated using MATLAB. By numerically computing the eigenvalues of the Jacobian matrix A evaluated at the numerical solution obtained at each time step, it is noted that the Jacobian matrix is not semi-stable

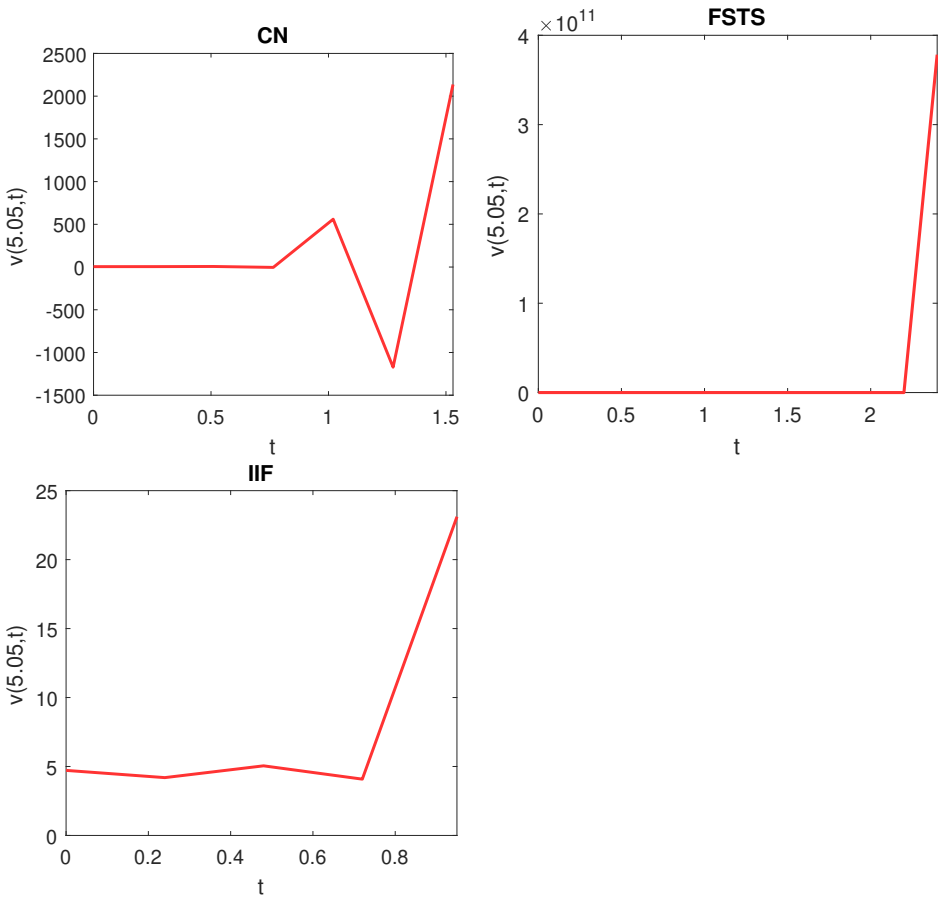


Figure 6.5: Blow-up of solution $v(5.05, t)$ for $\Delta t = 0.255$ for the CN, $\Delta t = 0.2$ for the FSTS and $\Delta t = 0.25$ for the IIF. One of the eigenvalues of the Jacobian has a positive real part at the time of blow-up.

6

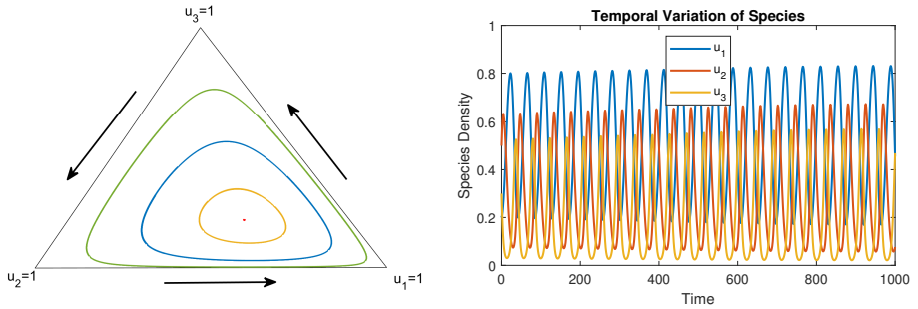


Figure 6.6: Dynamics of the ODE model system obtained from Eq. (6.72) by dropping the diffusion term. Species population densities move along periodic orbits around a coexistence equilibrium point (6.73). Left: The figure shows several such orbits for the invasion rates $\alpha_1 = 0.2$, $\alpha_2 = 0.5$ and $\alpha_3 = 0.3$. Here, u_3 ranges linearly from zero along the base of the triangle to unity at its peak; similarly u_1 and u_2 increase to unity at their respective corners. Right: The dynamics can also be visualized by plotting the population densities $u_i(t)$ as a function of time t . These simulations have been obtained by making use of MATLAB's standard ODE solver, `ode45`.

(as shown in Fig. 6.7), a necessary condition for the unconditional stability of the schemes discussed above. Thus the above schemes when applied to Eq. (6.72) are expected to be conditionally stable. In other words, there exists a critical time step size Δt^* at which the finite difference solution generated from a positive and bounded initial condition explodes (blows up) and becomes unstable in finite time.

To determine the Δt^* for which the blow-up occurs, we start by simulating the model Eq. (6.72) using the four schemes elaborated upon in this chapter starting with a relatively small Δt for which all schemes are stable and then gradually increase the time step while observing the behaviour of the resulting solution. Results from these simulations are shown in Figs. 6.8 to 6.11.

From these figures, it can be observed that for sufficiently small Δt , the densities of the three species form periodic orbits about the spatially homogeneous coexistence equilibrium (6.73), just like in the ODE case, albeit with a much smaller amplitude. As Δt is increased, a number of arbitrary dynamical behaviours can be witnessed depending on the numerical scheme being used. For example, when $\Delta t = 1.0$, the numerical solution from the FSTS scheme exhibits quasi-periodic orbits (as shown in Fig. 6.9(b)). This also happens when using the IMEX scheme when, for example, $\Delta t = 0.1$ (see Fig. 6.11(b)). A further increase in Δt for these two schemes produces two somewhat similar dynamics. Both solutions are quasi periodic at the beginning of the simulation but as time goes on, the product of the three population densities becomes exponentially small. That is, as time progresses, the quasi-periodic oscillations die out as the system appears asymptotically to move ever closer to an orbit carrying it along the lines $u_1 + u_2 = 1$, $u_2 + u_3 = 1$, $u_3 + u_1 = 1$. In other words, the system moves in population space from the neighborhood of the point where only species 1 is present, $(1, 0, 0)$, to

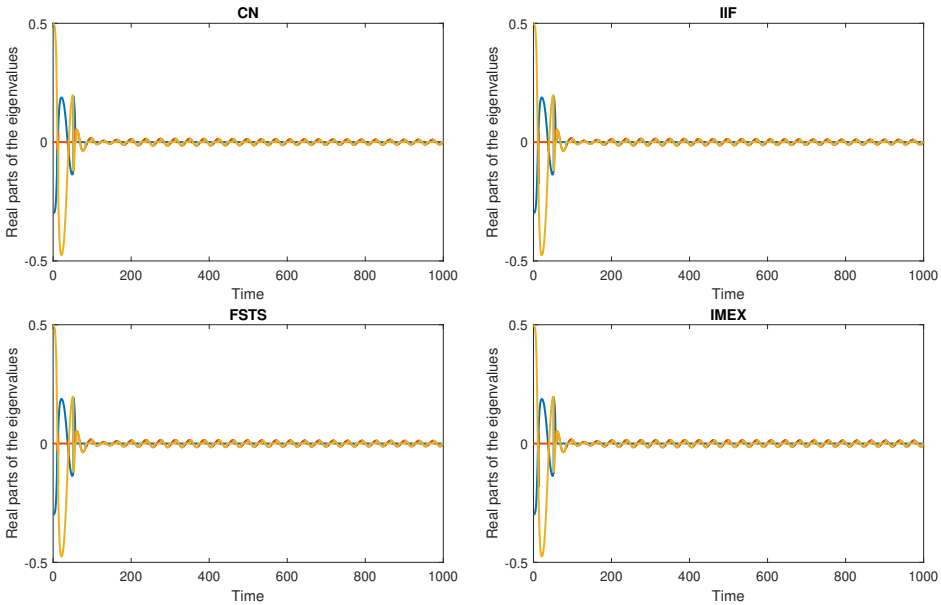


Figure 6.7: Real parts of the three eigenvalues of the Jacobian for for the invasion rates $\alpha_1 = 0.2$, $\alpha_2 = 0.5$ and $\alpha_3 = 0.3$ at the point $x = 5.05$. The space step size is $\Delta x = 0.1$, while the time step is $\Delta t = 0.1$ all the schemes (CN, FSTS and IIF) and $\Delta t = 0.01$ for the IMEX scheme.

the neighborhood of the point $(0, 0, 1)$, to the neighborhood of $(0, 1, 0)$, back to $(1, 0, 0)$, and so on, as shown in Figs. 6.9(c) and 6.11(c) for $\Delta t = 3.0$ for the FSTS and $\Delta t = 1.0$ for the IMEX scheme. A further increase in Δt enables us to obtain a critical value of the time step for which we witness a blow-up of the solutions, that is, at which the schemes are unstable. In the FSTS, this occurs at $\Delta t = 5.0$. The solutions behaves similarly to the one for $\Delta t = 3.0$ but only for a short transient before a blow-up occurs. For the IMEX scheme, blow-up occurs at $\Delta t = 2.2$. The behavior of the two solutions from the FSTS and IMEX as Δt is increased is arbitrary and unexpected. It is not clear whether this behaviour is a result of the nonlinearity, spatial aspects or the numerical properties of the scheme itself or a combination of the three. This behaviour, however, does not appear in the solution of the fully-implicit CN scheme and the semi-implicit IIF scheme.

These simulation results, like in the Brusselator model, also confirm results from the stability analysis that as long as the Jacobian of the reaction part is not semi-stable, the above analyzed schemes are not unconditionally stable. In short, there exists a Δt at which the numerical solution blows up. In addition, these results highlight the intricacies involved in using numerical methods to solve nonlinear PDEs where solution behavior could be affected not only by the mesh and time step sizes but also by the scheme used.

One important observation is that the behavior of the generated numerical solution

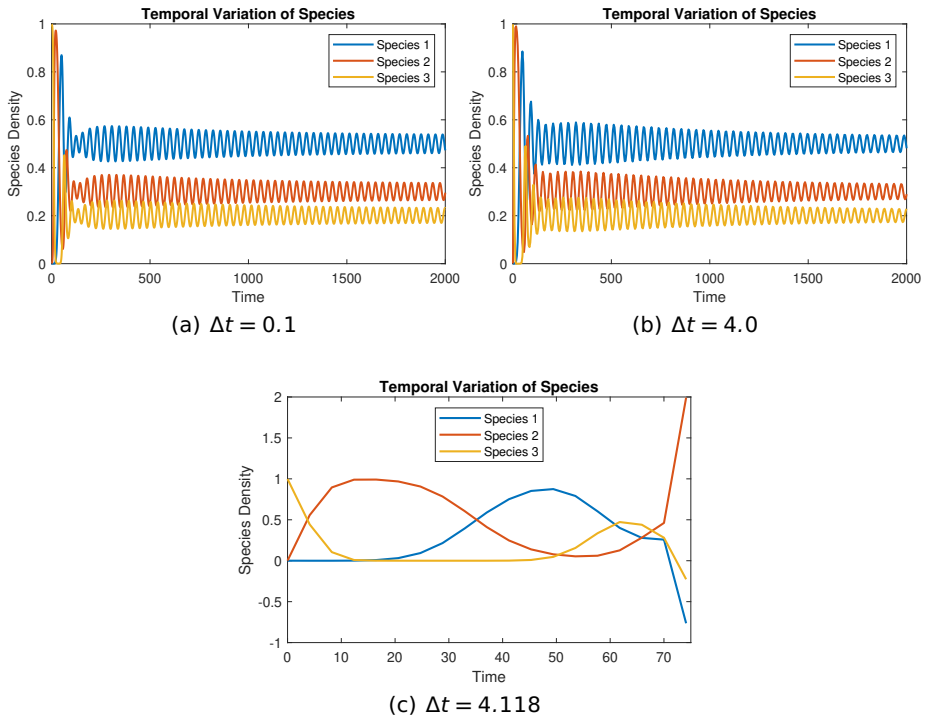


Figure 6.8: Numerical solutions of Eq. (6.72) using the CN scheme for the invasion rates $\alpha_1 = 0.2$, $\alpha_2 = 0.5$ and $\alpha_3 = 0.3$ at the point $x = 5.05$. The space step size is $\Delta x = 0.1$, while the time step is $\Delta t = 0.1, 4.0$ and 4.118 . It can be observed that the dynamics are similar for all Δt for which the scheme is stable. For $\Delta t = 4.118$, there is a blow-up of the finite difference solution and the scheme becomes unstable.

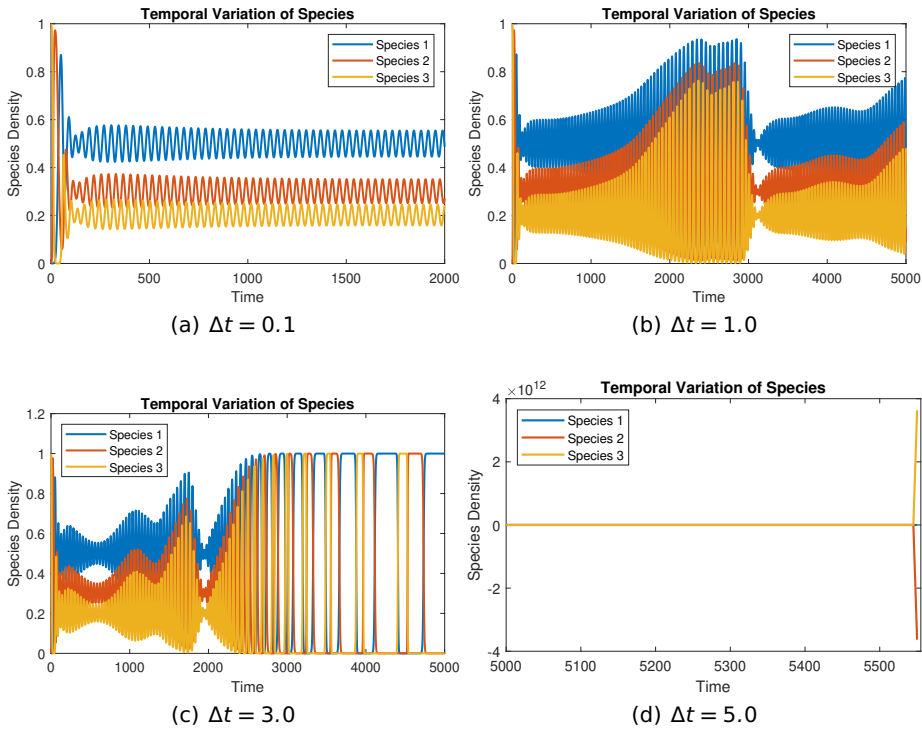


Figure 6.9: Numerical solutions of Eq. (6.72) using the FSTS scheme for the invasion rates $\alpha_1 = 0.2$, $\alpha_2 = 0.5$ and $\alpha_3 = 0.3$ at the point $x = 5.05$. The space step size is $\Delta x = 0.1$, while the time step size is $\Delta t = 0.1, 1.0, 3.0$ and 5.0 . It can be observed that as Δt is increased, the dynamics change from periodic orbits to quasi-periodic orbits and finally to a blow-up.

is similar among all the four schemes provided that the time step used in the simulation is sufficiently small. It can also be noted that the critical values of the time step at which instability (blow-up) occurs in the schemes is larger than the time step restriction set by the CFL condition for explicit schemes.

6.8 Matrix semi-stability

In the previous section, we have verified numerically the necessary condition of semi-stability of the Jacobian matrix of the reaction part for the stability of the analyzed finite difference schemes. A more difficult condition to verify, even numerically, is that of D-semi-stability of the Jacobian. However, for some very special cases, it is possible to mathematically verify the D-semi-stability (and hence semi-stability) of the Jacobian matrix without the need for numerical simulations.

In this section, we show one application of the results of this chapter to the area of chemical reaction networks. Specifically, for a single *non-autocatalytic* chemical

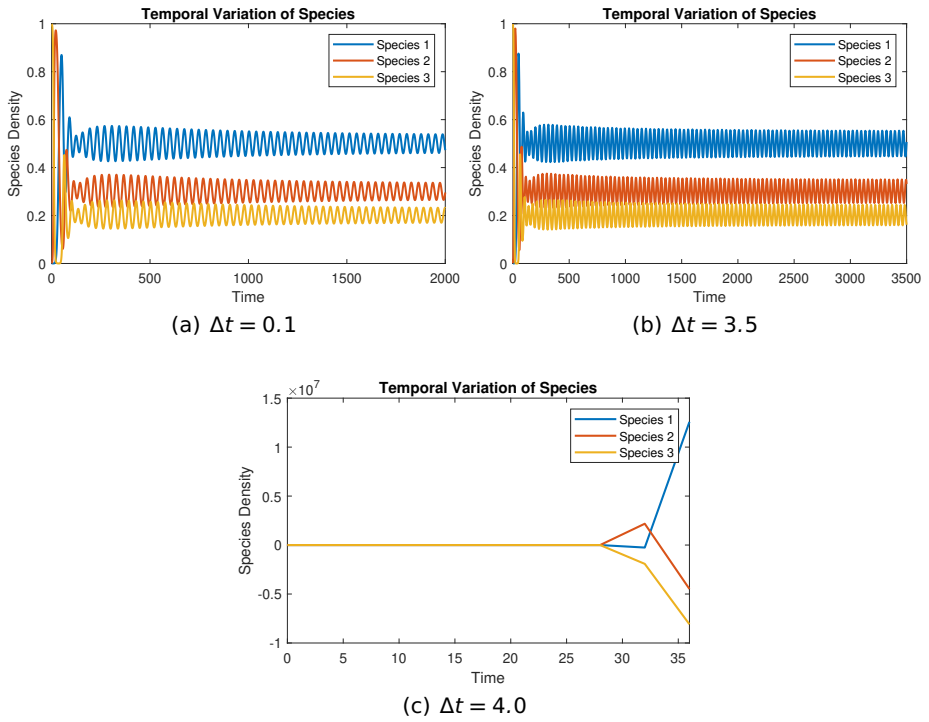


Figure 6.10: Numerical solutions of Eq. (6.72) using the IIF scheme for the invasion rates $\alpha_1 = 0.2$, $\alpha_2 = 0.5$ and $\alpha_3 = 0.3$ at the point $x = 5.05$. The space step size is $\Delta x = 0.1$, while the time step size is $\Delta t = 0.1, 3.5$ and 4.0 . It can be observed that the dynamics are similar for all Δt for which the scheme is stable. For $\Delta t = 4.0$, there is a blow-up of the finite difference solution and the scheme becomes unstable.

reaction, by making some reasonable assumptions on the kinetics of the reaction, we prove that the Jacobian matrix evaluated at any positive solution, is indeed both semi-stable and D-semi-stable. In addition, we show that the assumptions that we make in order to prove the semi-stability of Jacobian hold for reactions governed by a variety of enzyme-kinetic rate governing laws.

6.8.1 Monotone kinetics

Here we give a brief description about the assumption that we make on the kinetics of the reaction. Consider a reversible chemical reaction involving n chemical species X_1, X_2, \dots, X_n that takes the form:



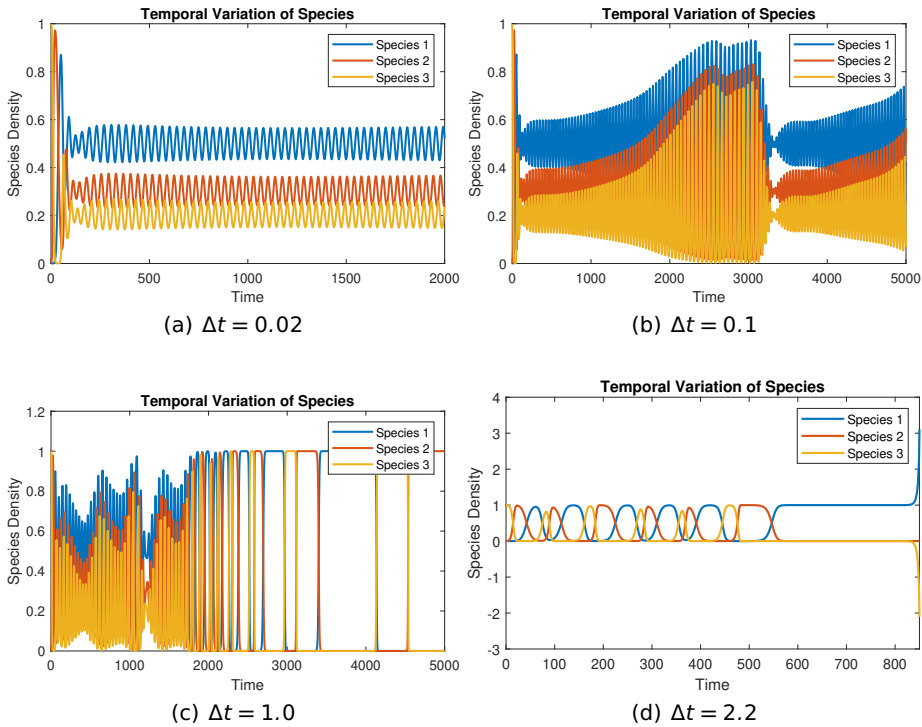


Figure 6.11: Numerical solutions of Eq. (6.72) using the IMEX scheme for the invasion rates $\alpha_1 = 0.2$, $\alpha_2 = 0.5$ and $\alpha_3 = 0.3$ at the point $x = 5.05$. The space step size is $\Delta x = 0.1$, while the time step size is $\Delta t = 0.02, 0.1, 1.0$ and 2.2 . It can be observed that as Δt is increased, the dynamics change from periodic orbits to quasi-periodic orbits and finally to a blow-up.

6

where α_i and β_i are nonnegative integers, known as the stoichiometric coefficients of species X_i on the substrate and product sides of the equation, respectively and v_f and v_r are the reaction rates in the forward and backward directions, respectively.

Denote by x_i the concentration of chemical species X_i and let $\mathbf{x} = (x_1, \dots, x_n)^T \in \mathbb{R}_+^n$ denote the vector of species concentrations at any time t . Assume that reaction (6.74) satisfies the following properties:

- (a) The reaction is *non-autocatalytic*, that is, no chemical species appears on both the left (substrates) and right (products) side of the reaction. This means that for each i , either $\alpha_i = 0$ or $\beta_i = 0$.
- (b) The forward and backward reaction rates are continuously differentiable functions of the species concentrations \mathbf{x} . Thus the overall reaction rate v in the forward direction, given by $v = v_f - v_r$, is a continuously differentiable function of species concentrations. That is $v = v(\mathbf{x})$.

- (c) Define $\gamma_i := \beta_i - \alpha_i$. For each X_i , if $\gamma_i < 0$, then $\frac{\partial v(\mathbf{x})}{\partial x_i} \geq 0$, while if $\gamma_i > 0$, then $\frac{\partial v(\mathbf{x})}{\partial x_i} \leq 0$.

All reactions whose reaction rates satisfy properties (b) and (c) above are said to obey *monotone kinetics* (Siegel, 2014).

We now proceed to show that the Jacobian of the reaction part of an RD system modelling the dynamics of a non-autocatalytic reaction with monotone kinetics is D-semi-stable.

6.8.2 D-semi-stability

The concept of D-stability is commonly encountered in mathematical economics and there are many necessary and sufficient conditions for a matrix to be D-stable, although many of them are hard to prove (Giorgi and Zuccotti, 2015). Recall that a matrix A is said to be D-semi-stable if for all positive diagonal matrices D , the matrix DA is semi-stable. In addition, we have already seen that every D-stable matrix is also a stable matrix although the converse is not generally true (Giorgi and Zuccotti, 2015). Thus in order for us to show that a matrix A is both semi-stable and D-semi-stable, we only need to show that A is D-semi-stable and use this to infer the semi-stability of A .

Suppose the chemical reaction (6.74) is non-autocatalytic. Let us order the chemical species in such a way that the first m chemical species, X_1, \dots, X_m , appear as reactants, while the remaining $(n - m)$ species, X_{m+1}, \dots, X_n , appear as products. Then Eq. (6.74) can be written as;



The stoichiometric matrix S for reaction (6.75) is given by

$$N = \begin{bmatrix} -\alpha_1 & \cdots & -\alpha_m & \beta_{m+1} & \cdots & \beta_n \end{bmatrix}^T. \quad (6.76)$$

The time evolution of the concentrations of the chemical species in reaction (6.75) is governed by the RD system

$$\frac{\partial \mathbf{x}}{\partial t} = D\nabla^2 \mathbf{x} + Sv(\mathbf{x}), \quad (6.77)$$

where $v(\mathbf{x})$ is the overall reaction rate. D-semi-stability of the Jacobian for the reaction part is established in the following theorem.

Theorem 6.6. Consider the non-autocatalytic reaction (6.75) with stoichiometric matrix S given by Eq. (6.76) and overall reaction rate $v(\mathbf{x})$. Suppose the reaction kinetics are monotone. Then the Jacobian matrix A of $f(\mathbf{x}) := Sv(\mathbf{x})$, evaluated at any $\mathbf{x} \in \mathbb{R}_+^n$, is D -semi-stable.

Proof. Since S is a column vector, denote by s_k the k -th-entry of S . The Jacobian A of $f(\mathbf{x})$ is the n -square matrix $A = [a_{ij}]$ with

$$a_{ij} = s_i \frac{\partial v(\mathbf{x})}{\partial x_j}, \quad \text{for } i, j = 1, \dots, n.$$

Denote by D a positive diagonal matrix given by $D = \text{diag}(\delta_1, \delta_2, \dots, \delta_n)$. Matrix DA is given by

$$DA = \begin{bmatrix} -\delta_1 \alpha_1 \frac{\partial v(\mathbf{x})}{\partial x_1} & \cdots & -\delta_1 \alpha_1 \frac{\partial v(\mathbf{x})}{\partial x_m} & -\delta_1 \alpha_1 \frac{\partial v(\mathbf{x})}{\partial x_{m+1}} & \cdots & -\delta_1 \alpha_1 \frac{\partial v(\mathbf{x})}{\partial x_n} \\ & \ddots & & & & \\ -\delta_m \alpha_m \frac{\partial v(\mathbf{x})}{\partial x_1} & \cdots & -\delta_m \alpha_m \frac{\partial v(\mathbf{x})}{\partial x_m} & -\delta_m \alpha_m \frac{\partial v(\mathbf{x})}{\partial x_{m+1}} & \cdots & -\delta_m \alpha_m \frac{\partial v(\mathbf{x})}{\partial x_n} \\ \delta_{m+1} \beta_{m+1} \frac{\partial v(\mathbf{x})}{\partial x_1} & \cdots & \delta_{m+1} \beta_{m+1} \frac{\partial v(\mathbf{x})}{\partial x_m} & \delta_{m+1} \beta_{m+1} \frac{\partial v(\mathbf{x})}{\partial x_{m+1}} & \cdots & \delta_{m+1} \beta_{m+1} \frac{\partial v(\mathbf{x})}{\partial x_n} \\ & & & & \ddots & \\ \delta_n \beta_n \frac{\partial v(\mathbf{x})}{\partial x_1} & \cdots & \delta_n \beta_n \frac{\partial v(\mathbf{x})}{\partial x_m} & \delta_n \beta_n \frac{\partial v(\mathbf{x})}{\partial x_{m+1}} & \cdots & \delta_n \beta_n \frac{\partial v(\mathbf{x})}{\partial x_n} \end{bmatrix}$$

Our aim is to show that matrix DA is semi-stable.

Note that the matrix DA has rank 1. From linear algebra, it is known that the number of nonzero eigenvalues of a matrix is less than or equal to the rank of the matrix. Therefore matrix DA has at most one nonzero eigenvalue and thus zero is an eigenvalue of a DA with algebraic multiplicity of at least $n - 1$. Since matrix DA is supposed to have n eigenvalues counting multiplicity, the remaining one eigenvalue of DA is therefore real and is given by the trace of DA . Let us denote this eigenvalue by λ . Thus

$$\lambda = \sum_{i=1}^m -\alpha_i \delta_i \frac{\partial v(\mathbf{x})}{\partial x_i} + \sum_{j=m+1}^n \beta_j \delta_j \frac{\partial v(\mathbf{x})}{\partial x_j}. \tag{6.78}$$

Since we have monotone kinetics,

$$\frac{\partial v(\mathbf{x})}{\partial x_i} \geq 0$$

for $i = 1, \dots, m$ and

$$\frac{\partial v(\mathbf{x})}{\partial x_j} \leq 0$$

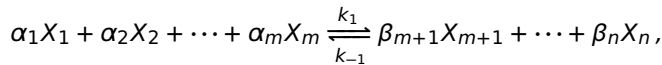
for $j = m + 1, \dots, n$.

Thus each term in both the first and second summations in (6.78) are negative and

hence both sums are negative. Therefore $\lambda \leq 0$ and the matrix DA is semi-stable. This proves that the matrix A is D-semi-stable. From the properties of D-stable matrices, we conclude that matrix A is also semi-stable. \square

We now demonstrate on some examples that the assumption we made about the kinetics of the reaction being monotone is a reasonable assumption that is satisfied by many rate governing laws.

Example 1: Consider the reversible chemical reaction



governed by mass-action kinetics. Here, k_1 and k_{-1} are positive rate constants. Denote by x_i the concentration of species X_i . The overall rate of reaction v in the forward direction is given by

$$v(\mathbf{x}) = k_1 \prod_{i=1}^m x_i^{\alpha_i} - k_{-1} \prod_{i=m+1}^n x_i^{\beta_i}.$$

For $i = 1, \dots, m$, we have $\gamma_i = -\alpha_i < 0$ and

$$\frac{\partial v(\mathbf{x})}{\partial x_i} = k_1 \alpha_i x_i^{\alpha_i - 1} \prod_{\substack{j=1 \\ j \neq i}}^m x_j^{\alpha_j} > 0, \quad \text{since } \mathbf{x} \in \mathbb{R}_+^n.$$

Similarly, for $i = m+1, \dots, n$, we have $\gamma_i = \beta_i > 0$ and

$$\frac{\partial v(\mathbf{x})}{\partial x_i} = -k_{-1} \beta_i x_i^{\beta_i - 1} \prod_{\substack{j=m+1 \\ j \neq i}}^n x_j^{\beta_j} < 0.$$

Thus the reaction rate $v(\mathbf{x})$ satisfies the properties of monotone kinetics.

Example 2: Consider the reversible enzymatic reaction:



Here S is the substrate, E is the enzyme that acts as a catalyst for the reaction and P the product. Let s and p denote the substrate and product concentrations, respectively, at any time t , and $\mathbf{x} = \begin{bmatrix} s & p \end{bmatrix}^T \in \mathbb{R}_+^2$. Note that $\gamma_s = -1$ while $\gamma_p = 1$. Suppose the reaction is governed by Michaelis–Menten kinetics, then

$$v(\mathbf{x}) = \frac{\frac{V_f}{K_s} s - \frac{V_r}{K_p} p}{1 + \frac{s}{K_s} + \frac{p}{K_p}},$$

where V_f, V_r, K_s and K_r are positive constants.

It can be verified that $\frac{\partial v(\mathbf{x})}{\partial s} > 0$ and $\frac{\partial v(\mathbf{x})}{\partial p} < 0$. Thus the reaction obeys monotone kinetics.

6.9 Discussion and conclusion

In this chapter, we have explored the use of finite difference schemes in solving RD equations that model the dynamics of competing populations in which the habitat is a continuum. In particular, we have analyzed the stability of some well-known finite difference schemes and established sufficient conditions for the local linear stability of these schemes in the multivariable case.

It should be noted, however, that the conditions derived for the stability of the schemes applied to the localized linear system may not guarantee stability of the same schemes when applied to the nonlinear RD system (6.2). Nonetheless, linear stability is a necessary condition for nonlinear stability and it provides a useful way of weeding out obviously unsuitable schemes.

In addition to the stability analysis, we have also been able to highlight some of the complexities involved in the use of numerical methods to solve nonlinear PDEs. The numerical solutions are affected by not only the nonlinearities in the model but also by the scheme employed and the time step. However, a notable observation is that for a sufficiently small time step size, the long-term behavior of the solutions from all the schemes is similar.

6 Because conclusions based on ecological models are often used in monitoring biodiversity and in environmental planning and management, it is important to have numerical solutions that are consistent and accurately represent the unknown analytical solution. Thus care should be taken when choosing the numerical scheme and in selecting the time step size for the simulations. Some schemes are more suited to problems in which the diffusion terms dominate, for example, the IIF scheme was designed for diffusion-dominated problems and does not seem to work well for problems where the reactions dominate. On the other hand, the time step should be chosen in such a way so as to strike a balance between accuracy, stability and computational effort.

From the stability analysis, one notable sufficient condition for stability of the analyzed schemes is that the Jacobian matrix of the reaction part evaluated at any known positive solution is either semi-stable or D-semi-stable. This is an eigenvalue problem which is difficult to verify analytically in many multivariable RD models of the form (6.2). In many practical models, this condition has to be verified numerically like we have done in Sections 6.7.1 and 6.7.2.

However, for chemical reaction whose kinetics are monotone, we have been able to prove analytically in Section 6.8 that the Jacobian matrix is always D-semi-stable (and hence semi-stable). In addition, we have also demonstrated using examples that the assumption on the kinetics of the reaction being monotone is reasonable and is satisfied by a number of kinetic rate governing laws.

We hope that the stability results of this chapter could act as a guide when deciding on a finite difference scheme to use whenever RD equations have to be used as a model for studying intransitive competition. Future work related to this chapter could involve extending the D-semi-stability that has been proven for a single non-autocatalytic reaction with monotone kinetics to a network of chemical reactions.

7

Conclusions and future work

Coexistence mechanisms, like intransitive competition, that only emerge in systems with more than two competitors, present a largely unexplored control over the preservation of diversity in species rich communities. In studying the effects of intransitive competition on species coexistence, ecologists have traditionally approached the problem via a graph-theoretic representation of an ecological community with a directed graph or network. An analysis of the structure of such a network should enable us to anticipate some of the dynamical properties of an ecological community. However, till now, how the structure of the network influences coexistence is still an open question.

In this thesis, by making use of a number of mathematical tools borrowed from fields outside ecology, such as graph theory, game theory, chemical reaction network theory, and the theory of dynamical systems, we have explored a number of questions relating to the dynamics of species involved in intransitive competition networks in a bid to provide insights to some of community ecology's open questions, such as the prediction of community structure at equilibrium. The interdisciplinary nature of the thesis has also allowed us to explore an existing mathematical problem regarding the stability of finite difference schemes for the

numerical solution of reaction-diffusion equations, which are ubiquitous in the field of mathematical modelling of biological and chemical systems.

In the following, we summarize the main conclusions that can be drawn from this thesis, and list several pending issues that might be included in future work.

7.1 Conclusions

In this thesis, we explored two key issues; one regarding the dynamics of species involved in intransitive competition networks, and two regarding the stability of finite difference schemes commonly used for the numerical solution of reaction-diffusion equations in ecology.

In Chapter 4, we have highlighted an approach that can be used to predict the dynamical properties of ecological communities governed by intransitive competition, by considering the competition networks, represented by complete directed graphs (tournaments) directly rather than via numerical simulations of their mean-field differential equation models. This approach, which we have named the method of triads, first makes use of the pairwise competitive abilities of species in a tournament to partition the species into two disjoint groups, kings and non-kings. Then by using game-theoretic methods, we have been able to show that every non-king is competitively excluded from the tournament, thus reducing it to a smaller tournament in which every species is a king, and each species is involved in at least one intransitive triad with every other species. In the resulting all-kings community, final community structure can be deduced from an analysis of the interactions among the intransitive triads of the all-kings tournament. Using the method of triads, we have been able to deduce the final community structure (both species richness and composition) in a number of ecological networks composed of five to nine species as shown in Table 4.1. This chapter highlights the intuition held by many that final community structure is a function of some intransitive structures within the network, although it is not yet clear which exact intransitive structures greatly influence community composition at equilibrium. It also opens the door for future research on network properties and their relation to final community composition.

In Chapter 5, we explored the question on how dynamics within a single metapopulation habitat patch are influenced by migrations from and to other patches. Note that in the absence of migrations, coexistence of species is a result of limit cycles around the neutral equilibrium point. With the introduction of migrations between patches, the dynamics can be significantly different depending on whether the dispersal graph is homogeneous or heterogeneous. In this chapter, we have mathematically proven, using concepts from chemical reaction network theory and the theory of dynamical systems, that the coexistence equilibrium point is locally

asymptotically stable for a heterogeneous dispersal graph, yet it stays neutrally stable if migrations are homogeneous. In deriving the proof, we have assumed that between any two patches, if there is migration between the two patches, this migration has to be bidirectional. This allows us to make use of the concept of detailed balancing from CRNT which ensures that at equilibrium, the net migration of each species between any two patches is zero. These results provide mathematical support to already existing numerical simulations in the literature and demonstrates that the existing numerical results, which have been derived for three-species cyclic systems, apply to networks with more than three species. The results also confirm the intuition held by many ecologists that spatial heterogeneities in the landscape, which in this case come in the form of differences in dispersal rates, can have profound effects on the dynamics of populations within an environment.

In Chapter 6, we have tackled a different mathematical problem to the ones studied in Chapters 4 and 5. We have explored the problem of numerical stability of finite difference schemes that are commonly used for the numerical solution of reaction-diffusion equations that appear, not only in ecology, but also in the modelling of a number of biological and physical phenomena. We have already stated that for spatial models in which the environment is a continuum, the mathematical models take the form of reaction-diffusion equations whose analytical solutions are very hard, if not impossible, to find. Thus numerical methods, in particular, finite difference schemes, are used to find approximate solutions to the equations. But the use of numerical methods leads to a different mathematical problem of establishing whether a given numerical scheme is stable or not. In this chapter, we have established sufficient conditions for the stability of a number of finite difference schemes in the case of systems of equations. Many stability conditions in the literature had been derived based on the analysis of systems of linear diffusion equations. It was not clear whether the same conditions would still apply if the methods are applied to systems of the reaction-diffusion equations. Our results have shown that additional constraints are needed, particularly on the Jacobian of the nonlinear reaction part to guarantee stability of the schemes.

7.2 Possible future research directions

In Chapter 4 of this thesis, we have demonstrated how structural properties of a competition network, represented by a complete directed graph, can be used to answer one of community ecology's central aims, to predict community structure at equilibrium. However, as stated before, our method, which makes use of interactions among the intransitive triads, is only able to deduce community structure at equilibrium for some networks, but fails for others. The method fails particularly for those networks whose triads interaction graph (TIG) contains multiple cycles

with different numbers of unique species in the triads forming the cycles. But we still believe that community structure at equilibrium can be fully predicted from an analysis of the structure of the graph, without the need for numerical simulations.

In addition, the intransitive competition models of this chapter have been derived with an assumption that the interactions in a community operate only between pairs of species and that these pairwise interactions then combine to generate the dynamics of the full community. Such models, however, often lead to species abundances to neutrally cycle around a coexistence equilibrium point, which is problematic as such cycles are not observed in nature (Grilli et al., 2017). In addition, there are also instances when such pairwise models fail to predict multi-species coexistence in a number of ecological communities (Dormann and Roxburgh, 2005; Momeni et al., 2017). To overcome these problems, recent studies have suggested that interactions between species should not be constrained to species pairs, but should include higher-order interactions (Grilli et al., 2017; Levine et al., 2017; Mayfield and Stouffer, 2017), where the per capita effect of one competitor on another can be modified by the presence of a third (or even more) species. Grilli et al. (2017) have shown that incorporating higher-order interactions does not alter the equilibrium values of the pairwise model but has a dramatic stabilizing effect on the dynamics leading to convergence to the equilibrium point instead of neutral cycles. Such a stabilizing effect has also been observed in the metapopulation model of Chapter 5, where heterogeneity in the migrations moves the coexistence equilibrium point within each patch from neutral stability to local asymptotic stability.

Finally, we have studied communities whose dynamics are well-described by systems of ODEs (assuming a large number of interacting individuals) in which species coexistence is often equated to the existence of a stable equilibrium that is bounded away from the extinction states and where coexistence holds indefinitely. However, when the number of individuals is finite, these deterministic ODE models fail to account for random fluctuations due to demographic and environmental stochasticity which are experienced by all natural populations. Demographic stochasticity describes the random fluctuations in population size that occur because the death and birth of each individual is a discrete and probabilistic event (Melbourne, 2012), and environmental stochasticity is the stochastic variation in the physical and biological environment and thereby in the parameters affecting the system (Feng et al., 2011). Incorporating stochasticity in models can introduce qualitative changes in the nature of long-term dynamics that depart dramatically from the predictions of a deterministic attractor (Hening et al., 2021). It also allows one to derive expressions for probabilities of extinctions, expected times to extinction, and other properties of relevant distributions.

Thus future research directions on the problem of predicting community structure could involve the following;

1. Deriving an alternative method for ranking dominance relations among the intransitive triads to the one used in this paper. This could probably lead to a different TIG where the number of cycles of triads within the graph is less or even just one.
2. Determination of general properties of tournament matrices corresponding to all coexistence networks.
3. The method of triads focuses on the number of species that go extinct (and the number of those that don't) as an endpoint of the model simulation, but ignores the time until extinction, which is a highly relevant ecological aspect. It would be interesting to study the time until all non-kings have gone extinct and the community reaches its final composition and see if this varies between different tournaments, and to what extent.
4. How can we incorporate higher-order interactions into the method of triads? Do the predictions from the method still hold with the incorporation of higher-order interactions?
5. What is the effect of stochasticity (e.g. time-dependent parameters) on the method of triads predictions?

In Chapter 5, we have provided a mathematical proof for existing numerical simulations regarding the effects of dispersal on the dynamics of species living in discrete habitat patches of a metapopulation modelled by a deterministic system of ordinary differential equations. In particular, we have shown that dispersal has the ability to shift the stability properties of the coexistence equilibrium, which is neutrally stable in the absence of dispersal, to local asymptotic stability in the presence of dispersal.

In our model, we have assumed that all coefficients (parameters) in the model equations are constant leading to the time-invariant differential equations used. However, in realistic scenarios, parameters involved in ecological models are not constants but rather they depend upon several ecological and environmental factors that induce seasonality in the parameters. Thus differential equations with time-varying parameters can be used to account for temporal changes in the parameters. Such models have been used to, for example, study the extinction of species in communities modelled by competitive Lotka-Volterra systems (Vance and Coddington, 1989; de Oca and Zeeman, 1996; Ahmad, 1999; Ahmad and Lazer, 2000). In fact, Ahmad and Lazer (2000) have derived sufficient conditions that guarantee the persistence and global stability of such time-varying systems. However, to our knowledge, the time-varying differential equations of the metapopulation models used in this chapter have not been studied in generality.

Thus possible future work on such deterministic metapopulation models could involve the following;

1. Deriving sufficient conditions for the persistence and stability of a more realistic metapopulation model in which the coefficients are time-varying.
2. Determination of dynamical characteristics (e.g., frequency, amplitude of oscillations) in such deterministic metapopulation models and how these mathematical results connect with ecological theory.
3. Exploring the effects of local habitat quality on the metapopulation dynamics. The effect of habitat quality crucially depends on migration rate. Thus we can assume that the more favourable patches have high immigration rates compared to the less favourable patches with low immigration and high emigration rates.

Another very promising future direction that is related to Chapters 4 and 5 involves the integration of intransitive competition in modern coexistence theory (MCT). Ecologists have embraced MCT as a framework for understanding the factors that lead to ecological coexistence versus competitive exclusion. According to MCT (Chesson, 2000), stable coexistence of a set of n competing species is only possible if each species is able to increase from low density when introduced in a subcommunity of the remaining $n - 1$ species. This is termed as the *invasibility criterion*, where the species at low density is termed the invader, with the rest of the community termed the residents. In other words, species coexistence is only possible if each species has a positive growth rate when invading the rest of the community. However, this theoretical framework seems insufficient to account for all the diversity observed in many natural communities. In addition, the theory has been developed with an exclusive focus on interactions between two species and is not easily extended to include mechanisms, such as intransitive loops, that only emerge with more than two species.

On the other hand, studies on the role of intransitive competition in promoting species coexistence have been typically done outside the framework of MCT. Thus little is known on how intransitivity interacts with the more traditional drivers of species coexistence such as niche partitioning. The key question is then: how can we integrate intransitive competition into MCT? Can intransitive competitive cycles preserve diversity in situations where coexistence is not possible via MCT mechanisms alone? Exploring these and more questions would provide a contribution to the development of a more unified theory for species coexistence.

Finally, in Chapter 6, we have derived sufficient conditions for the stability of some well-known finite difference schemes for the numerical solution of the systems of reaction-diffusion equations in ecology. Since the equations are nonlinear, these conditions have been derived through a local linearization. It is hoped that results from this stability analysis could act as a guide when deciding on a finite difference scheme to use whenever nonlinear RD equations are encountered. Future work related to this chapter could involve extending the proof of D-semi-stability that has

been established for a single non-autocatalytic reaction with monotone kinetics to a network of chemical reactions.

Bibliography

- Aarssen, L. W., 1983. Ecological combining ability and competitive combining ability in plants: Toward a general evolutionary theory of coexistence in systems of competition. *Am. Nat.* 122 (6), 707–731.
- Aarssen, L. W., 1989. Competitive ability and species coexistence: A 'plant's-eye' view. *Oikos* 56 (3), 386–401.
- Adler, I., 2013. The equivalence of linear programs and zero-sum games. *Int. J. Game Theory* 42 (1), 165–177.
- Adler, P. B., HilleRisLambers, J., Levine, J. M., 2007. A niche for neutrality. *Ecol. Lett.* 10, 95–104.
- Ahmad, S., 1999. Extinction of species in nonautonomous Lotka-Volterra systems. *Proc. Am. Math. Soc.* 127 (10), 2905–2910.
- Ahmad, S., Lazer, A. C., 2000. Average conditions for global asymptotic stability in a nonautonomous lotka-volterra system. *Nonlinear Anal. Theory Methods Appl.* 40 (1), 37–49.
- Alcántara, J. M., Rey, P. J., 2012. Linking topological structure and dynamics in ecological networks. *Am. Nat.* 180 (2), 186–199.
- Aldous, J. M., Wilson, R. J., 2003. *Graphs and Applications: An Introductory Approach*. Springer.
- Allesina, S., Levine, J. M., 2011. A competitive network theory of species diversity. *PNAS* 108 (14), 5638–5642.

- Amarasekare, P., 1998. Allee effects in metapopulation dynamics. *Am. Nat.* 152 (2), 298–302.
- Armstrong, R. A., McGehee, R., 1980. Competitive exclusion. *Am. Nat.* 115 (2), 151–170.
- Artzy-Randrup, Y., Stone, L., 2010. Connectivity, cycles, and persistence thresholds in metapopulation networks. *PLoS Comput. Biol.* 6 (8), 1–10.
- Ascher, U. M., Ruuth, S. J., Wetton, B. T. R., 1995. Implicit-explicit methods for time-dependent partial differential equations. *SIAM J. Numer. Anal.* 32 (3), 797–823.
- Bacaër, N., 2011. Verhulst and the logistic equation (1838). Springer London, London, pp. 35–39.
- Barabás, G., J. Michalska-Smith, M., Allesina, S., 2016. The effect of intra- and interspecific competition on coexistence in multispecies communities. *Am. Nat.* 188 (1), E1–E12.
- Bascompte, J., Jordano, P., 2007. Plant-animal mutualistic networks: The architecture of biodiversity. *Annu. Rev. Ecol. Evol. Syst.* 38 (1), 567–593.
- Begon, M., Townsend, C., Harper, J., 2006. *Ecology: From Individuals to Ecosystems*. Blackwell Publishing.
- Berr, M., Reichenbach, T., Schottenloher, M., Frey, E., 2009. Zero-one survival behavior of cyclically competing species. *Phys. Rev. Lett.* 102, 048102.
- Bersier, L.-F., 2007. A history of the study of ecological networks. *World Scientific*, Ch. 11, pp. 365–421.
- Bezembinder, T. G. G., 1981. Circularity and consistency in paired comparisons. *Br. J. Math. Stat. Psychol.* 34, 16–37.
- Bollobás, B., 1998. *Modern Graph Theory*. Graduate Texts in Mathematics, 184, Springer, New York.
- Boros, B., 2019. Existence of positive steady states for weakly reversible mass-action systems. *SIAM J. Math. Anal.* 51 (1), 435–449.
- Brémaud, P., 1988. *An Introduction to Probabilistic Modeling*. Springer.
- Broom, M., Koenig, A., Borries, C., 2009. Variation in dominance hierarchies among group-living animals: modeling stability and the likelihood of coalitions. *Behav. Ecol.* 20, 844–855.
- Brown, J. H., Kodric-Brown, A., 1977. Turnover rates in insular biogeography: Effect of immigration on extinction. *Ecology* 58 (2), 445–449.

- Brugnano, L., Mazzia, F., Trigiante, D., 2011. Fifty years of stiffness. In: Simos, T. E. (Ed.), *Recent Advances in Computational and Applied Mathematics*. Springer Netherlands, Ch. 1, pp. 1–21.
- Bunn, A., Urban, D., Keitt, T., 2000. Landscape connectivity: A conservation application of graph theory. *J. Environ. Manage.* 59 (4), 265–278.
- Burrows, M. T., Hawkins, S. J., 1998. Modelling patch dynamics on rocky shores using deterministic cellular automata. *Mar. Ecol. Prog. Ser.* 167, 1–13.
- Buss, L. W., Jackson, J. B. C., 1979. Competitive networks: Nontransitive competitive relationships in cryptic coral reef environments. *Am. Nat.* 113 (2), 223–234.
- Cameron, D. D., White, A., Antonovics, J., 2009. Parasite-grass-forb interactions and rock-paper-scissor dynamics: predicting the effects of the parasitic plant *rhinanthus minor* on host plant communities. *J. Ecol.* 97, 1311–1319.
- Cantrell, R. S., Cosner, C., 2003. *Spatial ecology via reaction-diffusion equations*. John Wiley & Sons, Ltd.
- Chao, A., Chiu, C.-H., 2016. *Species Richness: Estimation and Comparison*. John Wiley & Sons, Ltd, pp. 1–26.
- Charney, J. G., Fjørtoft, R., Von Neumann, J., 1950. Numerical integration of the barotropic vorticity equation. *Tellus* 2 (4), 237–254.
- Chase, I. D., Tovey, C., Spangler-Martin, D., Manfredonia, M., 2002. Individual differences versus social dynamics in the formation of animal dominance hierarchies. *PNAS* 99 (8), 5744–5749.
- Chen, A.-H., Chang, J.-M., Cheng, Y., Wang, Y.-L., 2008. The existence and uniqueness of strong kings in tournaments. *Discrete Math.* 308, 2629–2633.
- Cheng, H., Yao, N., Huang, Z.-G., Park, J., Do, Y., Lai, Y.-C., 2014. Mesoscopic interactions and species coexistence in evolutionary game dynamics of cyclic competitions. *Sci. Rep.* 4, 7486.
- Chesson, P., 2000. Mechanisms of maintenance of species diversity. *Annu. Rev. Ecol. Syst.* 31 (1), 343–366.
- Cohen, J. E., 1994. Lorenzo camerano's contribution to early food web theory. In: Levin, S. A. (Ed.), *Frontiers in Mathematical Biology*. Springer Berlin Heidelberg, Berlin, Heidelberg, pp. 351–359.
- Conway, E., Hoff, D., Smoller, J., 1978. Large time behavior of solutions of systems of nonlinear reaction-diffusion equations. *SIAM J. Appl. Math.* 35 (1), 1–16.
- Cosner, C., 2008. *Reaction-Diffusion Equations and Ecological Modeling*. Springer Berlin Heidelberg, pp. 77–115.

- Costa, A., Martin Gonzalez, A., Guizien, K., Doglioli, A., Gomez, J., Petrenko, A., Allesina, S., 11 2019. Ecological networks: Pursuing the shortest path, however narrow and crooked. *Sci. Rep.* 9, 17826.
- Courant, R., Friedrichs, K., Lewy, H., 1928. Ueber die partiellen differenzengleichungen der mathematischen physik. *Math. Ann.* 100 (1), 32–74.
- Cowden, C., 01 2012. Game theory, evolutionary stable strategies and the evolution of biological interactions. *Nature Education Knowledge* 3 (10), 6.
- Cox, S. M., Mathews, P. C., 2002. Exponential time differencing for stiff systems. *J. Comput. Phys.* 176, 430–455.
- Dale, M., Fortin, M.-J., 2010. From graphs to spatial graphs. *Annu. Rev. Ecol. Evol. Syst.* 41 (1), 21–38.
- Daly, A. J., 2017. Putting ecological theories to the test: individual-based simulations of synthetic microbial community dynamics. Ph.D. thesis, Department of Mathematical Modelling, Statistics and Bioinformatics, Ghent University, Ghent, Belgium.
- Dasgupta, B., 2006. *Applied Mathematical Methods*. Dorling Kindersley (India) Pvt. Ltd.
- Daun, S., Rubin, J., Vodovotz, Y., Clermont, G., 2008. Equation-based models of dynamic biological systems. *J. Crit. Care* 23 (4), 585–594.
- de Oca, F. M., Zeeman, M. L., 1996. Extinction in nonautonomous competitive Lotka-Volterra systems. *Proc. Am. Math. Soc.* 124 (12), 3677–3687.
- de Souza Júnior, M. B., Ferreira, F. F., de Oliveira, V. M., 2014. Effects of the spatial heterogeneity on the diversity of ecosystems with resource competition. *Physica A* 393, 312–319.
- DeAngelis, D. L., Grimm, V., 2014. Individual-based models in ecology after four decades. *F1000Prime Rep.* 6, 39.
- Delmas, E., Besson, M., Brice, M.-H., Burkle, L. A., Dalla Riva, G. V., Fortin, M.-J., Gravel, D., Guimarães Jr., P. R., Hembry, D. H., Newman, E. A., Olesen, J. M., Pires, M. M., Yeakel, J. D., Poisot, T., 2019. Analysing ecological networks of species interactions. *Biol. Rev.* 94 (1), 16–36.
- Dormann, C. F., Roxburgh, S. H., 2005. Experimental evidence rejects pairwise modelling approach to coexistence in plant communities. *Proc Biol Sci.* 272 (1569), 1279–1285.
- Durrett, R., Levin, S., 1998. Spatial aspects of interspecific competition. *Theor. Popul. Biol.* 53 (1), 30 – 43.

- Dym, C. L., 2004. *Principles of Mathematical Modeling*. Elsevier Academic Press.
- Ehlers, W., Zinatbakhsh, S., Markert, B., 2013. Stability analysis of finite difference schemes revisited: A study of decoupled solution strategies for coupled multi-field problems. *Int. J. Numer. Methods Eng.* 94 (8), 758–786.
- Ellis, A. M., Post, E., 2004. Population response to climate change: linear vs. non-linear modeling approaches. *BMC Ecol.* 4 (1), 2.
- Etienne, R. S., 2000. Local populations of different sizes, mechanistic rescue effect and patch preference in the levins metapopulation model. *Bull. Math. Biol.* 62 (5), 943–958.
- Fahrig, L., 2007. *Landscape heterogeneity and metapopulation dynamics*. Cambridge Studies in Landscape Ecology. Cambridge University Press, pp. 78–91.
- Feinberg, M., 1987. Chemical reaction network structure and the stability of complex isothermal reactors-i. the deficiency zero and deficiency one theorems. *Chem. Eng. Sci.* 42 (10), 2229–2268.
- Feinberg, M., 1989. Necessary and sufficient conditions for detailed balancing in mass action systems of arbitrary complexity. *Chem. Eng. Sci.* 44 (9).
- Feng, Z., Liu, R., Qiu, Z., Rivera, J., Yakubu, A.-A., 2011. Coexistence of competitors in deterministic and stochastic patchy environments. *J. Biol. Dyn.* 5 (5), 454–473.
- Fisher, D. C., Ryan, J., 1992. Optimal strategies for a generalized scissors, paper, and stone game. *Am. Math. Mon.* 99 (10), 935–942.
- Frean, M., Abraham, E. R., 2001. Rock-scissors-paper and the survival of the weakest. *Proc. R. Soc. Lond. B* 268, 1323–1327.
- French, A. R., Smith, T. B., 2005. Importance of body size in determining dominance hierarchies among diverse tropical frugivores. *Biotropica* 37 (1), 96–101.
- Gallien, L., 2017. Intransitive competition and its effects on community functional diversity. *Oikos* 126 (5), 615–623.
- Gallien, L., Zimmermann, N. E., Levine, J. M., Adler, P. B., 2017. The effects of intransitive competition on coexistence. *Ecol. Lett.* 20, 791–800.
- Garvie, M. R., 2007. Finite-difference schemes for reaction-diffusion equations modeling predator-prey interactions in matlab. *Bull. Math. Biol.* 69 (3), 931–956.
- Gause, G. F., 1934. *The struggle for Existence*. Dover Publications, New York.
- Gertsev, V., Gertseva, V., 2004. Classification of mathematical models in ecology. *Ecol. Model.* 178 (3), 329–334.

- Gibert, J. P., Yeakel, J. D., 2019. Laplacian matrices and turing bifurcations: revisiting Levin 1974 and the consequences of spatial structure and movement for ecological dynamics. *Theor. Ecol.* 12, 265–281.
- Gilg, O., Hanski, I., Sittler, B., 2003. Cyclic dynamics in a simple vertebrate predator-prey community. *Science* 302 (5646), 866–868.
- Gilpin, M. E., 1975. Limit cycles in competition communities. *Am. Nat.* 109 (965), 51–60.
- Giorgi, G., Zuccotti, C., Feb. 2015. An overview on d-stable matrices. Università Di Pavia, DEM Working Paper Series.
URL <ftp://ftp.repec.org/opt/ReDIF/RePEc/pav/demwpp/DEMWP0097.pdf>
- Glowinski, R., 2003. Finite element methods for incompressible viscous flow. *Handb. Numer. Anal.* 9, 3–1176.
- Godoy, O., Stouffer, D. B., Kraft, N. J. B., Levine, J. M., 2017. Intransitivity is infrequent and fails to promote annual plant coexistence without pairwise niche differences. *Ecology* 98 (5), 1193–1200.
- Gorban, A., Yablonsky, G., 2011. Extended detailed balance for systems with irreversible reactions. *Chem. Eng. Sci.* 66 (21), 5388–5399.
- Gordon, C. E., 2000. The coexistence of species. *Rev. Chil. de Hist. Nat.* 73, 175–198.
- Gray, P., Scott, S. K., Merkin, J. H., 1988. The brusselator model of oscillatory reactions. relationships between two-variable and four-variable models with rigorous application of mass conservation and detailed balance. *J. Chem. Soc., Faraday Trans. 1* 84, 993–1011.
- Grilli, J., Barabás, G., Michalska-Smith, M. J., Allesina, S., 2017. Higher-order interactions stabilize dynamics in competitive network models. *Nature* 548, 210–213.
- Grime, J. P., 2006. Trait convergence and trait divergence in herbaceous plant communities: Mechanisms and consequences. *J. Veg. Sci.* 17 (2), 255–260.
- Grinnell, J., 1917. The niche-relationships of the california thrasher. *The Auk* 34 (4), 427–433.
- Hairer, E., Wanner, G., 1996. *Solving Ordinary Differential Equations II: Stiff and Differential-Algebraic Problems*. Springer Berlin Heidelberg, Berlin, Heidelberg.
- Hanski, I., 1983. Coexistence of competitors in patchy environment. *Ecology* 64 (3), 493–500.
- Hanski, I., 1998. Metapopulation dynamics. *Nature* 396, 41–49.

- Hanski, I., Gilpin, M., 1997. *Metapopulation Biology: Ecology, Genetics, and Evolution*. Elsevier Science.
- Hanski, I., Ovaskainen, O., 2000. The metapopulation capacity of a fragmented landscape. *Nature* 404 (6779), 755–758.
- Hardin, G., 1960. The competitive exclusion principle. *Science* 131, 1292–1297.
- Harrison, S., Taylor, A. D., 1997. 2 - empirical evidence for metapopulation dynamics. In: Hanski, I., Gilpin, M. E. (Eds.), *Metapopulation Biology*. Academic Press, San Diego, pp. 27–42.
- Hart, S. P., Usinowicz, J., Levine, J. M., 2017. The spatial scales of species coexistence. *Nat. Ecol. Evol.* 1 (8), 1066–1073.
- Hastings, A., Harrison, S., 1994. Metapopulation dynamics and genetics. *Annu. Rev. Ecol. Syst.* 25 (1), 167–188.
- Hening, A., Nguyen, D. H., Chesson, P., 2021. A general theory of coexistence and extinction for stochastic ecological communities. *J. Math. Biol.* 82, 56.
- Higashi, M., Burns, T. P., 1991. *Theoretical Studies of Ecosystems: The Network Perspective*. Cambridge University Press, Cambridge.
- Hirsch, C., 1988. *Numerical Computation of Internal and External Flows: Fundamentals of Numerical Discretization*. John Wiley & Sons.
- Ho, T.-Y., Chang, J.-M., 2003. Sorting a sequence of strong kings in a tournament. *Inform. Process. Lett.* 87, 317–320.
- Hofbauer, J., Sigmund, K., 1988. *The Theory of Evolution and Dynamical Systems*. Cambridge University Press.
- Hofbauer, J., Sigmund, K., 1998. *Evolutionary Games and Population Dynamics*. Cambridge University Press.
- Holland, M. D., Hastings, A., 2008. Strong effect of dispersal network structure on ecological dynamics. *Nature* 456 (7223), 792–794.
- Holmes, E. E., Lewis, M. A., Banks, J. E., Veit, R. R., 1994. Partial differential equations in ecology: Spatial interactions and population dynamics. *Ecology* 75 (1), 17–29.
- Horn, R. A., Johnson, C. R., 2013. *Matrix Analysis*. Cambridge.
- Hubbell, S. P., 2001. *The Unified Neutral Theory of Biodiversity and Biogeography*. Princeton University Press.
- Hutchinson, G. E., 1951. Copepodology for the ornithologist. *Ecology* 32, 571–577.

- Hutchinson, G. E., 1957. Concluding remarks. *Cold Spring Harb. Symp. Quant. Biol.* 22, 415–427.
- Hutchinson, G. E., 1961. The paradox of the plankton. *Am. Nat.* 95 (882), 137–145.
- Hyman, J. M., October 1976. The method of lines solution of partial differential equations. Tech. Rep. C00-3077-139, New York University.
- Jackson, L. J., Trebitz, A. S., Cottingham, K. L., 2000. An Introduction to the Practice of Ecological Modeling. *BioScience* 50 (8), 694–706.
- Jacoby, D. M. P., Brooks, E. J., Croft, D. P., Sims, D. W., 2012. Developing a deeper understanding of animal movements and spatial dynamics through novel application of network analyses. *Methods Ecol. Evol.* 3 (3), 574–583.
- Jensen, A., 1987. Simple models for exploitative and interference competition. *Ecol. Model.* 35 (1), 113–121.
- Kaplansky, I., 1945. A contribution to von Neumann's theory of games. *Ann. Math.* 46 (3), 474–479.
- Kaplansky, I., 1995. A contribution to von Neumann's theory of games. ii. *Linear Algebra Appl.* 226-228, 371–373.
- Kareiva, P., Mullen, A., Southwood, R., 1990. Population dynamics in spatially complex environments: theory and data. *Phil. Trans. R. Soc. Lond. B* 330, 175–190.
- Kendall, M. G., Babington Smith, B., 1940. On the method of paired comparisons. *Biometrika* 31 (3/4), 324–345.
- Kenyon-Mathieu, C., Schudy, W., 2007. How to rank with few errors. In: *STOC 2007*. ACM Press, New York, pp. 95–103.
- Kerr, B., Riley, M. A., Feldman, M. W., Bohannan, B. J. M., 2002. Local dispersal promotes biodiversity in a real-life game of rock-paper-scissors. *Nature* 418, 171–174.
- Khalil, H. K., 1996. *Nonlinear Systems*. Prentice Hall.
- Kim, D., Ohr, S., 2020. Coexistence of plant species under harsh environmental conditions: an evaluation of niche differentiation and stochasticity along salt marsh creeks. *J. Ecol. Environ.* 44 (1), 19.
- Kirkup, B. C., Riley, M. A., 2004. Antibiotic-mediated antagonism leads to a bacteria game of rock-paper-scissors in vivo. *Nature* 428, 412–414.
- Koide, R. T., Fernandez, C., Petprakob, K., 2011. General principles in the community ecology of ectomycorrhizal fungi. *Ann. Forest Sci.* 68, 45–55.

- Koivisto, M., Westerbom, M., Arnkil, A., 2011. Quality or quantity: small-scale patch structure affects patterns of biodiversity in a sublittoral blue mussel community. *Aquat. Biol.* 12 (3), 261–270.
- Laird, R. A., Schamp, B. S., 2006. Competitive intransitivity promotes species coexistence. *Am. Nat.* 168 (2), 182–193.
- Laird, R. A., Schamp, B. S., 2008. Does local competition increase the coexistence of species in intransitive networks? *Ecology* 89 (1), 237–247.
- Laird, R. A., Schamp, B. S., 2009. Species coexistence, intransitivity, and topological variation in competitive tournaments. *J. Theor. Biol.* 256, 90–95.
- Laird, R. A., Schamp, B. S., 2018a. Calculating competitive intransitivity: Computational challenges. *Am. Nat.* 191 (4), 547–552.
- Laird, R. A., Schamp, B. S., 2018b. Exploring the performance of intransitivity indices in predicting coexistence in multispecies systems. *J. Ecol.* 106, 815–825.
- Lambert, J. D., 1992. *Numerical Methods for Ordinary Differential Systems: The Initial Value Problem*. Wiley.
- Landau, H. G., 1953. On dominance relations and the structure of animal societies: III. the condition for a score structure. *Bull. Math. Biophys.* 15, 143–148.
- Lankau, R. A., Wheeler, E., Bennett, A. E., Strauss, S. Y., 2011. Plant-soil feedbacks contribute to an intransitive competitive network that promotes both genetic and species diversity. *J. Ecol.* 99, 176–185.
- Laub, A. J., 2005. *Matrix Analysis for Scientists and Engineers*. SIAM.
- LeBrun, E. G., 2005. Who is the top dog in ant communities? resources, parasitoids, and multiple competitive hierarchies. *Oecologia* 142, 643–652.
- Levin, S. A., 1974. Dispersion and population interactions. *Am. Nat.* 108 (960), 207–228.
- Levin, S. A., 1976. Population dynamic models in heterogeneous environments. *Annu. Rev. Ecol. Syst.* 7, 287–310.
- Levin, S. A., Carpenter, S. R., Godfray, H. C. J., Kinzig, A. P., Loreau, M., Losos, J. B., Walker, B., Wilcove, D. S., Morris, C. G. (Eds.), 2009. *The Princeton Guide to Ecology*. Princeton University Press.
- Levine, J. M., Bascompte, J., Adler, P. B., Allesina, S., 2017. Beyond pairwise mechanisms of species coexistence in complex communities. *Nature* 546, 56–64.
- Levine, W. S., 1996. *The Control Handbook*. CRC Press.

- Levins, R., 1969. Some demographic and genetic consequences of environmental heterogeneity for biological control. *Bull. Ent. Soc. Amer.* 15 (3), 237–240.
- Levins, R., Culver, D., 1971. Regional coexistence of species and competition between rare species. *PNAS* 68 (6), 1246–1248.
- Liska, R., Steinberg, S., 1993. Applying quantifier elimination to stability analysis of difference schemes. *Comput. J.* 36 (5), 497–503.
- Logan, J. D., 2008. *An Introduction to Nonlinear Partial Differential Equations*. Wiley.
- Lotka, A. J., 1910. Contribution to the theory of periodic reactions. *J. Phys. Chem.* 14 (3), 271–274.
- Lotka, A. J., 1925. *Elements of Physical Biology*. Williams & Wilkins Company, Baltimore.
- MacArthur, R. H., Wilson, E. O., 1967. *The Theory of Island Biogeography*. Princeton University Press.
- Madzvamuse, A., Chung, A. H., 2014. Fully implicit time-stepping schemes and non-linear solvers for systems of reaction diffusion equations. *Appl. Math. Comput.* 244, 361–374.
- Mahdi, A., Law, R., Willis, A. J., 1989. Large niche overlaps among coexisting plant species in a limestone grassland community. *J. Ecol.* 77 (2), 386–400.
- Marek, M., Schreiber, I., 1991. *Chaotic behaviour of deterministic dissipative systems*. Cambridge University Press.
- Maurer, S. B., 1980. The king chicken theorems. *Math. Mag.* 53 (2), 67–80.
- May, R. M., 1972. Will a large complex system be stable? *Nature* 238, 413–414.
- May, R. M., 1974. *Stability and Complexity in Model Ecosystems*. Vol. 1. Princeton University Press.
- May, R. M., 1976. Simple mathematical models with very complicated dynamics. *Nature* 261 (5560), 459–467.
- May, R. M., Leonard, W. J., 1975. Nonlinear aspects of competition between three species. *SIAM J. Appl. Math.* 29 (2), 243–253.
- Mayfield, M. M., Stouffer, D. B., 2017. Higher-order interactions capture unexplained complexity in diverse communities. *Nat. Ecol. Evol.* 1, 0062.
- Maynard Smith, J., 1974. The theory of games and the evolution of animal conflicts. *J. Theor. Biol.* 47 (1), 209–221.

- Maynard Smith, J., 1979. Game theory and the evolution of behaviour. *Proc. Royal Soc. B, Biol. Sci.* 205 (1161), 475–488.
- Maynard Smith, J., Price, G. R., 1973. The logic of animal conflict. *Nature* 246 (5427), 15–18.
- McGill, B. J., Enquist, B. J., Weiher, E., Westoby, M., 2006. Rebuilding community ecology from functional traits. *Trends Ecol. Evol.* 21 (4), 178–185.
- Melbourne, B. A., 2012. Demographic stochasticity. In: Hastings, A., Gross, L. (Eds.), *Encyclopedia of Theoretical Ecology*. University of California Press, Berkeley, California, USA, pp. 706–712.
- Metz, J. A., Diekmann, O., 1986. *The Dynamics of Physiologically Structured Populations*. Springer-Verlag Berlin Heidelberg.
- Miller, R. S., 1967. Pattern and process in competition. Vol. 4 of *Advances in Ecological Research*. Academic Press, pp. 1–74.
- Momeni, B., Xie, L., Shou, W., 2017. Lotka-volterra pairwise modeling fails to capture diverse pairwise microbial interactions. *eLife* 6, e25051.
- Moon, J. W., 1968. *Topics on Tournaments*. Holt, Rinehart and Winston.
- Moore, J. C., 2013. Diversity, taxonomic versus functional. In: Levin, S. A. (Ed.), *Encyclopedia of Biodiversity (Second Edition)*, second edition Edition. Academic Press, Waltham, pp. 648–656.
- Morozov, A., Poggiale, J.-C., 2012. From spatially explicit ecological models to mean-field dynamics: The state of the art and perspectives. *Ecol. Complex.* 10, 1–11.
- Murray, R. M., Li, Z., Sastry, S. S., 1994. *A Mathematical Introduction to Robotic Manipulation*. CRC Press.
- Muyinda, N., Baetens, J. M., De Baets, B., Rao, S., 2019. Using intransitive triads to determine final species richness of competition networks. *Physica A*.
- Muyinda, N., De Baets, B., Rao, S., 2020. Non-king elimination, intransitive triad interactions, and species coexistence in ecological competition networks. *Theor. Ecol.* 13 (3), 385–397.
- Nagatani, T., Ichinose, G., Tainaka, K.-i., 2018. Heterogeneous network promotes species coexistence: metapopulation model for rock-paper-scissors game. *Sci. Rep.* 8 (7094).
- Nash, J., 1951. Non-cooperative games. *Ann. Math.* 54 (2), 286–295.
- Nash, J. F., 1950. Equilibrium points in n-person games. *PNAS* 36 (1), 48–49.

- Nie, Q., Zhang, Y.-T., Rui, Z., 2006. Efficient semi-implicit schemes for stiff systems. *J. Comput. Phys.* 214, 521–537.
- Nisbet, R. M., Briggs, C. J., Gurney, W. S. C., Murdoch, W. W., Stewart-Oaten, A., 1993. Two-patch metapopulation dynamics. In: Levin, S. A., Powell, T. M., Steele, J. W. (Eds.), *Patch Dynamics*. Springer Berlin Heidelberg, Berlin, Heidelberg, pp. 125–135.
- Okubo, A., Levin, S. A., 2001. *Diffusion and Ecological Problems: Modern Perspectives*. Springer, New York.
- Olinick, M., 2014. *Mathematical Modeling in the Social and Life Sciences*. Wiley.
- Otto, S. P., Day, T., 2007. *A Biologist's Guide to Mathematical Modeling in Ecology and Evolution*. Princeton University Press.
- Paquin, C. E., Adams, J., 1983. Relative fitness can decrease in evolving asexual populations of *s. cerevisiae*. *Nature* 306, 368–371.
- Perelson, A. S., 1978. Self-organization in nonequilibrium systems. from dissipative structures to order through fluctuations. *g. nicolis , i. prigogine. Q. Rev. Biol.* 53 (3), 362–363.
- Permogorskiy, M. S., 2015. Competitive intransitivity among species in biotic communities. *Biol. Bull. Rev.* 5 (3), 213–219.
- Perry, G. L. W., Lee, F., 2019. How does temporal variation in habitat connectivity influence metapopulation dynamics? *Oikos* 128 (9), 1277–1286.
- Petraltis, P. S., 1979. Competitive networks and measures of intransitivity. *Am. Nat.* 114 (6), 921–925.
- Pierce, W. D., Cushman, R. A., Hood, C. E., 1912. *The insect enemies of the cotton boll weevil*. U.S. Dept. of Agriculture, Bureau of Entomology.
- Prigogine, I., Lefever, R., 1968. Symmetry breaking instabilities in dissipative systems. ii. *J. Chem. Phys.* 48 (4), 1695–1700.
- Proulx, S. R., Promislow, D. E., Phillips, P. C., 2005. Network thinking in ecology and evolution. *Trends in Ecology & Evolution* 20 (6), 345–353.
- Rao, S., Jayawardhana, B., van der Schaft, A., 2012. On the graph and systems analysis of reversible chemical reaction networks with mass action kinetics. In: *2012 American Control Conference (ACC)*. pp. 2713–2718.
- Reichenbach, T., Mobilia, M., Frey, E., 2007. Mobility promotes and jeopardizes biodiversity in rock-paper-scissors games. *Nature* 448, 1046–1049.
- Richtmyer, R. D., Morton, K. W., 1967. *Difference Methods for Initial-Value Problems*. New York: Interscience Publishers.

- Rohani, P., May, R. M., Hassell, M. P., 1996. Metapopulation and equilibrium stability: The effects of spatial structure. *J. Theor. Biol.* 181 (2), 97–109.
- Rushen, J., 1982. The peck orders of chickens: How do they develop and why are they linear? *Anim. Behav.* 30, 1129–1137.
- Saavedra, S., Rohr, R. P., Bascompte, J., Godoy, O., Kraft, N. J. B., Levine, J. M., 2017. A structural approach for understanding multispecies coexistence. *Ecol. Monogr.* 87 (3), 470–486.
- Saiz, H., Le Bagousse-Pinguet, Y., Gross, N., Maestre, F. T., 2019. Intransitivity increases plant functional diversity by limiting dominance in drylands worldwide. *J. Ecol.* 107 (1), 240–252.
- Schaft, A. V. D., Rao, S., Jayawardhana, B., 2013. On the mathematical structure of balanced chemical reaction networks governed by mass action kinetics. *SIAM J. Appl. Math.* 73 (2), 953–973.
- Serre, D., 2010. *Matrices; Theory and Applications*. Springer.
- Shannon, C., 1948. A mathematical theory of communication. *Bell Syst. Tech. J.* 27 (1), 379–423, 623–656.
- Shigesada, N., Kawasaki, K., Teramoto, E., 1984. The effects of interference competition on stability, structure and invasion of a multi-species system. *J. Math. Biol.* 21, 97–113.
- Shmida, A., Ellner, S., 1984. Coexistence of plant species with similar niches. *Veg. etatio* 58 (1), 29–55.
- Siegel, D., 2014. Chemical reaction networks as compartmental systems. Presented at the 21st International Symposium on Mathematical Theory of Networks and Systems, July 7–11, 2014. Groningen, The Netherlands.
- Sigmund, K., 2011. Introduction to evolutionary game theory. In: *Proceedings of Symposia in Applied Mathematics*. Vol. 69.
- Simpson, E., 1949. Measurement of diversity. *Nature* 163, 688.
- Sinervo, B., Lively, C. M., 1996. The rock-paper-scissors game and the evolution of alternative male strategies. *Nature* 380, 240–243.
- Slater, P., 1961. Inconsistencies in a schedule of paired comparisons. *Biometrika* 48 (3/4), 303–312.
- Smith, B., Wilson, J. B., 1996. A consumer's guide to evenness. *Oikos* 76 (1), 70–82.

- Soliveres, S., Lehmann, A., Boch, S., Altermatt, F., Carrara, F., Crowther, T. W., Delgado-Baquerizo, M., Kempel, A., Maynard, D. S., Rillig, M. C., Singh, B. K., Trivedi, P., Allan, E., 2018. Intransitive competition is common across five major taxonomic groups and is driven by productivity, competitive rank and functional traits. *J. Ecol.* 106 (3), 852–864.
- Soliveres, S., Maestre, F. T., Ulrich, W., Manning, P., Boch, S., Bowker, M. A., Prati, D., Delgado-Baquerizo, M., Quero, J., Schöning, I., Gallardo, A., Weisser, W., Müller, J., Socher, S. A., García-Gómez, M., Ochoa, V., Schulze, E.-D., Fischer, M., Allan, E., 2015. Intransitive competition is widespread in plant communities and maintains their species richness. *Ecol. lett.* 18 (8), 790–798.
- Sommer, U., Worm, B., 2002. *Competition and Coexistence*. Springer-Verlag Berlin Heidelberg.
- Song, H.-S., Cannon, W. R., Beliaev, A. S., Konopka, A., 2014. Mathematical modeling of microbial community dynamics: A methodological review. *Processes* 2 (4), 711–752.
- Stuble, K. L., Jurić, I., Cerdá, X., Sanders, N. J., 2017. Dominance hierarchies are a dominant paradigm in ant ecology (Hymenoptera: Formicidae), but should they be? And what is a dominance hierarchy anyways? *Myrmecol. News* 24, 71–81.
- Sultan, A., 1993. *Linear Programming. An Introduction with Applications*. Academic Press, Inc.
- Summerhayes, V. S., Elton, C. S., 1923. Contributions to the ecology of spitsbergen and bear island. *J. Ecol.* 11, 214–286.
- Tahara, T., Gavina, M. K. A., Kawano, T., Tubay, J. M., Rabajante, J. F., Ito, H., Morita, S., Ichinose, G., Okabe, T., Togashi, T., Tainaka, K.-I., Shimizu, A., Nagatani, T., Yoshimura, J., 2018. Asymptotic stability of a modified lotka-volterra model with small immigrations. *Sci. Rep.* 8 (1), 7029–7029.
- Taylor, D. R., Aarssen, L. W., 1990. Complex competitive relationships among genotypes of three perennial grasses: Implications for species coexistence. *Am. Nat.* 136 (3), 305–327.
- Thomas, J. W., 1995. *Numerical Partial Differential Equations: Finite Difference Methods*. Springer.
- Tilman, D., 1982. *Resource Competition and Community Structure*. Princeton University Press.
- Tilman, D., 1994. Competition and biodiversity in spatially structured habitats. *Ecology* 75 (1), 2–16.
- Turing, A., 1952. The chemical basis of morphogenesis. *Phil. Trans. R. Soc. Lond. B* 237, 37–72.

- Urban, D., Keitt, T., 2001. Landscape connectivity: A graph-theoretic perspective. *Ecology* 82 (5), 1205–1218.
- van der Schaft, A. J., Rao, S., Jayawardhana, B., 2013. On the mathematical structure of balanced chemical reaction networks governed by mass action kinetics. *SIAM J. Appl. Math.* 73 (2), 953–973.
- van der Schaft, A. J., Rao, S., Jayawardhana, B., 2015. Complex and detailed balancing of chemical reaction networks revisited. *J. Math. Chem.* 53, 1445–1458.
- Vance, R. R., Coddington, E. A., 1989. A nonautonomous model of population growth. *J. Math. Biol.* 27 (5), 491–506.
- Vandermeer, J., 2011. Intransitive loops in ecosystem models: from stable foci to heteroclinic cycles. *Ecol. Complex.* 8, 92–97.
- Vandermeer, J., 2013. Forcing by rare species and intransitive loops creates distinct bouts of extinction events conditioned by spatial pattern in competition communities. *Theor. Ecol.* 6, 395–404.
- Vandermeer, J., Perfecto, I., 2018. *Ecological Complexity and Agroecology*. Routledge.
- Vandermeer, J., Yitbarek, S., 2012. Self-organized spatial pattern determines biodiversity in spatial competition. *J. Theor. Biol.* 300, 48–56.
- Vellend, M., 2016. *The Theory of Ecological Communities*. Princeton University Press.
- Volpert, V., Petrovskii, S., 2009. Reaction-diffusion waves in biology. *Phys. Life Rev.* 6 (4), 267–310.
- Volterra, V., 1927. Fluctuations in the abundance of a species considered mathematically. *Nature* 119, 12–13.
- von Neumann, J., Morgenstern, O., 1944. *Theory of Games and Economic Behavior*. Princeton University Press.
- Wang, H., Shu, C.-W., Zhang, Q., 2015. Stability and error estimates of local discontinuous galerkin methods with implicit-explicit time-marching for advection-diffusion problems. *SIAM J. Numer. Anal.* 53, 206–227.
- Webb, J. N., 2007. *Game Theory: Decisions, Interaction and Evolution*. Springer.
- Wegscheider, R., 1902. Über simultane gleichgewichte und die beziehungen zwischen thermodynamik und reaktionskinetik homogener systeme. *Z. Phys. Chem.* 39, 257–303.
- Wesseling, P., 2001. *Principles of Computational Fluid Dynamics*. Springer, Berlin, Heidelberg.

- White, L. A., Forester, J. D., Craft, M. E., 2018. Dynamic, spatial models of parasite transmission in wildlife: their structure, applications and remaining challenges. *J. Anim. Ecol.* 87, 559–580.
- Williams, S. A., Chow, P.-L., 1978. Nonlinear reaction-diffusion models for interacting populations. *J. Math. Anal. Appl.* 62 (1), 157–169.

Curriculum vitae

Personalialia

Name	Nathan Muyinda
Gender	Male
Date of birth	31/08/1984
Place of birth	Kampala, Uganda
Nationality	Ugandan
E-mail	Nathan.Muyinda@UGent.be

Education

University

2011 - 2013

M.Sc. Mathematical Modelling, Makerere University, Uganda

2009 - 2010

Masterclass in Numerical Bifurcation Analysis of Dynamical Systems, Mathematical Research Institute (MRI), Utrecht University, Netherlands

2008 - 2009

PG. Dip. (Mathematical Sciences), African Institute for Mathematical Sciences (AIMS)/ University of Cape Town, South Africa

2004 - 2007

BSc. Education (Mathematics, Chemistry), Makerere University, Uganda

Secondary education

2002 - 2003

Uganda Advanced Certificate of Education (UACE), Makerere College School, Kampala, Uganda

1998 - 2001

Uganda Certificate of Education (UCE), Kitante Hill School, Kampala, Uganda

Employment

December 2014 - Present

Assitant Lecturer at the Department of Mathematics, Makerere University

September 2015 - October 2020

7 Full-time Research and Teaching Assistant at Ghent University Global Campus, Incheon, South Korea

November 2010 - November 2014

Teaching Assistant at the Department of Mathematics, Makerere University

Tutorship Master and Bachelor theses

Effects of diffusion on the coexistence of species under intransitive competition.
Bachelor thesis, Academic year 2019-2020 (Jongdo Im).

Scientific output

Publications in international journals (ISI-papers)

- S. Rao, N. Muyinda, B. De Baets (2021). Stability analysis of the coexistence equilibrium of a balanced metapopulation model. *Scientific Reports* 11, 14084.
- N. Muyinda, B. De Baets, S. Rao (2020). Non-king elimination, intransitive triad interactions, and species coexistence in ecological competition networks. *Theoretical Ecology* 13, 385-397.
- N. Muyinda, J.M. Baetens, B. De Baets, S. Rao (2020). Using intransitive triads to determine final species richness of competition networks. *Physica A*, 123249.

Publications in international journals (non-ISI-papers)

- N. Muyinda, B. De Baets, S. Rao (2018). On the linear stability of some finite difference schemes for nonlinear reaction-diffusion models of chemical reaction networks. *Communications in Applied and Industrial Mathematics*, 9(1), 121-140.

Conference proceedings

- N. Muyinda, B. De Baets, S. Rao (2018). On the stability of finite difference schemes for nonlinear reaction-diffusion systems. *AIP Conference Proceedings*, 1978.

Conference Abstracts

- N. Muyinda, B. De Baets, S. Rao (2019). The role of intransitive triads in the determination of final species richness of competition networks. 24th National Symposium on Applied Biological Sciences, NSABS 2019, February 2019, Ghent, Belgium.
- N. Muyinda, B. De Baets, S. Rao (2017).. Stability of difference schemes for reaction-diffusion models of chemical reaction networks. 22nd National Symposium on Applied Biological Sciences, NSABS 2017, February 2017, Leuven, Belgium.

Index

- amplification factor, 75
- amplification matrix, 125
- balanced metapopulation model
 - heterogeneous, 109
 - homogeneous, 109
- boundary conditions
 - Dirichlet, 63
 - Neumann, 63
 - Robin, 63
- Brusselator model, 143
- chemical reaction network
 - reversible, 53
 - weakly reversible, 53
- coexistence equilibrium, 41
- competition
 - cyclic, 20
 - exploitative, 14
 - interference, 13
- competitive-exclusion principle, 1
- completely mixed game, 50
- completely mixed strategy, 44
- complex graph, 53
- complex stoichiometric matrix, 55
- Courant-Friedrichs-Lewy, 76
- detailed balanced, 108
- detailed balanced equilibrium, 56, 106
- diffusion-driven instability, 120
- discrete Fourier transform, 74, 125
- dominated strategy, 45
- ecological community, 11
- ecological niche, 2
- equilibrium stability
 - global stability, 37
 - local asymptotic stability, 36
 - local stability, 36
 - neutral stability, 104
- evolutionarily stable state, 49
- evolutionarily stable strategy, 46
- Fick's law, 61
- food web, 12
- fugitive species, 100
- function
 - positive definite, 37
 - positive semidefinite, 37

- graphs
- adjacency matrix, 16
 - complete graph, 18
 - connected, 18, 53
 - degree, 16
 - incidence matrix, 16
 - path, 18
 - subgraph, 15
 - tournament, 18
 - walk, 18
 - weighted, unweighted, 16
- heterogeneous graph, 100, 109
- homogeneous graph, 100, 109
- interspecific interactions, 13
- intransitive competition, 19, 82
- intransitive triad, 20, 87
- intransitivity indices
- Kendall's d , 22
 - relative intransitivity, 23
 - Slater's i , 22
- invariant set, 39
- Jordan canonical form, 129
- kings in a tournament, 23
- Laplacian, 62
- LaSalle's invariance principle, 40
- Lax equivalence theorem, 70
- Lipschitz condition, 35
- Lyapunov function, 38
- Lyapunov's stability theorem, 38
- mass-action kinetics, 54
- matrix
- bounded, 128
 - D-semi-stable, 128
 - diagonalizable, 127
 - semi stable, 127
 - semi-stable, 127
- mean-field ODE model, 34
- metapopulation, 66, 100
- method of lines, 70
- monotone kinetics, 155
- Nash equilibrium, 45
- neutral theory, 3
- niche overlap, 2
- niche theory, 2
- numerical stability, 65, 73
- omega limit point, 39
- Parseval's identity, 126
- phase portrait, 31
- phase space, 31
- reaction-diffusion model, 63
- replicator equation, 47
- species diversity, 12
- species evenness, 12
- species richness, 12
- spectral radius, 126
- stiffness, 71
- stoichiometric compatibility class, 51
- stoichiometric matrix, 52
- symmetric game, 43, 45
- triad-interaction graph, 84
- truncation error, 70
- von Neumann stability condition, 75, 126
- Wegscheider conditions, 57
- well-posed, 65
- zero-sum game, 43